Measuring the effects of a novel Titania (TiO_2) coating on microbial survival, adaptation and ecology

A Thesis

Submitted in partial fulfilment

of the requirements for the

Degree

Of

Doctor of Philosophy in Microbiology at the

University of Canterbury

By

Wasa Alibe Ahmed

University of

Canterbury

2021

Dedication

This thesis is dedicated to my late father Mallam Ahmed Wasa.

Acknowledgments

I would first like to thank God almighty for giving me life, strength and the opportunity to complete this program. My wife Yinasim, my son Zephath-Ahmed, Mother, brothers and sisters have all been a source of encouragement.

I would also like to express my gratitude to my supervisory team: Prof. Jack Heinemann, Asso. Prof. Catherine Bishop and Dr William Godsoe for allowing me to work on this project. Your support, guidance, enthusiasm and constructive criticisms have helped me a lot. Thank you for responding to questions and providing excellent feedback on this thesis. It was a great privilege to work with you.

I want to thank all members of the MolBio lab group, most especially Dr Brigitta Kurenbach, for the encouragement, guidance and support. She has always provided advice, help and feedback whenever I call on her. I am incredibly grateful for the inputs she made at group meetings. I am also indebted to members of the MRE lab group led by Dr Mitja Remus-Emsermann for providing technical support and teaching me some fundamental skills needed to carry out this work.

I would also wish to thank the entire staff of the School Biological Sciences headed by Prof. Mathew Turnbull for providing funding for my PhD tuition. I also wish to thank Matt Walters, Craig Galilee, Thomas Evans and Jan McKenzie for technical assistance. Mike Flaws, Shaun Mucalo and Rukmini Gorthy for helping with SEM. Johann Land and Daryl Lee for making NsARC depositions. Hyunwoo Jun and Jack Aitkens for helping to make the reporter strains.

Last but not the least I would like to thank the members of the “Saving lives with NsARC” group led by Prof. Susan Krumdieck for allowing me into the group and providing me with materials. I am very grateful to you all and wish you the best in your future endeavour. God bless you

Table of Contents

List of Figures

List of Tables

Abbreviations

ABA	Antibiofilm activity
Ag	Silver
AMA	Antimicrobial activity
CAM	chloramphenicol
CDC	Centre for disease control
cfu	colony forming units
Cip	Ciprofloxacin
Cu	Copper
DNA	Deoxyribonucleic acid
EOP	Efficiency of plating
EPS	Extracellular polymeric substance
Ery	Erythromycin
EVOH	ethylene-vinyl alcohol
FA	Fusidic acid
FP	Fluorescent proteins
GDP	Gross domestic product
HAI	Hospital acquired infections
HGT	Horizontal gene transfer
HMDS	Hexamethyldisilazane
H_2O_2	Hydrogen peroxide
kan	Kanamycin
LB	Lauria Broth
MDR	Multidrug resistant
MIC	Minimum inhibitory concentration

ml	Millilitre
mm	Millimetre
nm	Nanometre
NsARC	Nanostructured anatase rutile and carbon
Oxa	Oxacillin
PBP	Penicillin binding proteins
PP-MOCVD	pulsed-pressure metal-organic chemical vapour deposition process
PBS	Phosphate buffer saline
RNA	Ribonuceic acid
RND	Resistance nodulation division
ROS	Reactive oxygen species
SEM	Scanning electron microscopy
tet	Tetracycline
TiO_2	titania
TSA	Tryptic soy agar
TSB	Trytic soy broth
TTIP	Titanium tetraisopropoxide
UK	United Kingdom
USA	United States of America
UV	Ultraviolet
Van	Vancomycin
WHO	World Health Organization
YPB	Yeast potato broth
µg	microgram
µl	microlitre

Abstract

Contaminated surfaces are a major vehicle for the spread of infectious diseases. A strategy to prevent the spread of the organisms causing these infections is through making these surfaces antimicrobial. Photo-activated titania (TiO_2) is an antimicrobial agent with self-cleaning properties and could be used to coat door handles and similar surfaces. This coating can reduce viability, spread and colonization of the surface by pathogens.

The focus of my thesis is testing a nanostructured anatase rutile and carbon (NsARC) coating that was deposited on various substrates (stainless steel and fused silica). This material is shown to be photoactive. Photoactivity results in antimicrobial activity due to the production of reactive oxygen species (ROS) and other free radicals (H_2O_2 and OH^+) that can distort cell membranes.

I tested the survival of *Escherichia coli*, *Pseudomonas aeruginosa*, *Staphylococcus aureus* and *Saccharomyces cerevisiae* on the surface of NsARC under a variety of light wavelengths and intensities (high intensity visible, UV and ambient light) adopting a modified version of the standard ISO 27447:2009 "test method for antimicrobial activity of photocatalytic materials". Scanning electron microscopy (SEM) was used to visualize the morphology of the tested organisms.

There was significantly less survival of all the species of the microorganisms tested on NsARC compared to uncoated stainless steel. From the SEM images, I observed that cells that were on NsARC look more distorted compared to the ones that were on stainless steel. I observed that in addition to inhibiting the survival of laboratory strains of bacteria, NsARC was also able to inhibit the survival of bacteria that were recently isolated from the environment.

I was also interested in finding out if biofilms can form on NsARC. Attachment of microbial cells onto the surface of NsARC was used as a model to describe biofilm formation.

The number of microbes that were still attached onto the surface of NsARC after a period of 12, 24 and 48 hours exposure under high intensity visible, UV, ambient light and no light was significantly less than on stainless steel for the same period of time. SEM also corroborated the result.

I was also interested in finding out if exposing organisms to NsARC could lead to the development of unintended phenotypes like resistance to antibiotics.

To determine if exposing bacteria to NsARC changes the way bacteria respond to antibiotics, I exposed *E. coli* and *S. aureus* directly to various antibiotics after they had survived 8 hours

exposure to NsARC. I observed that *E. coli* that survived 8 hours exposure to NsARC were more susceptible to kanamycin than *E. coli* that were on stainless for the same period. No significant change in susceptibility to tetracycline, chloramphenicol, ciprofloxacin, vancomycin, erythromycin, oxacillin, tetracycline and fusidic acid was observed. There was also no significant change in susceptibility of *S. aureus* that was on either NsARC or stainless steel to all the antibiotics tested.

Previous research has shown that copper, an antimicrobial agent that is used in making antimicrobial surfaces can induce higher levels of antibiotic resistance. I was interested in investigating the possibility of NsARC inducing some form of resistance to antibiotics in bacteria. To determine if exposure of bacteria to NsARC could induce a form of resistance to antibiotics, known as adaptive resistance I used two reporter strains of *E. coli*, each having a plasmid with a reporter gene construct that expressed the mScarlet fluorescent protein (FP) under the control of the promoters of either the *tolC* or *soxS* genes. The *tolC* and *soxS* genes are regulators of multidrug resistance and stress response. The reporter strains were designed to "report" when the expression of *tolC* and *soxS* changes. When these genes are induced there is an increase in the production of the FP leading to a corresponding increase in fluorescence of the reporter strains. Reporter strains that were on NsARC were significantly brighter than the ones that were on stainless steel indicating that NsARC was able to induce the *tolC* or *soxS* genes.

Finally, these results suggest that NsARC can be used as a self-cleaning and self-sterilizing antimicrobial surface coating for the prevention and reduction in the spread of infections.

UNIVERSITY OF CANTERBURY
Te Whare Wānanga o Waitaha
CHRISTCHURCH NEW ZEALAND

Deputy Vice-Chancellor's Office
Postgraduate Research Office

Co-Authorship Form

This form is to accompany the submission of any thesis that contains research reported in co-authored work that has been published, accepted for publication, or submitted for publication. A copy of this form should be included for each co-authored work that is included in the thesis. Completed forms should be included at the front (after the thesis abstract) of each copy of the thesis submitted for examination and library deposit.

Please indicate the chapter/section/pages of this thesis that are extracted from co-authored work and provide details of the publication or submission from the extract comes:

Chapter Two /Page 13-49/ Section 2.3, 2.4.2, 2.4.4 and 2.5 / Figure 2.2, 2.8-2.11 and 2.13-2.16

Title: Antimicrobial and biofilm-disrupting nanostructured TiO_2 coating demonstrating photoactivity and dark activity.

Authors: Alibe Wasa[a], Johann G Land[b], Rukmini Gorthy[b], Susan Krumdieck[b], Catherine Bishop[b], William Godsoe[c] and Jack A. Heinemann[a]

Journal: FEMS Microbiology Letters,

Please detail the nature and extent (%) of contribution by the candidate:

Author roles: Alibe Wasa: (45%) Original draft preparation, Investigation, Methodology, Writing, statistical analysis – Review and Editing; **Johann Land**: (5%) Production of test samples, Writing – Original Draft Preparation; **Rukmini Gorthy**: (5%) Characterisation of NsARC, SEM, Writing – Review & Editing; **Susan Krumdieck**: (5%) Funding Acquisition, Project Administration, Writing – Review & Editing; **Catherine Bishop**: (10%) Resources, Supervision, Writing – Review & Editing; **Godsoe William**: (10%) Statistical Analysis, Methodology, Supervision, Writing – Review & Editing; **Jack A. Heinemann**: (20%) Conceptualization, Methodology, Project Administration, Resources, Funding Acquisition, Supervision, Writing and Editing – Original Draft Preparation

Revised manuscript submitted awaiting decision from editors

Certification by Co-authors:

If there is more than one co-author then a single co-author can sign on behalf of all

The undersigned certifies that:

- The above statement correctly reflects the nature and extent of the Doctoral candidate's contribution to this co-authored work
- In cases where the candidate was the lead author of the co-authored work he or she wrote the text

Name: *Rukmini Gorthy* Signature: *RG* Date: 22/001/21

UNIVERSITY OF CANTERBURY
Te Whare Wānanga o Waitaha
CHRISTCHURCH NEW ZEALAND

Deputy Vice-Chancellor's Office
Postgraduate Research Office

Co-Authorship Form

This form is to accompany the submission of any thesis that contains research reported in co-authored work that has been published, accepted for publication, or submitted for publication. A copy of this form should be included for each co-authored work that is included in the thesis. Completed forms should be included at the front (after the thesis abstract) of each copy of the thesis submitted for examination and library deposit.

Please indicate the chapter/section/pages of this thesis that are extracted from co-authored work and provide details of the publication or submission from the extract comes:

Chapter 2, section 2.4.3. Figure 2.3, 2.12

Title: Effects of post-deposition heat treatment on nanostructured TiO2-C composite structure and antimicrobial properties

Authors: Rukmini Gorthy, Alibe Wasa; Johann G Land, PhD; Zhendi Yang, PhD; Jack A Heinemann, PhD; Catherine M Bishop, PhD; Susan P Krumdieck, PhD

Journal: Surface and Coatings Technology

Please detail the nature and extent (%) of contribution by the candidate:

Rukmini Gorthy: (40) Original draft preparation, Investigation, Methodology, Writing, statistical analysis – Review and Editing; Alibe Wasa: (20%) Investigation, Methodology, Writing, statistical analysis – Review and Editing; Johann G Land: (10%) Production of test samples, Writing – Original Draft Preparation; Zhendi Yang: (5%) Investigation, Methodology, Writing, Review and Editing; Jack A Heinemann: (5%) Resources, Supervision, Writing – Review & Editing; Catherine M Bishop: (10%) Resources, Supervision, Writing – Review & Editing; Susan P Krumdieck: (10%) supervision, Funding Acquisition, Project Administration, Writing – Review & Editing

revised manuscript accepted for publication

Certification by Co-authors:

If there is more than one co-author then a single co-author can sign on behalf of all

The undersigned certifies that:

- The above statement correctly reflects the nature and extent of the Doctoral candidate's contribution to this co-authored work
- In cases where the candidate was the lead author of the co-authored work he or she wrote the text

Name: *Rukmin Gorthy* Signature: *RG* Date: 22/01/21

Chapter One

1.1 Introduction

Nanomaterials are generating attention because of their importance in pharmaceutical and biological applications. These nanomaterials with antimicrobial properties could be of value because disease causing microorganisms are becoming resistant to the conventional methods of prevention and treatment (Djurišić et al., 2015; Leung et al., 2016). Conventional methods such as the use of prescription medicines, antiseptics and disinfectants are not uniformly effective against microorganisms (Dancer, 2008; Foster et al., 2011; Griffith et al., 2000). Therefore, the diseases caused by these microorganisms are difficult or impossible to treat with antibiotics (Heinemann, 1999; Metcalfe et al, 2016; Williamson et al., 2015). Disease-causing microorganisms may transfer through touching contaminated surfaces (Finley et al., 2013), making them particularly troublesome in public places and hospitals. The infections they cause are serious public health issues that increases hospital costs, morbidity and mortality (Griffith et al., 2000).

Presently, measures taken to reduce infections are geared towards personal hygiene and cleaning of surfaces, but this has yielded limited success (Airey and Verran, 2007; Griffith et al., 2000) and so research towards developing antifouling, antiadhesive and antimicrobial coatings on surfaces that are constantly touched by people is ongoing (Krumdieck et al., 2015). Recently, metals, physical and chemical compounds such as cationic polymers, metal nanoparticles, and antimicrobial peptides has received a great deal of attention because of their antimicrobial activity against microorganisms (Dancer, 2008).

One of the strategies to reduce infections by bacteria transferring through direct contact with contaminated surfaces is to make these surfaces antimicrobial (Krumdieck et al., 2015).

I tested antimicrobial activity of a titania surface coating product, called nanostructured anatase rutile carbon "NsARC", that was developed through collaboration between Koti Technologies and the University of Canterbury. This surface coating is a robust nanostructured composite comprising of titanium dioxide and carbon (Krumdieck et al., 2017). Titania is an interesting material because it is photoactive. Photoactivity is a light induced mechanism, where photoexcitation of titania causes a series of chemical reactions that leads to the release of reactive oxygen species (ROS) such as hydrogen peroxide (H_2O_2), super oxides (O^+) and other free radicals that are toxic to cell membranes of microorganisms (Castellote and Bengtsson, 2011; Pelaez et al., 2012; Verdier et al., 2014). This toxic effect that titania has on microorganisms makes it a good choice material for making antimicrobial coating (Kim et al., 2007). Antimicrobial surface coatings are anti-adhesive and or biocides releasing surfaces that can affect the ability of microorganisms to survive and proliferate on them (Ramyadevi et al., 2012). In addition to their anti-adhesive properties, titania, copper and silver are examples of materials that can also release or facilitate in the release of ions and other molecules that are toxic microorganisms. They have been applied successfully to a wide variety of touch surfaces because of their antimicrobial properties (Ahamed et al., 2014; Cheng et al., 2009; Grass et al., 2011).

1.2 Titania (TiO_2)

TiO_2 exists in three mineral forms: rutile, anatase and brookite. Rutile got its name from the Latin word "rutilus" meaning red, because of its deep red coloration. It is the most thermodynamically stable form of TiO_2, due to its low molecular volume compared to anatase and brookite. It is also commonly seen in igneous and metamorphic rocks (Sikora, 2005). Anatase on the other hand, exhibits the most photocatalytic activity, and is the most photoactive and commonly occurring form found as small, isolated and sharply developed crystals shaped like a pyramid (Yu et al.,

2014). The name anatase comes from the Greek word “anastasis” meaning extension because its vertical axis is longer than that of rutile. Anatase can revert to rutile structure at temperature above 90°C (Hanaor and Sorrell, 2011). Brookite is the rarest form of titania when compared to anatase and rutile. It is not easily found because of its instability and thus not much is known about its photocatalytic potential even though it is believed to have the highest photocatalytic activity per surface area (Zhang et al., 2014). Difficulty in the synthesis of brookite makes getting its pure form quite challenging (Zhao et al., 2009).

Recently, TiO_2 has been attracting attention because it could cause decomposition of organic matter under UV light irradiation (Brook et al., 2007; Piszczek et al., 2013; Wu et al., 2010).

No matter how polymorphic titania may seem, it is a semi-conductive material that during illumination acts as a strong oxidizing agent lowering the activation energy for the decomposition of organic and inorganic compounds. Illumination of the surface of the TiO_2 induces the separation of two types of carriers: an electron (e^-) and a hole (h^+). To produce these two carriers, sufficient energy must be supplied by a photon to promote an e^- from the valence band to the conduction band, leaving a h^+ behind in the valence band.

Its interaction with light with wavelength 388 nm or below leads to excitation of e^- and h^+ that can participate in redox reactions with water and oxygen molecules adsorbed onto the surface. These redox reactions lead to formation of reactive oxygen species (Castellote and Bengtsson, 2011), free radicals, hydroxyl radicals and hydrogen peroxide that causes leakage of cellular content of the cell leading to cell damage and death (See Figure 1.1) (Foster et al., 2011; Kubacka et al., 2014). This photo-activation process is known as photocatalysis. It is a photon-assisted generation of active reactive oxygen species that are involved in killing microbes (Gomes et al., 2011; Sadowski et al., 2015), rather than the action of light as a catalyst in a reaction (Pelaez et al., 2012).

Studies have suggested that toxicity of photoactivated TiO_2 occurs through membrane damage. Kiwi and Nadtochenko (2005) showed that TiO_2 caused oxidative degradation of lipopolysaccharides, phosphatidyl-ethanolcholine and peptidoglycan components of the cell wall of *E. coli* (Kiwi and Nadtochenko, 2005; Nadtochenko et al., 2005). Maness et al. (1999) had earlier demonstrated that polyunsaturated fatty acids and lipids were the major targets for oxidative attack from reactive oxygen species (Maness et al., 1999). Wei et al. (2014) also demonstrated that bacterial membrane bound proteins were also sensitive targets for ROS activity. They found out that there was a decline in Amide I and Amide II in bacterial cells exposed to TiO_2 coating when compared to bacterial cells that were not exposed to TiO_2. This reduction in proteins was as a result of membrane damage caused by the increase in the permeability of the membrane (Wei et al., 2014; Yu et al., 2014). The bactericidal effect of photocatalysis is believed to be due to the production of hydrogen peroxide, super oxides and hydroxyl radicals, however, the particular radical responsible for cell death is debatable (Cho et al., 2004; Gogniat and Dukan, 2007). Some studies demonstrated that the killing of *E. coli* exposed to TiO_2 was due to hydrogen peroxide alone, because of its ability to penetrate into cell membranes compared to hydroxyl radical (Cho et al., 2004). It was proposed that the mechanism of killing involved entry of hydrogen peroxide and super oxides into the cell by diffusion and the subsequent generation of hydroxyl radicals through the Harber-Weiss reaction. In fact, hydroxyl radical generated by this process is considered as the main cause of the cell death (Cho et al., 2004; Dodd and Jha, 2009; Gogniat and Dukan, 2007). Sunasda et al. (2003) summarized that there are 3 possible steps involved in the killing. ROS cause an increase in permeability of the outer membrane in the first step. The cell is still viable at this stage. The second step involves ROS entering into the cell and disrupting the cytoplasmic membrane leading to cell death. The decomposition of the cell occurs at the final step

(Sunada et al., 2003). This killing mechanism confers on TiO_2 broad spectrum antimicrobial activity, making it also effective against multidrug resistant strains (Allahverdiyev et al., 2011; Josset et al., 2008).

The use of TiO_2 as a biocide was first demonstrated by Matsunaga and co-workers in the early 1980s (Maness et al., 1999). Subsequently, the photocatalytic property of this compound was documented and it is believed to have many applications which include removal of organic contaminants and disinfection of surfaces (Kubacka et al., 2014). Photo-activated TiO_2 is capable of facilitating the killing of a wide range of microorganisms.

The killing effect of this photocatalyst is most efficient when TiO_2 is in close contact with the organism. The presence of other antimicrobial agents like copper in combination with it further increases its potency (Foster et al., 2011).

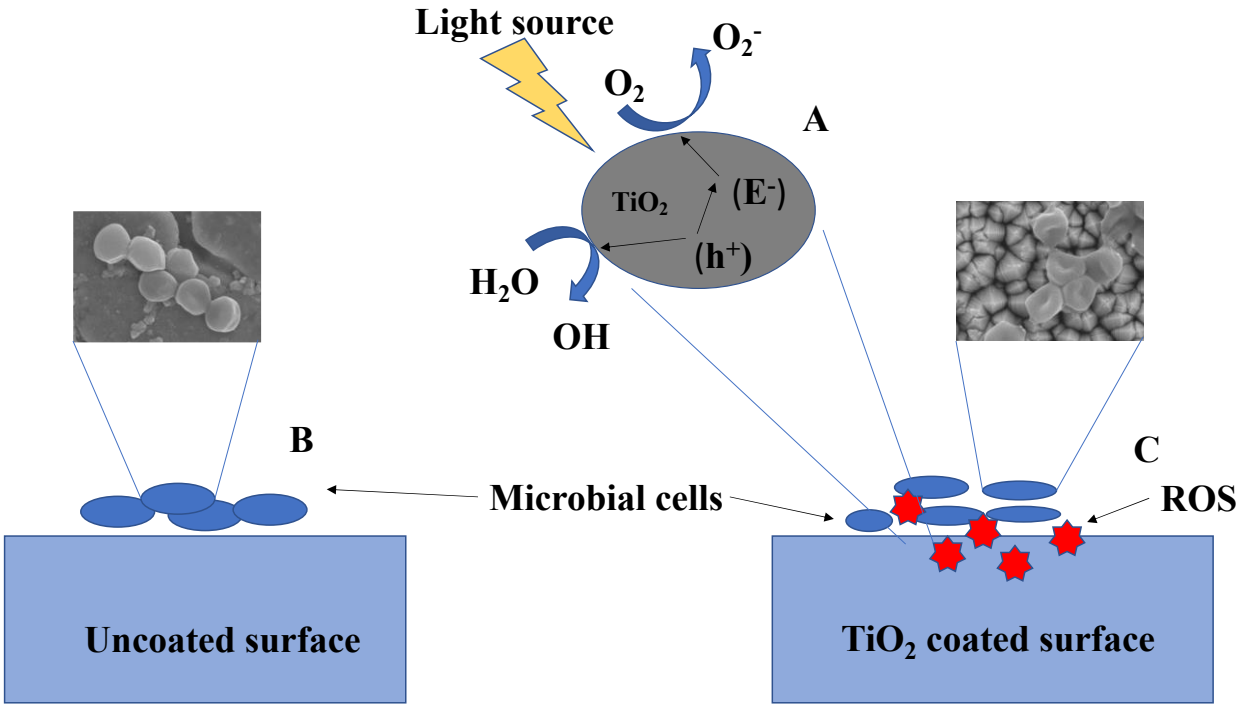

Figure 1.1: Schematic illustration of the mechanism of killing by TiO_2.

(A) Photo-activation of TiO_2 leads to ROS generation (B) Cells on uncoated surface remain intact, while (C) ROS causes death of microbial cells on TiO_2 coated surface**.**

1.2.1 Nanostructured anatase rutile and carbon (NsARC)

The TiO_2 formulation called nanostructured anatase rutile and carbon (NsARC) is a composite of titania and carbon. It was deposited using the direct liquid injection pulsed-pressure metal-organic chemical vapour deposition process (PP-MOCVD) technique and can be applied in conformal coatings onto complex geometries (Krumdieck et al., 2015; Krumdieck et al., 2017; Krumdieck et al., 2019; Lee et al., 2013). NsARC depositions were done using the same number of pulses, temperature, concentration and injection rate of titanium tetraisopropoxide (TTIP) in dilute toluene solution in the deposition reactor. The deposited films had a black tint that was opaque (Krumdieck et al., 2019). NsARC on either fused silica or stainless-steel substrate also had higher surface wettability than the corresponding inert uncoated surfaces (Krumdieck et al., 2019), indicating that NsARC is also very hydrophilic.

This material was tested for photoactivity (Krumdieck et al., 2017), using the standard ISO methylene blue test as adopted by Mills (2012). Methylene blue dye degraded faster on NsARC coated surface compared to on uncoated stainless surface (Krumdieck et al., 2015), indicating photoactivity. NsARC is robust, super-hydrophilic and photoactive under UV and visible light. This property that makes it suitable as an antimicrobial surface coating.

There is a lot of interest in using metals and metal ions such as copper, silver oxides and titania as antimicrobial agents because they could be alternatives to antibiotics for which resistance is common (Foster et al., 2011; Krumdieck et al., 2015). The use of copper and silver in making door knobs and handles in public places and hospitals is quite popular (Abboud et al., 2014; Hassan et al., 2014). Even though copper and silver are effective in preventing the spread of infections they are more expensive compared to titania (Table 1.1).

Table 1.1: Global market price of metals (2019)

S/N	metal	Price in US dollars (USD)
1	copper	6.79/kg
2	silver	469.6/kg
3	titanium	4.9/kg

Source: ("Commodity and Metal Prices, Metal Price Charts - Investment Mine," n.d.)

Titania is less expensive than silver and copper but has one drawback, which is that it is only active upon excitation by light within the ultraviolet (UV) range (De Falco et al., 2017). Efforts have been made to develop titania formulations that are effective under visible light with little success, with no significant activity observed under visible light (Cendrowski et al., 2014; De Falco et al., 2017; Xu et al., 2015). Preliminary antimicrobial testing of NsARC using *E. coli* as the test organism adopting the standard ISO 27447:2009, "test method for antimicrobial activity of semi conducting photocatalytic materials" showed that activation of NsARC by visible light reduced

viable *Escherichia coli* populations by 3 orders of magnitude in 4 hours. In addition, a 2 orders of magnitude reduction in viability was observed even in the dark (Krumdieck et al., 2019).

1.3 Copper (Cu)

Cu has attracted attention due to its unique optical, electronic, magnetic properties and thus, it is utilized in diverse applications (Ramyadevi et al., 2012; Shankar & Rhim, 2014; Stoimenov et al., 2002). It can easily be mixed with other materials that have stable chemical and physical properties (Hassan et al., 2014; Ramyadevi et al., 2012). It exists naturally as a red metal found in the soil and rocks and it is about 50 parts per million (ppm) in average concentration in the earth's crust (Ahamed et al., 2014; Grass et al., 2011). Living organisms require copper in small amounts as cofactors for metalloproteins and enzyme biosynthesis. However, in high concentrations it can have a toxic effect and can induce inhibition in growth of most microorganisms. This is possible through substitution of essential ions and blocking of functional amino acid groups, inactivation of enzymes, alteration of membrane integrity and production of radicals (Kiaune & Singhasemanon, 2011). When microorganisms are exposed to high concentrations of copper, extensive breakdown of plasma membrane can occur leading to loss of cell viability (Grass et al., 2011).

A bacterium has a stable "transmembrane potential", which is the electrochemical potential difference between the inside and the outside of a cell. Short circuiting of the current in the cell membrane can occur on contact with copper surface, leading to weakening of the membrane and creation of pores (Lemire et al., 2013; Shankar and Rhim, 2014). Influx of copper ions into the cell occurs obstructing cell metabolism and eventually causing cell death (See Figure 1.2) (Abboud et al., 2014; Grass et al., 2011; Souli et al., 2013).

Copper nanoparticles are active against various bacterial species and can be used as an antibacterial agent in surface coatings on various substrates to prevent microorganisms from attaching, colonizing and formation and spread of biofilms (Ahamed et al., 2014; Gyawali ea al., 2011). Copper and its alloys such as brass and bronze are used as biocides in paints, water purification systems and in agriculture to prevent plants from fungal diseases of the leaves (Kiaune and Singhasemanon, 2011). Copper alloys are also used on coating surfaces because of their antimicrobial activity and their availability in different range of colours (Michels et al., 2009).

To reduce the spread of hospital acquired infections (HAI), copper has been used on surface such as bed rails and doorknobs (Schmidt et al., 2012).

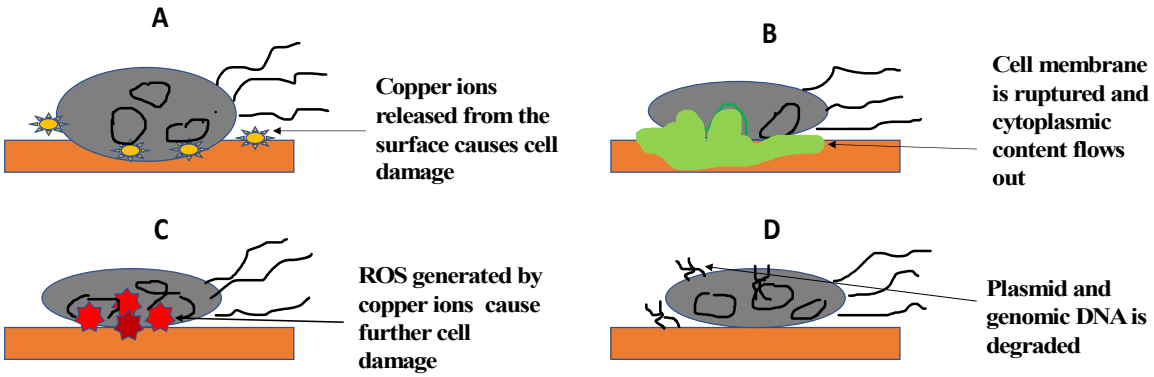

Figure 1.2: Illustration of the mechanism of contact killing by copper.

(A) Copper ions are released from the surface of copper and cause cell membrane damage (B) The cell membrane then ruptures causing the cell cytoplasmic contents to flow out (C) The copper ions also induce the generation of reactive oxygen species (ROS) that can cause further cell damage (D) And finally, the degradation of the plasmid and genomic DNA occurs.

1.4 Silver (Ag)

Silver is material that is known for its antimicrobial activity. The ancient Greeks and Romans have put silver coins in water to maintain its purity (Page et al., 2009). Silver has also been used to coat medical devices such as dental fillings and catheter (Kim et al., 2007; Peng et al., 2012; Silver et al., 2006). Silver is not toxic to non-targeted cells but is effective against a wide range of

microorganisms such as gram-positive and gram-negative bacteria (Kim et al., 2007; Wang et al., 2016). That is why it is incorporated into a wide range of materials such as electric appliances, textiles and food storage containers (Jung et al., 2006). Taylor et al. (2009) reported a 98% reduction in bacterial counts on surfaces that were treated with silver in the hospital, when compared with the untreated surface (Taylor et al., 2009). The antimicrobial activity of silver depends on the release of silver ions (Ag^+) (Kim et al., 2007; Wu et al., 2010). Ag^+ that are released can enter into bacterial cell and prevent cell division and also cause damage to the cell envelop. Ag^+ can bind to electron donors in biological molecules like phosphate, amino and carboxyl groups in DNA and proteins. The interaction between Ag^+ and these groups of molecules can lead to the denaturation of proteins and subsequent inactivation of the bacteria. Even low levels of Ag^+ can cause protons to leak through the cell membrane leading to cell death (Kim et al., 2011). Studies have also shown that silver can inhibit the activity of succinate dehydrogenase that catalyses the uptake of succinate by membrane vesicles of *E. coli* (Sondi and Salopek-Sondi, 2004).

1.5 Mechanism of microbial resistance to nanomaterials

The diverse nature of the antimicrobial activity of nanomaterials might make it more difficult for bacteria to develop resistance. However, recently it was observed that bacteria are able to generate resistance to nanomaterials through electrostatic repulsion, efflux pumps (Webber and Piddock, 2003; Weston et al., 2018), mutation (Walsh, 2000) and biofilm formation mechanisms (Graves Jr et al., 2015).

Microorganisms have been exposed to both essential and toxic nanomaterial for over billions of years, and this exposure is likely the major driving force for the ability of these microorganisms to control the cellular concentration of these nanomaterials (Barkay et al., 2010; Lemire et al., 2013). Nanomaterials are sometimes found in high concentrations in the environment as a result of natural

geological events such as volcanos and or human activities such as mining, smelting, fossil fuel burning and other industrial activities (Ali et al., 2019; Barkay et al., 2010). Thus, because of the abundance of these nanomaterials in the environment, microorganisms have evolved mechanisms by which they can acquire essential metals, maintain the intracellular concentrations of these metals and eliminate these metals when they are in excess (Ali et al., 2019; Chandrangsu et al., 2017). Microorganisms have also evolved systems for removing and or modifying toxic metals into useful or nontoxic materials (Das et al., 2016). Nanomaterial have multiple cellular targets and therefore the options available for microorganisms to mitigate the effects of nanomaterials is limited (Lemire et al., 2013; Wright et al., 2006). However, the strategy microorganism employ involves extracellular and or intracellular sequestration of metals, modification of target sites, reduction in outer membrane porins (OMP), enzymatic detoxification and or increase in efflux of metals (Nies, 2003). The most common mechanism by which microorganism are able to develop resistance to nanomaterials is usually through detoxification or efflux of metals from the cells. This is because nanomaterials are not easily broken down and the import systems or porins in microorganisms cannot sufficiently discriminate between useful and toxic metals (Das et al., 2016). There are several metal ion-specific response regulators in microorganisms that control the expression of structural resistance genes involved in resistance to specific metal ions. These genes produce metal ion-specific efflux proteins or protein complexes and or enzymes that alter metal ions into less toxic forms in a microbial cell (Silver and Phung, 1996). Bacteria are able to tolerate copper through transmembrane copper export (Abboud et al., 2014), sequestration of copper by metallothioneins and oxidation of copper (Airey and Verran, 2007; Shankar and Rhim, 2014; Tong et al., 2015). The *cue* and *cus* systems are two chromosomally encoded copper homeostasis mechanisms in *E. coli*. Both systems can modify the charge copper ions in a cell and then expel

the copper ion by efflux (Munson et al., 2000). Widespread resistance to Ag^+ is not very common, but as seen with other nanomaterials, energy-dependent ion efflux systems rather than chemical detoxification may be responsible for resistance of microorganisms to Ag^+ (Percival et al., 2005). Furthermore, studies have shown that *E. coli* mutants that don't have OMP were more resistant to Ag^+ (Munson et al., 2000).

1.6 Antibiotics

Antimicrobial agents are chemical compounds or physical agents that kill or inhibit the growth of microorganisms by interfering with their metabolism, growth and reproduction (Corona and Martinez, 2013). Antimicrobial agents are not only naturally produced by organisms or synthetic molecules, as in the case of antibiotics, but also include physical agents such as ultraviolet light and chemical agents like antiseptics, disinfectants, metal and metal oxides (Denyer and Russell, 2004). Commonly prescribed antibiotics are beta lactams, aminoglycoside, quinolones, tetracycline and chloramphenicol, all having their own modes of action (von Nussbaum et al., 2006).

1.6.1 Beta lactams

These represent one of the most important groups of antibiotics. Antibiotics such as ampicillin, amoxicillin, cephalosporins and penicillin belong to this group (Page, 2012). These antibiotics are grouped together based on a shared structural feature which is the beta lactam ring. This group of antibiotics are bactericidal and their mode of action is simply inhibition of bacterial peptidoglycan cell wall layer biosynthesis (Yao et al., 2012). They bind to the active site of penicillin binding proteins (PBPs) inhibiting their activity. This PBPs form peptide crosslinks within the peptidoglycan layer that maintains cell shape and turgidity. Inhibition of protein by the antibiotic results in the inability to form crosslinks resulting in cell lysis (Yao et al., 2012). Gram negative

bacteria normally develop resistance to this antibiotic by the production of beta lactamase enzymes that attack the beta lactam ring, rendering it ineffective (Page, 2012).

1.6.2 Aminoglycosides

This group of antibiotics contains amino-sugar structures that have high affinities for certain portions of RNAs and hammerhead ribosomes (Kotra et al., 2000), with different classes binding to different site on the ribosomes and ribosomal RNA's. Most are bactericidal, and their mode of action is through inhibition of protein synthesis, leading to cell death. Once the antibiotic gets into the bacterium, it binds to the 30S ribosomal subunit at the aminoacyl-tRNA acceptor site (A) on the 16S ribosomal RNA. This induces codon misreading and inhibition of protein translation, directly resulting in a non-functional protein synthesis. Resistance to this group may be due to reduced uptake of the drug or decreased cell wall permeability, alterations at the ribosomal binding sites making it difficult for the drug to bind with its target site, or production of aminoglycoside modifying enzymes that will directly alter the antibiotic. Antibiotics such as: kanamycin, gentamycin, streptomycin and tobramycin belongs this group (Garneau-Tsodikova and Labby, 2016).

1.6.3 Quinolones

This group of antibiotics contain fused aromatic (quinolone) rings with a carboxylic acid group attached. Members of this group include ciprofloxacin, levofloxacin and trovafloxacin. Most are bactericidal and interfere with DNA replication and transcription. They inhibit DNA gyrase enzyme that is responsible for unwinding DNA during replication and transcription, by binding to the A-subunit of the enzyme thus making the bacteria unable to replicate or even synthesize proteins (Garneau-Tsodikova & Labby, 2016). Resistance to quinolones can be target mediated, plasmid mediated or chromosome mediated (Aldred et al., 2014; Mehta, 2011).

1.6.4 Tetracyclines

Doxycycline, limecyline, oxytetracycline belong to this group. All the members of this group contain four adjacent cyclic hydrocarbon rings that enable them to inhibit protein synthesis. This is possible by inhibiting the binding of aminoacyl-tRNA to the mRNA-ribosome complex. They do so mainly by binding to the 30S ribosomal subunit in the mRNA translation complex (Aldred et al., 2014; Mehta, 2011). Resistance to this form of antibiotic is through genetic acquisition and expression of *tet* genes by the invading bacteria (Chopra and Roberts, 2001).

1.6.5 Chloramphenicol

This antibiotic is bacteriostatic, inhibiting protein biosynthesis thus preventing growth due to peptide chain elongation inhibition. It reversibly binds to the peptidyltransferase centre at the 50S ribosomal subunit. It is also believed that it may interact with mitochondrial ribosomes. Resistance to it is usually due to enzymatic inactivation by acetylation of the drug mainly through different types of chloramphenicol acetyltransferases (CATs) (Schwarz et al., 2004).

1.7 Resistance to antimicrobial agents

The discovery of antibiotics in the early 19th century has led to a reduction in the use of metal and metal ions (Clardy et al., 2009; Zaffiri et al., 2012), and an increase in the use of antibiotics (Hyldgaard et al., 2012; Keren et al., 2013; Page, 2012) for the prevention and treatment of diseases. The overuse of antibiotics has caused a crisis of resistance to antibiotics, leading to increase in health-care costs and mortality (Jones et al., 2004; Zaffiri et al., 2012).

Resistance can be in three forms: Intrinsic, acquired and adaptive. Intrinsic resistance is the baseline tolerance of an organism toward any given drug. It is innate and occurs when a drug does not have affinity for an organism (Blair et al., 2015). Acquired resistance arises from mutation or gene acquisition (Witte, 2004). It is inheritable, stable, and the phenotype is independent of the

environment. Adaptive resistance is a form of intrinsic resistance. It develops due to changes in gene expression triggered by environmental factors such as pH, oxygen levels and presence of ions or even presence of antimicrobials (Fernández et al., 2011). That leads to induction of efflux pumps or reduction in porins (Fernández and Hancock, 2013; Mangalappalli-Illathu and Korber, 2006). The interesting story about adaptive resistance is the fact that it is dependent on the environment, it can last for several generations and is lost upon removal of the inducing signal (Fernández et al., 2011). Bacteria can also form biofilms in order to tolerate higher concentration of drugs without a change in genotype (Sandoval-Motta and Aldana, 2016).

In this study I assessed interactions between NsARC and bacteria, testing survival and non-lethal effects of exposure like biofilm formation and impact on antibiotic resistance.

1.8 Aims and Objectives

1.8.1 Aim

Specific aim of the study is to measure the antimicrobial activity of NsARC and to describe potential effects it has on target microbes.

1.8.2 Objectives

My four objectives were to:

1. Assess the antimicrobial activity of NsARC

The research questions I answered were:

i. Does exposing microorganisms to NsARC ± light reduce their survival compared to when they were exposed to other inert surfaces?

ii. Since NsARC is photoactive, what light regime was most effective in reducing microbial survival?

My hypothesis was that there was less microbial survival on NsARC compared to when the same species of microbes were exposed to inert control materials.

2. Determine if NsARC prevented biofilm formation

The research questions I tried to answer were:

i. Were microorganisms able to form biofilm on NsARC?

ii. If biofilms are able to formed on NsARC, was there a reduction in the amount of biofilm that formed on NsARC compared to on an inert material?

My hypothesis was that the amount of biofilm that can form on NsARC was less compared to on an inert material

3. Determine if exposing bacteria to NsARC caused the bacteria to develop adaptive resistance to antibiotics

The research question I tried to answer was:

i. Does exposing bacteria to NsARC induce an increase in the expression of genes associated with adaptive resistance to antibiotics?

My hypothesis was that there was an increase in expression of genes associated with adaptive resistance on exposure of bacteria to NsARC, compared to when the same bacteria were exposed to an inert material.

4. Determine if resistance to NsARC provides cross resistance to antibiotics

The research question I tried to answer was:

i. Were bacteria that were resistant to NsARC also cross resistant to antibiotics?

My hypothesis is that bacteria resistant to NsARC will also be cross resistant to antibiotic.

5. Determine if NsARC was active against bacteria isolated from the environment.

The research question I tried to answer was:

i. Were bacteria isolated from the environment susceptible to NsARC?

My hypothesis is that bacteria isolated from the environment was also susceptible to NsARC.

2 Chapter Two

2.1 Introduction

The increase in cases of communicable diseases is a serious public health problem that requires urgent attention (Dancer, 2008; Griffith et al., 2000). The ability of pathogens to survive on solid surfaces for very long periods is a major reason for this increase (Airey and Verran, 2007; Kramer and Assadian, 2014; Li et al., 2006). Microorganisms can survive on frequently touch surfaces such as light switches, doorknobs, elevator buttons and other furniture in health care facilities for hours, days and even months increasing the chances for the spread of hospital acquired infections (Chowdhury et al., 2018; Griffith et al., 2000; Inweregbu et al., 2005). Hospital acquired infections (HAI) also referred to as nosocomial infections may affect patients during their stay on admission in hospitals and can also manifest after they are discharged (Page, 2012; Tzeng et al., 2014; Wagenvoort et al., 2005). The World Health Organization (WHO) estimates that hundreds of millions of patients globally are affected by HAI, with the burden several folds higher in low- and middle-income developing countries than in higher income developed countries (Leyland et al., 2016). Standard protocols for the prevention and control of HAI includes: Hand hygiene, constant cleaning of frequently touch surface and the use of self-cleaning antimicrobial surfaces (Khan et al., 2017). Self-cleaning surfaces has led to a 70% decrease in HAI (Dancer, 2008; Griffith et al., 2000; Li et al., 2006).

2.2 Structure of nanostructured anatase, rutile and carbon (NsARC)

NsARC is a composite of titania and carbon. It has a unique crystalline microstructure and adheres tightly onto stainless steel and fused silica substrates (Krumdieck et al., 2019). NsARC is black in colour, robust, super-hydrophilic and photoactive under UV and visible light. These qualities make it promising as an antimicrobial surface coating.

Raman spectroscopy carried out to identify the crystallographic orientation of NsARC revealed the presence of amorphous carbon. The amorphous carbon was in the form of aromatic rings and carboxylate groups within the spaces between the anatase and rutile plates on the surface of NsARC (figure 2.3) (Krumdiek et al., 2019). Carbon, though inert as an element, can be chemically active when combined with other compounds or elements (Cheng et al., 2009; Dizaj et al., 2015). In order to remove the carbon, NsARC samples were heat-treated. Heat-treatment (annealing) of NsARC samples at 500 °C in the air for 2 hours resulted in a change in colour from black to white indicating oxidation with the removal the carbon (see Figure 2.4) (Krumdieck et al., 2019). There was not change in the structure of the TiO_2 surface after the heat treatment (Krumdieck et al., 2019; Krumdieck et al., 2017). As-deposited NsARC samples are black and completely opaque, while annealed NsARC samples are white and translucent.

2.2.1 Survival curve

Microorganisms can be transmitted from contaminated surfaces because they are able to survive on these surfaces for periods ranging from hours to months. The risk of transmission of these microorganisms depends on their persistence on the surface. The longer microorganisms survive on these surfaces, the more likely the contaminated surface is to be a source of transmission. In order to determine how long *E. coli* can survive on NsARC surface I exposed *E. coli* to NsARC and monitored its survival at 30 minutes intervals for a period of up to 8 hours and determine the survival curve.

2.2.2 Antimicrobial activity of NsARC against different species of microorganisms

I also explored the potential of as-deposited NsARC to reduce viable populations of other species of microorganism using a set of microbial species that serve as representatives of various kinds of pathogens. The microorganisms were *Escherichia coli, Staphylococcus aureus, Pseudomonas*

aeruginosa and *Saccharomyces cerevisiae*. Microorganisms generally differ from each other based on their size, morphology, cellular content, metabolism and cell wall and as such they normally respond differently to the killing effects of antimicrobial agents (Yao et al., 2012; Keren et al., 2013). For example, *S. aureus* a gram positive bacteria has a thick peptidoglycan cell wall that is made up of phospholipids, surface protein and teichoic acid linked together by phosphodiester bonds making the cell wall thick and negatively charged (Arciola et al., 2012; Michels et al., 2009). While *E. coli* and *P. aeruginosa* are both gram negative bacteria that possess an additional outer membrane layer beyond the peptidoglycan wall. Their cell wall is less permeable, but more negatively charged compared to gram positive bacteria (Rohde, 2019). This increases their ability to resist conventional antimicrobial agents (Hartmann et al., 2010). *S. cerevisiae* (yeast) has a plasma membrane consisting of primarily lipids and proteins in-between the cell wall and cytoplasm. The plasma membrane regulates movement of different compounds in and out of the cell, thus playing a very key role in defence against antimicrobials (Hapala et al., 2013).

I was able to determine the role light regimes play in the effectiveness of NsARC. I had reported reduction in viable *E. coli* under high intensity light (450-650 nm wavelength) and no light in a previous study (Krumdieck et al., 2019), but in practice light of such intensity may not be available in all public places. I then decided to test the survival of four different species of microorganisms on NsARC under ambient light (>650 nm wavelength), UV light (>300 nm wavelength) and no light.

2.2.3 Antibiofilm activity of NsARC

I was also interested in finding out if NsARC could prevent biofilms from forming on it.

Biofilm is a community of microorganisms that can develop on any kind of material surface.

Biofilms formation helps bacteria such as *E. coli* and *S. aureus* to be able to survive and adapt to life in different types environments (Fleming and Randle, 2006; Flemming and Wingender, 2010; Jefferson, 2004; Koseki et al., 2014). Biofilms are very difficult to eradicate when compare with planktonic cells (Kubacka et al., 2014). Biofilms production also help microorganisms to protect themselves from environmental stress and abiotic factors such as cell damaging free radicals (Arciola et al., 2012). Over 65% of chronic microbial infections are associated with biofilm formation. Surgical implants, catheter and other materials used in hospitals are often times colonized by biofilms (Arciola et al., 2012; Koseki et al., 2014). And these biofilms are resilient and difficult to eradicate with conventional disinfectants (Flemming and Wingender, 2010). Currently, there is no known drug that is specifically effective in preventing biofilm formation (Arciola et al., 2012; Flemming and Wingender, 2010), So the best option is through the use of surface coatings with antimicrobial properties and implants with anti-adhesive properties (Ganewatta et al., 2015; Lee et al., 2013; Yang et al., 2016).

In addition to antimicrobial activity testing of NsARC that I discussed earlier, it was important to determine if accumulation of bacteria on the surface of NsARC leads to the formation of biofilms. These biofilms form through a series of steps (See Figure 2.1). Attachment to surfaces is the first step in biofilm formation, followed by release of extracellular polymeric substance (EPS) that shrouds these cells providing physical and mechanical support (Fleming and Randle, 2006). EPS also helps in adhesion to surfaces and protects the organisms from UV radiation, desiccation and toxic effect of antibiotics and other biocides (Flemming and Wingender, 2010; Jefferson, 2004). Formation of biofilm would enable microorganisms to survive and proliferate, with the possibility of developing resistance to antibiotics. I compared the effectiveness of NsARC towards preventing or reducing biofilm formation with stainless steel.

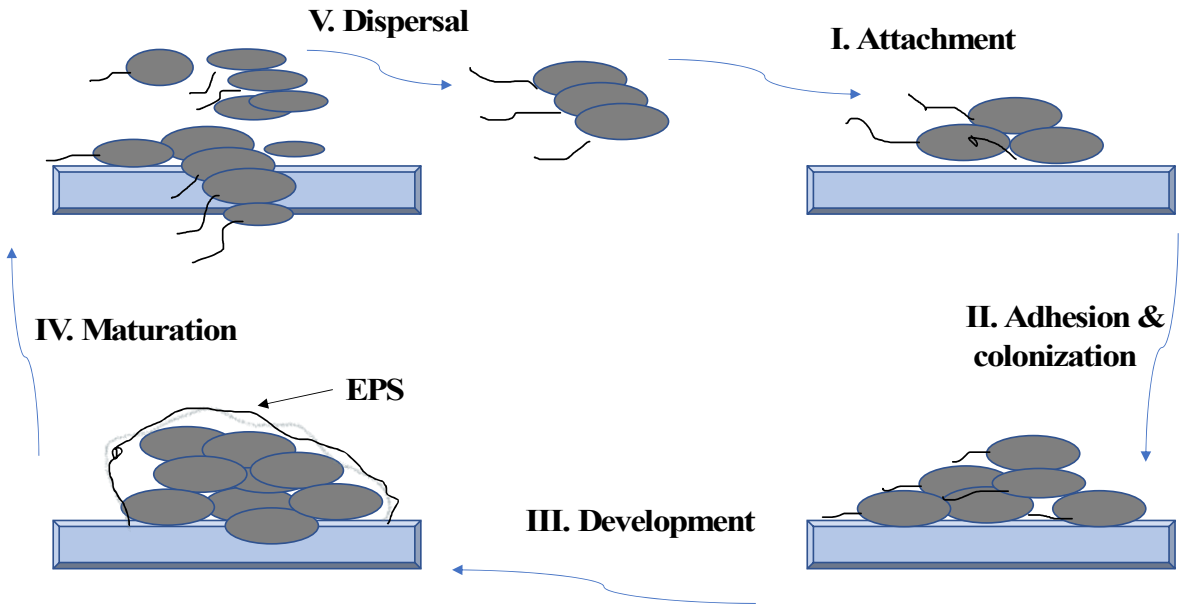

Figure 2.1: Stages of biofilm formation.

(I) The first stage begins with the attachment of cells onto a surface (II) The interaction between the cell membrane of microorganisms and the surface triggers the microorganisms to synthesize and release extracellular polymeric substances that further strengthens adhesion and colonization of the surface (III) The colony grows and further develops with the attachment of other species of microorganisms (IV) The biofilm matures and is capable of releasing part of its colonies into the environment (V) planktons are then dispersed into the environment, to further colonize other surfaces.

2.2.4 Role of carbon in the antimicrobial activity of NsARC

To investigate if carbon play a role in antimicrobial activity in NsARC, I tested the survival of *E. coli* for a period of 4 hours on NsARC samples that have been heat-treated (annealed) at 500 ^{0}C in air to remove the carbon (Krumdieck et al., 2019).

2.3 Methodology

2.3.1 Selection of test materials

NsARC deposited on 25 × 25 mm stainless steel or fused silica coupons were used as test material, 25 × 25 mm stainless steel or fused silica coupons were used as negative (inert) controls materials (see Figure 2.2) as recommended by the ISO 27447:2009 (Mills et al., 2012), and 24 × 24 mm commercially pure copper coupon which is well-known for its antimicrobial activity (Grass et al., 2011), was selected as positive control material.

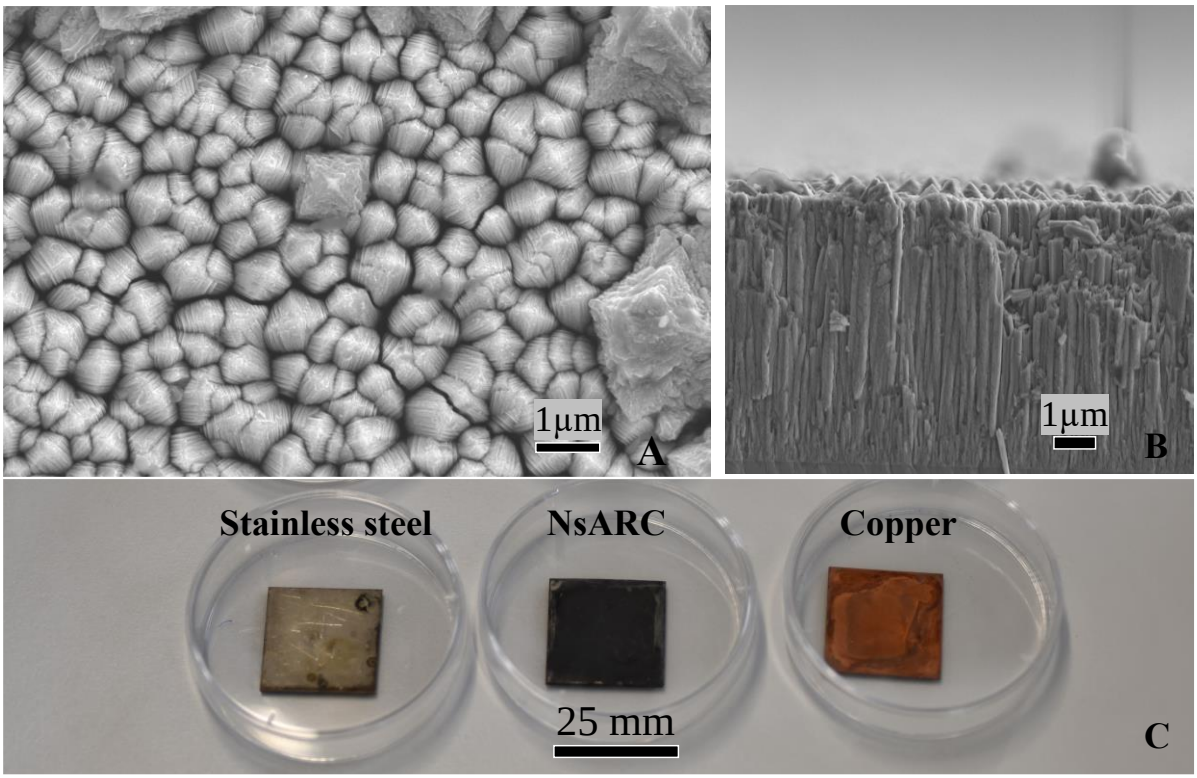

Figure 2.2: Images of the test samples

(a) SEM image of the top view of the coating surface morphology (b) SEM fracture cross-section of the surface NsARC. (c) Photographs (left to right) of negative control (stainless steel), sample (NsARC), positive control (copper).

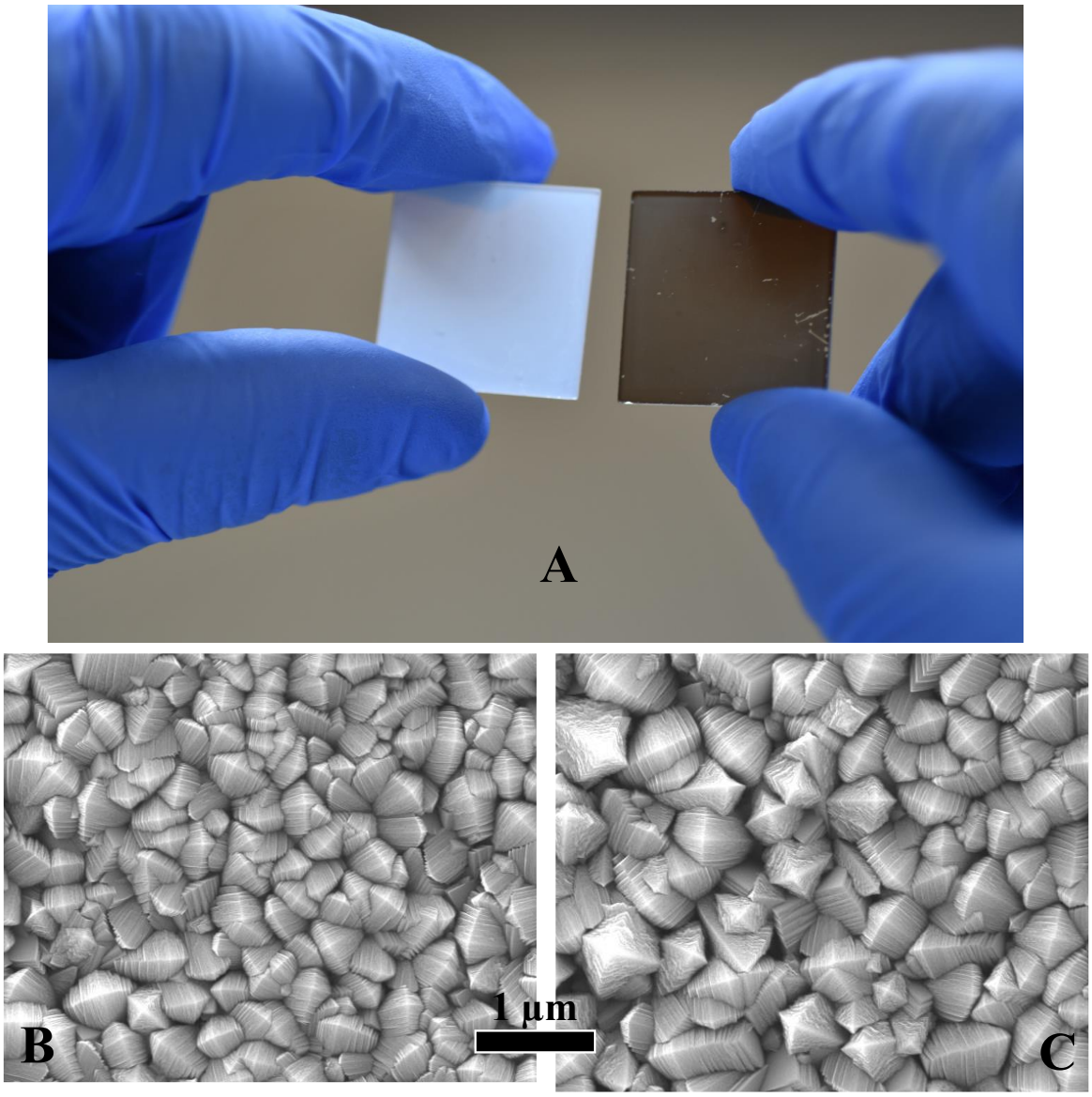

Figure 2.3: Typical image of black as-deposited and white (after annealing) NsARC coating on fused silica and SEM of the top view of the surface morphology of (B) As-deposited (C) Annealed NsARC coating.

NsARC and control (stainless steel and copper) samples were sterilised using 70% ethanol and the NsARC test pieces were aseptically stored in the dark for >48 hours to discharge before the experiment.

2.3.2 Bacterial strains, media and cultivation

Escherichia coli ATCC8739, *Pseudomonas aeruginosa* ATCC10145 and *Staphylococcus aureus* 25923 used in this study are shown in Table 2.1. These bacterial strains were stored in 15%

glycerol solution at -80°C. To recover these strains, Lauria Bertani (LB) agar plates (Lennox-L-Broth Base, Invitrogen (USA) and agar (Bacteriological Agar No.1, Oxoid (UK)) were inoculated with loopfuls of the samples and the plates incubated at 37°C for 18-24 hours. These plates are stored at 4°C for not longer than one week. To recover the bacteria, LB broth (Lennox-L-Broth Base, Invitrogen (USA)) was inoculated with a colony that was picked from the plates and aerated using a rotary shaker at 37°C and grown to saturation. Phosphate buffer saline (PBS) was used to wash and re-suspend the organisms.

2.3.3 Fungal strain, media and cultivation

Saccharomyces cerevisiae SY1229 used in this study is shown in Table 2.1. This strain is stored in 30% glycerol solution at -80°C. To recover the strain, a loopful of the sample was transferred onto Yeast Peptone Dextrose (YPD) agar plates (Sigma-Aldrich (USA) and agar (Bacteriological Agar No.1, Oxoid (UK)) and the plates incubated at 30°C for up to 48 hours. These plates are stored at 4°C for not longer than one week. A colony from the plate was picked and inoculated into YPD broth (Sigma-Aldrich (USA)) and then aerated using a rotary shaker platform at 30°C and grown to saturation. Phosphate buffer saline (PBS) used to wash and re-suspend the cells.

Table 2.1: List of Organisms used for the study.

Organism	**Reference**
Escherichia coli ATCC 8739	(Mills et al., 2012)
Staphylococcus aureus ATCC 25923	(Mun et al., 2013)
Pseudomonas aeruginosa ATCC 10145	(Kwiatek et al., 2017)
Saccharomyces cerevisiae SY1229	(Heinemann and Sprague, 1989)

A modified version of the ISO 27447:2009, “test method for antimicrobial activity of semi conducting photocatalytic materials” (Mills et al., 2012; Sadowski et al., 2015) was the standard

method that was used for the antimicrobial and antibiofilm activity testing. All experiments were conducted three times to obtain biological replicates. Three samples of each (test and control) were used for each experiment to obtain technical replicates (*Quick-R: Power Analysis*, n.d.). The entire set up is shown in Figure 2.4 and 2.5.

2.3.4 Survival of *E. coli* on As-deposited NsARC samples

50 µl of the culture containing ~500,000 *E. coli* cells were placed on the test and control surfaces (25 mm × 25 mm) under a sterile cover slip (24 mm × 24 mm) used to spread the culture on the surface. The samples were placed in petri dishes (60 mm × 15 mm) containing damp filter paper. Replicates were simultaneously exposed to high intensity visible light of 2100 lux (450-650 nm) for period of ½, 1, 2, 4, 6 and 8 hrs. The cells were recovered in 1.95 ml tryptic soy broth with 0.05% Tween (TSB-Tween) (Sigma-Aldrich (USA)). Dilutions were made in PBS. 10 µl of samples of different dilutions of were transferred onto the surface of tryptic soy agar (TSA) (Sigma-Aldrich (USA)). The inoculated plates were incubated at 37℃ for 18 hours (see Figure 2.5). The colonies from the plates were counted and normalised to volume of solution to give colony forming units per ml (cfu/ml). This was compared for the various treatments (material and exposure conditions). There were variations in the values, thus, the cfu/ml counts were normalised to efficiency of plating (EOP) values, which is the ratio of live cells on the test samples to the initial cell counts on the negative control. The EOP values were then used to plot graphs using graphpad prism software (*Prism - Graphpad.Com*, n.d.). R was used for statistical analysis (Rosario-Martinez et al., 2015).

Equation 2.1: Formula used to calculate efficiency of plating (EOP)

$$\text{EOP} = \frac{titre\ of\ treatments\ (t{=}8hrs)}{titre\ of\ control\ (t{=}0hrs)}$$

2.3.5 Antimicrobial activity testing against different species of microorganisms

2.3.5.1 Antibacterial testing

50 µl of the culture containing ~500,000 cells were placed on the test and control surfaces (25 mm × 25 mm) under a sterile cover slip (24 mm × 24 mm) used to spread the culture on the surface. The samples were placed in petri dishes (60 mm × 15 mm) containing damp filter paper. Replicates were simultaneously exposed to high intensity visible light of 2100 lux (450-650 nm), UV light (365 nm), ambient light (650-750 nm) and also kept in the dark for a period of up to 8 hrs. The cells were recovered in 1.95 ml tryptic soy broth with 0.05% Tween (TSB-Tween) (Sigma-Aldrich (USA)). Dilutions were made in PBS. 10 µl of samples of different dilutions of *E. coli, S. aureus* and *P. aeruginosa* were transferred onto the surface of tryptic soy agar (TSA) (Sigma-Aldrich (USA)). The inoculated plates were incubated at 37℃ for 18 hours. The colonies from the plates were counted and the values converted to EOP as described in section 2.3.4.

2.3.5.2 Antifungal testing

50 µl of the culture containing ~500,000 cells were placed on the test and control surfaces (25 mm × 25 mm) under a sterile cover slip (24 mm × 24 mm) used to spread the culture on the surface. The samples were placed in petri dishes (60 mm × 15 mm) containing damp filter paper. Replicates were simultaneously exposed to high intensity visible light of 2100 lux (450-650 nm), UV light (365 nm), ambient light (650-750 nm) and also kept in the dark for a period of up to 8 hrs. The cells were recovered in 1.95 ml tryptic soy broth with 0.05% Tween (TSB-Tween) (Sigma-Aldrich (USA)). Dilutions were made in PBS. 10 µl of the dilutions was then transferred onto the surface of YPD agar (Sigma-Aldrich (USA)). The inoculated plates were then incubated at 30℃ for 48 hrs. The colonies from the plates were counted and the values converted to EOP as described in section 2.3.4.

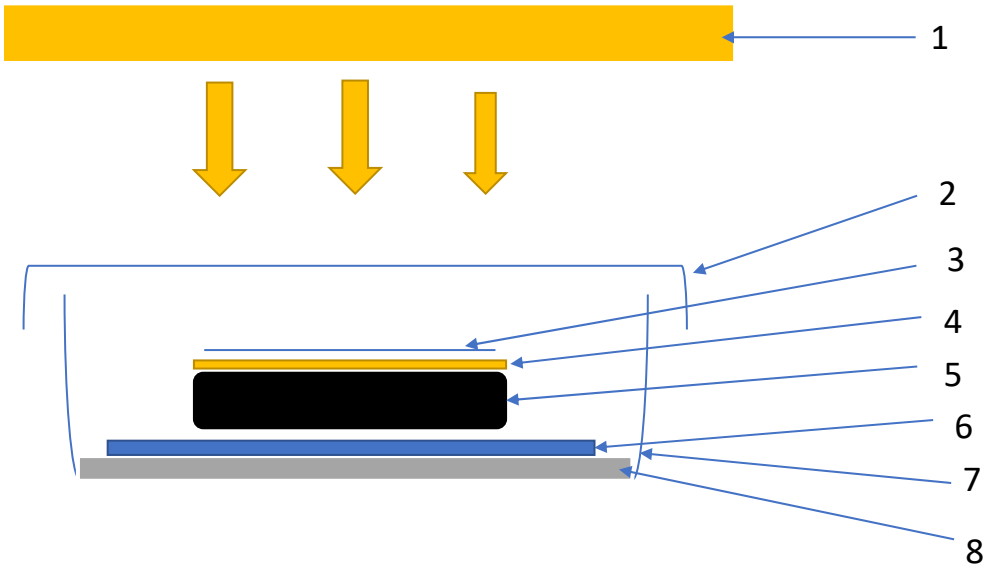

Figure 2.4: Experimental set up for testing antimicrobial activity of surfaces under different exposure conditions.

1: light source (high intensity visible light of 2100 lux (450-650 nm), UV light (365 nm wavelength) and ambient light of 650-750 nm) 2: Petri dish cover to prevent evaporation and contamination 3: 24 × 24 mm microscope coverslip. 4: liquid culture containing bacteria or fungi 5: test material (25 × 25 mm) NsARC, stainless steel or glass, copper coupon 6: steel or glass rod to serve as barrier between material and filter paper 7: filter paper dampened with sterile distilled water to preserve moisture.8: petri dish to limit contamination and preserve moisture.

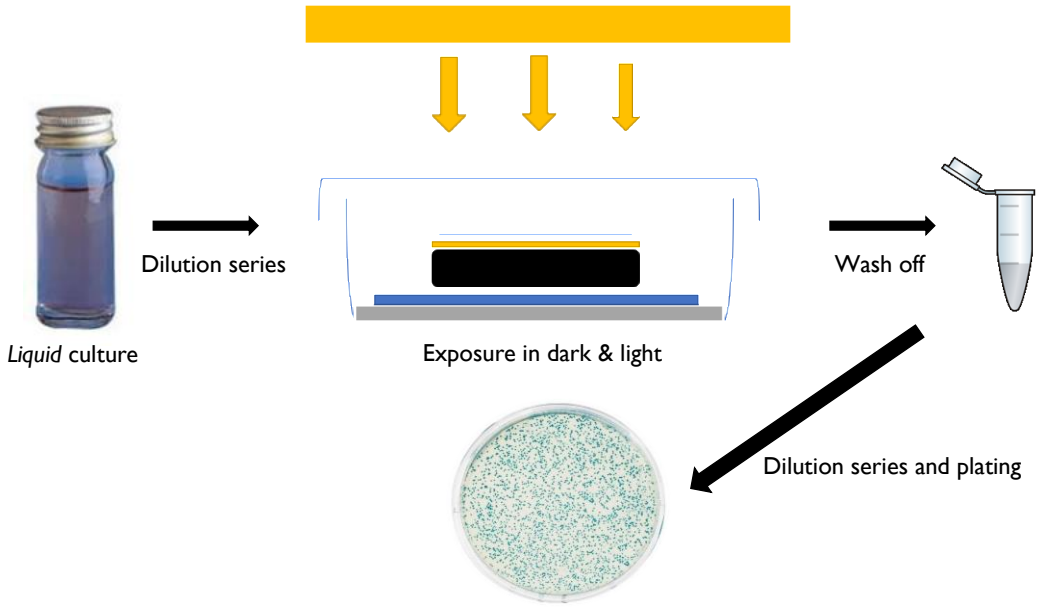

Figure 2.5: Experimental set up showing the various steps.

Step 1: Microorganisms grown to saturation in a liquid culture. Culture is then diluted two-fold. Step2: Diluted culture is then placed on the surface of the test samples and exposed to light or kept in the dark for 8 hours. After the 8 hours the cells are washed off. Step3: The washed off cells are then diluted three-fold. Step 4: cells are then recovered on a solid culture media.

2.3.6 Antimicrobial testing of as-deposited and annealed NsARC

50 µl of the culture containing ~500,000 *E. coli* cells were placed on as-deposited and annealed NsARC samples and control fused silica surfaces (25 mm × 25 mm) under a sterile cover slip (24 mm × 24 mm) used to spread the culture on the surface (see Figure 2.4). The samples were placed in petri dishes (60 mm × 15 mm) containing damp filter paper. Replicates were also simultaneously exposed to high intensity visible light of 2100 lux (450-650 nm), UV light (365 nm), ambient light (650-750 nm) and also kept in the dark for 4 hrs. The bacterial cells were recovered on tryptic soy agar (TSA) (Sigma-Aldrich (USA)). The colonies from the plates were counted and the values converted to EOP as described in section 2.3.4.

2.3.7 Biofilm adhesion and Antibiofilm formation test

Attachment of microorganisms onto the surface NsARC was used as a model to determine biofilm formation (Naik and Kowshik, 2014). Quantification of the biofilm that adhere to the surface of NsARC was carried out adopting a revised method described by Pantanella et al (2011) (Pantanella et al., 2011).

The test organisms (100 µl of each corresponding to ~1000, 000 cells) were transferred to the NsARC or stainless-steel samples (25 mm × 25 mm) and a sterile cover slip (24 mm × 24 mm) was placed on it to spread the culture on the surface of the samples. The samples were placed in petri dishes (60 mm × 15 mm) containing damp filter paper. Replicates were simultaneously exposed to high intensity visible light of 2100 lux (450-650 nm), UV light (365 nm), ambient light (650-750 nm) and also kept in the dark for a period of 12, 24 and 48 hrs respectively. After which the surface of the samples was washed with PBS to remove loosely bound cells, and the samples were placed into a sonication water bath (ultrasonic bath, Sigma-Aldrich, USA) and sonicated for up to 5 minutes to elute the attached biofilm. Then 100 µl of the recovered cells was serially diluted in PBS, and 10µl of the bacteria transferred onto the surface of TSA agar (Sigma-Aldrich (USA)), the yeast was transferred onto the surface of YPD agar (Sigma-Aldrich (USA)).

The inoculated plates were then incubated at 37℃ for 18 hrs for the bacteria, and at 30℃ for 48 hrs for the yeast. All experiments were conducted three times to obtain biological replicates. Three samples of each (test and control) were used for each experiment to obtain technical replicates (*Quick-R: Power Analysis*, n.d.). The experimental setup is shown in Figure 2.6.

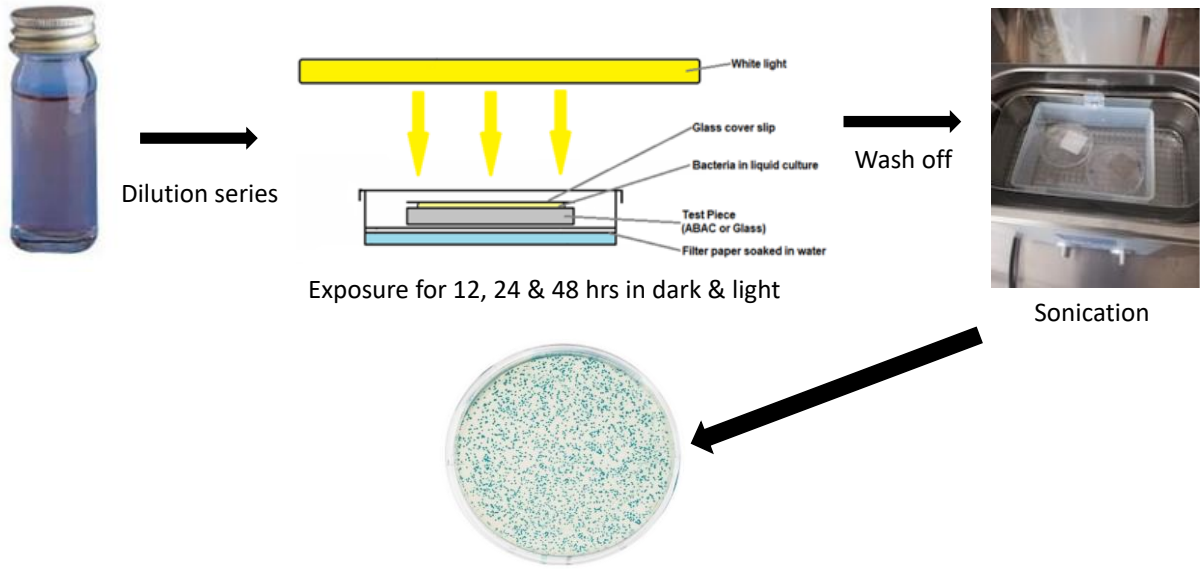

Figure 2.6 Experimental set up showing how biofilms were developed and recovered.

Step 1: Microorganisms grown to saturation in a liquid culture. Culture is then diluted two fold. Step2: Diluted culture is then placed on the surface of the test samples and exposed to light or kept in the dark for either 12, 24 or up to 48 hours. After the exposure period, loosely bound cells are washed off. Step3: Sonication is then used to detach the cells in the biofilms. Step 4: cells are then recovered on a solid culture media.

2.3.8 Scanning Electron Microscopy (SEM)

Visualization of the morphology of cells that were on NsARC and stainless steel under high intensity visible light was performed by SEM. This works on the principle of scattering of electrons on the surface of samples when electrons are released from the source onto the sample. The behaviour of these electrons are then used to create images. (Golding et al., 2016; Hartmann et al., 2010; Sondi & Salopek-Sondi, 2004; Walker, 2003).

2.3.8.1 Procedure

For the antimicrobial activity test, microbial cultures were grown as described earlier and placed on the test samples as describes earlier in this section, after the 8 hours exposure period, the cells on the surface of the samples were washed and re-suspended in 100µl PBS. 100 µl of 4% Paraformaldehyde fixing solution was then added and the set up stored at 4°C for 2 hours. The cells were then washed twice with 100 µl PBS before re-suspending in 100 µl of PBS. The fixed

cells were then dehydrated using various concentration series of ethanol (30%, 50%, 70%, 90% and 100%) and hexamethyldisilane (HMDS). The cells were then air-dried at room temperature. The dried cells are then coated with gold using a sputter coater (sputter current: 120 mA, sputter pressure: 1×10^{-2} psi, Argon pressure: 12600 psi and distance: 800 nm). The samples with the treated cells were mounted onto an SEM sample stub with a double-sided sticky tape for imaging in a JEOL JSM-7000F field emission scanning electron microscope. 20 images from each sample replicate was capture and saved (Walker, 2003).

For the antibiofilm activity test, SEM was also performed to visualize the cells that were still attached to the surface of NsARC and stainless steel samples after 48 hours under high intensity visible light. The *in situ* biofilm samples were prepared in the same manner as described above.

2.3.9 Statistical analysis

R was used for this statistical analysis (Rosario-Martinez et al., 2015). For all the experiments, residual plots were examined to determine if the data were normally distributed, which is an assumption for ANOVA (Crawley, 2007). The plots were not normally distributed. So the values were log transformed to meet the assumption.

2.3.9.1 Antimicrobial (AMA) testing

For the experiment that I determined the survival *E. coli* on NsARC over a period of time, I performed an Analysis of variance (ANOVA) on log transformed EOP values to test for significant effects of the material (NsARC and stainless steel) over the ½, 1, 2, 4, 6 and 8 hours periods. In each case, I tested for significant difference between materials. The null hypothesis was that there was no difference between the EOP values from the materials over the period of time. A Bonferroni's post hoc test was used to compare the EOP to determine if there is a significant

difference between NsARC and the controls. The value for statistical significance was set at $P<0.05$. The ANOVA table and results of each post hoc are available in Appendix A,

In the experiment to determine AMA of NsARC on different microorganisms, I used a statistical model that was based on analyses of variance (ANOVAs) of EOP scores. A multifactor analysis of variance (ANOVA) was performed on the log transformed EOP values to test for significant effect of the materials (NsARC and control) and exposure conditions (high intensity visible light, UV light, ambient light and dark). In each case, I tested for significant difference between materials. The null hypothesis was that there was no difference between the EOP values from the materials under the various exposure conditions. I also tested for interaction between materials and exposure conditions. A Bonferroni's post hoc test was used to compare the EOP to determine if there is a significant difference between NsARC and the controls. The value for statistical significance was set at $P<0.05$. The ANOVA table and results of each post hoc are available in Appendix A, however, I was most interested in the differences in EOP between individual treatment combinations as follows: NsARC under ambient light vs steel under ambient light, NsARC under ambient light vs NsARC in the dark, NsARC in the dark vs steel in the dark, NsARC under high intensity visible light vs steel under high intensity visible light, NsARC under high intensity visible light vs NsARC under UV light and NsARC under UV light vs steel under UV light. Contrast matrices listing the contrast of interest mentioned were drawn up and the test Interactions function in the phia package in R was used to evaluate the contrasts as described in the result section (Rosario-Martinez et al., 2015).

For the experiment that I compared AMA of as-deposited and annealed sample, I performed a multifactor analysis of variance (ANOVA) on the log transformed EOP values to test for relationship between samples (as-deposited and annealed) and the different illumination conditions

(high intensity visible light, UV light, ambient light and dark). The null hypothesis was that there was no difference between the EOP values from the samples at different illumination conditions. A Bonferroni's post hoc test was used to compare the EOP and determine if there was difference between samples. P value for significance was set as $P<0.05$. The ANOVA table and results of each post hoc are available in Appendix A.

2.3.9.2 Biofilm adhesion and Antibiofilm formation test

In the experiment to determine antibiofilm activity (ABA) of NsARC, I also used a statistical model that was based on analyses of variance (ANOVAs) of cfu/ml scores. A multifactor analysis of variance (ANOVA) was performed to test for significant effect of the materials (NsARC and control) and exposure conditions (high intensity visible light, UV light, ambient light and dark) after the 12, 24 or 48 hours. In each case, I tested for significant difference between materials. The null hypothesis was that there was no difference between the cfu/ml values from the materials under the various exposure conditions. I also tested for interaction between materials and exposure conditions. Again, a Bonferroni's post hoc test was also used to compare the cfu/ml to determine if there is a significant difference between NsARC and the controls. The value for statistical significance was also set at $P<0.05$. The ANOVA table and results of each post hoc are available in Appendix B, however, I was most interested in the difference of cfu/ml between individual treatment combinations as follows: NsARC under ambient light vs steel under ambient light, NsARC under ambient light vs NsARC in the dark, NsARC in the dark vs steel in the dark, NsARC under high intensity visible light vs steel under high intensity visible light, NsARC under high intensity visible light vs NsARC under UV light and NsARC under UV light vs steel under UV light. Contrast matrices listing the contrast of interest mentioned were also drawn up and the test

Interactions function in the phia package in R was used to evaluate the contrasts as described in the result section (Rosario-Martinez et al., 2015).

2.4 Results

2.4.1 Survival curve of *E. coli* on NsARC and copper overtime

The was no significant reduction in viable *E. coli* (P>0.05) after ½ an hour, but a greater than 4 logs reduction in viability to below the detection limit of the experiment was observed for *E. coli* that were on copper (Figure 2.7). Significant reduction in viable *E. coli* on NsARC was observed after 1 hour. A greater than 1 log reduction was observed after 2 hours and subsequently a greater than 3 log reduction was observed after 4, 6 and 8 hours. There was no significant difference in the reduction observed after 4, 6 and 8 hours (Appendix A) (Figure 2.7).

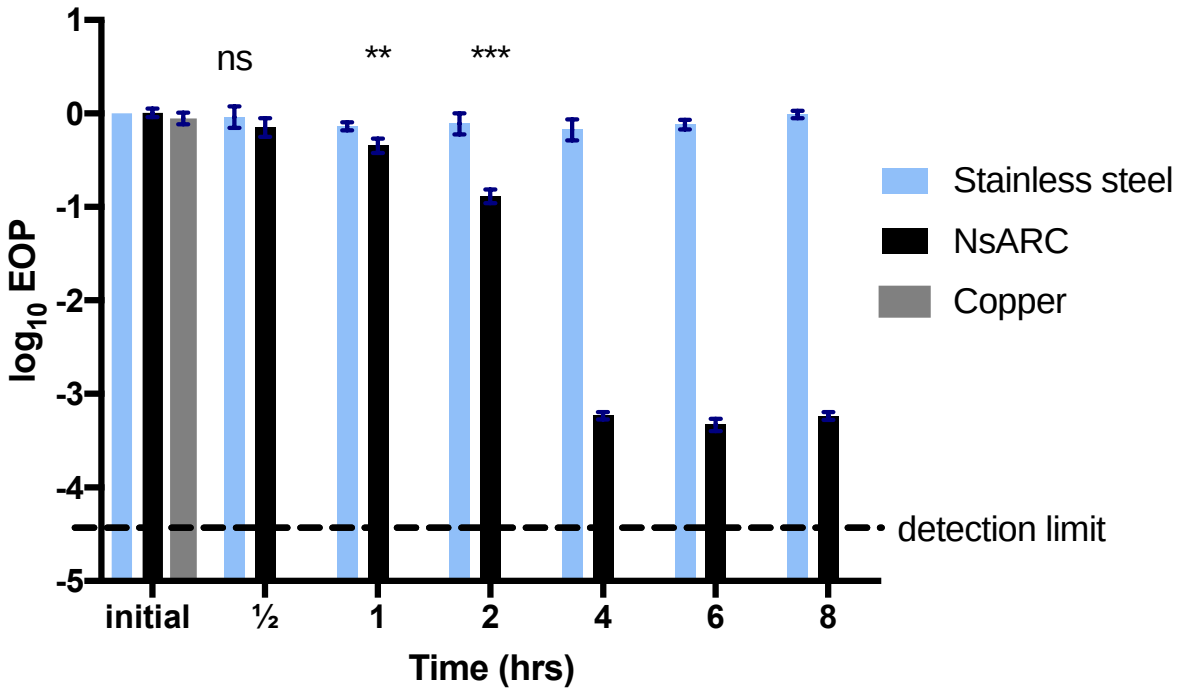

Figure 2.7: Survival curve of *E. coli* on NsARC under high intensity visible light. Error bars are standard error of means (SEM). Asterisks indicate P values. *: P<0.05; **: P<0.01; ***: P<0.001; ns: not significant

2.4.2 AMA testing of NsARC for different microorganisms

The viable population of all the organisms tested on NsARC under all the light exposure conditions were reduced by greater than 2 logs compared to those that were on stainless steel (Figure 2.8-

2.11). In contrast, a greater than 4 logs reduction in viability to below the detection limit of the experiment was observed for all the organisms that were on copper.

2.4.2.1 *E. coli*

There was a greater than 3 log reduction in EOP of viable *E. coli* that were on NsARC exposed to UV and high intensity visible light, while a 2 log reduction was observed using ambient light or no light (dark), when compared to viability on stainless steel (Figure 2.8A). There was no significant difference in the effectiveness of NsARC in killing under high intensity visible and UV light ($P=0.966$). But there was significantly greater killing under ambient light compared to no light ($P<0.001$) (Appendix A2). *E. coli* on NsARC under high intensity visible light looked distorted compared to the cells on stainless steel that looked intact (Figure 2.8B).

2.4.2.2 *S. aureus*

A greater than 4 logs reduction in viability was achieved using UV and visible light, and a greater than 2 log reduction was observed using ambient light or no light (Figure 2.9A). There was no significant difference in the effectiveness of NsARC in killing under high intensity visible and UV light ($P=0.867$). But there was significantly greater killing under ambient light compared to no light ($P<0.001$) (Appendix A4). *S. aureus* cells that were on NsARC under high intensity visible light were also distorted with pores in them, while the ones that were on stainless steel were looking intact (Figure 2.9B).

2.4.2.3 *P. aeruginosa*

P. aeruginosa viability on NsARC was reduced by more than 3 logs using either UV or visible light compared to on stainless steel. A 2 log reduction was observed using ambient light and no light (Figure 2.10A). Interestingly, there was significantly greater killing on NsARC under high intensity visible than under UV light ($P<0.0003$). There was significantly greater killing under

ambient light compared to no light (P<0.001) (Appendix A6). Similar to what was observed in *E. coli* cells that were on NsARC under high intensity visible light, *P. aeruginosa* cells also looked distorted compared to the fresh looking cells that were on stainless steel (Figure 2.10B).

2.4.2.4 *S. cerevisiae*

Viability of the fungus *S. cerevisiae* reduced by more than 3 logs using either UV or visible light compared to the same light exposures on stainless steel. About 2 log reduction in viability was also achieved using ambient light and no light exposure (Figure 2.11A). There was significantly greater killing on NsARC under UV light than under high intensity visible (P<0.0066). But as seen in all the other organisms tested, there was significantly greater killing under ambient light compared to no light (P<0.001) (Appendix A8). *S. cerevisiae* cells on NsARC were also deformed and were relatively smaller than the ones that were on stainless steel (Figure 2.11B).

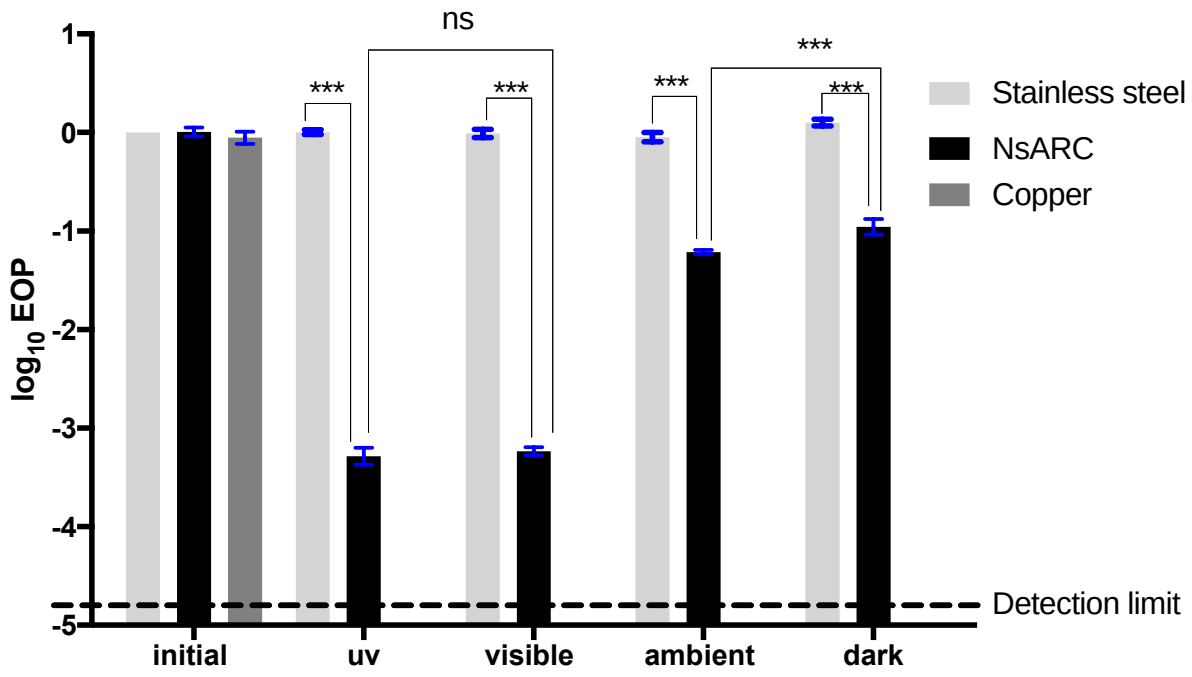

Figure 2.8A: Survival of *E. coli* on NsARC and stainless steel for 8 hours. Error bars are standard error of means (SEM). Asterisks indicate P values. *:P<0.05; **:P<0.01; ***:P<0.001; ns: not significant.

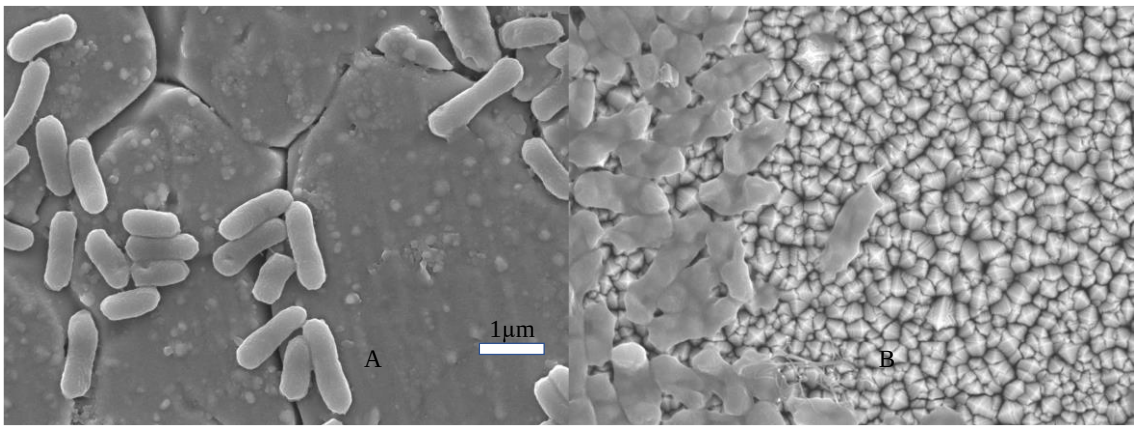

Figure 2.8B: SEM images of (A) intact *E. coli* cells that were on stainless steel and (B) *E. coli* cells looking distorted on NsARC after a period of 8 hours under high intensity visible light.

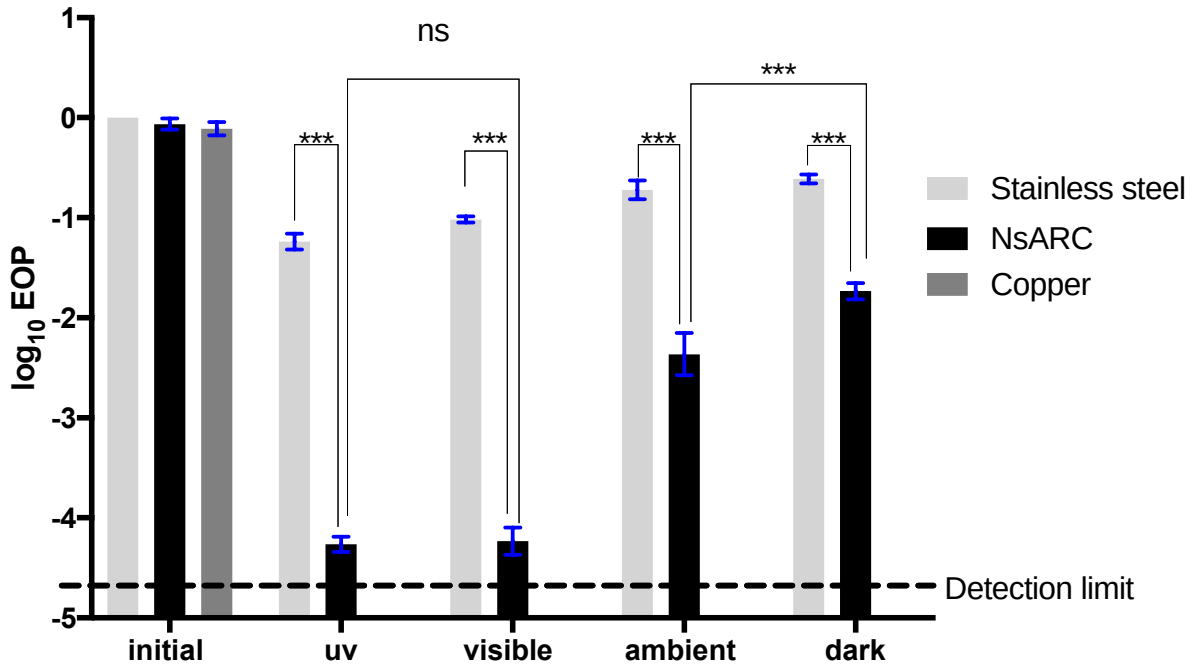

Figure 2.9A: Survival of *S. aureus* on NsARC and stainless steel for 8 hours. Error bars are standard error of means (SEM). Asterisks indicate P values. *:P<0.05; **:P<0.01; ***:P<0.001; ns: not significant.

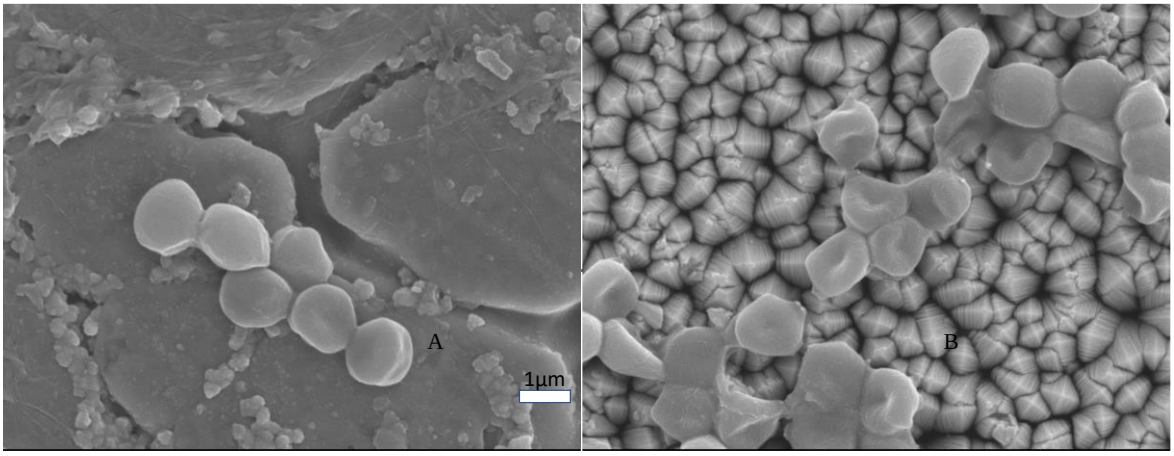

Figure 2.9B: SEM images of (A) intact *S. aureus* cells that were on stainless steel and (B) *S. aureus* cells looking distorted on NsARC after a period of 8 hours under high intensity visible light.

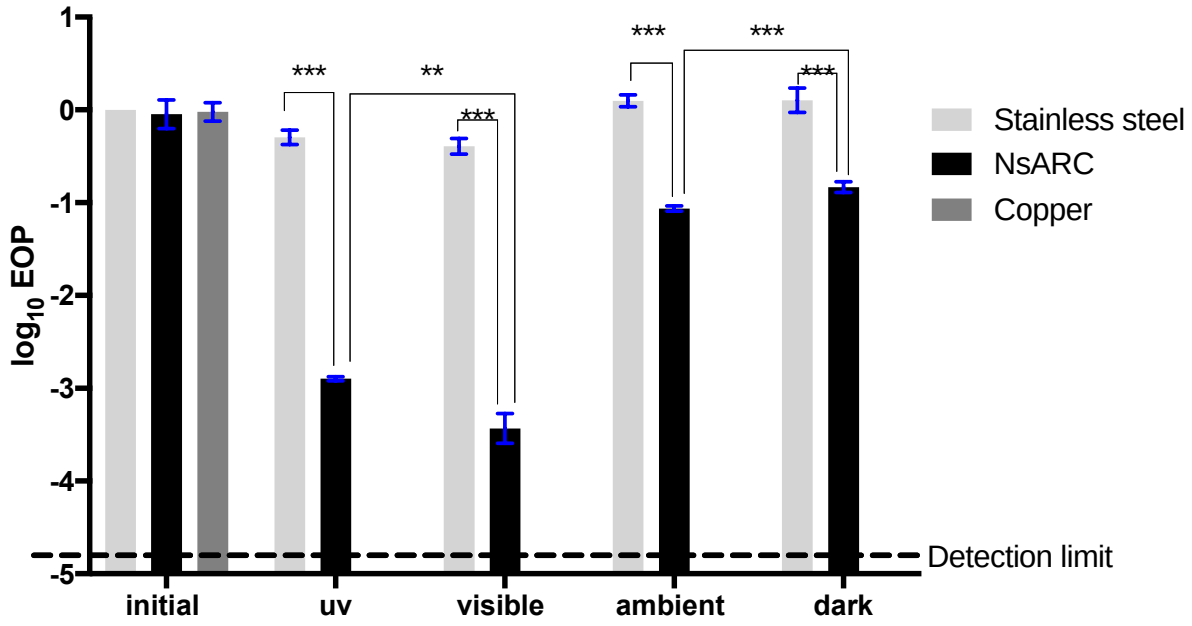

Figure 2.10A: Survival of *P. aeruginosa* on NsARC and stainless steel for 8 hours. Error bars are standard error of means (SEM). Asterisks indicate P values. *:P<0.05; **:P<0.01; ***:P<0.001; ns: not significant.

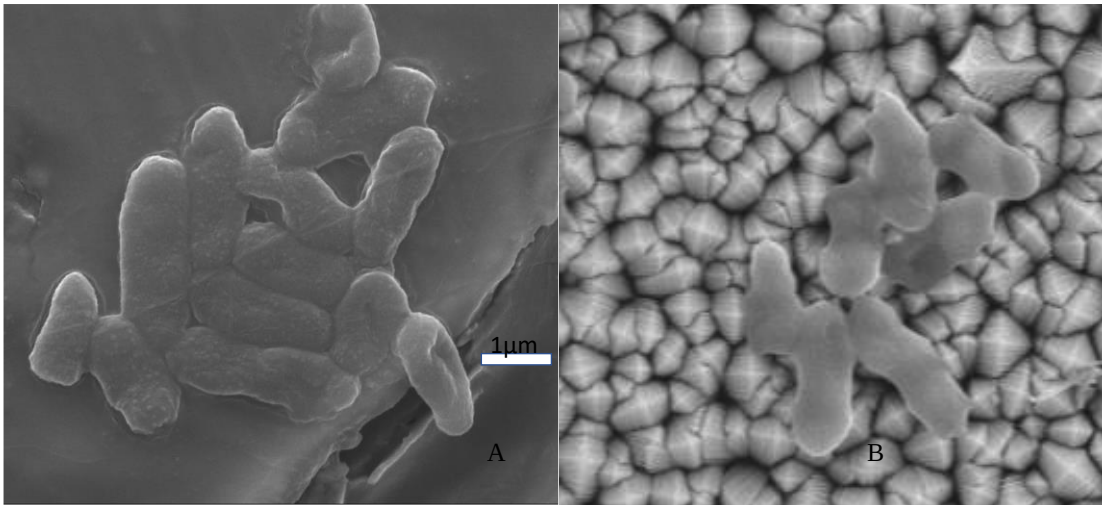

Figure 2.10B: SEM images of (A) intact *P. aeruginosa* cells that were on stainless steel and (B) *P. aeruginosa* cells looking distorted on NsARC after a period of 8 hours under high intensity visible light.

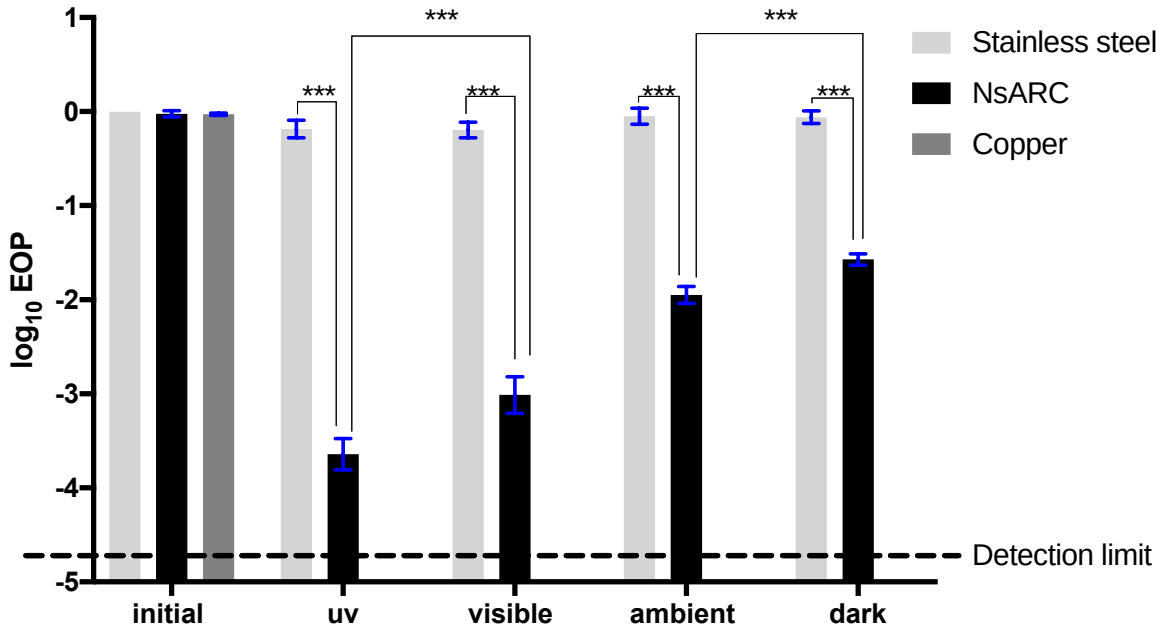

Figure 2.11A: Survival of *S. cerevisiae* on NsARC and stainless steel for 8 hours. Error bars are standard error of means (SEM). Asterisks indicate P values. *:P<0.05; **:P<0.01; ***:P<0.001; ns: not significant.

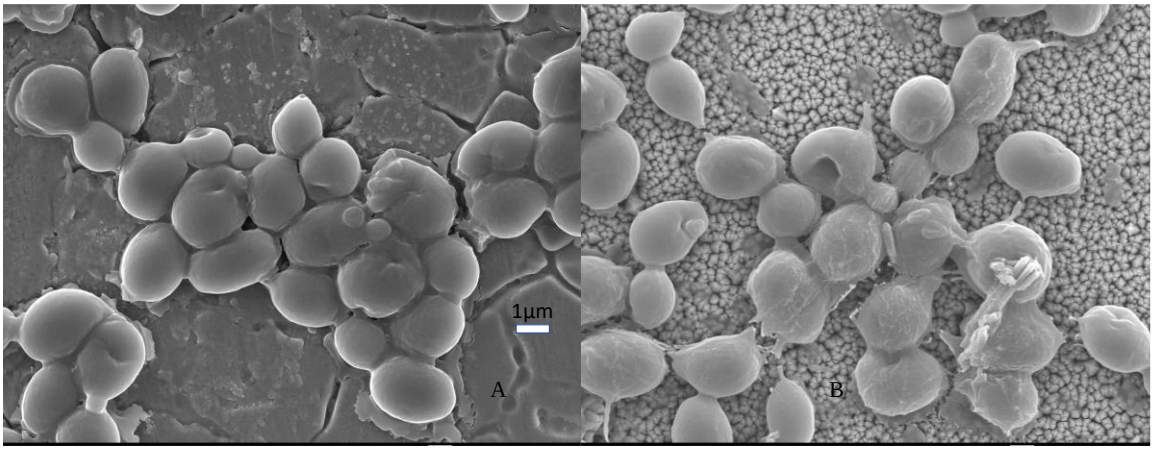

Figure 2.11B: SEM images of (A) intact *S. cerevisiae* (yeast) cells that were on stainless steel and (B) *S. cerevisiae* cells looking distorted on NsARC after a period of 8 hours under high intensity visible light.

2.4.3 Comparing the AMA of as-deposited and annealed NsARC samples

The antimicrobial activities of as-deposited and annealed NsARC coatings are shown in Figure 2.12. A greater than 3 log (99.9%) reduction was achieved on both as-deposited and annealed NsARC coatings using UV and visible light, and a 2 log reduction was achieved using ambient light, while a greater than 1 log reduction was observed without any form of photonic irradiation

(dark). There was no significant difference in the effectiveness of annealed and as-deposited NsARC coated samples under visible light (P=0.196). But there was significantly greater reduction in viable *E. coli* populations that were on annealed NsARC coated samples under UV (P=0.00342) and ambient light (P<0.001) compared with those that were on as-deposited NsARC coated samples. On the other hand, significantly greater reduction was observed on as-deposited NsARC than on annealed NsARC coated samples without photo irradiation (P<0.012). Annealed samples exhibited higher AMA than as-deposited samples under photo irradiation, while as-deposited samples exhibited higher AMA than annealed samples without photo irradiation.

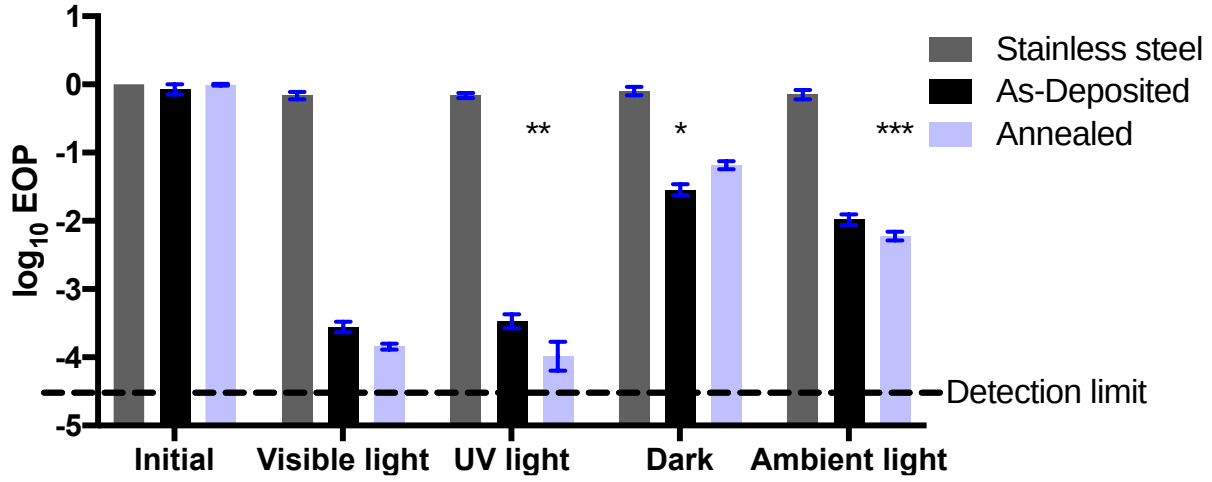

Figure 2.12: Comparison of the survival of *E. coli* on pristine and annealed NsARC and stainless steel samples for a period of 8 hours. Error bars are standard error of means (SEM). Asterisks indicate P values. *:P<0.05; **:P<0.01; ***:P<0.001; ns: not significant.

2.4.4 Antibiofilm activity testing

Biofilm formation on the test surfaces was analyzed in two ways: firstly, by determining the number of viable cells from the biofilm that were detached from the surfaces after sonication and secondly, by using SEM to observe the surface area covered by the biofilm. The number of the viable cells of all the organisms recovered from NsARC were significantly (P<0.01) less than those recovered from stainless steel. This number also differed significantly (P<0.01) by type of exposure condition (Figure 2.13-2.16).

2.4.4.1 *E. coli*

The amount of viable *E. coli* cells recovered from the surface of NsARC was significantly less than the ones recovered from the surface of stainless steel. (Figure 2.13). After 12 hours exposure, there was a significantly greater than 2 log reduction ($P<0.001$) in viable *E. coli* that were on NsARC under all the conditions when compared to viability on stainless steel (Figure 2.13A). There was no significant difference in the effectiveness of NsARC under high intensity visible and UV light ($P=0.243$). There was also no significant difference under ambient light compared to no light ($P=0.717$) (Appendix B2). After 24 hours, there was a significantly greater than 2 log reduction ($P<0.001$) in viable *E. coli* that were on NsARC under all the conditions when compared to viability on stainless steel (Figure 2.13A). There was a significant difference in the effectiveness of NsARC under high intensity visible and UV light ($P=0.0028$). There was no significant difference under ambient light compared to no light ($P=0.16$) (Appendix B4). Similarly, after 48 hours, there was a significantly greater than 2 log reduction ($P<0.001$) in viable *E. coli* that were on NsARC under all the conditions when compared to viability on stainless steel (Figure 2.13A). There was significant difference in the effectiveness of NsARC under high intensity visible and UV light ($P<0.001$). There was also a significant difference under ambient light compared to no light ($P=0.00717$) (Appendix B6).

E. coli biofilms occupied noticeably smaller areas of the surface of NsARC after 48 hours under high intensity visible light compared to stainless steel (Figure 2.13B).

2.4.4.2 *S. aureus*

Viable *S. aureus* cells from biofilms that formed on NsARC were significantly less than those formed on stainless steel (Figure 2.14). After 12 hours exposure, there was a significantly greater than 2 log reduction ($P<0.001$) in viable *S. aureus* that were on NsARC under all the conditions

when compared to viability on stainless steel (Figure 2.14A). There was no significant difference in the effectiveness of NsARC under high intensity visible and UV light (P=0.934). There was also no significant difference under ambient light compared to no light (P=0.864) (Appendix B8). After 24 hours, there was a significantly greater than 2 log reduction (P<0.001) in viable *S. aureus* that were on NsARC under all the conditions when compared to viability on stainless steel (Figure 2.14A). There was a significant difference in the effectiveness of NsARC under high intensity visible and UV light (P<0.001). But there was no significant difference under ambient light compared to no light (P=0.10) (Appendix B10). Similarly, after 48 hours, there was a significantly greater than 2 log reduction (P<0.001) in viable *S. aureus* that were on NsARC under all the conditions when compared to viability on stainless steel (Figure 2.14A). There was no significant difference in the effectiveness of NsARC under high intensity visible and UV light (P=1). But there was a significant difference under ambient light compared to no light (P=0.0098) (Appendix B12). *S. aureus* biofilms occupied noticeably smaller areas of the surface of NsARC after 48 hours under high intensity visible light compared to stainless steel (Figure 2.14B).

2.4.4.3 *P. aeruginosa*

Viable *P. aeruginosa* cells recovered from biofilms that formed on NsARC were significantly less than those formed on stainless steel (Figure 2.15). After 12 hours exposure, there was a significantly greater than 2 log reduction (P<0.001) in viable *P. aeruginosa* that were on NsARC under all the conditions when compared to viability on stainless steel (Figure 2.15A). There was no significant difference in the effectiveness of NsARC under high intensity visible and UV light (P=0.996). There was also no significant difference under ambient light compared to no light (P=0.213) (Appendix B14). After 24 hours, there was a significantly greater than 2 log reduction (P<0.001) in viable *P. aeruginosa* that were on NsARC under all the conditions when compared

to viability on stainless steel (Figure 2.15A). There was no significant difference in the effectiveness of NsARC under high intensity visible and UV light (P=0.545). There was no significant difference under ambient light compared to no light (P=0.869) (Appendix B16). Similarly, after 48 hours, there was a significantly greater than 2 log reduction (P<0.001) in viable *P. aeruginosa* that were on NsARC under all the conditions when compared to viability on stainless steel (Figure 2.15A). There was no significant difference in the effectiveness of NsARC under high intensity visible and UV light (P=972). There was also no significant difference under ambient light compared to no light (P=0.067) (Appendix B18). *P. aeruginosa* biofilms occupied noticeably smaller areas of the surface of NsARC after 48 hours under high intensity visible light compared to stainless steel (Figure 2.15B).

2.4.4.4 *S. cerevisiae*

Viable *S. cerevisiae* cells recovered from biofilms that formed on NsARC were significantly less than those formed on stainless steel (Figure 2.16). After 12 hours exposure, there was a significantly greater than 2 log reduction (P<0.001) in viable *S. cerevisiae* that were on NsARC under all the conditions when compared to viability on stainless steel (Figure 2.16A). There was no significant difference in the effectiveness of NsARC under high intensity visible and UV light (P=0.479). But there was a significant difference under ambient light compared to no light (P<0.001) (Appendix B20). After 24 hours, there was a significantly greater than 2log reduction (P<0.001) in viable *S. cerevisiae* that were on NsARC under all the conditions when compared to viability on stainless steel (Figure 2.16A). There was no significant difference in the effectiveness of NsARC under high intensity visible and UV light (P=0.988). There was also no significant difference under ambient light compared to no light (P=0.950) (Appendix B22). Similarly, after 48 hours, there was a significantly greater than 2 log reduction (P<0.001) in viable *S. cerevisiae*

that were on NsARC under all the conditions when compared to viability on stainless steel (Figure 2.16A). There was no significant difference in the effectiveness of NsARC under high intensity visible and UV light (P=375). There was also no significant difference under ambient light compared to no light (P=1.0) (Appendix B24). *S. cerevisiae* biofilms occupied noticeably smaller areas of the surface of NsARC after 48 hours under high intensity visible light compared to stainless steel (Figure 2.16B)

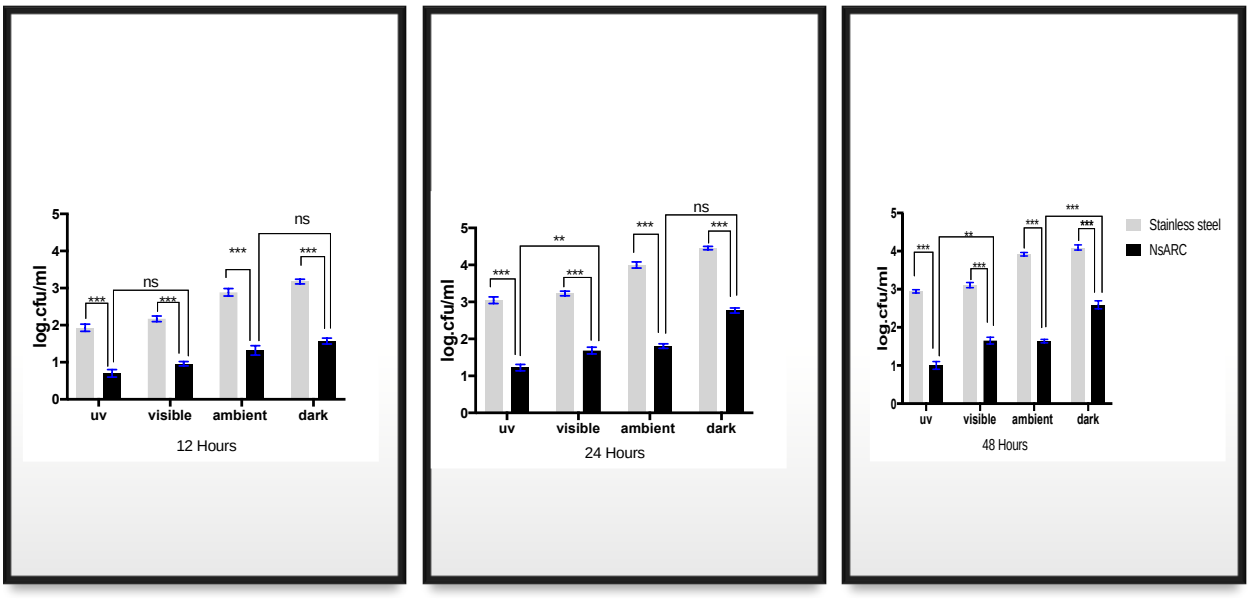

Figure 2.13A: Number of viable *E. coli* cells recovered from biofilm from stainless steel and NsARC after 12, 24 and 48 hours in the dark and exposure to UV, ambient and high intensity visible light. Error bars are standard error of means (SEM). Asterisks indicate P values. *: P<0.05; **: P<0.01; ***: P<0.001; ns: not significant.

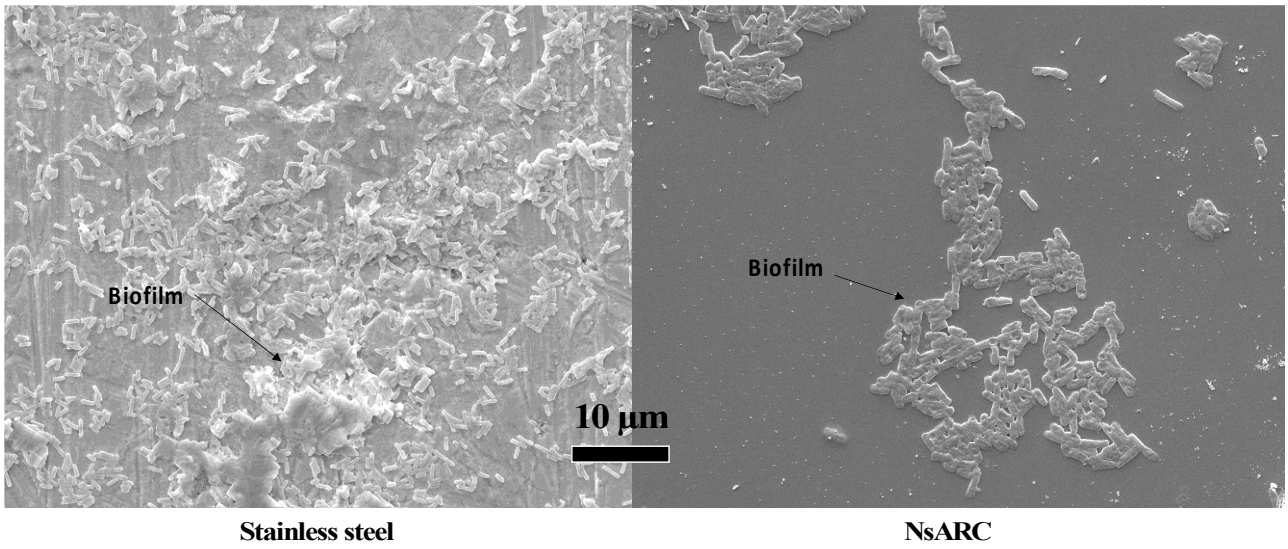

Figure 2.13B: SEM images of *E. coli* biofilms that formed on stainless steel and NsARC after 48 hours under high intensity visible light.

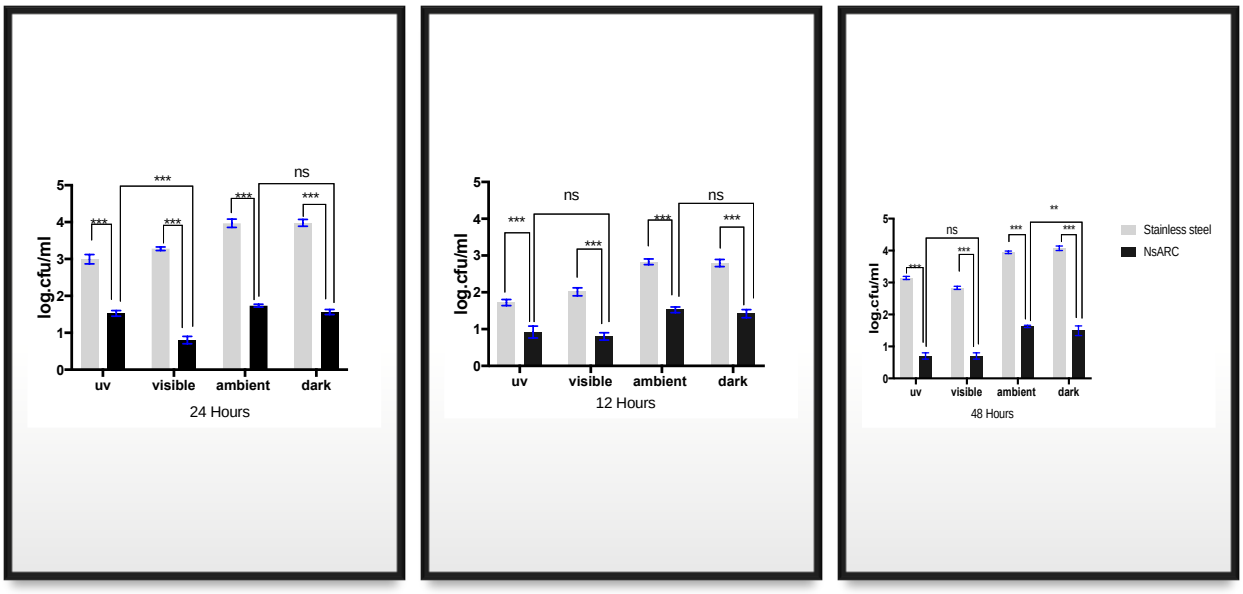

Figure 2.14A: Number of viable *S. aureus* cells recovered from biofilms from the surfaces of stainless steel and NsARC after 12, 24 and 48 hours in the dark and exposure to UV, ambient and high intensity visible light. Error bars are standard error of means (SEM). Asterisks indicate P values. *: P<0.05; **: P<0.01; ***: P<0.001; ns: not significant.

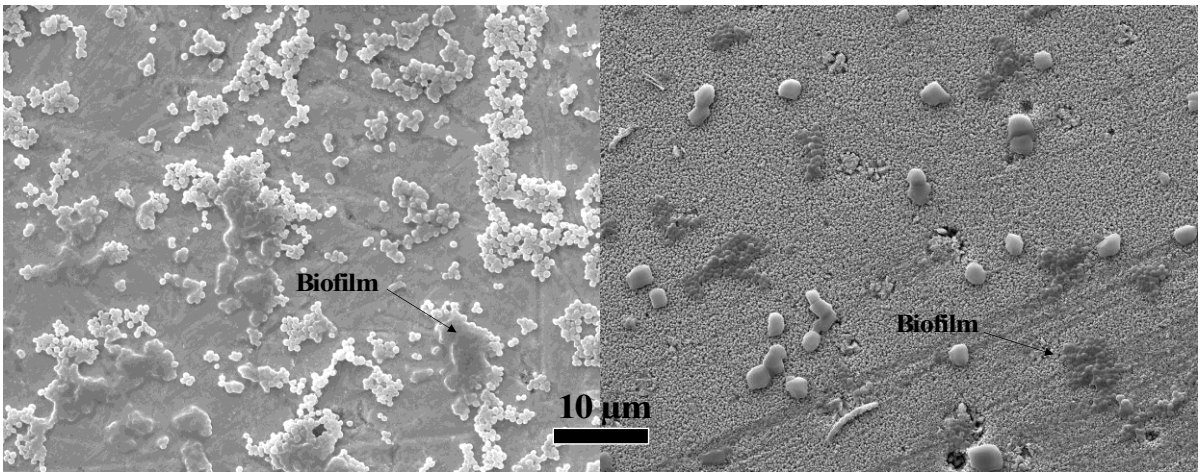

Figure 2.14B: SEM images of *S. aureus* biofilms that formed on stainless steel and NsARC after 48 hours under high intensity visible light

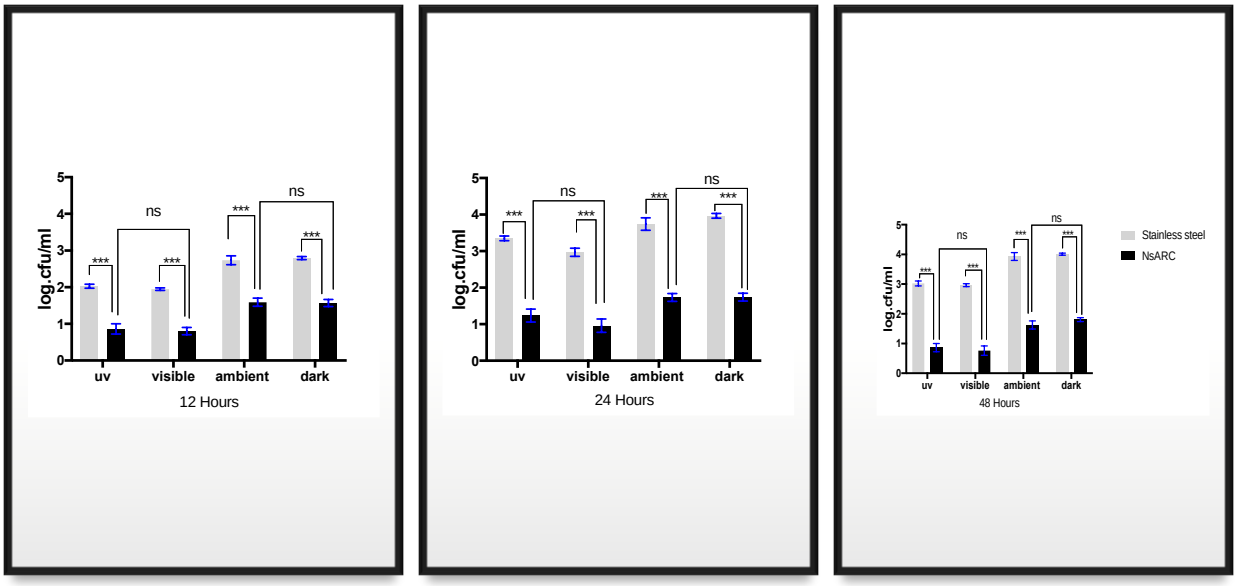

Figure 2.15A: Number of viable *P. aeruginosa* cells recovered from biofilms from the surfaces of stainless steel and NsARC after 12, 24 and 48 hours in the dark and exposure to UV, ambient and high intensity visible light. Error bars are standard error of means (SEM). Asterisks indicate P values. *: P<0.05; **: P<0.01; ***: P<0.001; ns: not significant.

.

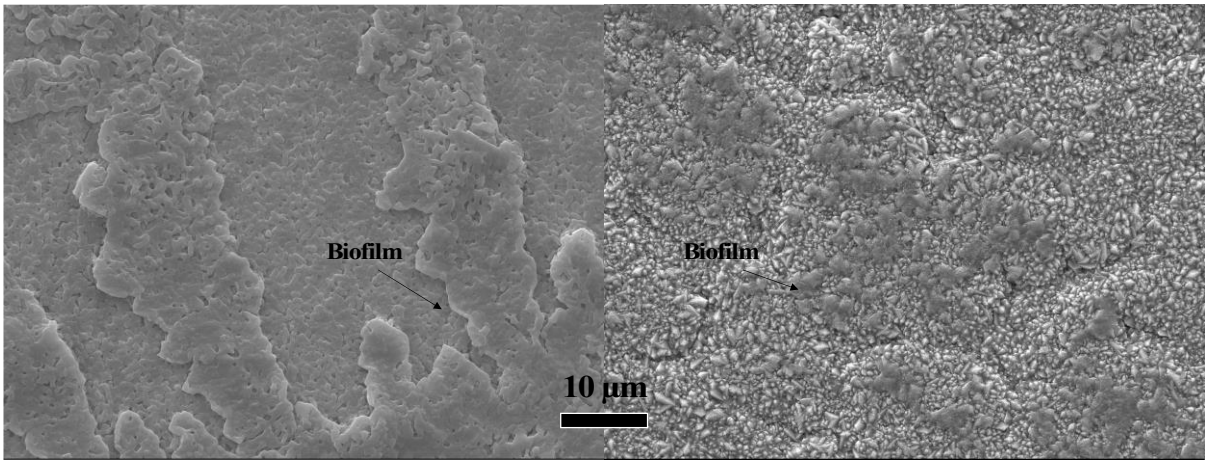

Figure 2.15B: SEM images of *P. aeruginosa* biofilms that formed on stainless steel and NsARC after 48 hours under high intensity visible light

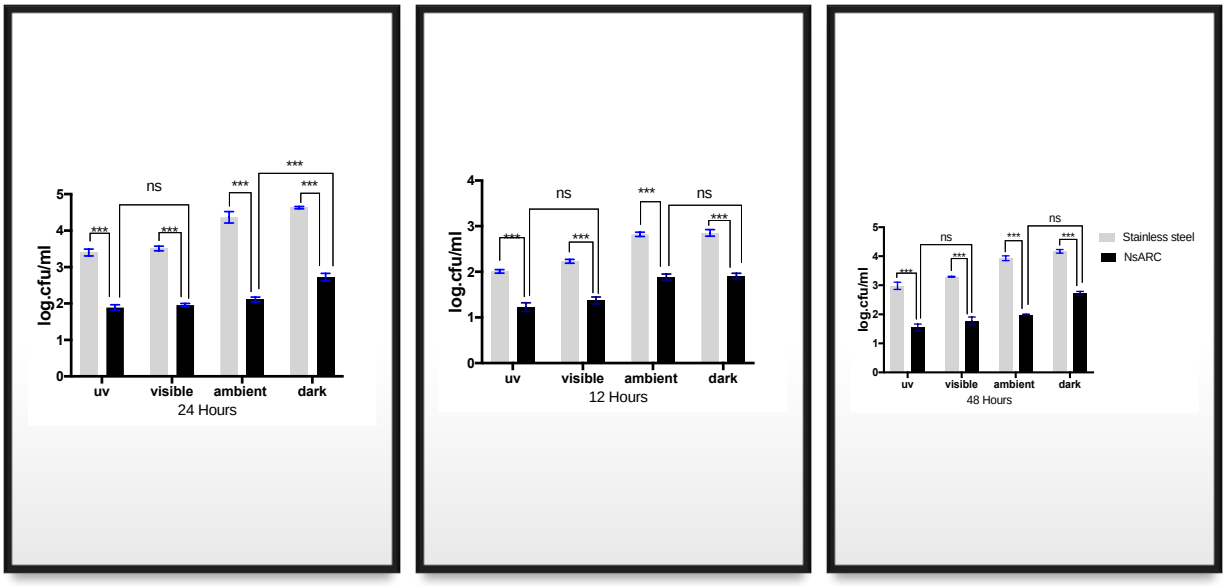

Figure 2.16A: Number of viable *S. cerevisiae* cells recovered from biofilm from the surfaces of stainless steel and NsARC after 12, 24 and 48 hours in the dark and exposure to UV, ambient and high intensity visible light. Error bars are standard error of means (SEM). Asterisks indicate P values. *:P<0.05; **:P<0.01; ***:P<0.001; ns: not significant.

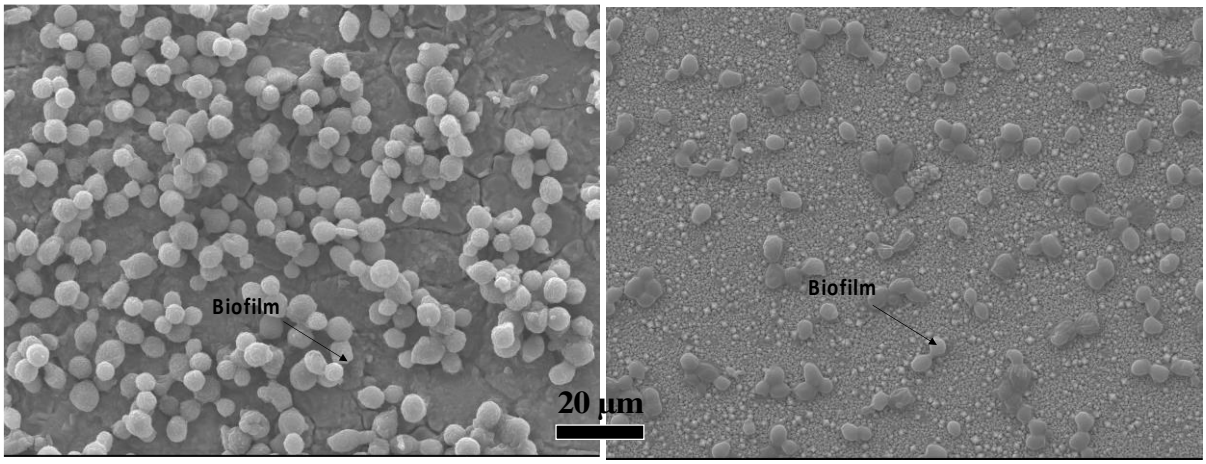

Stainless steel **NsARC**

Figure 2.16B: SEM images of *S. cerevisiae* biofilms that were formed on stainless steel and NsARC after 48 hours under high intensity visible light.

2.5 Discussion

2.5.1 Antimicrobial activity

NsARC caused reduction in viability of microorganisms in the dark and after photoactivation. This demonstrates that ROS generated by photoactivation are not the only mechanism for cellular degradation. While the killing mechanisms are not known, there are several possibilities. This activity could arise from the carbon component of the NsARC. Carbon is also an antimicrobial agent that is inert as an element, but can be chemically active when combined with other compounds or elements (Cheng et al., 2009; Dizaj et al., 2015). Another possible reason for the AMA in the dark is that direct contact between the cell membrane of microorganism and NsARC can cause the modification of the zeta potential of the cell membranes. This modification can lead to an increase in permeability of the cell membranes (Halder et al., 2015). The hydrophilic surface of NsARC, possibly linked to the very high specific surface area of the nanostructured coating (Gardecka et al., 2019; Krumdieck et al., 2019), may also desiccate cells over time (Yu et al., 2014).

I observed that NsARC samples that were annealed in air to remove the carbon showed greater AMA under UV and visible light compared with the as-deposited samples. My hypothesis for this observation is that removal of the carbon made the TiO_2 surfaces cleaner and increased the specific surface area available for redox reactions to occur, thus increasing the ROS concentration to which the bacteria were exposed. The results in the dark showed greater killing AMA for the as-deposited coatings, possibly because co-deposited carbon stabilized high energy facets of TiO_2, leading to a possible increase in activity.

NsARC killed all the organisms tested. This confirms that NsARC is a broad-spectrum antimicrobial agent, similar to what has been observed of other TiO_2 materials (Pelaez et al., 2012;

Sadowski et al., 2015; Xu et al., 2015). We observed cellular morphologies of the cells recovered after 8 hour exposure under high intensity visible light using SEM. The cells that were on NsARC looked distorted compared to those that were on steel. The cell morphologies that we have observed are consistent with deformity on the cell membrane of *E. coli* (Foster et al., 2011; Leung et al., 2016) and *S. aureus* (Cheng et al., 2009) after exposure to photoactivated TiO_2 nanoparticles. Similar effects were observed when *Candida albicans* and *S. aureus* were exposed to flame-synthesized nano-TiO_2 coatings (De Falco et al., 2017). Distortion in cell morphology with loss in viability or cell death is a consistent feature in the activity of TiO_2 (Dizaj et al., 2015).

2.5.2 Antibiofilm activity

Fewer *E. coli, S. aureus, P. aeruginosa* and *S. cerevisiae* biofilm were found on NsARC compared to stainless steel. This reduction was observed under all the light exposure conditions. Kubacka et al (2014) had observed a similar result with ethylene-vinyl alcohol copolymer (EVOH) embedded with Ag-TiO_2 nanoparticles as their material. In their study, they demonstrated photocatalysis upon ultraviolet (UV) light activation of their material and resistance to bacteria and yeast biofilm formation. Another study by Santhosh and Natarajan (2015), also demonstrated the antibiofilm activity of a Ag-TiO_2 nanocomposite coating against *S. aureus* and *E. coli* (M. and Natarajan, 2015). The biocidal ability and prevention of bacterial attachment to TiO_2 nanocomposite is said to be as a result of radical-mediated photocatalytic action (Jung et al., 2006). And the antibiofilm efficacy of NsARC could be attributed to release of free radicals that prevent initial microbial attachment (Krumdieck et al., 2019; Naik & Kowshik, 2014), and the hydrophilic nature of the surface coating that also does not support attachment (Krumdieck et al., 2019). Contrary to what is observed in other TiO2 formulations, where only photo-excitation can lead to prevention of

biofilm formation (Cheng et al., 2009; Gomes Silva et al., 2011), NsARC inhibits biofilms even in the dark.

In this study I was able to demonstrate the reduction in survival and distortion in the morphology of microbial cells caused by NsARC. However, I was however not able to ascertain the actual mechanism of killing. The hypothesis is that damage to bacterial enzymes or plasma membrane, disruption of metabolic pathways and leakage of the cytoplasmic content may be responsible for the killing (Cheng et al., 2009). It is also not absolutely certain that the killing effect in the dark is fully explained by the carbon component of NsARC. Therefore, I tested NsARC films that have been annealed in air to remove the carbon (Gardecka et al., 2018). This enabled me to monitor the AMA effect and see the significant changes that occurred when microorganisms are exposed to the annealed NsARC samples in the presence and absence of photoexcitation.

3 Chapter Three

3.1 General Introduction

Antibiotics are considered one of the most iconic discoveries of the 20th century. Sadly, the rise in resistance to antibiotics in hospitals, communities and the environment seem to have taken over the spotlight (Caniça et al., 2015; Heinemann, 1999). About 700,000 people die globally from bacterial diseases associated with antimicrobial resistance. If this current trend continues by 2050, an estimated 10 million people will be dying yearly according to The World Health Organization (WHO), making antimicrobial resistance more dangerous than tuberculosis, HIV/AIDS and diabetes combined (Khan et al., 2017; Leyland et al., 2016). The World Bank also warns that because of this rise in antibiotic resistance, people are seeking alternative methods of treatment at extra cost. This extra cost is placing enormous financial pressure on the global economy. About $1 trillion of the extra medical cost per year is causing a 5% loss in GDP per year for most countries, pushing over 25 million people in most developing countries into extreme poverty (Khan et al., 2017). Information explaining the dangers associated with resistance is available, but unfortunately, we have not been able to successfully address the problem of resistance to antimicrobial agents (Caniça et al., 2015).

It is difficult to prevent microorganisms from developing resistance to antibiotics because microorganisms utilize multiple mechanisms to develop resistance to antibiotics. They can acquire antibiotic resistance genes from the environment, which in addition to mutation is a pathway for them to evolve multidrug resistance (Davies and Davies, 2010). Other pathways to developing resistance to antibiotics may include inactivation of the antimicrobial agent by enzymes such as beta-lactamase. Mutations that affect the target, and or expulsion of the antibiotic from the cell

(efflux) or reduced entrance of the antimicrobial into the cell by modification of the cell surface and reduction in the number of entry channels called porins. Microorganisms can tolerate new therapeutic agents used for the treatment of some infectious and chronic diseases even from the first time of usage (Davies and Davies, 2010). The inappropriate use of antibiotics may not be the only cause for the growing increase in antibiotic resistance we are observing today. Exposing bacteria to non-antibiotic chemicals could predispose them to develop resistance to antibiotics (Jun et al., 2019; Kurenbach et al., 2015, 2017, 2018).

Kurenbach et al. (2015) had reported that *Salmonella typhimurium* exposed to sublethal concentration of the herbicides kamba® and 2, 4-D® became more tolerant to ampicillin, chloramphenicol, ciprofloxacin and tetracycline antibiotics. In a similar study, Jun et al. (2019) also reported that *E. coli* exposed to the fungicide copper ammonium acetate became more resistant to tetracycline, While *E. coli* exposed to atrazine became more resistant to ciprofloxacin, kanamycin and streptomycin. Furthermore, food preservatives and emulsifiers used in food and medicines could also cause these changes. The way bacteria respond after exposure to chemicals may vary depending on their genetic and physiological differences. The response in form of resistance to antibiotic may be intrinsic, acquired or adaptive.

3.1.1 Intrinsic resistance

This form of resistance is the naturally occurring resistance that is present in most strains of a particular type of microorganism. In this form of resistance, bacteria may have traits that are common to an entire species of bacteria. Such as constitutive efflux pumps that are used as a channel to selectively remove and prevent accumulation of antibiotics and other chemicals. This type of resistance is not dependent on selective pressure from antimicrobial agents (Fernández et al., 2011). A good example is the drug resistant phenotype seen in gram-negative bacteria. Gram-

negative bacteria possess an outer membrane that is impermeable to many molecules. The outer membrane of gram-negative bacteria contains tightly packed lipopolysaccharides chains that also acts as a barrier that decreases permeability and prevents molecules such as antibiotics that are larger than 500 Da from entering the bacterium. Vancomycin antibiotic is not active against gram-negative bacteria because the molecules are unable to penetrate the outer membrane of gram-negative bacteria (Caniça et al., 2015; Davies and Davies, 2010).

3.1.2 Acquired resistance

This is the type of resistance that occurs when bacteria that are previously sensitive to an antibiotic become resistant to the same or other types of antibiotics. There are several pathways of developing acquired resistance to antibiotics, many of which are specific to a particular type or class of antibiotic (Metcalfe et al., 2016; Williamson et al., 2015). Acquired resistance is associated with a change in genotype and can arise within a population via mutation or gene acquisition. These changes make it impossible for the antibiotic molecule to bind to its target on the bacteria (Fernández and Hancock, 2013). Mutations in some genes, for example, *gyrA* and *parC* genes can lead to changes in DNA maintenance proteins. These changes can cause resistance to quinolone antibiotics, such as ciprofloxacin and ofloxacin (Davies and Davies, 2010). Bacteria can also acquire new antibiotic resistance genes (ARGs) from the environment through conjugation, transduction and or transformation (Fernández et al., 2011).

3.1.3 Adaptive resistance

The presence of a biocide and stress in the environment can cause microbes to alter their protein or gene expression to increase their chances of survival under such conditions (Jun et al., 2019; Kurenbach et al., 2017). This modification is called adaptive resistance (Fernández and Hancock, 2013). Adaptive resistance enables the microorganisms to be able to tolerate higher concentrations

of antimicrobial agents that it usually would not tolerate, leading to a decrease in susceptibility to antimicrobial agents and an increase in the concentration needed to inhibit the growth of the microorganism (Fernández et al., 2011; Fernández and Hancock, 2013). This concentration is known as the minimum inhibitory concentration (MIC).

Adaptive resistance can lead to changes in cell permeability, with an increase in efflux and decrease in influx (Davies and Davies, 2010; Hughes and Andersson, 2012). Unlike acquired resistance mechanisms that are stable and transmissible, adaptive resistance is dependent on the environment, can last for only several generations and is lost upon removal of the inducing signal (Fernández et al., 2011). The increase in MIC caused by adaptive resistance to antibiotics is usually less than when the resistance is caused by mutation or horizontally acquired genes (acquired resistance) (Russell, 2002). Unfortunately, this small change in MIC could lead to more substantial changes with a significant effect on treatment outcome for patients with a bacterial infection. Bacteria with a small change in MIC has the potential of producing mutants with higher MIC and these mutants with higher MICs have a fitness advantage and can accumulate differentially to their low MIC cousins (Niño-Martínez et al., 2019). Higher MIC mutants will then replace the ones with low MIC. This means that since treatment targeted at a particular species of organism is usually based on government advice on regional phenotypes, and these small changes in MIC can render the government-approved baseline treatment dosage insufficient. Thus, for effective treatment of the bacterial infection, a higher concentration of the drug may be required and/or treatment might have to be for longer periods, than anticipated by guidance authorities (Sader et al., 2019).

3.1.4 Efflux systems in bacteria

Bacteria have genes that encode a system called "Efflux pump" that it uses to prevent the accumulation internally of toxic compounds. Efflux pumps remove unwanted materials. Several different efflux pumps are used to transport a variety of molecules (Walsh, 2000). Some of these efflux pumps enable bacteria to export antibiotics out of the cell, thereby reducing the concentration of the drug inside the cell, increasing the apparent MIC of the drug. Some efflux pumps can transport more than one type of antibiotic and thus confer multidrug resistance (MDR) on bacteria (Fernández and Hancock, 2013). Increase in tolerance to antibiotics by some bacteria is linked with the increase in expression of efflux pumps and a reduction in porins (Kurenbach et al., 2015).

There are five classes of bacterial efflux pumps:

(i) Major facilitator superfamily (MFS)

(ii) Adenosine triphosphate binding cassette superfamily (ABC)

(iii) Small multidrug resistant family (SMR)

(iv) Multidrug and toxic compound extrusion family (MATE) and

(v) Resistance nodulation division family (RND).

These pumps are classified based on their transmembrane spanning regions, substrates and sources of energy (Fernández et al., 2011). They can transport minerals and other cellular components out of the cell, and in some cases, pumps are essential in virulence to the host (Fernández et al., 2011; Fernández and Hancock, 2013). All the five classes are found in both gram-positive and gram-negative bacteria except for the RND that is found only in gram negative bacteria. The ABC pump is powered by the hydrolysis of ATP, while the other four pumps utilize energy from the electrochemical potential of the cell membrane (Weston et al., 2018).

Efflux pumps can be single component or multi component transporters that have both inner and outer membrane channels for transport. The RND type is a multicomponent transporter, existing as a tripartite system (Blair et al., 2014, 2015) and is found to be associated with multidrug resistance (Weston et al., 2018), such as *AcrB* found in *E. coli* and some species of Salmonella and *MexB* found in *P. aeruginosa*. While MFS pumps such as *NorA* are found in *S. aureus* and *PmrA* found in *S. pneumonia* (Blair et al., 2014). The most characterized RND pump is AcrAB-tolC. This pump is made up of an inner membrane *AcrB* transporter, outer membrane TolC protein channel and an *AcrA* periplasmic adaptor protein (Weston et al., 2018). This system under the control of transcriptional regulators such as *MarA*, *SoxA* and *SoxS* is vital for gram-negative bacteria to be able to resist antibiotics such as quinolones, macrolides, chloramphenicol and beta lactams (Weston et al., 2018).

3.2 Nanomaterials and resistance to antibiotics

The growing increase in bacterial resistance to antibiotics observed since the discovery of antibiotics in the 1920s has led to the growing interest in using nanomaterials as tools against multi-drug resistant bacterial (Niño-Martínez et al., 2019). Nanomaterials are used individually as nano-drugs or in combination with other antimicrobial agents. Nanomaterials can be metals such as silver, titanium, copper, aluminium, zinc etc or metal oxides such as silver oxide, titanium dioxide, copper oxide, zinc oxide etc. Studies have shown that these nanomaterials have broad-spectrum antimicrobial activity because of their diverse antimicrobial mechanisms. These mechanisms include:

- Direct contact killing by damaging bacterial cell wall, proteins and internal cellular components (Foster et al., 2011).
- release of ions that are toxic to bacteria (Page et al., 2009)

- DNA damage as a result of oxidative stress (Gogniat et al., 2007)

The diverse nature of the antimicrobial activity of nanomaterials might make it more difficult for bacteria to develop resistance (Niño-Martínez et al., 2019). However, recently it was observed that bacteria through electrostatic repulsion, efflux pumps (Webber and Piddock, 2003; Weston et al., 2018), mutation (Walsh, 2000) and biofilm formation (Graves Jr et al., 2015) mechanism have been able to generate resistance to nanomaterials. *E. coli* and *Pseudomonas aeruginosa* are able to produce extracellular substances (ECS) and also increase the expression of a flagellin matrix (see Figure 3.1) that can modify the charge or zeta potential around nanomaterials causing them to aggregate and thus preventing direct contact with the bacteria (Niño-Martínez et al., 2019).

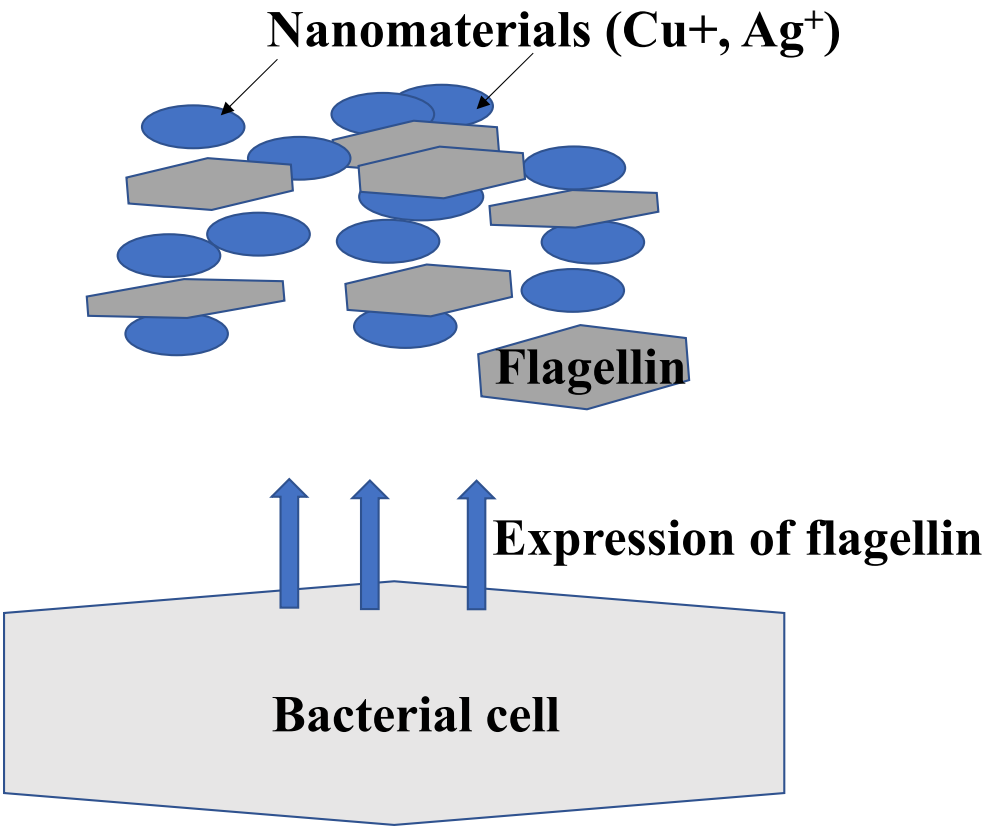

Figure 3.1: Schematic representation of bacterial mechanism of defence against nanoparticles.

Presence of Cu+, Ag+ can induce the expression of flagellin that can attach to the ions and prevent entry of the ions into the cell.

Nonlethal concentrations of nanomaterials such as silver nanoparticles (AgNPs), Zinc oxide (ZnO) and copper oxide (CuO) can cause an increase in mutation rates in bacteria by inducing stress responses and oxidative damage (Zhang et al., 2018). Interaction between bacteria and nanomaterials can facilitate the generation of ROS. Increase in ROS production can cause an increase in mutation, leading to the development of resistant phenotypes. Nanomaterials can also interact with organic matter such as lipids and proteins in the environment under aerobic condition. This interaction can cause a redox reaction that will lead to solubilization of the lipids and proteins.

These soluble lipids and proteins will then bind to charge ions that are being released by the nanomaterials, causing a decrease in the number of ions and ROS that can interact with the cell membrane of bacteria. Sublethal concentrations of ROS are still able to stimulate the expression of bacterial defence mechanisms. This defence mechanisms include the expression of ROS scavenger enzymes responsible for inactivating ROS. And the upregulation of oxidative stress resistance mechanism via SoxRS and OxyRS regulon (See Figure 3.2) (Koutsolioutsou et al., 2005; Niño-Martínez et al., 2019).

The quantity of ions released, and ROS generated during the interaction between bacteria and nanoparticles also depends on environmental factors such as the presence of light and oxygen (Niño-Martínez et al., 2019). For example, there is an increase in the release of ions and ROS from CuO under aerobic conditions compared to anaerobic conditions (Niño-Martínez et al., 2019). There is an increase in the photocatalytic activity of TiO_2 in the presence of light, compared to in the absence of light (Krumdieck et al., 2015).

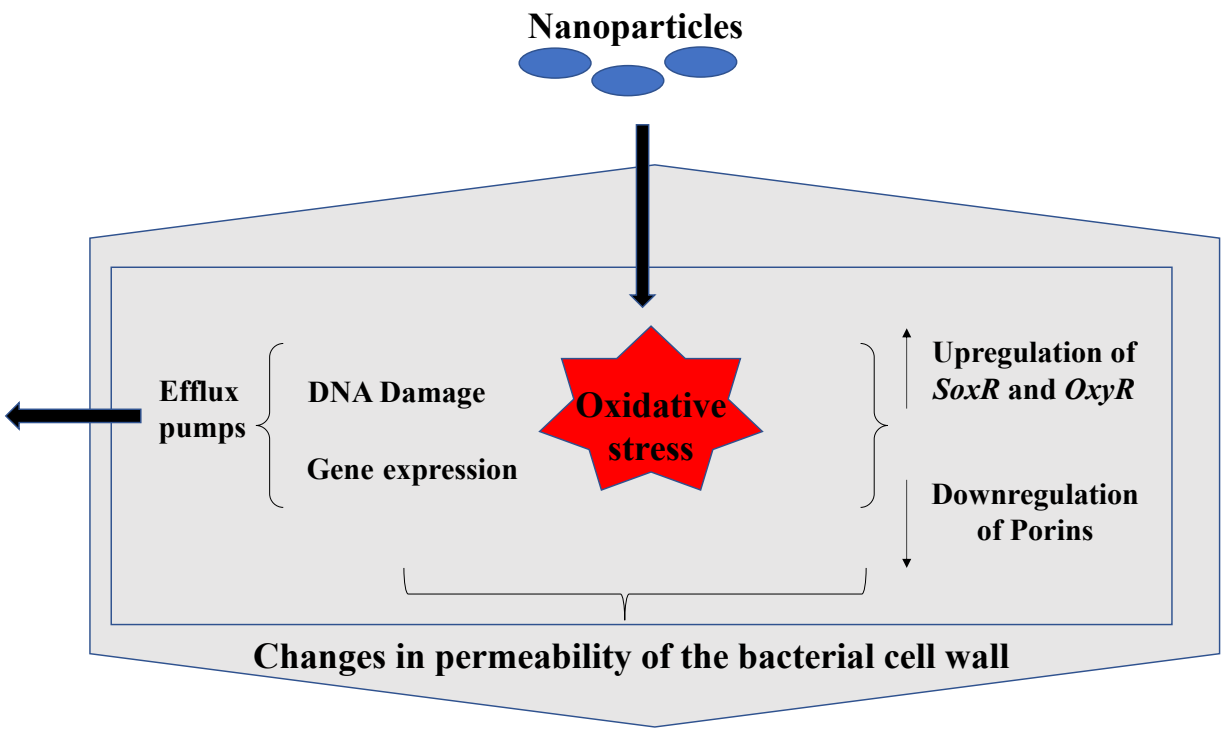

Figure 3.2: Schematic representation of how bacteria develop resistance to nanomaterials.

Nanoparticles can induce oxidative stress that can cause DNA damage and or a change in gene expression, upregulation of SoxR and OxyR and downregulation of porins that can cause changes in the way molecules move in and out of the cell.

3.2.1 Reactive Oxygen species (ROS) and antibiotic lethality

During respiration in bacteria, ROS are continuously being produced. These ROS can accumulate in the cell causing damage to cellular DNA, proteins and lipids, leading to cell death (Fraud and Poole, 2011). Bactericidal antibiotics such as beta lactams, quinolones and aminoglycosides can also induce cell death through the production of ROS (Kohanski et al., 2007). The model for ROS mediated cellular death pathway induced by bactericidal antibiotics suggests that they can stimulate oxidation of NADPH to NAD^+ through the electron transport chain, leading to superoxide production. These superoxides will then cause damage of iron-sulphur-cluster proteins, and the release of iron (II), that reacts with H_2O_2 and hydroxyl radicals are then generated through the Fenton reaction (Kohanski et al., 2007). Increase in ROS production has been observed in

gram-negative bacteria during treatment with quinolone antibiotics (Kohanski et al., 2007). Oxidative stress is also induced during ciprofloxacin treatment of *Proteus mirabilis* (Aiassa et al., 2012).

3.2.2 Reactive Oxygen species (ROS) and antibiotic resistance

Bacteria have enzymes such as superoxide dismutases (*sodA*) and catalase that it uses to prevent the accumulation and harmful effects of ROS and other regulatory mechanisms such as *soxRS*, *OxyRS* and *SOS* regulon (Fraud and Poole, 2011). *SodA* converts O_2^- to oxygen and hydrogen peroxide (H_2O_2). H_2O_2 can then react with iron (II), leading to the generation of highly reactive hydroxyl radicals (OH^+): $Fe^{2+} + H_2O_2 \rightarrow Fe^{3+} + OH^- + OH^+$

For example, when *E. coli* is treated with nalidixic acid, there is a significant increase in the expression of *sodA*. The increase in expression of *sodA* induces the activation of oxidative stress response system called *soxRS* regulon. The *soxRS* regulon is a system that confers multiple-antibiotic resistance in most Gram-negative bacteria (Kohanski et al., 2007). The increase in the expression of *soxS* and the constitutive activation of the *soxRS* regulon in gram-negative bacteria such as *E. coli* and *Salmonella enterica* increases the level of resistance to quinolones. ROS can cause the oxidation and nitrosylation of the *SoxR* protein, which in turn induces the transcription of *soxS* gene. The increase in the expression of the *SoxS* protein then directly induces the expression the AcrAB-TolC efflux pump responsible for resistance to some antibiotics and other biocide. Oxidative stress from reactive oxygen species (ROS) such as hydrogen peroxide and other superoxides can also induce the expression of RND type multidrug efflux pumps system that confers multidrug resistance to the bacteria (Fraud and Poole, 2011).

3.2.3 NsARC and antibiotic resistance

The possibility of NsARC (TiO_2) inducing changes to antibiotic response is highly likely because nanomaterials such as Ag (Niño-Martínez et al., 2019), Cu (Jun et al., 2019), and Zn (Zhang et al., 2018) with antimicrobial properties are shown to cause bacteria to develop multidrug resistant phenotypes. Developing a strategy to investigate the possibility of bacteria developing acquired and adaptive resistance to antibiotics after they are exposed to NsARC is necessary because NsARC is a new material that is been introduced and has not been tested for this potential effect. I therefore, decided to adopt the following strategy.

- Directly exposing bacteria to antibiotics after they have been exposed to NsARC to observe if the exposure has affected their susceptibility to the antibiotics
- Determine if NsARC was able to cause a change in expression of genes associated with adaptive resistance to antibiotics
- Determine if NsARC could directly affect the availability and potency of antibiotics

3.2.3.1 NsARC causing a change in susceptibility to antibiotics

Non-antibiotic biocides such as sodium nitrite, sodium hypochlorite (Molina-González et al., 2014), and copper (Tong et al., 2015) at sub-inhibitory concentrations can affect tolerance of bacteria to antibiotics. For example, sodium nitrite and sodium hypochlorite are known to alter the tolerance of various *S. enterica* strains to aminoglycoside and cephalosporin antibiotics (Molina-González et al., 2014). Copper also can induce an increase in tolerance of *E. coli* to tetracycline (Jun et al., 2019). I decided to test how *E. coli* and *S. aureus* will respond to some antibiotics after exposure to NsARC. The antibiotics were ampicillin (Amp), ciprofloxacin (Cip), chloramphenicol (Cam), erythromycin (Ery), fusidic acid (FA), kanamycin (Kan), oxacillin (Oxa), tetracycline (Tet)

and vancomycin (Van). These antibiotics were selected because they represent a broad range of common antibiotics used in treating microbial infections and have been utilized in related studies. *E. coli* and *S. aureus* were exposed to NsARC for a period of 8 hours and survivors were transferred to culture media supplemented with various types of antibiotics.

3.2.3.2 NsARC inducing genes associated with efflux pumps

The *tolC* and *soxS* genes are part of the system that regulate RND efflux pump and are associated with stress responses to biocides and can be used to serve as indicators of adaptive resistance to antibiotics. H_2O_2, super oxides, ROS and other free radicals that are produced from the reaction that takes place upon light excitation of TiO_2 are known inducers of *tolC* and *soxS* genes (Wang et al., 2017; Weston et al., 2018; Wu et al., 2012). To determine if NsARC can induce the expression of the *tolC* and *soxS* genes, I decided to use a reporter system that monitor the expression of these genes in *E. coli* when they were exposed to NsARC.

3.2.3.3 Reporter system

Reporter genes can be fused to the regulatory sequence of gene of interest to monitor expression levels of the gene. The reporter system can be used for the analysis of gene expression, protein interactions, microbial detection and quantification, interactions between pathogens and hosts, therapeutics and diagnosis (Gerlach et al., 2007; Leveau and Lindow, 2002; Remus-Emsermann and Leveau, 2010). The fluorescence-based reporter system is an example of a system that is used for microbial analysis to measure and distinguish phenotypes. Several fluorescent proteins are available, for example red fluorescent protein (RFP), green fluorescent protein (GFP), yellow fluorescent protein (YFP). Each of these fluorescent proteins have been used extensively in a variety of applications in molecular biology (Jun et al., 2019; Remus-Emsermann and Schlechter, 2018; Schlechter et al., 2018). An important application of the fluorescence-based reporter is for

analysing promoter activity. The promoter region of a gene of interest can be cloned into a reporter plasmid to generate gene fusions (Gerlach et al., 2007; Remus-Emsermann and Schlechter, 2018). These gene fusions combine the DNA sequence of the reporter gene under a single promoter. When the promoter is induced, the reporter gene is expressed (Gerlach et al., 2007; Jun et al., 2019; Schlechter et al., 2018).

I used two reporter strains of *E. coli* that "report" efflux activity (Jun et al., 2019), each of these reporter strain have a plasmid construct that expressed the mScarlet red fluorescent protein (RFP) under the control of the promoters of either the *tolC* or *soxS* genes. These designed constructs are strains that "report" when *tolC* and or *soxS* expression changes.When these genes are induced there was an increase in the production of the RFP leading to a corresponding increase in fluorescence of the reporter strains (Mangalappalli-Illathu and Korber, 2006; Remus-Emsermann et al., 2016).

3.2.3.4 Interaction of NsARC with Antibiotics

Antibiotics, heavy metals and nanomaterials are often detected to coexist in the environment (Tong et al., 2015; Zhao et al., 2013). These compounds that coexist can interact with each other with a potential effect on the ecosystem (Gao et al., 2013; Tong et al., 2015). Interaction between antibiotics and metals in the soil is potentially hazardous to the soil microbiota (Gao et al., 2013; Lu et al., 2014). There may also be an increase or decrease in the efficacy of the antibiotic or/and the metal. For example, the efficacy of the antibiotics oxytetracycline (OTC) and sulfamethazine (SMZ) against *E. coli* is increased by 2 folds, when the antibiotics were used in combination with Zn and Cu (Tong et al., 2015). In contrast, the interaction between tetracycline (tet) and copper Cu causes a decrease in the efficacy of both compounds (Hao et al., 2014; Zhao et al., 2013). The decrease in efficacy seen in both tet and Cu may be as a result of chelation of tet by Cu or the induction of an adaptive resistance pathway (Jun et al., 2019; Tong et al., 2015). In addition to

investigating if NsARC can induce the adaptive pathway of developing resistance to antibiotics, I was also interested in determining if NsARC can interact with tetracycline and affects its efficacy, as seen with copper. For this experiment, I placed NsARC, copper and stainless steel coupons in LB agar with or without *E. coli* + tetracycline (see section 3.4.4).

3.3 Methodology

3.3.1 Bacterial Strains, culture conditions, materials and chemicals

Bacterial strains used in this study are shown in Table 3. The type strain of *E. coli* used in the reporter strains was BW25113 (Baba et al., 2006). This strain was chosen as a model organism to describe changes in gene expression because of the availability of credible literature describing its response to many antimicrobial agents.

These strains are stored in 15% glycerol solution at -80°C. To recover these strains, Lauria Bertani (LB) agar plates (Lennox-L-Broth Base, Invitrogen (USA) and agar (Bacteriological Agar No.1, Oxoid (UK)) were inoculated with loopfuls of the samples and the plates incubated at 37°C for 18-24 hours. These plates are stored at 4°C for not longer than one week.

Table 3.1: Bacterial strains and plasmids used in this study

	Characteristics/Genotype	Reference
E. coli ATCC 8739	cook strain	(Mills et al., 2012)
S. aureus ATCC25923	agr-III strain	(Mun et al., 2013)
E. coli BW25113	F^-, λ^-, Δ(*araD-araB*)567, Δ*lacZ*4787(::*rrnB*-3), rph-1,Δ(*rhaD-rhaB*)568, *hsdR*514	(Baba et al., 2006)
Plasmids		
pFru-p_{tolC}-mScarlet	Kan^R, cat, nptII, pBBR1, *tolC* promoter:mScarlet-I	(Jun et al., 2019)
pFru-p_{SoxS}-mScarlet	Kan^R, cat, nptII, pBBR1, *soxS* promoter:mScarlet-I	(Jun et al., 2019)
E. coli with plasmids		
BWtolC	BW25113 (pFru-p_{tolC}-mScarlet)	(Jun et al., 2019)
BWsoxS	BW25113 (pFru-p_{soxS}-mScarlet)	(Jun et al., 2019)

The copper used in the experiment was liquid copper (Yates, Auckland, NZ), a. commercial fungicide. The active ingredient in this product was copper (92.8g/L) (Cu) present as copper ammonium acetate. The concentration used was used at sub-lethal levels 4.73g/L (Jun et al., 2019). Tetracycline (tet) used was purchased from Sigma, Auckland (NZ). The concentration of 2 μg/ml used in the experiment involving the use of coupons embedded in LB + tet was twice higher than the MIC (Jun et al., 2019). Ampicillin (Amp), ciprofloxacin (Cip), chloramphenicol (Cam), erythromycin (Ery), fusidic acid (FA), kanamycin (Kan), oxacillin (Oxa) and vancomycin (Van) used were purchased from Sigma-Aldrich (USA).

Paraformaldehyde used for fixation of cells prior to fluorescence microscopy was purchased from Sigma-Aldrich (USA) and stored as powdered stock at 4^{o}C. 4% solution of paraformaldehyde was made up on the day it was to be used and kept at 4^{o}C.

Stainless steel (25 × 25 mm) coupons was used as an inert control material as recommended by the ISO 27447:2009 (Mills et al., 2012), and commercially pure copper (25 × 25 mm) coupons which is well-known for its antimicrobial activity (Grass et al., 2011), was selected as positive control material. NsARC (25 × 25 mm) coupons and Control (stainless steel and copper) samples were sterilised using 70% ethanol and the NsARC test pieces were aseptically stored in the dark for >48 hours to discharge before the experiment.

Gelatine coated slides were made by washing glass microscopy slides (Mareinfeld-Superior, 76 × 26 mm, approx. 1 mm thick) in 70% ethanol for 1 hour. They were then air dried and dipped in 0.1% gelatine solution at 70^{o}C before air drying. After drying they were kept at 4^{o}C and disposed of after 1 week if not used.

3.3.2 Experiment to determine if NsARC can cause a change in susceptibility of *E. coli* and *S. aureus* to antibiotics

The bacterial culture was prepared as described in section 2.3. After exposure for 8 hours either under visible light or in the dark, and washing off using PBS, 100 µl of the wash off from NsARC which contains about ~10^2 cells were transferred to the surface of LB plates containing 0, 0.01, 0.02, 0.03, 0.04 , 0.05 µg/ml of ciprofloxacin, 0, 5, 6, 7, 8, 9 µg/ml of chloramphenicol, 0, 4, 5, 6, 8, 9 µg/ml of kanamycin and 0, 0.5, 0.7, 1, 1.5, 2 µg/ml of tetracycline antibiotics for *E. coli* and 0, 1, 2, 3, 4, 5, 6 µg/ml of erythromycin, 0, 0.09, 0.1, 0.2, 0.3, 0.4 µg/ml of fusidic acid, 0, 0.9, 1, 2, 3, 4 µg/ml of kanamycin, 0, 0.07, 0.08, 0.09, 0.1, 0.2 µg/ml of oxacillin, 0, 0.09, 0.1, 0.2, 0.3, 0.4 µg/ml of tetracycline and 0, 0.5, 0.8, 1, 1.5, 2 µg/ml of vancomycin for *S. aureus*. The wash off from stainless steel was diluted threefold to get cells that correspond to ~10^2 cells and the cells also transferred to the surface of LB plates containing various concentration of antibiotics. Plates were then incubated at 37°C for 24 hours. All experiments were conducted three times to obtain biological replicates. Three samples of each (test and control) were used for each experiment to obtain technical replicates. The plates were monitored for up to three days and colonies were counted and normalised to volume of solution to give colony forming units per ml (cfu/ml). This was compared for the various treatments (material and exposure conditions). There were variations in the values, thus, the cfu/ml counts were normalised to efficiency of plating (EOP) values using the formula described in equation 3.1. The EOP values were then used to plot graphs using graphpad prism software (*Prism - Graphpad.Com*, n.d.). R was used for statistical analysis (Rosario-Martinez et al., 2015).

Equation 3.1: Formula used to calculate efficiency of plating (EOP)

$$\text{EOP} = \frac{titre\ of\ treatments\ (\text{LB + antibiotics})}{titre\ of\ control\ (LB\ only\ )}$$

3.3.3 Experiment to determine if NsARC can induce genes associated with efflux pumps

For this experiment, the setup is shown in Figure 3.4. The design and construction of the two reporter strains is as described in Appendix D (Jun et al., 2019).

Each of the *E. coli* BW*tolC* and BW*soxS* reporter strains were individually picked and placed into LB broth (Lennox-L-Broth Base, Invitrogen (USA)) supplemented with kanamycin and then placed on a shaker platform at 37°C and grown to exponential phase. 100µl of each of the strains containing about ~10^7cells was then placed on separate NsARC (test), stainless steel (negative control) and stainless steel (positive control). 10µl of copper ammonium acetate (4.73g/L) was then added to the culture on the stainless steel sample marked as positive control. Sterile cover slips (24 mm × 24 mm) were used to spread the cultures on the sample surfaces. The samples were placed in petri dishes (60 mm × 15 mm) containing damp filter paper. Replicates were simultaneously exposed to high intensity visible light of 2100 lux (450-650 nm), UV light (365 nm), ambient light (650-750 nm) (see Figure 3.3) and also kept in the dark for a period of not more than 2 hours before washing off with PBS and the cells fixed with paraformaldehyde (Chao and Zhang, 2011).

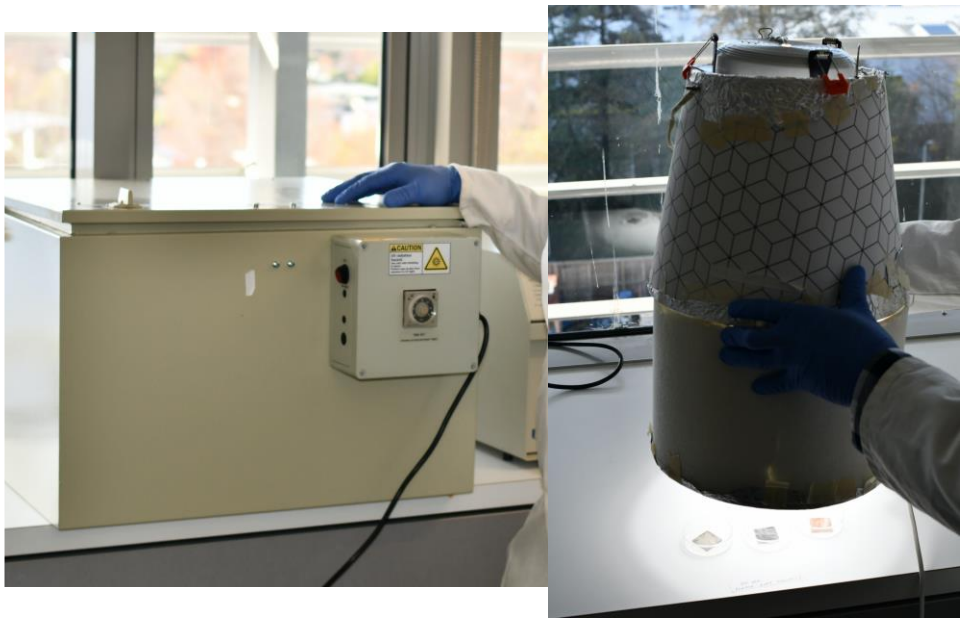

A B

Figure 3.3: Light source used for the experiment. (A) UV light box (B) High intensity LED light

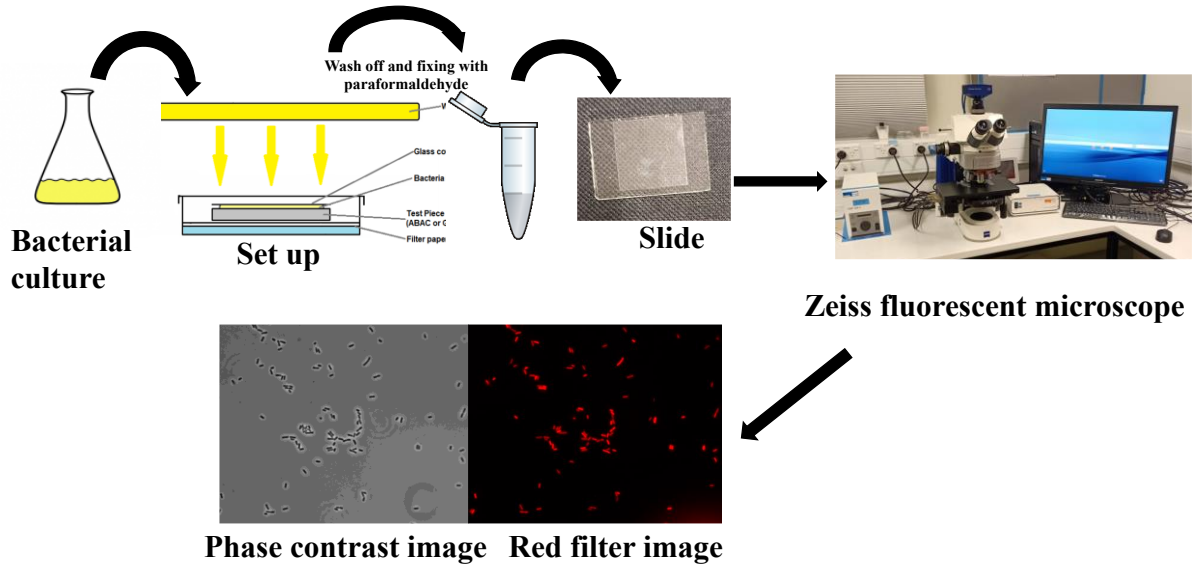

Figure 3.4: Experimental set up showing the various steps.

Bacteria in a liquid culture is placed on the samples and exposed to light, after which the bacteria was recovered and fix with paraformaldehyde. Cell are placed on gelatine coated slide and viewed under a fluorescent microscope and the images capture in phase contrast and using red filter.

3.3.3.1 Mounting of the fixed cells on gelatine coated slides

2 µl of fixed cells from section 3.4.3 was smeared onto a gelatine-coated glass slide and allowed to dry at room temperature. 6 µl of 50% glycerol was then added to the dried smear and a 25 × 25 mm glass cover slip was used to spread it over the dried smear.

3.3.3.2 Fluorescence microscopy imaging

Fixed and mounted cells were examined with an Axio Imager.M1 (Zeiss, Oberkochen, Germany) using 556/20 nm excitation bandpass. Digital images were captured at 100× magnification with an AxioCam MRm camera (Zeiss) in phase contrast and through a 556/20 nm (red) filter set (as shown in Figure 3.5). Approximately 10 NsARC and 10 control samples each were used for this experiment. And about 50 images were captured from each individual sample. A total of 500 images from each treatment was taken for each treatment replicate.

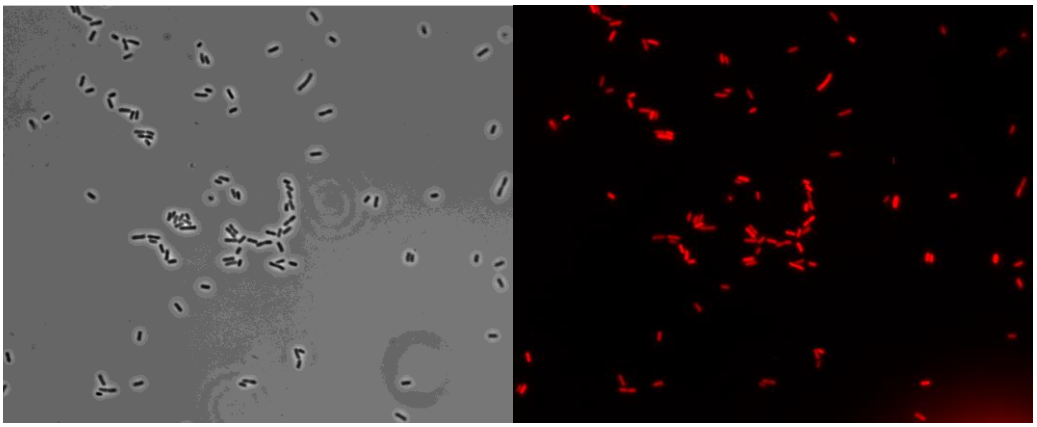

A B

Figure 3.5: Typical digital image of *E. coli* BW cell captured at 100× magnification in (A) Phase contrast and (B) 556/20 nm (red) filter set.

3.3.3.3 Image processing

Images were analysed using Fiji ImageJ (Schindelin et al., 2012). 100 separate images for each sample was analysed. Single-cell fluorescence intensity of the individual cells was obtained by acquiring multichannel images of the fluorescence signals and phase contrast signals. Multichannel images were imported into the Fiji ImageJ program. Thresholding command and standard settings were used to separate cells from the background based on the phase contrast. The analyse particles command was then used to add cells to the region of interest manager and the average fluorescence of the individual cells was determined using the "multi-measure" command (Remus-Emsermann et al., 2016). The relative fluorescence is also just an arbitrary unit (au) of measurement.

3.3.4 Experiment to determine if NsARC can interact with and affect the potency of antibiotics

Stainless steel, NsARC and copper coupons (24 × 24 mm) were individually placed in sterile Petri dishes (90 × 15 mm). Lauria Bertani (LB) (Lennox-L-Broth Base, Invitrogen (USA) and agar (Bacteriological Agar No.1, Oxoid (UK)) containing 2 µg/ml tetracycline (Sigma, Auckland) was

poured into each dish and allowed to set. A replicate of the set up was made, with just the LB agar and no tetracycline. Pure colonies of freshly grown *E. coli* BW25113 was then inoculated onto each petri dish using the spread plating method. And the petri dishes are then placed in the incubator and left for 3-4 day at 37^{o}C. Set up is shown in Figure 3.6.

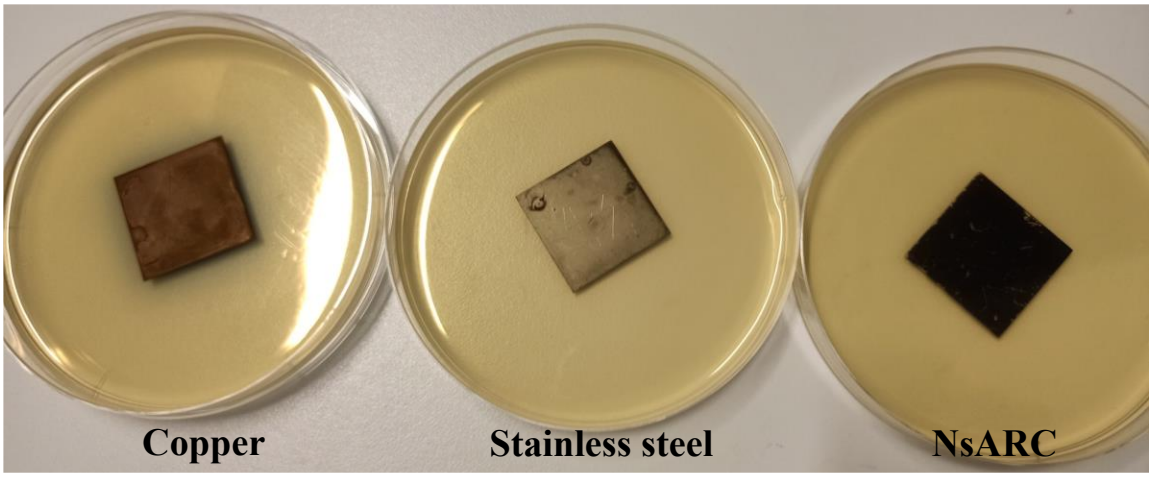

Figure 3.6: Set up showing copper, stainless steel and NsARC coupons embedded in petri dishes containing LB agar with or without tetracycline.

3.4 Statistical analysis

R was used for this statistical analysis (Rosario-Martinez et al., 2015).

3.4.1 Determine if NsARC can cause a change in susceptibility of *E. coli* and *S. aureus* to antibiotics

In the experiment to determine if exposure of bacteria to NsARC caused a change in susceptibility to antibiotics. A multifactor analysis of variance (ANOVA) was performed on EOP values to test for effect of the materials (NsARC and control) and antibiotic concentration under two exposure conditions (light and dark). Residual plots were examined to determine if EOP values were normally distributed, which is an assumption for ANOVA (Crawley, 2007). The plots were not normally distributed. So, the EOP scores were log transformed to meet the assumption. In each

case, I tested for significant difference between materials. The null hypothesis was that there was no difference between the EOP values from the materials at various antibiotic concentrations. I also tested for interaction between materials, antibiotic concentrations and exposure conditions. A Bonferroni's post hoc test was used to compare the EOP to determine if there is a significant difference between NsARC and the controls. The value for statistical significance was set at $P<0.05$. The ANOVA table and results of each post hoc are available in Appendix C, however, i was most interested in the differences in EOP between individual treatment combinations as follows: NsARC vs steel under light and NsARC vs steel in the dark. Contrast matrices listing the contrast of interest mentioned were drawn up and the test Interactions function in the phia package in R was used to evaluate the contrasts as described in the result section (Rosario-Martinez et al., 2015).

3.4.2 Determine if NsARC can induce genes associated with efflux pumps

For the experiment to determine if there was significant difference in fluorescence between reporter strains that were on NsARC and the control samples, a statistical model based on Analysis of variance (ANOVA) was used. A Tukey's post hoc test was used to compare the means of the relative fluorescence to determine if there is a difference between NsARC and the controls. The value for statistical significance was set at $P<0.05$. The ANOVA tables and results of each post hoc are available in Appendix E. However, I was most interested in the differences between individual treatment combinations, these include NsARC vs positive control (copper), Negative control (steel) vs Positive control (copper) and NsARC vs Negative control (steel). These were calculated using contrasts and are described in the results section. Violin plots were then made using ggplot2 (Wickham, 2016).

3.5 Results

3.5.1 Determine if NsARC can cause a change in susceptibility of *E. coli* and *S. aureus* to antibiotics

E. coli that have survived after exposure to NsARC was tested for survival on exposure to ciprofloxacin, chloramphenicol, kanamycin and tetracycline, respectively. *S. aureus* was tested against kanamycin, vancomycin, erythromycin, oxacillin, tetracycline and fusidic acid antibiotics, respectively. *E. coli* and *S. aureus* that were exposed NsARC with and without light for about 8 hours were cultured on LB agar supplemented with different concentrations of the selected antibiotics. Changes in response to a particular concentration of the antibiotic because of the previous exposure to NsARC were shown as differential EOP (Figure 3.7 & 3.8 and Figure A.1 & A.2). A significant change ($P<0.001$) in the EOP was observed for *E. coli* that was on NsARC under both light and no light before transfer to LB containing various concentrations of kanamycin (Figure 3.7 and 3.8). For *E. coli* that was on NsARC under UV light before transferring to LB + kan, there was a significant ($P<0.01$) 2 log decrease in EOP at kan concentrations of 4, 5 and 6 µg/ml (Figure 3.7 and Appendix C2). For *E. coli* that was on NsARC in the dark before transferring to LB + kan, there was also a significant ($P<0.01$) 2 log decrease in EOP at concentration 5, 6 and 8 µg/ml of kan as shown in Figure 3.8 (Appendix C4). However, no significant change in susceptibility was observed for tetracycline (Appendix C6&8), chloramphenicol (Appendix C10&12) and ciprofloxacin (Appendix C14&16) (Figures A.1).

No significant change in susceptibility to kanamycin (Appendix C18&20), vancomycin (Appendix C22&24), erythromycin (Appendix C26&28), oxacillin (Appendix C30&32), tetracycline (Appendix C34&36) or fusidic acid (Appendix C38&40) antibiotics was observed when *S. aureus* was exposed to NsARC (Figure A.2).

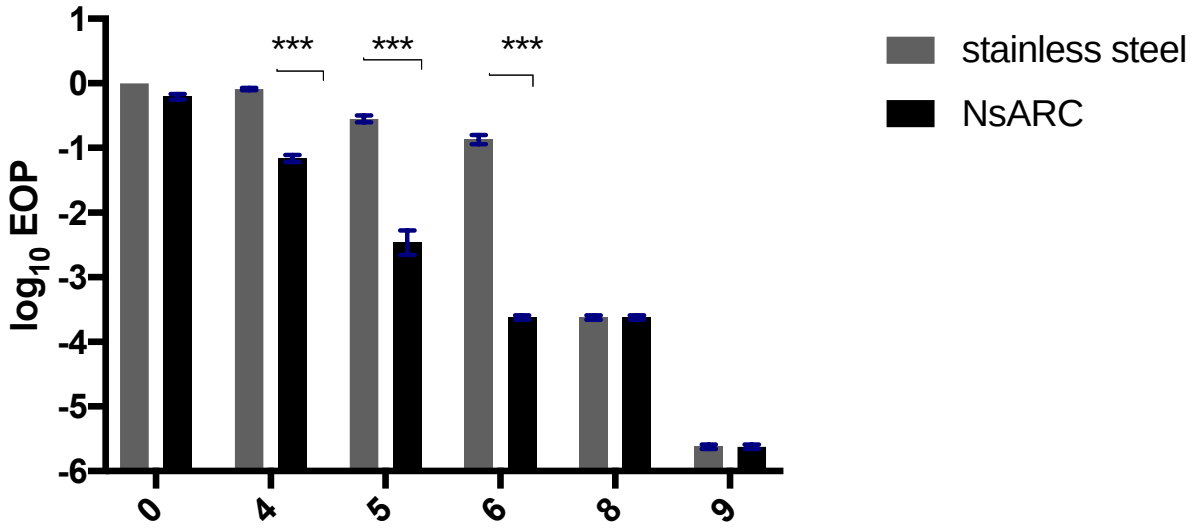

Figure 3.7: Response of *E. coli* to various concentrations (µg/ml) of kanamycin after exposure to NsARC under UV light.

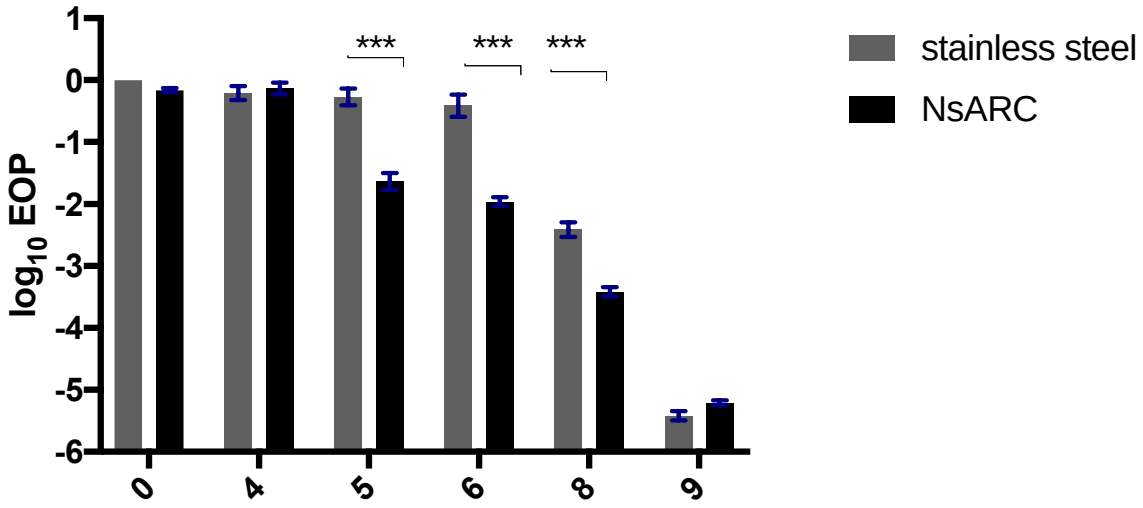

Figure 3.8: Response of *E.coli* to various concentrations (µg/ml) of kanamycin after exposure to NsARC in the dark.

3.5.2 Determine if NsARC can induce genes associated with efflux pumps

This section describes the experiment done to investigate the possible effects of NsARC on genes associated with efflux pump. The experiment was carried out as described in section 3.4.3. Two

reporter strains expressing *PtolC*-mScarlet and *PsoxS*-mScarlet were exposed to NsARC, stainless steel and copper and their fluorescence intensities measured. Reporter strains expressing *PtolC*-mScarlet were brighter than the reporter strains expressing *PsoxS*-mScarlet. There were also variations in the fluorescence of the strains that were on NsARC, stainless steel and stainless steel + copper under all the exposure conditions (high intensity visible, UV, ambient light and no light) ($P<0.001$) indicating that both material type and exposure conditions are major causes for the variation in the fluorescence intensities. Both reporter strains were brighter on steel + copper under all exposure conditions compared to when they were on NsARC and stainless steel (Figures 3.9-3.16).

For the reporter strains expressing *PtolC*-mScarlet, it was observed that under UV light (Figure 3.9), reporter strains that were on steel + copper were significantly brighter than the ones that were on NsARC ($P<0.001$) and steel alone ($P<0.001$). The strains that were on NsARC were significantly brighter ($P<0.001$) than the ones that were on steel (Appendix E2). Under high-intensity visible light (Figure 3.10), reporter strains that were on NsARC were significantly brighter ($P<0.001$) than the ones on steel (Appendix E4). But, under ambient light (Figure 3.11), reporter strains on NsARC were not significantly brighter ($P=0.357$) than the ones on steel (Appendix E6). Also, in the dark (Figure 3.12) Reporter strains on NsARC were not significantly brighter ($P=0.479$) than on steel (Appendix E8).

For the reporter strains expressing *PsoxS*-mScarlet, it was observed that under UV light (Figure 3.13), reporter strains on NsARC were significantly brighter ($P<0.001$) than on steel (Appendix E10). Under high-intensity visible light (Figure 3.14), reporter strains that were on NsARC were also significantly brighter ($P=0.003$) than the ones that were on steel ($P=0.003$) (Appendix E12). Under ambient light (Figure 3.15), there was no significant difference ($P=0.105$) in the brightness

of the reporter strains that were on NsARC and steel (Appendix E14). Finally, in the dark (Figure 3.16), reporter strains were significantly brighter (P=0.009) on NsARC than on steel (Appendix E16).

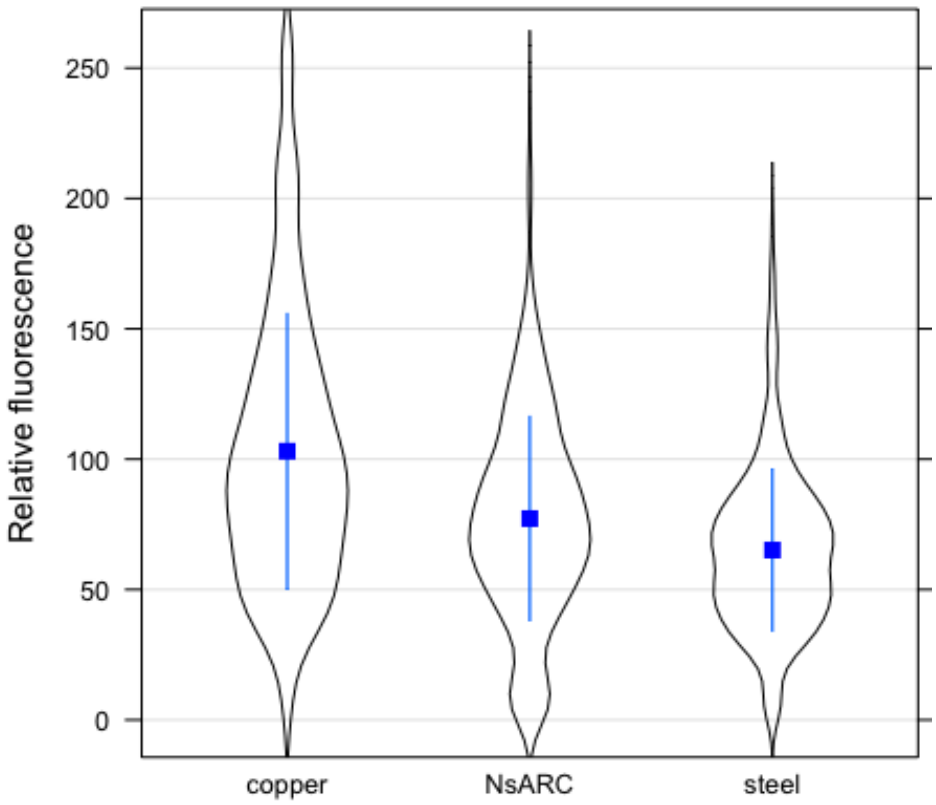

Figure 3.9: Single-cell fluorescence intensity of *E. coli* BWtolC expressing mScarlet red fluorescent protein under the control of the *tolC* promoter upon exposure to copper, NsARC and stainless steel under UV light.

The violin plots show the distribution of the single-cell fluorescence within the cell population. The bar in the box depicts the median and the box shows the 25% and 75% quartiles.

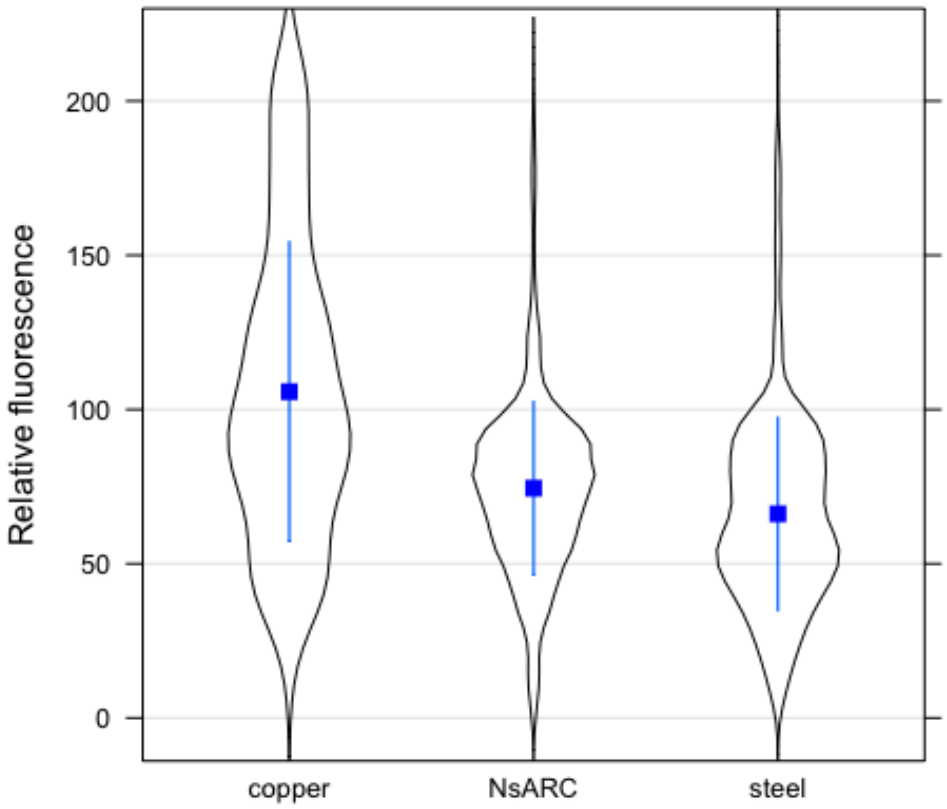

Figure 3.10: Single-cell fluorescence intensity of *E. coli* BWtolC expressing mScarlet red fluorescent protein under the control of the *tolC* promoter upon exposure to copper, NsARC and stainless steel under high intensity visible light.

The violins show the distribution of the single-cell fluorescence within the cell population. The bar in the box depicts the median and the box shows the 25% and 75% quartiles.

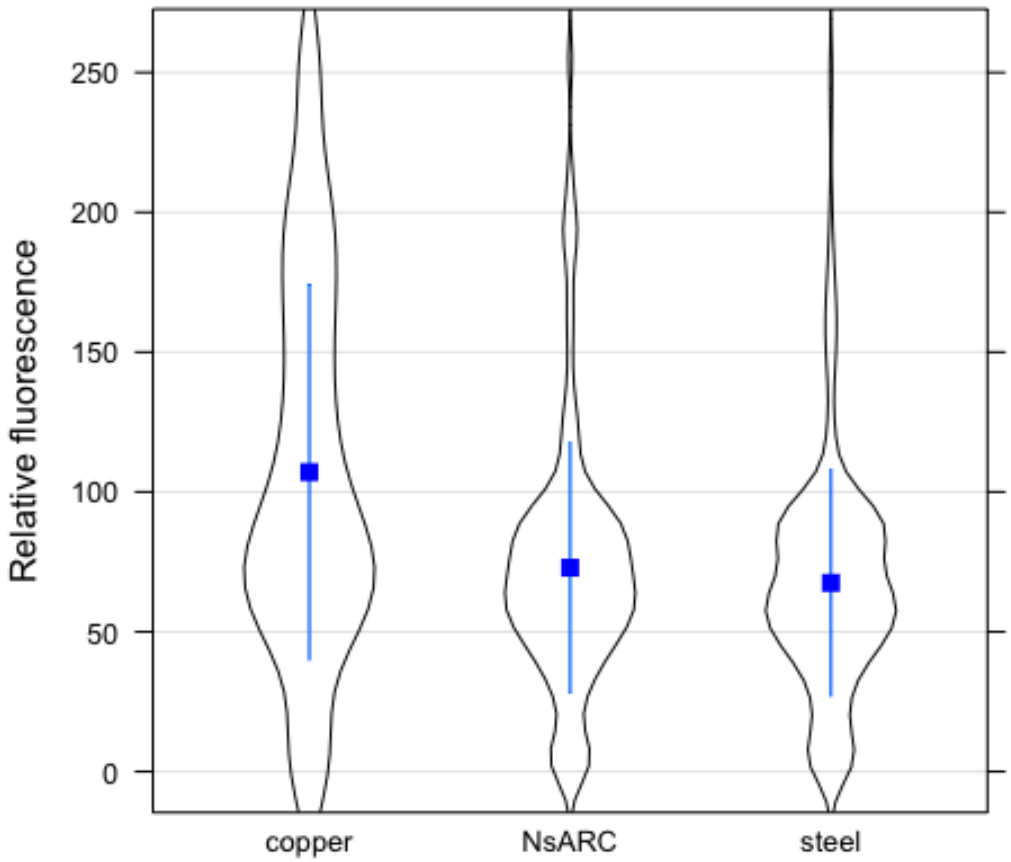

Figure 3.11: Single-cell fluorescence intensity of *E. coli* BWtolC expressing mScarlet red fluorescent protein under the control of the *tolC* promoter upon exposure to copper, NsARC and stainless steel under ambient light.

The violin show the distribution of the single-cell fluorescence within the cell population. The bar in the box depicts the median and the box shows the 25% and 75% quartiles.

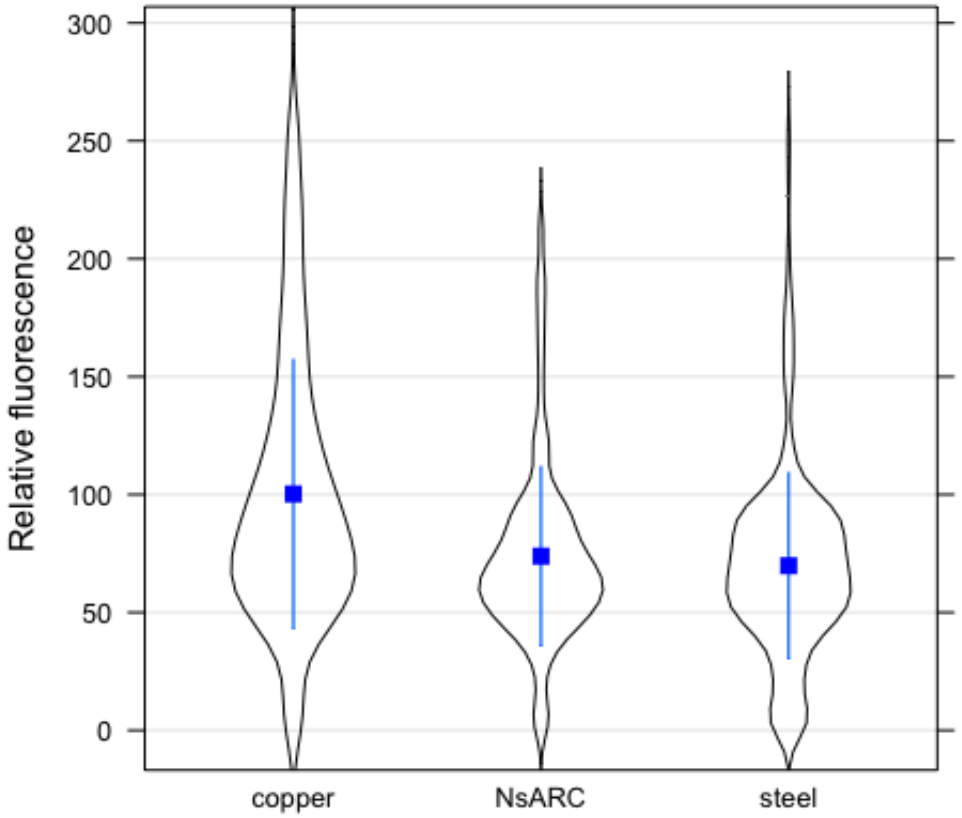

Figure 3.12: Single-cell fluorescence intensity of *E. coli* BWtolC expressing mScarlet red fluorescent protein under the control of the *tolC* promoter upon exposure to copper, NsARC and stainless steel in the dark.

The violin show the distribution of the single-cell fluorescence within the cell population. The bar in the box depicts the median and the box shows the 25% and 75% quartiles.

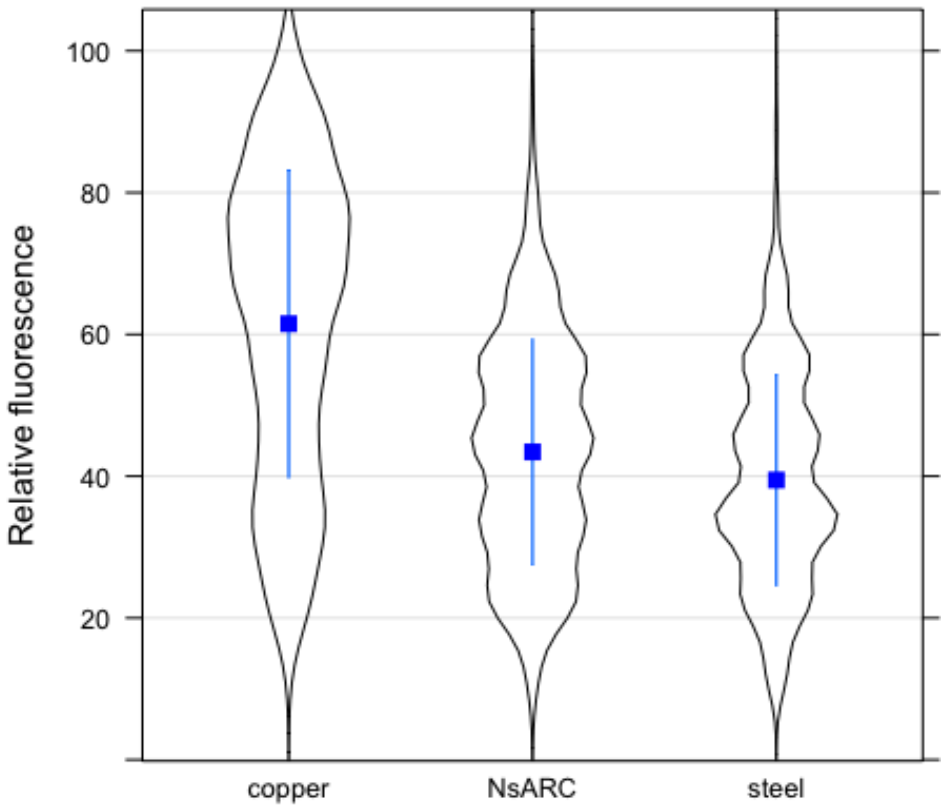

Figure 3.13: Single-cell fluorescence intensity of *E. coli* BWsoxS expressing mScarlet red fluorescent protein under the control of the *soxS* promoter upon exposure to copper, NsARC and stainless steel under UV light.

The violin show the distribution of the single-cell fluorescence within the cell population. The bar in the box depicts the median and the box shows the 25% and 75% quartiles.

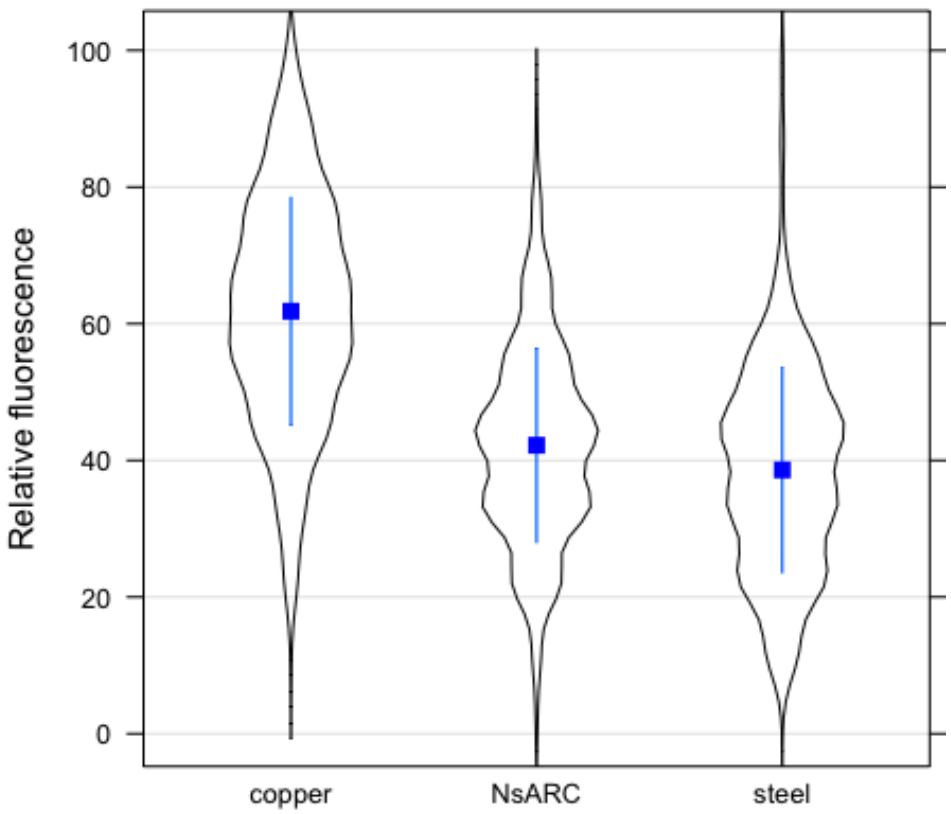

Figure 3.14: Single-cell fluorescence intensity of *E. coli* BWsoxS expressing mScarlet red fluorescent protein under the control of the *soxS* promoter upon exposure to copper, NsARC and stainless steel under high intensity visible light.

The violin show the distribution of the single-cell fluorescence within the cell population. The bar in the box depicts the median and the box shows the 25% and 75% quartiles.

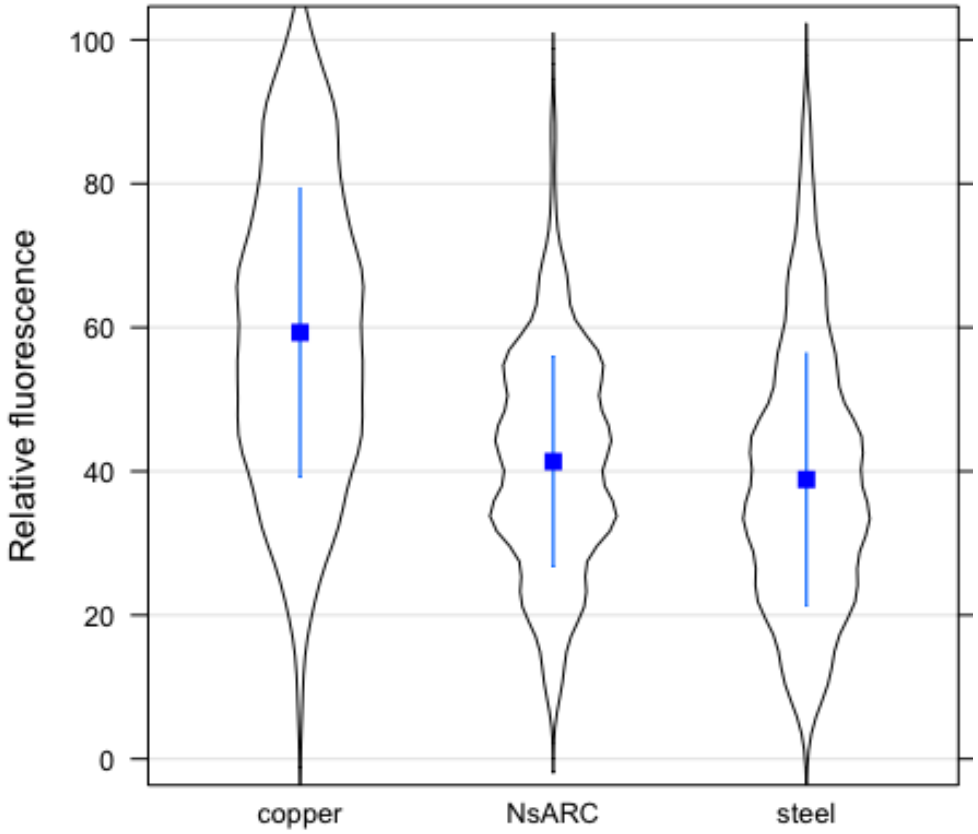

Figure 3.15: Single-cell fluorescence intensity of *E. coli* BWsoxS expressing mScarlet red fluorescent protein under the control of the *soxS* promoter upon exposure to copper, NsARC and stainless steel under ambient light.

The violin show the distribution of the single-cell fluorescence within the cell population. The bar in the box depicts the median and the box shows the 25% and 75% quartiles.

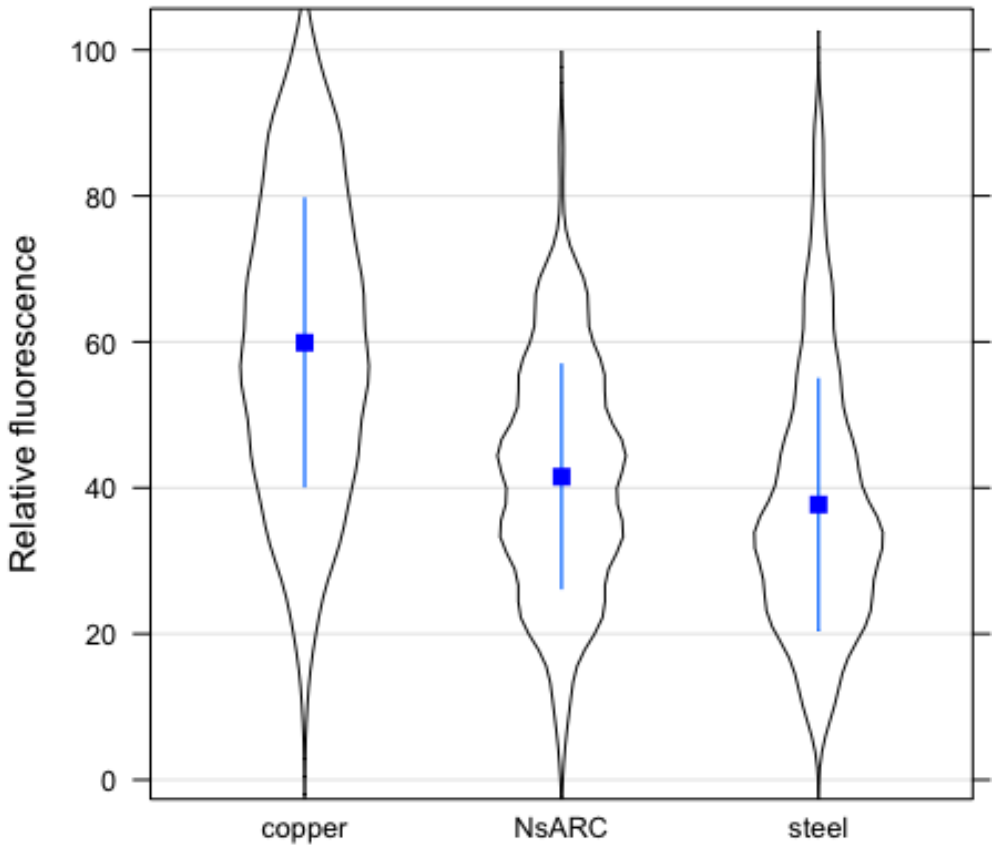

Figure 3.16: Single-cell fluorescence intensity of *E. coli* BWsoxS expressing mScarlet red fluorescent protein under the control of the *soxS* promoter upon exposure to copper, NsARC and stainless steel in the dark.

The violin show the distribution of the single-cell fluorescence within the cell population. The bar in the box depicts the median and the box shows the 25% and 75% quartiles.

3.5.3 Determine if NsARC can interact with and affect the potency of antibiotics

In a culture medium, tetracycline and copper can interact resulting in a reduction in the efficacy of tetracycline. This reduction in efficacy may be as a result of chelation of tetracycline by copper. To determine if a similar interaction is possible with NsARC, the experiment shown in Figure 3.6 was set up. The experiment was monitored daily for a week. The image of coupons embedded in media inoculated with *E. coli* is shown in Figure 3.17. The plates in A, B and C had stainless steel, NsARC and copper coupons, respectively, embedded in LB + tetracycline + *E. coli*, while D, E and F had stainless steel, NsARC and copper coupons embedded in LB + *E. coli* without tetracycline. There was no growth on tet plates A and B containing the stainless steel and the NsARC coupons, but there was a "ring" of growth on plate C with the copper coupon (Figure 3.17). There was uniform growth on plates D and F containing the stainless steel and the NsARC coupons, but in plate F with the copper coupon the growth was restricted to regions about 5mm in diameter away from the copper coupon.

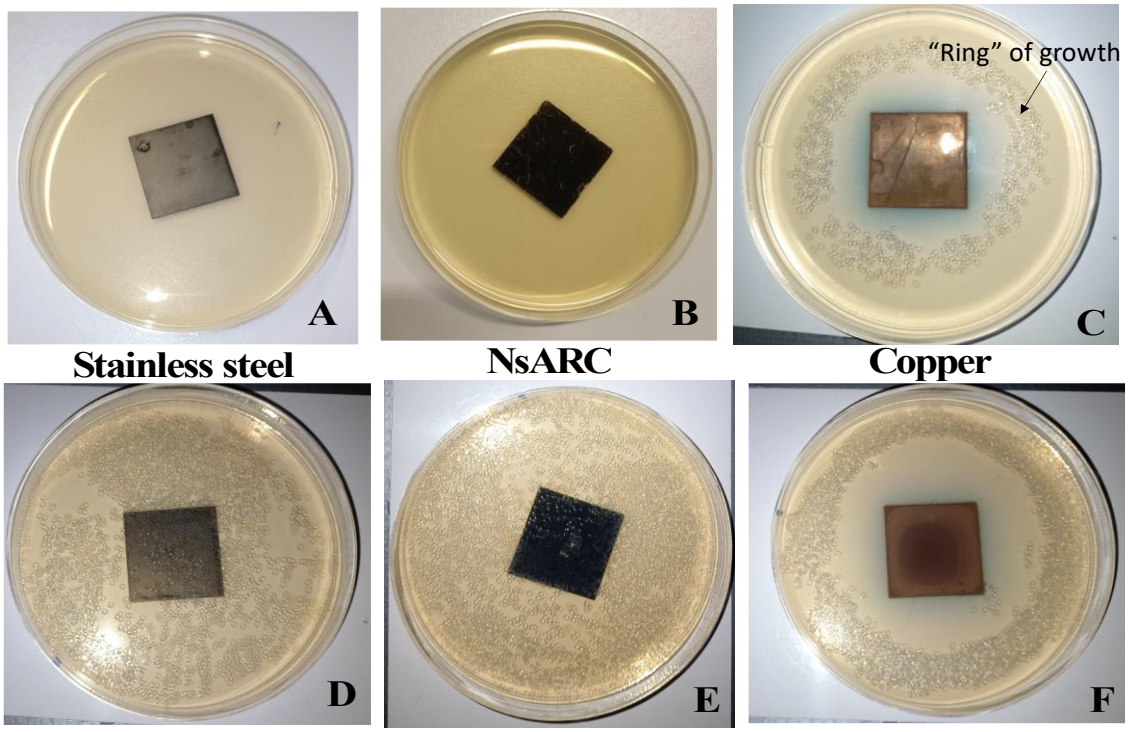

Figure 3.17: Typical image of (A) Stainless steel (B) NsARC (C) Copper coupons embedded in LB + tetracycline (2 µg/ml) inoculated with *E. coli* BW25113 and (D) Stainless steel (E) NsARC (F) Copper coupons embedded in LB and inoculated with *E. coli* BW25113

3.6 Discussion

In this section I discussed the outcome of some experiments that I carried out to determine if exposing bacteria to NsARC could cause the bacteria to develop resistance to some antibiotics.

3.6.1 NsARC can cause a change in susceptibility to antibiotics

Exposure of *E. coli* and *S. aureus* to non-antibiotic antimicrobials and antibiotics simultaneously can accelerate the evolution of genotypically antibiotic resistant mutants (Kurenbach et al., 2018). I tested *E. coli* and *S. aureus* that has survived exposure to NsARC on some selected antibiotics to find out if there was a change in their susceptibility to various antibiotics. I observed that there was a significant increase in susceptibility to kanamycin among *E. coli* strains that have survived exposure to NsARC, when compared to the *E. coli* strains that were not exposed to NsARC. A similar increase in susceptibility to kanamycin was observed when *E. coli* was exposed to sublethal concentrations of roundup (herbicide) (Kurenbach et al., 2015). There was no significant change in susceptibility to ciprofloxacin, chloramphenicol and tetracycline among *E. coli* strains that have survived exposure to NsARC and the ones that were not exposed to NsARC. I also observed that there was also no significant change in susceptibility to kanamycin, vancomycin, erythromycin, oxacillin, tetracycline and fusidic acid antibiotics among *S. aureus* strains that survived exposure to NsARC and the one that were not exposed to NsARC,

3.6.2 NsARC can induce genes associated with efflux pumps

The use of the described reporter strains to determine a change in efflux activity upon exposure to any material is a method for investigating the potential effects of NsARC. Reporter strains that were exposed to copper were significantly brighter than the ones that were exposed to NsARC and stainless steel (Figure 3.9-3.16). The increase in fluorescence of the reporter strains that were exposed to copper is not surprising because copper is a known inducer of *soxS* and *tolC*

transcription (Franke et al., 2003; Nishino et al., 2007). Copper can also induce *marR*, making *marR* an agent that acts as a copper sensor (Hao et al., 2014). The increase in cell fluorescence may be due to oxidative activity of the copper (Fenoglio Ivana et al., 2009).

Reporter strains that were exposed to NsARC under UV and high intensity light were significantly brighter than the strains that were on stainless under the same conditions. Cells that were exposed to both NsARC and stainless steel under ambient light or no light demonstrated no significant difference in brightness. The major reason for the difference in brightness in the presence or absence of light is not known, but possibly it is because light excitation of NsARC is needed in order to facilitates the production of ROS and other free radicals that can induce *soxS* and *tolC* genes (Koutsolioutsou et al., 2005; Verdier et al., 2014). Absence of light excitation affects the production of free radical and hence these gene are not induced with no corresponding effect on the brightness of the cell.

3.6.3 Copper can interact with and affect the potency of antibiotics

Copper is known to interact with tetracycline when they are in combination and it results in the decrease in the effective concentration of both. This decrease is usually due to chelation of tetracycline by copper and an adaptive resistance pathway induced by copper (Jun et al., 2019). In the LB + tetracycline plates containing the copper coupon (Figure 3.17), there was no growth in the region close to the coupon, attributed to the antimicrobial activity of the high concentration of copper ions around the region. But further away from the coupon the concentration of the soluble copper ion is lower, but is still able to interact and form a complex with tetracycline. Because tetracycline is a bacteriostatic antibiotic that inhibits the growth of bacteria without necessarily killing it, the bacteria is able to grow as seen from the “ring” of growth (Figure 3.17). Further away from the “ring” of growth, there was no growth probably because there was little or no interaction

between copper and tetracycline and so bacterial growth was inhibited by the tetracycline. There was no growth on the plate with the NsARC coupon probably because NsARC may not have been able to facilitate the release of free radicals that are able to interact with the tetracycline or induce an adaptive response from the bacteria. The plate assay may also not be sensitive enough for me to make a definite conclusion.

4 Chapter Four

4.1 General Introduction

Bacteria can acquire new traits such as resistance to antibiotics from the environment through mutations and horizontal gene transfer (HGT) (Blair et al., 2015; Finley et al., 2013). It is more likely for bacteria to acquire new genes from an environment with high bacterial cell density and microbial diversity than in an environment with a low density of bacteria and less microbial diversity (Metcalfe et al., 2016).

Microbes can be exposed to antibiotics, biocides, herbicides and pesticides in many environments (Kurenbach et al., 2018). Antibiotics and biocides used by humans and on animals for treatment of infections can get to the soil directly by irrigation with surface or wastewater (Wellington et al., 2013) (see Figure 4.1). Herbicides and insecticides used for the control of unwanted plants and insects, respectively, can also leach into the environment. Antibiotics, biocides and herbicides found in the environment even at sublethal doses can contribute to the selection of bacteria that are resistant to one or more types antimicrobial agents (Kurenbach et al., 2018). Therefore, contaminated environments are reservoirs of resistant bacteria and also sources of different types of genes. Bacteriophages, transposons and plasmids are mobile genetic elements found in the environment, and they carry many different types of genes, such as antibiotic resistance genes (Heinemann, 1999). Extended-spectrum beta-lactamase (ESBL) and other genes associated with antibiotic resistance have been detected in strains of *E. coli* isolated from the environment (Jang et al., 2017; Van Hamelsveld et al., 2019; Wellington et al., 2013).

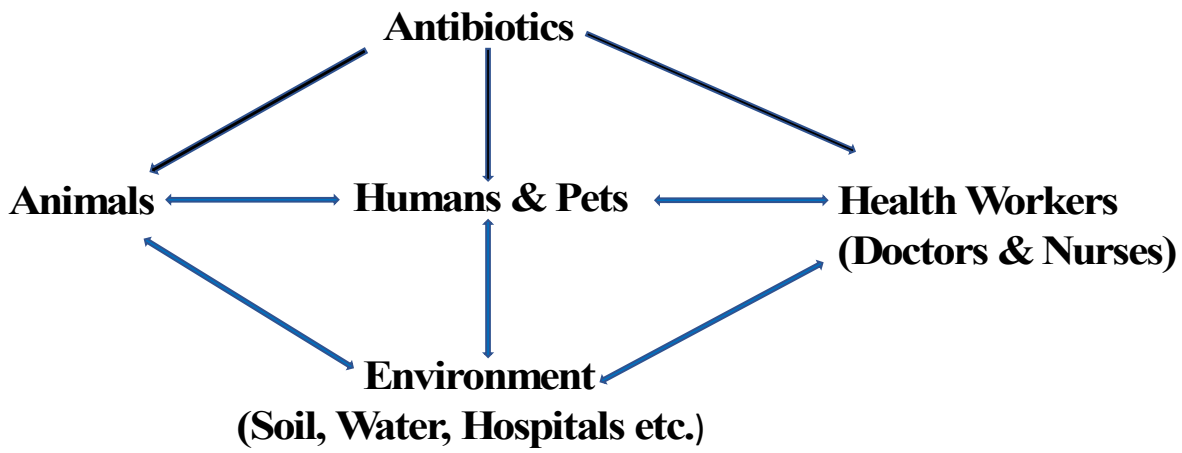

Figure 4.1: Representation of how antibiotic resistance is spread.

4.2 Laboratory strains vs environmental strains

Environmental and laboratory strains of bacteria have different characteristics. Environmental strains are likely to show higher tolerance to oxidative stress (Jang et al., 2017), change in temperature and pH compared to some laboratory strains (van Elsas et al., 2011). For example, environmental strains of *E. coli* showed higher levels of transcription for stress defence genes under unusual growth conditions such as limited oxygen, limited carbon and low-nutrient conditions (van Elsas et al., 2011). Comparative transcriptome analysis between environmental and laboratory strains suggests that environmental *E. coli* strains are more likely to adapt to an adverse environments compared to a laboratory strain (van Elsas et al., 2011). Niestepski et al. (2019) suggested that bacteria isolated from the environment were also more likely to be more tolerant to antibiotics and stress that can be caused by ROS, heat shock and freezing than laboratory strains. The possible reason for the increase in tolerance may be because laboratory strains have been sub-cultured for long periods since their first isolation and might have lost some genes associated with tolerance to environmental stress (Wellington et al., 2013). Environmental strains are also more likely to acquire plasmids and transposons that carry antibiotic resistant genes than

laboratory strains that are mostly grown in vitro in pure cultures and stored free from conditions that will likely induce mechanisms associated with the acquisition of antibiotic resistance (Wellington et al., 2013). The bacterial species that were used for AMA testing that I discussed in Chapter Two were laboratory strains and therefore may not be representative of those the NsARC will encounter if deployed in relevant environments. So, I was interested in finding out how bacteria isolated from the environment respond to exposure to NsARC, and I decided to carry out AMA testing of some selected strains of *E. coli* that were isolated from the environment.

4.2.1 Plasmids and resistance to biocides

Bacteria can carry self-replicating double-stranded circular DNA elements called plasmids. These plasmids are usually large, >50 kb, self-transmissible, and encode mechanisms that control their copy number and regulate the rate at which they replicate (Amaya et al., 2012). They can harbour genes that promote their stability and maintenance in a bacterial host under different environmental conditions. Plasmids contribute to the spread and dissemination of antimicrobial resistance and also promote horizontal gene transfer among unrelated bacteria (Jørgensen et al., 2017).

I was also interested in finding out how bacteria that carry a plasmid respond to the antimicrobial activity of NsARC. The questions I wanted to answer were:

i. Can bacteria carrying a plasmid with antibiotic resistance gene(s) survive on NsARC?
ii. If the bacteria carrying the plasmid are able to survive on NsARC, what part of the plasmid was responsible for the survival?

To answer these questions, I decided to test the survival of two *E. coli* strains that I had transformed using a plasmid construct that has antibiotic resistance genes. The design and development of these constructs is found in appendix D.

4.3 Methodology

4.3.1 Bacterial strains and cultivation

All the bacterial strains used in this study are shown in Table 4.1. The bacterial strains with the plasmid constructs were all transformed as described in appendix D. These bacterial strains were stored in 15% glycerol solution at -80°C. To recover these strains, Lauria Bertani (LB) agar plates (Lennox-L-Broth Base, Invitrogen (USA) and agar (Bacteriological Agar No.1, Oxoid (UK)) were inoculated with loopfuls of the samples and the plates incubated at 37°C for 18-24 hours. These plates are stored at 4°C for not longer than one week. To recover the bacteria, LB broth (Lennox-L-Broth Base, Invitrogen (USA)) was inoculated with a colony that was picked from the plates and aerated using a rotary shaker at 37°C and grown to saturation.

Table 4.1: *E. coli* strains and plasmids used in the study

E. coli	Notable feature	Reference
BW25113	F^-, λ^-, Δ(*araD-araB*)567, Δ*lacZ4787(::rrnB-3*), *rph-1*,Δ(*rhaD-rhaB*)568, *hsdR*514	(Baba et al., 2006)
CMB27	*aph*(3")-Ib, *aph*(6)-Id, *blaCTX*-M-27, *mph*(A), *sul2*, tet(A), Cip^R, Tet^R, Amp^R	(Van Hamelsveld et al., 2019)
CMB28	aph(3")-Ib, aph(6)-Id, *blaC*TX-M-27, *mph(*A), sul2, tet(A), Ctx^R, Amp^R, Tet^R, Cip^R	(Van Hamelsveld et al., 2019)
CMB42	none	(Van Hamelsveld et al., 2019)
CMB43	none	(Van Hamelsveld et al., 2019)
CMB44	none	(Van Hamelsveld et al., 2019)
CMB45	none	(Van Hamelsveld et al., 2019)
CMB70	tet^R	(Van Hamelsveld et al., 2019)

CMB73	IncFIA, IncFIB(AP001918)	(Van Hamelsveld et al., 2019)
Plasmid		
pFru97	nptII promoter, dsRed, Kan^R, Cam^R	(Tecon and Leveau, 2012)
pUC19	Amp^R	(Mendes et al., 2015)
pFru-p_{tolC}-mScarlet	cat, nptII, pBBR1, *tolC* promoter:mScarlet-I	(Jun et al., 2019)
pFru-p_{soxS}-mScarlet	cat, nptII, pBBR1, *soxS* promoter:mScarlet-I	(Jun et al., 2019)
pMRE132	sGFP, Kan^R, Cam^R	(Schlechter et al., 2018)
pMRE133	sYFP, Kan^R, Cam^R	(Schlechter et al., 2018)
pMRE135	RFP, Kan^R, Cam^R	(Schlechter et al., 2018)
pMRE145	RFP, Kan^R, Cam^R,$Gent^R$	(Schlechter et al., 2018)
pMRE165	RFP, Kan^R, Cam^R,Tet^R	(Schlechter et al., 2018)
***E. coli* with plasmids**		
BWtolC	BW25113 (pFru-p_{tolC}-mScarlet)	(Jun et al., 2019)
BWsoxS	BW25113 (pFru-p_{soxS}-mScarlet)	(Jun et al., 2019)
BWpFru97	BW25113(pFru97)	This study
CMB73tolC	CMB73 (pFru-p_{tolC}-mScarlet)	This study
CMB73soxS	CMB73 (pFru-p_{soxS}-mScarlet)	This study
BWpUC19	BW25113 (pUC19)	This study
BWpMRE132	BW25113 (pMRE132)	This study
BWpMRE133	BW25113 (pMRE133)	This study
BWpMRE135	BW25113 (pMRE135)	This study
BWpMRE145	BW25113 (pMRE145)	This study
BWpMRE165	BW25113 (pMRE165)	This study

4.3.2 Survival of environmental *E. coli* isolates on NsARC

Eight *E. coli* strains (Van Hamelsveld et al., 2019) isolated from water and sediments of two rivers in Christchurch, New Zealand were used for the experiments. ISO 27447:2009, "test method for antimicrobial activity of semi conducting photocatalytic materials" as previously described in Chapter Two was used to determine the survival of environmental *E. coli* strains on NsARC. All experiments were conducted three times to obtain biological replicates. Three samples of each (test and control) were used for each experiment to obtain technical replicates.

All environmental isolates were prepared as described in section 2.3.4, and kept under high intensity visible light of 2100 lux (450-650 nm) for a period of up to 8 hrs. The bacterial cells were then recovered on tryptic soy agar (TSA) (Sigma-Aldrich (USA)) plates. The plates were incubated at 37°C for 18 hours. The colonies from the plates were counted and the values converted to EOP as described in section 2.3.4.

4.3.3 Survival of *E. coli* BWtolC and *E. coli* BWsoxS on NsARC

E. coli BwtolC and BWsoxS that harbour pFru-p_{tolC}-mScarlet and pFru-p_{soxS}-mScarlet plasmid (see section 3.4.3), respectively, were used for this experiment. Each was individually transferred to separate McCartney bottles with LB broth (Lennox-L-Broth Base, Invitrogen (USA)) supplemented with kanamycin and then placed on a shaker platform at 37°C and grown to saturation. 50 µl of each of the strains containing about ~500,000 cells were then placed on separate NsARC and stainless steel (24 × 24 mm) coupons, sterile cover slips (24 mm × 24 mm) were used to spread the cultures on the surfaces of the coupons. The coupons were placed in petri dishes (60 mm × 15 mm) containing damp filter paper. Replicates were simultaneously exposed to high intensity visible light of 2100 lux (450-650 nm), UV light (365 nm), ambient light (650-750 nm)

and also kept in the dark for a period of 8 hours before washing off with PBS. The set-up is then treated as described section 2.3.4.

4.3.4 Survival of *E. coli* BWpruf97, BWtolC, BWsoxS and isogenic parent strain (*E. coli* BW25113) and CMBtolC and CMBsox on NsARC

E. coli BW25113 was picked and placed into separate LB broth (Lennox-L-Broth Base, Invitrogen (USA)), while BWpFru97, BWtolC and BWsoxS, CMBtolC and CMBsoxS were each individually picked and placed into separate LB broth (Lennox-L-Broth Base, Invitrogen (USA)) supplemented with kanamycin. All the organisms were then placed on a shaker platform at 37°C and grown to saturation. Phosphate buffer saline (PBS) was used to wash and re-suspend the organisms. The organisms were then each treated as described earlier in section 2.3.4

4.3.5 Survival of different *E. coli* BW25113 strains expressing fluorescent proteins

E. coli BW 25113 pMRE 132, pMRE 133, pMRE 135, pMRE 145 and pMRE 165 expressing green fluorescent protein (sGFP), yellow fluorescent protein (sYFP) and red fluorescent protein (RFP), respectively, (widefield microscopy images shown in Figure 4.9) were treated as described in section 2.3.4.

4.3.6 Survival of induced and uninduced *E. coli* pUC19 on NsARC

4.3.6.1 Induction of cultures with IPTG and experiment.

100 ml of overnight culture of *E. coli* pUC19 was transferred into McCartney bottles containing LB supplemented with ampicillin and the OD600 adjusted to 0.2. The culture was then divided into two equal portions; IPTG was added to a final concentration of 1 mM to one portion, while to the other, IPTG was not added. Miller's assay was carried out to determine if protein expression was induced in culture that was supplemented with IPTG.

Induced and uninduced strains of *E. coli* pUC19 were then treated as described in section 2.3.4

4.4 Statistical analysis

R was used for this statistical analysis (Rosario-Martinez et al., 2015).

4.4.1 Survival Environmental isolates on NsARC

For this experiment, I used ANOVA to test for effect of the materials (NsARC and control) on the survival of the test organisms. In each case, log transformed EOP values were tested for significant difference between materials. The null hypothesis was that there was no difference between the EOP values from the NsARC and stainless steel. A Bonferroni's post hoc test were used to compare the EOPs to determine if there is a significant difference between NsARC and stainless steel. The value for statistical significance was set at $P<0.05$. The ANOVA table and results of each post hoc are available in Appendix A

4.4.2 Survival *E. coli* BWtolC and BWsoxS on NsARC

For the experiment to determine the survival BWtolC and BWsoxS on NsARC under various exposure conditions, a multifactor analysis of variance (ANOVA) was performed on the EOP values to test for significant effect of the materials (NsARC and control) and exposure conditions (high intensity visible light, UV light, ambient light and dark). Log transformed EOP values were tested for significant difference between materials and exposure conditions. The null hypothesis was that there was no difference between the EOP values from the materials under the various exposure conditions. I also tested for interaction between materials and exposure conditions. A Bonferroni's post hoc test was used to compare the EOP to determine if there is a significant difference between NsARC and the controls. The value for statistical significance was set at $P<0.05$. The ANOVA table and results of each post hoc are available in Appendix A. Contrast matrices listing the contrast of interest were drawn up and the test Interactions function in the phia

package in R was used to evaluate the contrasts as described in the result section (Rosario-Martinez et al., 2015).

4.4.3 Survival of *E. coli* BW25113, BWpFru97, BWtolC and BWsoxS strains on NsARC

For this experiment, a multifactor analysis of variance (ANOVA) was used to test for effect of the materials (NsARC and control) on the survival of the isolates. Log transformed EOP values were tested for significant difference between materials. The null hypothesis was that there was no difference between the EOP values from the NsARC and stainless steel. A Bonferroni's post hoc test was used to compare the EOP to determine if there is a significant difference in survival between the different strains on NsARC and stainless steel. The value for statistical significance was set at $P<0.05$. The ANOVA table and results of each post hoc are available in Appendix A. Contrast matrices listing the contrast of interest were drawn up and the test Interactions function in the phia package in R was used to evaluate the contrasts as described in the result section (Rosario-Martinez et al., 2015).

4.4.4 Survival of parent *E. coli* CMB73, CMB73tolC and CMBsoxS on NsARC

For this experiment, ANOVA was used to test for effect of the materials (NsARC and control) on the survival of the isolates as described earlier in section 4.4.3

4.4.5 Survival of Fluorescent labelled bacteria on NsARC

For this experiment, ANOVA was used to test for effect of the materials (NsARC and control) on the survival of the isolates as described earlier in section 4.4.3.

4.4.6 Survival of induced and uninduced bacteria on NsARC

For this experiment, ANOVA was used to test for effect of the materials (NsARC and control) on the survival of the induced and uninduced isolates as described earlier in section 4.4.3.

4.5 Results

4.5.1 Survival of environmental isolates on NsARC

There was a greater than 3 log decrease in survival of all the environmental isolates on NsARC (Figure 4.2). There was also no significant difference (P>0.05) in the survival of the different strains on NsARC (Figure 4.2).

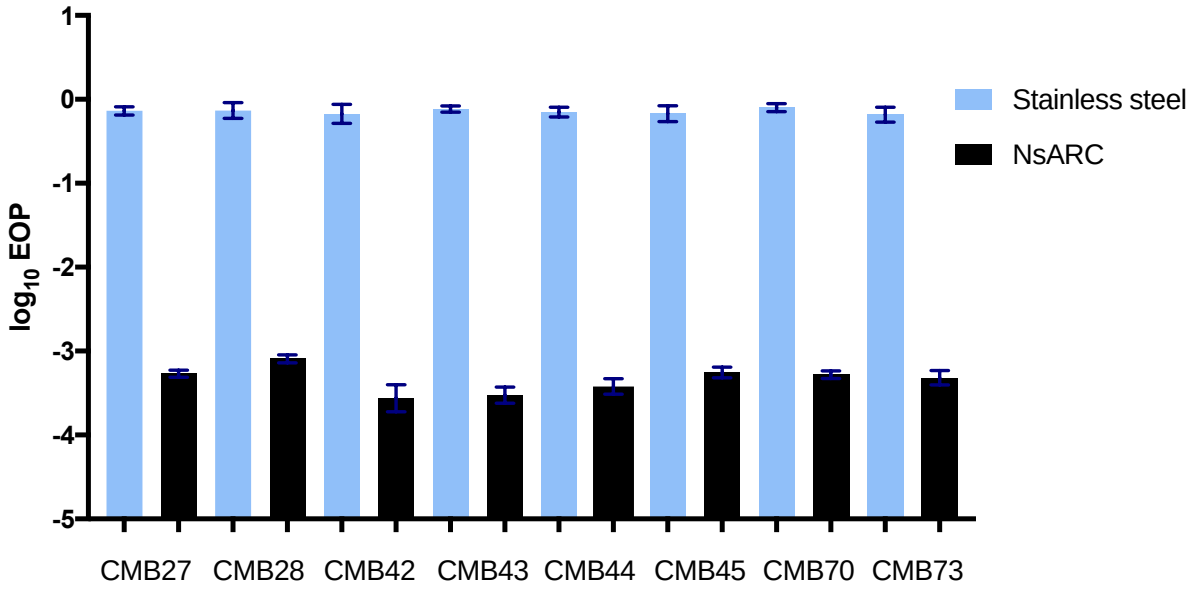

Figure 4.2: Survival of environmental isolates on NsARC and stainless steel for 8 hours under high intensity visible light.

4.5.2 Survival of *E. coli BWtolC* and *BWsoxS* on NsARC

Studies have shown that bacteria that harbor plasmids with multiple antibiotic genes are usually resistant to the AMA of biocides. I was interested in investigating how bacteria that carry a plasmid with antibiotic-resistant genes would respond to the AMA of NsARC. I decided to test the survival of two *E. coli* strains that were transformed using a plasmid construct. The survival of two strains of *E. coli* on NsARC was tested under various exposure conditions. BWtolC and BWsoxS were exposed to NsARC and stainless steel under visible, UV, ambient light and no light for a period of 8 hours. There was 1- 2 log reduction in viability of both strains under all the exposure conditions. There was a 2 log reduction in survival of BWtolC strains that were on NsARC under UV light,

while for those on NsARC under high intensity visible, ambient light and no light, there was a 1 log reduction in EOP (Figure 4.3). There was a < 2 log reduction in EOP of BWsoxS that were on NsARC under all the exposure conditions. There was also no significant difference (P>0.05) in the reduction in EOP of BWsoxS that were on NsARC under all the exposure conditions (Figure 4.4).

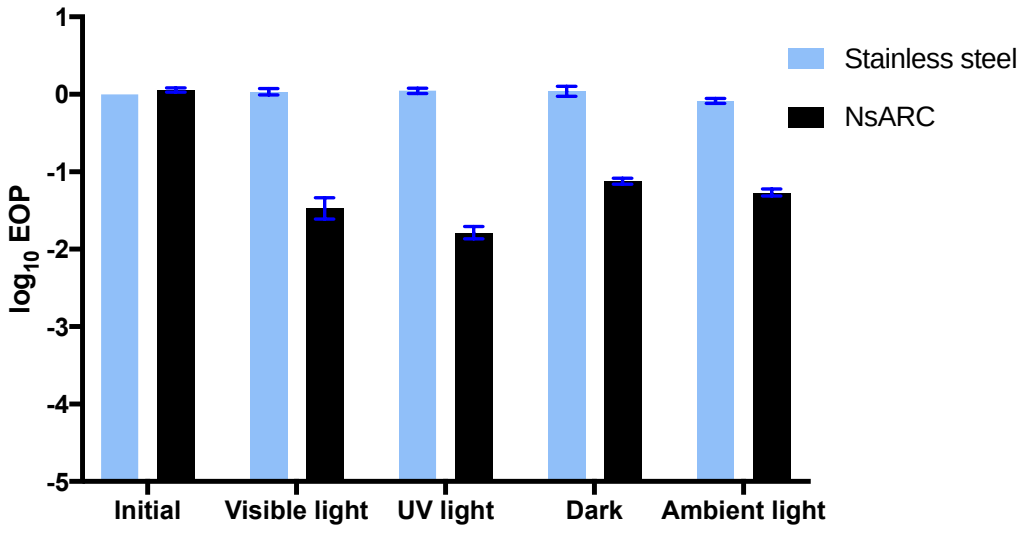

Figure 4.3: Survival of *E. coli* BWtolC on NsARC and stainless steel for a period of 8 hour in the dark and exposure to UV, ambient and high intensity visible light.

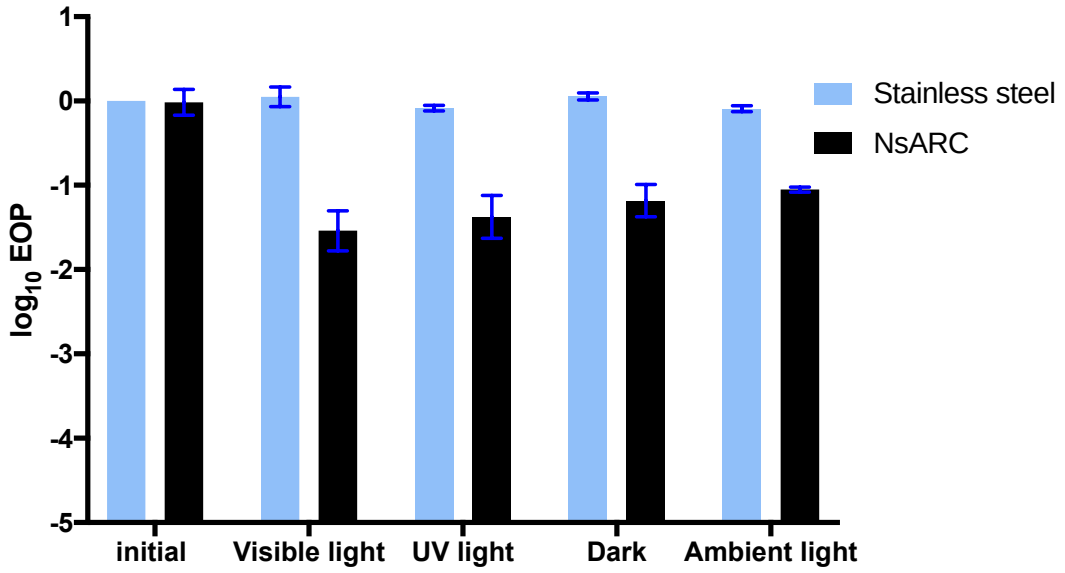

Figure 4.4: Survival of *E. coli* BWsoxS on NsARC and stainless steel for a period of 8 hour in the dark and exposure to UV, ambient and high intensity visible light.

4.5.3 Survival of *E. coli* BW25113, *BWpFru97*, *BWtolC* and *BWsoxS* strains on NsARC

The 1- 2 log reduction in viability of both strains under all the exposure conditions, indicated an increase in survival compared to the 3-4 log reduction that was observed in previous AMA experiments. To confirm if there was a significant increase in survival of two *E. coli* strains harboring plasmids, I then compared the survival of the two transformed strains with the isogenic parent strain and another *E. coli* strain (BWpFru97) harboring the pFru97 plasmid before insertion of the reporter construct. There was a 4 log reduction in survival of *E. coli* BW25113 and BWpFru97 on NsARC, and a 2 log reduction in the survival of BWtolC and BWsoxS on NsARC (Figure 4.5). There was no significant difference ($P>0.05$) in the reduction of *E. coli* BW25113 compared with BWpFru97. There was also no significant difference ($P>0.05$) in the reduction of *E. coli* BWtolC compared with *E. coli* BWsoxS. But there was significantly greater reduction of *E. coli* BW25113 compared with BWtolC ($P<0.01$) and BWsoxS ($P<0.01$). There was significantly greater reduction of *E. coli* pFru97 compared with BWtolC ($P<0.01$) and BWsoxS ($P<0.01$) (Appendix A). BWtolC and BWsoxS were more tolerant to the AMA of NsARC compared to their

parent isogenic strain and the *E. coli* BW25113 strain harboring the pFru97 plasmid before insertion of the reporter construct.

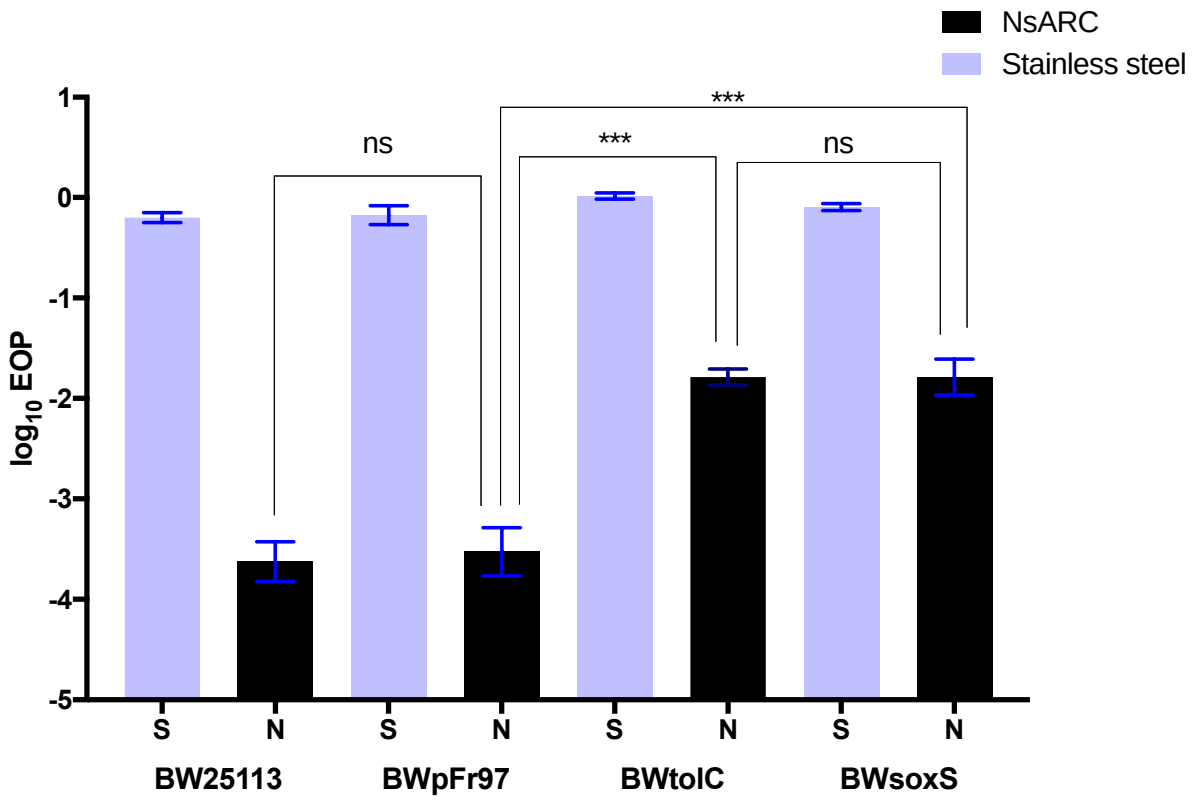

Figure 4.5: Survival of the isogenic parent strain of *E. coli* BW25113 and the mutants pFfu97, BWtolC and BWsoxS on NsARC for 8 hours under high intensity visible light. Error bars are standard error of means (SEM). Asterisks indicate P values. *: P<0.05; **: P<0.01; ***: P<0.001; ns: not significant.

4.5.4 Survival of parent *E. coli* CMB73, CMB73tolC and CMBsoxS on NsARC

The significant difference in survival between the two strains, the isogenic parent strains and the strain harbouring the pFru97 plasmid, suggests that the reporter construct inserted into the plasmid in the two strains may be responsible for the increase in survival. To confirm if the reporter construct inserted into the plasmid was responsible for the increase in survival, pFru-p_{tolC}-mScarlet and pFru-p_{soxS}-mScarlet plasmids were extracted from BWtolC and BWsoxS, respectively, and used to transform CMB73 (Table 4.1) to CMB73tolC and CMB73soxS. The survival of CMB73tolC and CMB73soxS on NsARC under high intensity visible light for a period of 8 hours

was then compared with that of the isogenic parent strain (Figure 4.6 and 4.7, respectively). There was a 3 log reduction is survival of CMB73 on NsARC compared to the ones on stainless steel, while there was a less than 2 log reduction in survival of CMB73tolC and CMB73soxS on NsARC, when compared with the one that were on stainless steel (Figure 4.6 and 4.7 respectively). There was significant reduction in survival of CMB73 when compared with CMBtolC ($P<0.001$) and CMBsoxS ($P<0.001$).

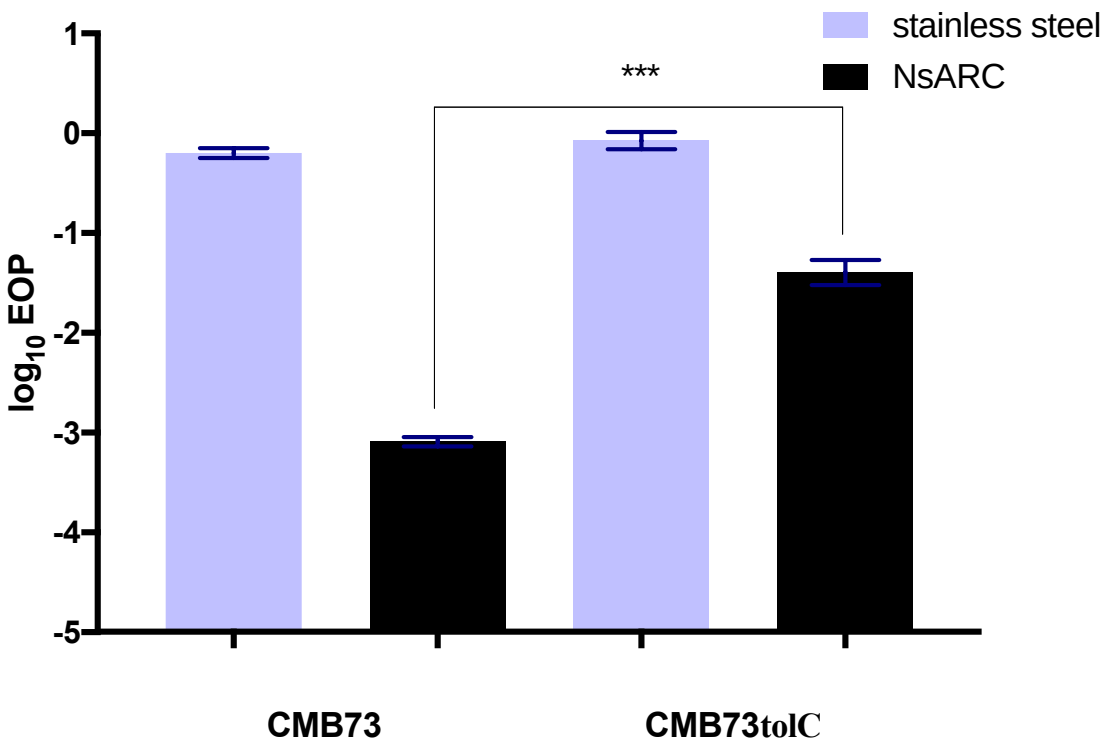

Figure 4.6: Survival of the isogenic parent strain of *E. coli* CMB73 and the mutant CMB73tolC on NsARC and stainless steel for a period of 8 hours under high intensity visible light. Error bars are standard error of means (SEM). Asterisks indicate P values. *: P<0.05; **: P<0.01; ***: P<0.001; ns: not significant.

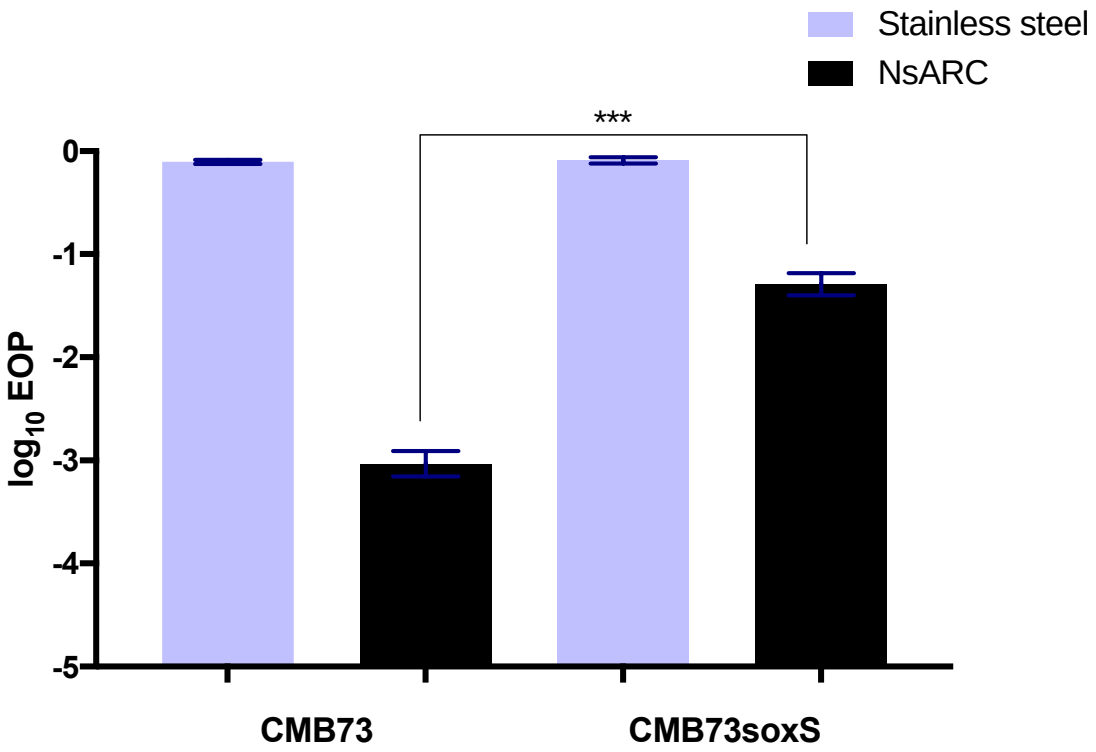

Figure 4.7: Survival of the isogenic parent strain of *E. coli* CMB73 and CMB73soxS on NsARC and stainless steel for a period of 8 hours under high intensity visible light. Error bars are standard error of means (SEM). Asterisks indicate P values. *: P<0.05; **: P<0.01; ***: P<0.001; ns: not significant.

4.5.5 Survival of Fluorescent labelled bacteria on NsARC

The transformed strains CMB73tolC and CMB73soxS were more resistant to NsARC compared to the isogenic parent strain. I then hypothesized that the increase in survival of the strains harbouring the plasmid construct was due to the expression of the fluorescent protein (FP) in the reporter construct. To investigate if the expression of FP was responsible for the increased resistance to NsARC, a set of pFru97-based pMRE plasmids (Schlechter et al., 2018) conferring fluorescent phenotypes in a wide range of bacteria was used to transform BW25113. Five BW25113 strains, each harbouring one of the pMRE132, 133, 135, 145 and 165 plasmids, were exposed to NsARC under high intensity visible light for a period of 8 hours before recovery on a culture media. pMRE132 express the sGFP, *E. coli* pMRE133 express the sYFP, and *E. coli* pMRE135, 145 and 165 express the RPF (see widefield microscopy in Figure 4.9). There was a 2

log reduction in pMRE132 and pMRE133 that were on NsARC, while pMRE135, pMRE145 and pMRE165 reduced by <2 log (Figure 4.8). There was no significant difference in the reduction between pMRE132 and pMRE133 (P>0.05) (Appendix A). However, there was significant reduction in EOP of both pMRE132 and pMRE133 on NsARC compared to pMRE135, pMRE145 and pMRE165 (P<0.001) (Appendix A). There was also greater reduction in EOP of pMRE135 on NsARC compared to pMRE165 (P<0.01), while EOP of pMRE165 was significantly reduced on NsARC compared to pMRE145 (P<0.01) (Appendix E). The pMRE133 strain was the most susceptible to NsARC, followed by pMRE132, pMRE135 and pMRE165, while pMRE145 was the least susceptible to killing effect of NsARC (Figure 4.8). *E. coli* pMRE145 strains were brighter than pMRE165 and pMRE135 (Figure 4.10).

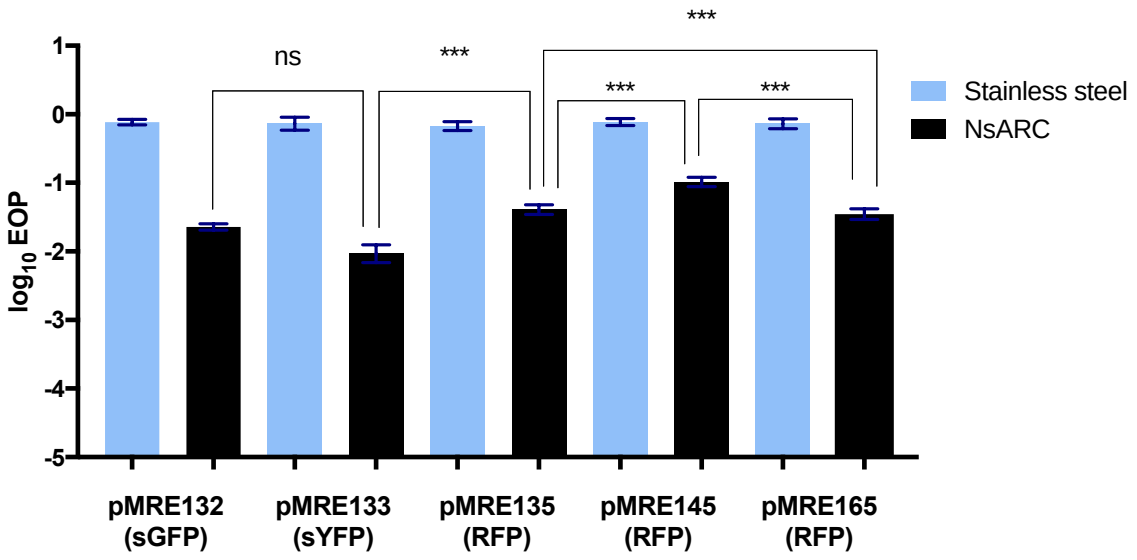

Figure 4.8: Survival of five *E. coli* strains expressing green fluorescent proteins (sGFP), yellow fluorescent proteins (sYFP) and red fluorescent proteins (RFP) on NsARC and stainless steel for a period of 8 hours under high intensity visible light. Error bars are standard error of means (SEM). Asterisks indicate P values. *: P<0.05; **: P<0.01; ***: P<0.001; ns: not significant.

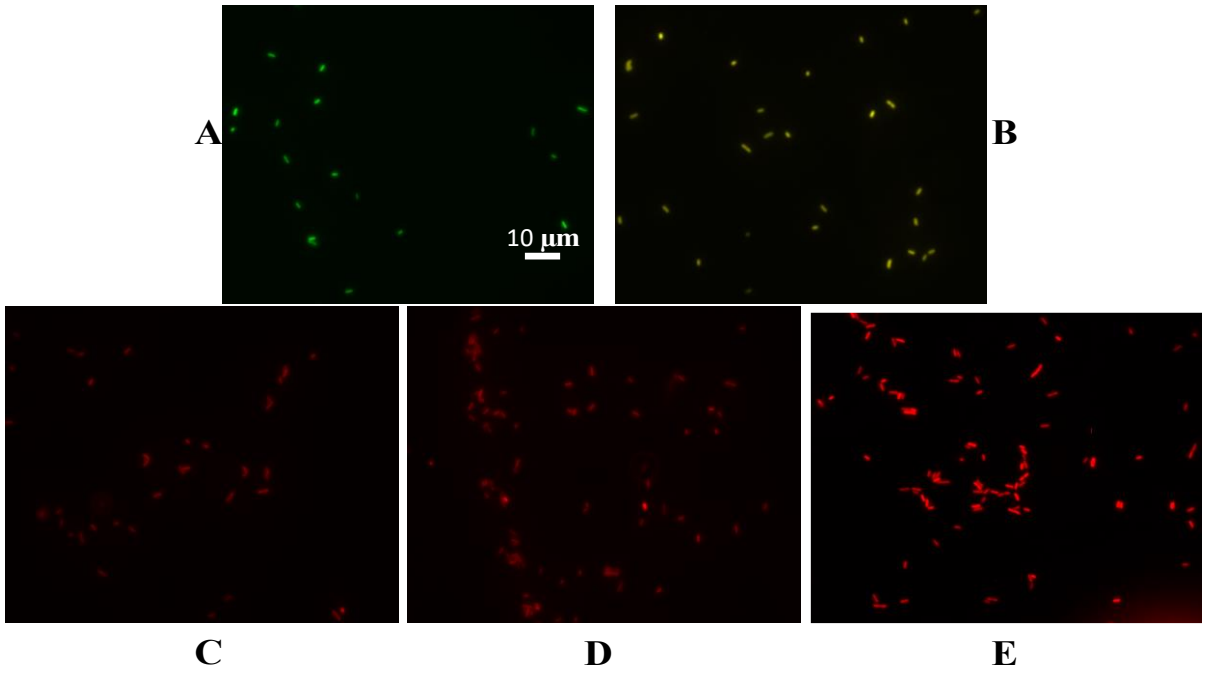

Figure 4.9: Widefield microscopy of *E. coli* expressing fluorescent proteins. (A) *E. coli* BW25113 (pMRE132), (B) *E. coli* BW25113 (pMRE133), (C) *E. coli* BW25113 (pMRE135), (D) *E. coli* BW25113 (pMRE165) and (E) *E. coli* BW25113 (pMRE145).

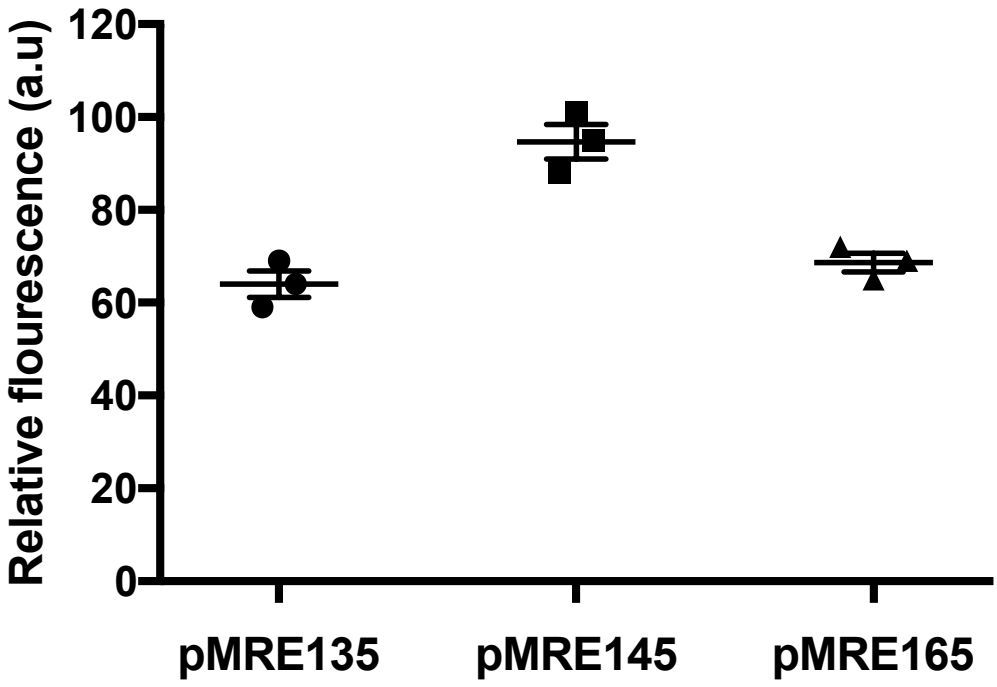

Figure 4.10: Fluorescent intensity of *E. coli* BW25113 cultures expressing mScarlet-1 from different pMRE plasmid series (pMRE145, pMRE145 and pMRE165). a.u indicates arbitrary units.

4.5.6 Survival of induced and uninduced bacteria on NsARC

To investigate if accumulation of protein biomass per se within a cell could increase the possibility of surviving AMA of NsARC, pUC19 plasmid was used to transform *E. coli* (see protocol in appendix D). Isopropyl-ß-D-thiogalactoside (IPTG) a compound that mimic allolactose and triggers transcription of the *lac* operon was used to induce protein (beta-galactosidase) expression in *E. coli* pUC19. Induced and uninduced *E. coli* pUC19 were then exposed to NsARC. There was a greater than 2 log reduction in EOP for the induced *E. coli* pUC19 and there was also a greater than 2 log reduction in the *E. coli* pUC19 uninduced strains (Figure 4.11). There was also no significant difference ($P>0.05$) in the reduction in EOP between the induced and uninduced strains.

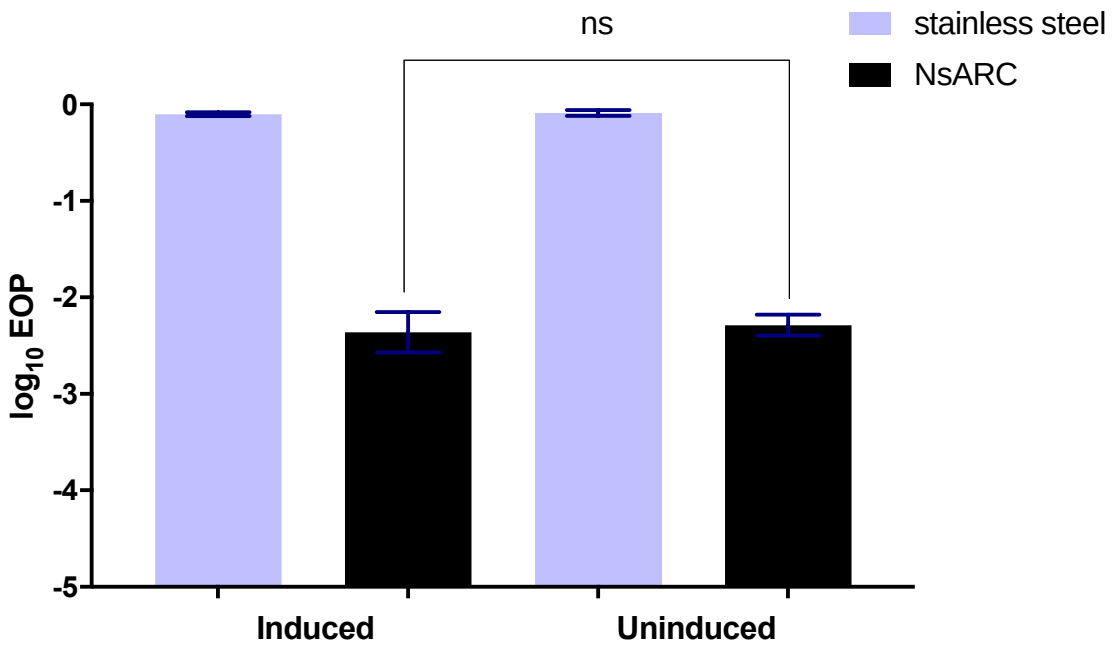

Figure 4.11: Survival of *E. coli* pUC19 on NsARC and stainless steel for a period of 8 hours under high intensity visible light. Error bars are standard error of means (SEM). Asterisks indicate P values. *: P<0.05; **: P<0.01; ***: P<0.001; ns: not significant.

4.6 Discussion

In this chapter, in an attempt to further evaluate the AMA performance of NsARC coatings against bacteria, a series of AMA experiments were conducted. AMA testing of NsARC against bacteria isolated from the environment was carried out, followed by AMA testing of NsARC against bacteria that are known to harbour plasmids that carry antibiotic resistance genes.

4.6.1 Survival of environmental isolates on NsARC

In previous chapters, I had demonstrated the AMA of NsARC against *E. coli*, *S. aureus*, *P. aeruginosa* and *S. cerevisiae* (Chapter 2), all of which were laboratory strains. These laboratory strains have been stored for decades and it is highly likely that they may respond in a different way to antimicrobial agents, when compared to the way the same species of organisms that are found in the environment will respond to the same antibiotics. Evaluating the AMA of NsARC against some *E. coli* strains that were isolated from the environment, it was observed that there was a greater than 3 log reduction in survival of all the organisms tested (Figure 4.2). This was similar to what was observed for laboratory strains of *E. coli* (Krumdieck et al., 2019). This indicates that NsARC is active against laboratory strains of *E. coli* recommended for use in AMA of photocatalytic materials (Mills, 2012) and *E. coli* strains isolated from the environment.

4.6.2 Survival of *E. coli* strains harbouring plasmids with multiple antimicrobial resistance genes on NsARC

Two strains of *E. coli*, each of which harbours a plasmid construct with mScarlett-I (red fluorescent protein) and antimicrobial resistance genes, were exposed to NsARC under various light exposure conditions. The highest reduction (2 log) for both strains was under high-intensity visible and UV light (Figure 4.3 and 4.4). This 2 log reduction is less compared to the 4 log reduction (Figure 4.5) observed when the isogenic parent strain was on NsARC for the same period. Furthermore, there

was also 4 log reduction in survival of an *E. coli* BW25113 strain harbouring the pFru97 plasmid prior to insertion of the reporter construct compared to the 2 log reduction observed for the two strains harbouring the plasmid with the reporter constructs.

This observation shows that the two strains harbouring the plasmid construct with mScarlet-I (red fluorescent protein) survived better on NsARC than the isogenic parent strains and the strain harbouring the plasmid backbone. The reporter construct inserted into the plasmid in the two strains may be responsible for the increase in survival. The plasmids were then extracted and used to transform strain CMB73, one of the *E. coli* strains isolated from the environment. The transformed strains and the isogenic parent strain were also exposed to NsARC for 8 hours under high intensity visible light. From the result, I also observed that the two strains, CMB73tolC and CMB73soxS, were more resistant to NsARC compared to the isogenic parent strain (Figure 4.6 and 4.7). The increase in survival of the strains harbouring the plasmid construct on NsARC when compared with the strain without the plasmid or with the plasmid backbone was hypothesised to be due to the expression of the fluorescent protein (see appendix D).

4.6.3 Survival of fluorescent labelled bacteria on NsARC

To investigate if expression of mScarlet-I increased resistance to NsARC, a set of pFru97-based pMRE plasmids (Schlechter et al., 2018) conferring fluorescent phenotypes in a wide range of bacteria was used to transform BW25113 (see protocol in appendix D). The five BW25113 transformants, each harbouring one of the pMRE132, 133, 135, 145 and 165 plasmids, were exposed to NsARC and it was observed that the bacteria were less susceptible to killing by NsARC. For the three strains expressing the red fluorescent proteins, it was observed that the bacteria with the pMRE145 survived better (Figure 4.8) on NsARC compared to pMRE165 and pMRE135

transformants. Also, pMRE145-harbouring bacteria were brighter (Figure 4.9 and 4.10) compared to pMRE165 and pMRE135-harbouring strains. Schlechter et al. (2018) had also observed that bacteria harbouring the pMRE145 plasmid were significantly brighter than the other bacteria that harbour the rest of the plasmid series. The reason for the increase in brightness of bacteria with pMRE 145 was probably because more red fluorescent proteins (RFP) were expressed from pMRE145 due to the read-through of a gentamycin antibiotic resistance gene promoter, which was cloned upstream of the RFP gene (Schlechter et al., 2018).

The increase in survival observed in the bacteria harbouring Fluorescent proteins (FP) may be as a result of the absorption of light needed for the photoexcitation of NsARC by the FP. Studies have shown that FP can absorb light within a range of wavelengths and also emit a range of wavelengths. Within these ranges, there are maximum excitation and maximum emissions (Bindels et al., 2017). The absorption of light by the FP can cause a reduction in the amount of light needed for photoexcitation of NsARC. This reduction in the photoexcitation of NsARC can cause a decrease in the AMA of NsARC, leading to an increase in survival of the strains harbouring the FPs. This could also explain why the strain that produced the most FP was more resistant to NsARC compared to the other strains.

There was also no significant difference ($P>0.05$) in reduction in survival on NsARC of the *E. coli* pUC19 strain whose protein expression was induced using IPTG and the strain that was not induced, which indicates that accumulation of heterologous proteins within a cell may not significantly lead to an increase in resistance to NsARC. But preferably proteins that can absorb light such as FP may be able to reduce the amount of light needed for maximum photoactivation of NsARC, leading to a reduction in ROS production and a subsequent increase in survival of bacteria.

5 Chapter Five

5.1 General discussion

This thesis forms a part of the physical and biological investigation of the antimicrobial activity (AMA) of nanostructured anatase, rutile and carbon (NsARC). The biological investigation began with an evaluation of AMA adopting the ISO 27447:2009, "test method for antimicrobial activity of semi conducting photocatalytic materials" (Mills et al., 2012; Sadowski et al., 2015). We had reported the reduction in viable populations of a laboratory strain of *E. coli* that was exposed to NsARC for 4 hours under UV, visible light or in the dark (Krumdieck et al., 2019). I then went further to test AMA of NsARC using *E. coli* strains isolated from the environment and three additional species of organisms (*S. aureus*, *P. aeruginosa* and *S. cerevisiae*) for an extended period of 8 hours. I also investigated the antibiofilm activity (ABA) of NsARC using *S. aureus*, *P. aeruginosa* and *S. cerevisiae*. Finally, I developed a suitable methodology for determining whether NsARC could cause microorganisms to develop resistance to antibiotics. For this, reporter strains were constructed and characterised based on their responses to biocides and ability to report changes in gene expression.

The discovery of antimicrobial agents is one of the most important discovery of the 20th century, sadly, the overuse of antimicrobials such as antibiotics, disinfectants and antiseptics for prevention and treatment of disease comes with its drawbacks. One drawback is in the form of antimicrobial resistance. Antimicrobial resistance usually occurs naturally over time, sometimes through genetic changes (Heinemann, 1999). The potential failure of antimicrobials has led to an increase in the spread of contagious diseases. The increase in cases of contagious diseases is a severe public health dilemma that requires urgent attention (Himmler et al., 2020; Mao et al., 2020). Microorganisms

can survive and persist on regularly touched surfaces such as light switches, doorknobs, elevator buttons and furniture in public facilities for hours, days and even months increasing the chances for the spread of infections (Chowdhury et al., 2018; Griffith et al., 2000; Inweregbu et al., 2005). The World Health Organization (WHO) estimates that hundreds of millions of people globally are affected by contagious diseases, with the burden several fold higher in countries with large populations and low- and middle-income developing countries (Leyland et al., 2016). WHO suggests that prevention and control measures against contagious diseases involve hand hygiene, constant washing of hands, cleaning of frequently touch surface, using antiseptics and disinfectants and the use of self-cleaning antimicrobial surfaces. Studies have also shown that the use of self-cleaning antimicrobial surfaces can lead to a 70% decrease in contagious diseases (Khan et al., 2017).

The use of antimicrobial surfaces in areas people frequently touch is not new. An example of such is the use of copper coated surfaces. Copper is readily available for use as a surface material and has been widely adopted (Mehtar et al., 2008; Schmidt et al., 2012). However, copper is expensive (Table 1.1). A lot of data on the photocatalytic properties of TiO_2 is available, but much of it is limited to TiO_2 working under UV light (Foster et al., 2011).

My work has significantly extended observations of antimicrobial properties of the particular TiO_2 formulation NsARC under various exposure conditions and light regimes. NsARC is a composite of titania and carbon, deposited using the direct liquid injection pulsed-pressure metal-organic chemical vapour deposition process (PP-MOCVD) technique (Krumdieck et al., 2017; Krumdieck et al., 2019; Lee et al., 2013). NsARC deposition was done using a fixed number of pulses, temperature, concentration and injection rate of titanium tetraisopropoxide (TTIP) in dilute toluene solution in the deposition reactor (Krumdieck et al., 2019). I assessed interactions between NsARC

and bacteria, testing survival and non-lethal effects of exposure such as biofilm formation and impact on antibiotic resistance.

5.2 Summary and conclusion

I first started by investigating the survival of *E. coli* on NsARC compared with inert stainless steel and antimicrobial copper. I observed that the reduction in survival of *E. coli* on NsARC starts after 1 hour, and peaks after 4 hours, after which there was no increase in the reduction in survival. There was no significant decrease, sometimes even an increase, in survival on stainless steel. While on copper, there was no detectable survival after half an hour.

I then tested the survival of *S. aureus*, *P. aeruginosa* and *S. cerevisiae* on NsARC. There was a 99.9% killing of all the microorganisms I tested on NsARC after 8 hours, confirming that NsARC is a broad-spectrum antimicrobial agent (Pelaez et al., 2012; Sadowski et al., 2015; Xu et al., 2015). Morphologies of the cells recovered from NsARC after the 8 hour exposures were more distorted compared to those that were on steel. Studies have shown similar forms of deformity and cell membrane damage have been seen in *E. coli* (Foster et al., 2011; Leung et al., 2016) and *S. aureus* (Cheng et al., 2009) that were exposed to oxidative stress.

I also observed that, the strains I used for the AMA testing were laboratory strains and therefore may not be representative of those the material will encounter if deployed in relevant environments. So, I decided to test if NsARC was also active against some *E. coli* strains that were isolated from the environment. I observed > 4 log reduction of all *E. coli* strains that were isolated from the environment, similar to what was seen for the laboratory *E. coli* strain, indicating that NsARC is active against laboratory strains of *E. coli* recommended for use in AMA testing of photocatalytic materials (Mills, 2012) and *E. coli* strains isolated from the environment.

The AMA results in this thesis show that NsARC has antimicrobial properties. The antimicrobial properties were under all the exposure conditions, which include UV light, high-intensity visible light, ambient light and even no light. The greatest AMA was usually under UV or high-intensity visible light. The fact that all forms of light enhance the AMA of NsARC shows that most of the effect was due to photocatalysis. Photocatalysis is a photon-assisted redox reaction that leads to the generation of reactive oxygen species (ROS) and other super oxides such as H_20_2 that are involved in killing microbes (Gomes Silva et al., 2011; Sadowski et al., 2015).

The antimicrobial activity in the dark indicated that photocatalysis might not be responsible for the entire AMA. The hypothesis was that the amorphous carbon component in NsARC was causing the production of active carbon-centred reactive oxygen species in the dark. The production of carbon-centred free radicals as a result of cleavage of C-H bond usually occur when carbon-based materials interact with TiO_2 (Fenoglio et al., 2009). Carbon is also known to be inert as an element but can be chemically active when combined with other compounds or elements (Cheng et al., 2009; Dizaj et al., 2015). The hydrophilic surface of NsARC, possibly linked to the very high specific surface area of the nanostructured coating (Gardecka et al., 2019; Krumdieck et al., 2019), may also desiccate cells over time (Yu et al., 2014).

I decided to investigate if the carbon component of NsARC was responsible for some form of AMA in the dark by testing annealed NsARC samples. The Annealing process involves heat-treatment of the NsARC in air to remove the carbon. Annealing did not cause a change in the structure of the TiO_2 surface (Krumdieck et al., 2017; Krumdieck et al., 2019). The only difference between the as-deposited NsARC and the annealed samples was that the as-deposited samples are black and completely opaque, while annealed NsARC samples are white and translucent. Annealed NsARC samples showed greater AMA under UV and visible light compared with the as-deposited

samples. My hypothesis for this observation is that removal of the carbon increased the specific surface area available for redox reactions to occur, thus increasing the ROS concentration to which the bacteria were exposed. The results in the dark showed greater AMA for the as-deposited coatings, possibly because co-deposited carbon stabilized high energy facets of TiO_2, leading to possible increased AMA.

Plasmids are circular double stranded DNA molecules that can exist naturally in bacteria and some eukaryotic cells. Some genes carried in plasmids provides resistance to antibiotics. I was interested in finding out how bacteria that carry a plasmid with antibiotic-resistant genes would respond to the antimicrobial activity of NsARC. To answer this question, I decided to test the survival of two *E. coli* strains that I had transformed using a plasmid construct with two antibiotic resistance genes. I observed that the strains with the plasmid survive better on NsARC compared to the strains without the plasmids. To confirm if the plasmid construct was responsible for the increase in survival, I extracted the plasmid and used it to transform an *E. coli* strain (CMB73) isolated from the environment. I then exposed the transformed strain and the isogenic parent strain to NsARC. I also observed that the transformed strain was more resistant to NsARC compared to the isogenic parent strain. I then hypothesized that the increase in survival of strains harbouring the plasmid was due to the expression of fluorescent proteins (FP) in the reporter element of the plasmid. To investigate if the expression of FP was responsible for the increased resistance to NsARC, a set of pFru97-based pMRE plasmids (Schlechter et al., 2018), conferring fluorescent phenotypes in a wide range of bacteria, was used to transform BW25113. The five BW25113 transformants, each harbouring one of the pMRE132, 133, 135, 145 and 165 plasmids, were exposed to NsARC, and it was observed that they were less susceptible to killing by NsARC. From the three strains expressing the red fluorescent proteins, it was observed that the bacteria with pMRE145 were

significantly brighter than those with pMRE165 and pMRE135 when viewed using fluorescence microscopy and they also survived better on NsARC compared to pMRE165 and pMRE135 transformants. The reason for the increase in brightness of transformants with pMRE 145 was probably because more RFP was expressed from pMRE145 due to read-through of a gentamycin antibiotic resistance gene promoter, which was cloned upstream of the RFP gene (Schlechter et al., 2018).

FP can absorb light within a range of wavelengths and also emit a range of wavelengths. Within these ranges, there are maximum excitation and maximum emission (Bindels et al., 2017). I hypothesize that FP may be responsible for absorption of light needed for the photoexcitation of NsARC, causing a decrease in the AMA of NsARC with an increase in survival of the strains harbouring the FP. The absorption of light needed for photoexcitation of NsARC could then explain why the strain that produced the most FP was more resistant to NsARC compared to the other strains. Since the presence of FP in bacteria was responsible for increase in resistance to NsARC, I decided to investigate if accumulation of any protein in bacteria could also cause an increase in resistance to NsARC. I transformed *E. coli* using the pUC19 plasmid. pUC19 is a plasmid cloning vector that has multiple cloning sites and encodes the N-terminal fragment of beta-galactosidase, an intracellular enzyme that cleaves lactose into glucose and galactose, whose synthesis can be induced by isopropyl-ß-D-thiogalactoside (IPTG). I used IPTG to induce the expression the expression of beta-galactosidase in *E. coli* pUC19. Induced and uninduced *E. coli* pUC19 were then exposed to NsARC. There was also no significant difference ($P>0.05$) in survival on NsARC between the induced and uninduced strains, which indicates that accumulation of heterologous proteins within a cell may not lead to a significant increase in resistance to NsARC. Proteins that can absorb light such as FP may be able to reduce the amount of light needed for

maximum photoactivation of NsARC, leading to a reduction in ROS production and a subsequent increase in survival of bacteria.

Aside from the potential usefulness of NsARC for its antimicrobial properties, there is a need also for the consideration of possible potential adverse effects NsARC may have. NsARC is a biocidal material, and like other antimicrobial agents, there is a possibility that it may induce higher levels of antibiotic resistance. The possibility of NsARC inducing changes to antibiotic response is possible because metals such as Ag (Niño-Martínez et al., 2019), Cu (Jun et al., 2019), and Zn (Zhang et al., 2018) with antimicrobial properties have cause bacteria to develop multidrug-resistant phenotypes.

Developing a strategy to investigate the possibility of bacteria developing resistance to antibiotics after exposure to NsARC is necessary because NsARC is a new material and not yet tested for this potential effect. I, therefore, decided to adopt the following strategies.

1. Take bacteria that have survived exposure to NsARC and directly expose them to antibiotics to see if there will be a change in their susceptibility to the antibiotics.
2. Determine if NsARC was able to cause a change in the expression of genes associated with adaptive resistance to antibiotics.
3. Determine if NsARC could directly interact with antibiotics and affect the availability and potency of antibiotics.

To determine how bacteria that have survived exposure to NsARC will respond to antibiotics, I selected ampicillin, ciprofloxacin, chloramphenicol, erythromycin, fusidic acid, kanamycin, oxacillin, tetracycline and vancomycin antibiotics. These antibiotics were selected because they represent a broad range of common antibiotics used in treating infections including those caused by the bacteria I have tested and have been utilized in related studies. I then tested *E. coli* and *S.*

aureus that have survived exposure to NsARC on these antibiotics. I observed that *E. coli* exposed to NsARC became more susceptible to only kanamycin, while its susceptibility to the other antibiotics remained unchanged. The susceptibility of *S. aureus* to antibiotics was unchanged.

To determine if NsARC can induce genes associated with adaptive resistance to antibiotics, two reporter strains of *E. coli* that "report" transcription of *tolC* or *soxS* genes were designed (Jun et al., 2019). Each of these reporter strains had a plasmid construct that expressed mScarlet red fluorescent protein under the control of the promoters of either the *tolC* or *soxS* genes. These designed constructs are strains wherein an increase in expression of FP is expected when the *tolC* or *soxS* genes are induced. I exposed the two reporter strains to NsARC, inert stainless steel and copper. Copper is a known inducer of *soxS* and *tolC* transcription (Franke et al., 2003; Nishino et al., 2007), and so it was used as a positive control. Reporter strains that were on copper were significantly brighter than the reporter strains that were on NsARC, while the strains that were on NsARC were also significantly brighter than the one on stainless steel. The fact that the reporter strains that were on NsARC were brighter than the ones on steel indicated there is a strong likelihood that NsARC may be able to induce genes associated with adaptive resistance to antibiotics in bacteria.

Copper interacts with tetracycline when they are in combination, and it results in a decrease in the effective concentration of both copper and tetracycline. This decrease was due to chelation of tetracycline by copper and an adaptive resistance pathway induced by copper (Jun et al., 2019). To determine if NsARC can also interact with tetracycline and maybe affect its potency, I set up an experiment in which copper, NsARC and stainless steel coupons were placed in separate Petri dishes containing LB + tetracycline + *E. coli.* A replicate of the set up was made without tetracycline. I observed that on plates with LB + tetracycline + *E. coli* and either NsARC or

stainless steel coupons there was no growth. However, with the copper coupon and tetracycline, there was no growth immediately around the coupon, but there was a "ring" of growth in the region between the coupon and the edge of the petri dish. In the replica set without tetracycline, there was uniform growth across the surface of the medium except. Plates that had a copper coupon, there was no growth in the region close to the coupon -a halo- but there was growth in the region further away from the coupon.

In the first set up, there was no growth in the region close to the copper coupon because copper is toxic. But further away from the coupon, as the concentration of copper decreases, there forms a local toxicity minima where the combination of tetracycline-copper chelation and efflux induction permit the bacteria to grow. Further away from the "ring" of growth, there was no growth probably because there was too little copper to neutralise tetracycline or induce efflux pathways before transcription was halted by tetracycline. On the other hand, there might not have been any tetracycline interaction with ROS produced from the photoactivation of NsARC, hence no growth was seen in the Petri dish with the NsARC coupon.

5.3 Future work

There has been further research aimed at optimizing and improving the production of NsARC. Several NsARC depositions were made using different parameters, such as the number of pulses (Gorthy et al., 2020), annealing temperatures (Krumdieck et al., 2017), and precursor solution concentrations (Gorthy et al., manuscript under review). There are also NsARC depositions made with a ten-time higher instantaneous precursor vapour flux (Krumdieck et al., 2019) compared to the samples that I used for AMA testing discussed in this thesis. These new depositions are yet to be tested for AMA and potential of inducing resistance to antibiotics. There is a need for AMA and ABA testing of these new NsARC depositions.

In this thesis, I was able to test only four different species of microorganisms. The organisms I tested included three bacteria (*E. coli, S. aureus* and *P. aeruginosa*) and one fungus (*S. cerevisiae*). There is a need to test more diverse species of microorganisms, including viruses.

Studies have shown that cross-resistance can exist between some antibiotics and photocatalysis. NsARC may have the effect of selecting for resistant strains of pathogens. It is necessary to investigate if some antibiotic resistance genes can also confer resistance to NsARC.

I demonstrated in this thesis that NsARC can induce the *tolC* and *soxS* genes associated with the AcrAB-TolC RND type multidrug-resistant efflux pumps. Therefore, there is also a need to investigate other genes, such as *marR*, *acrR*, *acrB* and *sodA*. To further investigate if NsARC can induce the adaptive resistance response via AcrAB-TolC efflux pump, a set of strains such as Δ *acr*A, Δ*acr*B and Δ *tol*C from an isogenic series carrying single gene deletions will also be tested.

The exposure of the reporter strains to NsARC increased the transcription of the red fluorescent protein gene *mScarlet* under the control of the *tolC* and *soxS* promoter, respectively. It is was not possible to quantify how much of this increase in fluorescence accounts for the increase in the expression of efflux pumps. Besides, only a specific efflux pump component was tested. The way NsARC may be inducing these components was not investigated. Whole transcriptome sequencing could provide an overview of mRNA levels of most genes that might be affected by NsARC.

The practical application of NsARC in public places has not yet taken place. So, there is a need to evaluate the in situ performance of NsARC coating. NsARC coated door handles, elevator buttons, bed rail should be made available in public places and the survival microorganisms on these surfaces evaluated over a period of time.

A post-antibiotic period is fast becoming a reality and the understanding of resistance and the various factors affecting the evolution of antibiotic resistance is essential, and all hands must be on deck to find a lasting solution to the menace of antibiotic resistance.

Reference

Abboud, Y., Saffaj, T., Chagraoui, A., El Bouari, A., Brouzi, K., Tanane, O., and Ihssane, B. (2014). Biosynthesis, characterization and antimicrobial activity of copper oxide nanoparticles (CONPs) produced using brown alga extract (Bifurcaria bifurcata). *Applied Nanoscience*, *4*(5), 571–576. https://doi.org/10.1007/s13204-013-0233-x

Ahamed, M., Alhadlaq, H. A., Khan, M. A. M., Karuppiah, P., and Al-Dhabi, N. A. (2014). Synthesis, characterization, and antimicrobial activity of copper oxide nanoparticles. *Journal of Nanomaterials*, *2014*, 1–4. https://doi.org/10.1155/2014/637858

Aiassa, V., Barnes, A. I., Smania, A. M., and Albesa, I. (2012). Sublethal ciprofloxacin treatment leads to resistance via antioxidant systems in *Proteus mirabilis*. *FEMS Microbiology Letters*, *327*(1), 25–32. https://doi.org/10.1111/j.1574-6968.2011.02453.x

Airey, P., and Verran, J. (2007). Potential use of copper as a hygienic surface; problems associated with cumulative soiling and cleaning. *Journal of Hospital Infection*, *67*(3), 271–277.

Aldred, K. J., Kerns, R. J., and Osheroff, N. (2014). Mechanism of quinolone action and resistance. *Biochemistry*, *53*(10), 1565–1574. https://doi.org/10.1021/bi5000564

Ali, H., Khan, E., and Ilahi, I. (2019). Environmental chemistry and ecotoxicology of hazardous heavy metals: Environmental persistence, toxicity, and bioaccumulation [Review Article]. *Journal of Chemistry*; Hindawi. https://doi.org/10.1155/2019/6730305

Allahverdiyev, A. M., Abamor, E. S., Bagirova, M., and Rafailovich, M. (2011). Antimicrobial effects of TiO_2 and Ag_2O nanoparticles against drug-resistant bacteria and leishmania parasites. *Future Microbiology*, *6*(8), 933–940. https://doi.org/10.2217/fmb.11.78

Amaya, E., Reyes, D., Paniagua, M., Calderón, S., Rashid, M.-U., Colque, P., Kühn, I., Möllby, R., Weintraub, A., and Nord, C. E. (2012). Antibiotic resistance patterns of *Escherichia*

coli isolates from different aquatic environmental sources in Leon, Nicaragua. *Clinical Microbiology and Infection*, *18*(9), E347–E354. https://doi.org/10.1111/j.1469-0691.2012.03930.x

Arciola, C. R., Campoccia, D., Speziale, P., Montanaro, L., and Costerton, J. W. (2012). Biofilm formation in Staphylococcus implant infections. A review of molecular mechanisms and implications for biofilm-resistant materials. *Biomaterials*, *33*(26), 5967–5982.

Baba, T., Ara, T., Hasegawa, M., Takai, Y., Okumura, Y., Baba, M., Datsenko, K. A., Tomita, M., Wanner, B. L., and Mori, H. (2006). Construction of *Escherichia coli* K-12 in-frame, single-gene knockout mutants: The Keio collection. *Molecular Systems Biology*, *2*(1), 2006.0008. https://doi.org/10.1038/msb4100050

Barkay, T., Kritee, K., Boyd, E., and Geesey, G. (2010). A thermophilic bacterial origin and subsequent constraints by redox, light and salinity on the evolution of the microbial mercuric reductase. *Environmental Microbiology*, *12*(11), 2904–2917. https://doi.org/10.1111/j.1462-2920.2010.02260.x

Bindels, D. S., Haarbosch, L., Van Weeren, L., Postma, M., Wiese, K. E., Mastop, M., Aumonier, S., Gotthard, G., Royant, A., and Hink, M. A. (2017). mScarlet: A bright monomeric red fluorescent protein for cellular imaging. *Nature Methods*, *14*(1), 53.

Blair, J. M., Richmond, G. E., and Piddock, L. J. (2014). Multidrug efflux pumps in Gram-negative bacteria and their role in antibiotic resistance. *Future Microbiology*, *9*(10), 1165–1177. https://doi.org/10.2217/fmb.14.66

Blair, J. M., Webber, M. A., Baylay, A. J., Ogbolu, D. O., and Piddock, L. J. (2015). Molecular mechanisms of antibiotic resistance. *Nature Reviews Microbiology*, *13*(1), 42.

Brook, L. A., Evans, P., Foster, H. A., Pemble, M. E., Sheel, D. W., Steele, A., and Yates, H. M. (2007). Novel multifunctional films. *Surface and Coatings Technology*, *201*(22–23), 9373–9377. https://doi.org/10.1016/j.surfcoat.2007.04.020

Caniça, M., Manageiro, V., Jones-Dias, D., Clemente, L., Gomes-Neves, E., Poeta, P., Dias, E., and Ferreira, E. (2015). Current perspectives on the dynamics of antibiotic resistance in different reservoirs. *Research in Microbiology*, *166*(7), 594–600. https://doi.org/10.1016/j.resmic.2015.07.009

Castellote, M., and Bengtsson, N. (2011). Principles of TiO_2 photocatalysis. In *Applications of Titanium Dioxide Photocatalysis to Construction Materials* (pp. 5–10). Springer.

Cendrowski, K., Peruzynska, M., Markowska-Szczupak, A., Chen, X., Wajda, A., Lapczuk, J., Kurzawski, M., Kalenczuk, R. J., Drozdzik, M., and Mijowska, E. (2014). Antibacterial performance of nanocrystallined titania confined in mesoporous silica nanotubes. *Biomedical Microdevices*, *16*(3), 449–458. https://doi.org/10.1007/s10544-014-9847-3

Chandrangsu, P., Rensing, C., and Helmann, J. D. (2017). Metal homeostasis and resistance in bacteria. *Nature Reviews Microbiology*, *15*(6), 338–350. https://doi.org/10.1038/nrmicro.2017.15

Chao, Y., and Zhang, T. (2011). Optimization of fixation methods for observation of bacterial cell morphology and surface ultrastructures by atomic force microscopy. *Applied Microbiology and Biotechnology*, *92*(2), 381.

Cheng, C.-L., Sun, D.-S., Chu, W.-C., Tseng, Y.-H., Ho, H.-C., Wang, J.-B., Chung, P.-H., Chen, J.-H., Tsai, P.-J., Lin, N.-T., Yu, M.-S., and Chang, H.-H. (2009). The effects of the bacterial interaction with visible-light responsive titania photocatalyst on the bactericidal

performance. *Journal of Biomedical Science*, *16*(1), 7. https://doi.org/10.1186/1423-0127-16-7

Cho, M., Chung, H., Choi, W., and Yoon, J. (2004). Linear correlation between inactivation of *E. coli* and OH radical concentration in TiO_2 photocatalytic disinfection. *Water Research*, *38*(4), 1069–1077. https://doi.org/10.1016/j.watres.2003.10.029

Chopra, I., and Roberts, M. (2001). Tetracycline antibiotics: Mode of action, applications, molecular biology, and epidemiology of bacterial resistance. *Microbiology and Molecular Biology Reviews*, *65*(2), 232–260. https://doi.org/10.1128/MMBR.65.2.232-260.2001

Chowdhury, D., Tahir, S., Legge, M., Hu, H., Prvan, T., Johani, K., Whiteley, G. S., Glasbey, T. O., Deva, A. K., and Vickery, K. (2018). Transfer of dry surface biofilm in the healthcare environment: The role of healthcare workers' hands as vehicles. *Journal of Hospital Infection*. https://doi.org/10.1016/j.jhin.2018.06.021

Clardy, J., Fischbach, M. A., and Currie, C. R. (2009). The natural history of antibiotics. *Current Biology*, *19*(11), R437–R441. https://doi.org/10.1016/j.cub.2009.04.001

Commodity and Metal Prices, Metal Price Charts—InvestmentMine. (n.d.). Retrieved August 31, 2018, from http://www.infomine.com/investment/metal-prices/

Corona, F., and Martinez, J. (2013). Phenotypic resistance to antibiotics. *Antibiotics*, *2*(2), 237–255. https://doi.org/10.3390/antibiotics2020237

Crawley, M. J. (2007). *Mixed-Effects Models*. Wiley Online Library.

Dancer, S. J. (2008). Importance of the environment in meticillin-resistant *Staphylococcus aureus* acquisition: The case for hospital cleaning. *The Lancet Infectious Diseases*, *8*(2), 101–113.

Das, S., Dash, H. R., and Chakraborty, J. (2016). Genetic basis and importance of metal resistant genes in bacteria for bioremediation of contaminated environments with toxic metal

pollutants. *Applied Microbiology and Biotechnology*, *100*(7), 2967–2984. https://doi.org/10.1007/s00253-016-7364-4

Davies, J., and Davies, D. (2010). Origins and evolution of antibiotic resistance. *Microbiology and Molecular Biology Reviews*, *74*(3), 417–433.

De Falco, G., Porta, A., Petrone, A. M., Del Gaudio, P., El Hassanin, A., Commodo, M., Minutolo, P., Squillace, A., and D'Anna, A. (2017). Antimicrobial activity of flame-synthesized nano-TiO_2 coatings. *Environmental Science: Nano*, *4*(5), 1095–1107. https://doi.org/10.1039/C7EN00030H

Denyer, S., and Russell, A. (2004). Non-antibiotic antibacterial agents: Mode of action and resistance. *Hugo and Russell's: Pharmaceutical Microbiology, Seventh Edition*, 306–322.

Dizaj, S. M., Mennati, A., Jafari, S., Khezri, K., and Adibkia, K. (2015). Antimicrobial activity of carbon-based nanoparticles. *Advanced Pharmaceutical Bulletin*, *5*(1), 19.

Djurišić, A. B., Leung, Y. H., Ng, A. M. C., Xu, X. Y., Lee, P. K. H., Degger, N., and Wu, R. S. S. (2015). Toxicity of metal oxide nanoparticles: Mechanisms, characterization, and avoiding experimental artefacts. *Small*, *11*(1), 26–44. https://doi.org/10.1002/smll.201303947

Dodd, N. J. F., and Jha, A. N. (2009). Titanium dioxide induced cell damage: A proposed role of the carboxyl radical. *Mutation Research*, *660*(1–2), 79–82. https://doi.org/10.1016/j.mrfmmm.2008.10.007

Faúndez, G., Troncoso, M., Navarrete, P., and Figueroa, G. (2004). Antimicrobial activity of copper surfaces against suspensions of S*almonella enterica* and *Campylobacter jejuni*. *BMC Microbiology*, 7.

Fenoglio, I., Greco, G., Livraghi, S., and Fubini, B. (2009). Non-UV-induced radical reactions at the surface of TiO_2 nanoparticles that may trigger toxic responses. *Chemistry – A European Journal*, *15*(18), 4614–4621. https://doi.org/10.1002/chem.200802542

Fenoglio Ivana, Greco Giovanna, Livraghi Stefano, and Fubini Bice. (2009). Non-UV-induced radical reactions at the surface of TiO_2 nanoparticles that may trigger oxic responses. *Chemistry – A European Journal*, *15*(18), 4614–4621. https://doi.org/10.1002/chem.200802542

Fernández, L., Breidenstein, E. B., and Hancock, R. E. (2011). Creeping baselines and adaptive resistance to antibiotics. *Drug Resistance Updates*, *14*(1), 1–21.

Fernández, L., and Hancock, R. E. (2013). Adaptive and mutational resistance: Role of porins and efflux pumps in drug resistance. *Clinical Microbiology Reviews*, *26*(1), 163.

Finley, R. L., Collignon, P., Larsson, D. J., McEwen, S. A., Li, X.-Z., Gaze, W. H., Reid-Smith, R., Timinouni, M., Graham, D. W., and Topp, E. (2013). The scourge of antibiotic resistance: The important role of the environment. *Clinical Infectious Diseases*, *57*(5), 704–710.

Fleming, K., and Randle, J. (2006). Toys-friend or foe? A study of infection risk in a paediatric intensive care unit. *Paediatric Nursing*, *18*(4), 14.

Flemming, H.-C., and Wingender, J. (2010). The biofilm matrix. *Nature Reviews Microbiology*, *8*(9), 623.

Foster, H. A., Ditta, I. B., Varghese, S., and Steele, A. (2011). Photocatalytic disinfection using titanium dioxide: Spectrum and mechanism of antimicrobial activity. *Applied Microbiology and Biotechnology*, *90*(6), 1847–1868.

Franke, S., Grass, G., Rensing, C., and Nies, D. H. (2003). Molecular analysis of the copper-transporting efflux system CusCFBA of *Escherichia coli*. *Journal of Bacteriology*, *185*(13), 3804–3812. https://doi.org/10.1128/JB.185.13.3804-3812.2003

Fraud, S., and Poole, K. (2011). Oxidative stress induction of the MexXY multidrug efflux genes and promotion of aminoglycoside resistance development in *Pseudomonas aeruginosa*. *Antimicrobial Agents and Chemotherapy*, *55*(3), 1068–1074.

Ganewatta, M. S., Miller, K. P., Singleton, S. P., Mehrpouya-Bahrami, P., Chen, Y. P., Yan, Y., Nagarkatti, M., Nagarkatti, P., Decho, A. W., and Tang, C. (2015). Antibacterial and Biofilm-Disrupting Coatings from Resin Acid-Derived Materials. *Biomacromolecules*, *16*(10), 3336–3344. https://doi.org/10.1021/acs.biomac.5b01005

Gao, M., Song, W., Zhou, Q., Ma, X., and Chen, X. (2013). Interactive effect of oxytetracycline and lead on soil enzymatic activity and microbial biomass. *Environmental Toxicology and Pharmacology*, *36*(2), 667–674. https://doi.org/10.1016/j.etap.2013.07.003

Gardecka, A. J., Bishop, C., Lee, D., Corby, S., Parkin, I. P., Kafizas, A., and Krumdieck, S. (2018). High efficiency water splitting photoanodes composed of nano-structured anatase-rutile TiO_2 heterojunctions by pulsed-pressure MOCVD. *Applied Catalysis B: Environmental*, *224*, 904–911. https://doi.org/10.1016/j.apcatb.2017.11.033

Gardecka, A. J., Polson, M. I. J., Krumdieck, S. P., Huang, Y., and Bishop, C. M. (2019). Growth stages of nano-structured mixed-phase titania thin films and effect on photocatalytic activity. *Thin Solid Films*, *685*, 136–144. https://doi.org/10.1016/j.tsf.2019.06.018

Garneau-Tsodikova, S., and J. Labby, K. (2016). Mechanisms of resistance to aminoglycoside antibiotics: Overview and perspectives. *MedChemComm*, *7*(1), 11–27. https://doi.org/10.1039/C5MD00344J

Gerlach, R. G., Hölzer, S. U., Jäckel, D., and Hensel, M. (2007). Rapid engineering of bacterial reporter gene fusions by using red recombination. *Applied and Environmental Microbiology*, *73*(13), 4234–4242. https://doi.org/10.1128/AEM.00509-07

Gogniat, G., and Dukan, S. (2007). TiO2 photocatalysis causes DNA damage via fenton reaction-generated hydroxyl radicals during the recovery period. *Applied and Environmental Microbiology*, *73*(23), 7740–7743.

Golding, C. G., Lamboo, L. L., Beniac, D. R., and Booth, T. F. (2016). The scanning electron microscope in microbiology and diagnosis of infectious disease. *Scientific Reports*, *6*(1). https://doi.org/10.1038/srep26516

Gomes Silva, C., Juárez, R., Marino, T., Molinari, R., and García, H. (2011). Influence of excitation wavelength (UV or Visible Light) on the photocatalytic activity of titania containing gold nanoparticles for the generation of hydrogen or oxygen from water. *Journal of the American Chemical Society*, *133*(3), 595–602. https://doi.org/10.1021/ja1086358

Gorthy, R., Krumdieck, S., and Bishop, C. (2020). Process-induced nanostructures on anatase single crystals via pulsed-pressure MOCVD. *Materials*, *13*(7), 1668. https://doi.org/10.3390/ma13071668

Grass, G., Rensing, C., and Solioz, M. (2011). Metallic copper as an antimicrobial surface. *Applied and Environmental Microbiology*, *77*(5), 1541–1547. https://doi.org/10.1128/AEM.02766-10

Graves Jr, J., Tajkarimi, M., Cunningham, Q., Campbell, A., Nonga, H., Harrison, S., and Barrick, J. (2015). Rapid evolution of silver nanoparticle resistance in *Escherichia coli*. *Frontiers in Genetics*, *6*, 42. https://doi.org/10.3389/fgene.2015.00042

Griffin, M. O., Ceballos, G., and Villarreal, F. J. (2011). Tetracycline compounds with non-antimicrobial organ protective properties: Possible mechanisms of action. *Pharmacological Research*, *63*(2), 102–107.

Griffith, C. J., Cooper, R. A., Gilmore, J., Davies, C., and Lewis, M. (2000). An evaluation of hospital cleaning regimes and standards. *Journal of Hospital Infection*, *45*(1), 19–28.

Gyawali, R., Ibrahim, S. A., Hasfa, S. H. A., Smqadri, S. Q., and Haik, Y. (2011). Antimicrobial activity of copper alone and in combination with lactic acid against *Escherichia coli* O157:H7 in laboratory medium and on the surface of lettuce and tomatoes. *Journal of Pathogens*, 1–9. https://doi.org/10.4061/2011/650968

Halder, S., Yadav, K. K., Sarkar, R., Mukherjee, S., Saha, P., Haldar, S., Karmakar, S., and Sen, T. (2015). Alteration of zeta potential and membrane permeability in bacteria: A study with cationic agents. *SpringerPlus*, *4*(1), 672. https://doi.org/10.1186/s40064-015-1476-7

Hanaor, D. A., and Sorrell, C. C. (2011). Review of the anatase to rutile phase transformation. *Journal of Materials Science*, *46*(4), 855–874.

Hao, Z., Lou, H., Zhu, R., Zhu, J., Zhang, D., Zhao, B. S., Zeng, S., Chen, X., Chan, J., He, C., and Chen, P. R. (2014). The multiple antibiotic resistance regulator MarR is a copper sensor in *Escherichia coli*. *Nature Chemical Biology*, *10*(1), 21–28. https://doi.org/10.1038/nchembio.1380

Hapala, I., Griac, P., Nosek, J., Sychrova, H., and Tomáška, L. (2013). Yeast membranes and cell wall: From basics to applications. *Current Genetics*, *59*. https://doi.org/10.1007/s00294-013-0408-8

Hartmann, M., Berditsch, M., Hawecker, J., Ardakani, M. F., Gerthsen, D., and Ulrich, A. S. (2010). Damage of the bacterial cell envelope by antimicrobial peptides gramicidin S and

PGLa as revealed by transmission and scanning electron microscopy. *Antimicrobial Agents and Chemotherapy*, *54*(8), 3132–3142. https://doi.org/10.1128/AAC.00124-10

Hassan, I. A., Parkin, I. P., Nair, S. P., and Carmalt, C. J. (2014). Antimicrobial activity of copper and copper (I) oxide thin films deposited via aerosol-assisted CVD. *Journal of Materials Chemistry B*, *2*(19), 2855–2860. https://doi.org/10.1039/C4TB00196F

Heinemann, J. A. (1999). How antibiotics cause antibiotic resistance. *Drug Discovery Today*, *4*(2), 72–79.

Heinemann, J. A., and Sprague, G. F. (1989). Bacterial conjugative plasmids mobilize DNA transfer between bacteria and yeast. *Nature*, *340*(6230), 205–209. https://doi.org/10.1038/340205a0

Himmler, S., van Exel, J., Perry-Duxbury, M., and Brouwer, W. (2020). Willingness to pay for an early warning system for infectious diseases. *The European Journal of Health Economics: HEPAC: Health Economics in Prevention and Care*, *21*(5), 763–773. https://doi.org/10.1007/s10198-020-01171-2

Hughes, D., and Andersson, D. I. (2012). Selection of resistance at lethal and non-lethal antibiotic concentrations. *Current Opinion in Microbiology*, *15*(5), 555–560. https://doi.org/10.1016/j.mib.2012.07.005

Hyldgaard, M., Mygind, T., and Meyer, R. L. (2012). Essential oils in food preservation: mode of action, synergies, and interactions with food matrix components. *Frontiers in Microbiology*, *3*. https://doi.org/10.3389/fmicb.2012.00012

Inweregbu, K., Dave, J., and Pittard, A. (2005). Nosocomial infections. *Continuing Education in Anaesthesia Critical Care & Pain*, *5*(1), 14–17. https://doi.org/10.1093/bjaceaccp/mki006

Jang, J., Hur, H.-G., Sadowsky, M. J., Byappanahalli, M. N., Yan, T., and Ishii, S. (2017). Environmental *Escherichia coli*: Ecology and public health implications—a review. *Journal of Applied Microbiology*, *123*(3), 570–581. https://doi.org/10.1111/jam.13468

Jefferson, K. K. (2004). What drives bacteria to produce a biofilm? *FEMS Microbiology Letters*, *236*(2), 163–173. https://doi.org/10.1111/j.1574-6968.2004.tb09643.x

Jones, S. A., Bowler, P. G., Walker, M., and Parsons, D. (2004). Controlling wound bioburden with a novel silver-containing HydrofiberR dressing. *Wound Repair and Regeneration*, *12*(3), 288–294. https://doi.org/10.1111/j.1067-1927.2004.012304.x

Jørgensen, S. B., Søraas, A. V., Arnesen, L. S., Leegaard, T. M., Sundsfjord, A., and Jenum, P. A. (2017). A comparison of extended spectrum β-lactamase producing *Escherichia coli* from clinical, recreational water and wastewater samples associated in time and location. *PloS One*, *12*(10), e0186576. https://doi.org/10.1371/journal.pone.0186576

Josset, S., Keller, N., Lett, M.-C., Ledoux, M. J., and Keller, V. (2008). Numeration methods for targeting photoactive materials in the UV-A photocatalytic removal of microorganisms. *Chemical Society Reviews*, *37*(4), 744. https://doi.org/10.1039/b711748p

Jun, H, Kurenbach, B., Aitken, J., Wasa, A., Remus-Emsermann, M. N. P., Godsoe, W., and Heinemann, J. A. (2019). Effects of sub-lethal concentrations of copper ammonium acetate, pyrethrins and atrazine on the response of *Escherichia coli* to antibiotics. *F1000Research*, *8*. https://doi.org/10.12688/f1000research.17652.1

Jung, J., Oh, H., Noh, H., Ji, J. H., and Kim, S. S. (2006). Metal nanoparticle generation using a small ceramic heater with a local heating area. *Journal of Aerosol Science - J AEROSOL SCI*, *37*, 1662–1670. https://doi.org/10.1016/j.jaerosci.2006.09.002

Keren, I., Wu, Y., Inocencio, J., Mulcahy, L. R., and Lewis, K. (2013). Killing by bactericidal antibiotics does not depend on reactive oxygen species. *Science*, *339*(6124), 1213–1216. https://doi.org/10.1126/science.1232688

Khan, H. A., Baig, F. K., and Mehboob, R. (2017). Nosocomial infections: Epidemiology, prevention, control and surveillance. *Asian Pacific Journal of Tropical Biomedicine*, *7*(5), 478–482. https://doi.org/10.1016/j.apjtb.2017.01.019

Kiaune, L., and Singhasemanon, N. (2011). Pesticidal copper (I) oxide: Environmental fate and aquatic toxicity. *Reviews of Environmental Contamination and Toxicology*, *213*, 1–26. https://doi.org/10.1007/978-1-4419-9860-6_1

Kim, J. S., Kuk, E., Yu, K. N., Kim, J.-H., Park, S. J., Lee, H. J., Kim, S. H., Park, Y. K., Park, Y. H., and Hwang, C.-Y. (2007). Antimicrobial effects of silver nanoparticles. *Nanomedicine: Nanotechnology, Biology and Medicine*, *3*(1), 95–101.

Kim, S. H., Lee, H. S., Ryu, D. S., Choi, S. J., and Lee, D. S. (2011). Antibacterial activity of silver-nanoparticles against *Staphylococcus aureus* and *Escherichia coli*. *Korean Journal of Microbiology and Biotechnology*. https://agris.fao.org/agris-search/search.do?recordID=KR2012001109

Kiwi, J., and Nadtochenko, V. (2005). Evidence for the mechanism of photocatalytic degradation of the bacterial wall membrane at the TiO2 interface by ATR-FTIR and laser kinetic spectroscopy. *Langmuir*, *21*(10), 4631–4641.

Kohanski, M. A., Dwyer, D. J., Hayete, B., Lawrence, C. A., and Collins, J. J. (2007). A Common Mechanism of Cellular Death Induced by Bactericidal Antibiotics. *Cell*, *130*(5), 797–810. https://doi.org/10.1016/j.cell.2007.06.049

Koseki, H., Yonekura, A., Shida, T., Yoda, I., Horiuchi, H., Morinaga, Y., Yanagihara, K., Sakoda, H., Osaki, M., and Tomita, M. (2014). Early Staphylococcal biofilm formation on solid orthopaedic implant materials: In Vitro Study. *PLoS ONE*, *9*(10), e107588. https://doi.org/10.1371/journal.pone.0107588

Kotra, L. P., Haddad, J., and Mobashery, S. (2000). Aminoglycosides: Perspectives on mechanisms of action and resistance and strategies to counter resistance. *Antimicrobial Agents and Chemotherapy*, *44*(12), 3249–3256.

Koutsolioutsou, A., Peña-Llopis, S., and Demple, B. (2005). Constitutive soxR mutations contribute to multiple-antibiotic resistance in clinical *Escherichia coli* isolates. *Antimicrobial Agents and Chemotherapy*, *49*(7), 2746–2752.

Kramer, A., and Assadian, O. (2014). Survival of Microorganisms on Inanimate Surfaces. In *Use of Biocidal Surfaces for Reduction of Healthcare Acquired Infections* (pp. 7–26). https://doi.org/10.1007/978-3-319-08057-4_2

Krumdieck, S., Miya, S. S., Lee, D., Davies-Talwar, S., and Bishop, C. M. (2015). Titania-based photocatalytic coatings on stainless steel hospital fixtures. *Physica Status Solidi (c)*, *12*(7), 1028–1035.

Krumdieck, S. P., Boichot, R., Gorthy, R., Land, J. G., Lay, S., Gardecka, A. J., Polson, M. I. J., Wasa, A., Aitken, J. E., Heinemann, J. A., Renou, G., Berthomé, G., Charlot, F., Encinas, T., Braccini, M., and Bishop, C. M. (2019). Nanostructured TiO_2 anatase-rutile-carbon solid coating with visible light antimicrobial activity. *Scientific Reports*, *9*(1), 1883. https://doi.org/10.1038/s41598-018-38291-y

Krumdieck, S, Gorthy, R., Gardecka, A. J., Lee, D., Miya, S. S., Talwar, S. D., Polson, M. I., and Bishop, C. (2017). Characterization of photocatalytic, wetting and optical properties of

TiO_2 thin films and demonstration of uniform coating on a 3-D surface in the mass transport controlled regime. *Surface and Coatings Technology*, *326*, 402–410.

Kubacka, A., Diez, M. S., Rojo, D., Bargiela, R., Ciordia, S., Zapico, I., Albar, J. P., Barbas, C., Dos Santos, V. A. M., and Fernández-García, M. (2014). Understanding the antimicrobial mechanism of TiO_2-based nanocomposite films in a pathogenic bacterium. *Scientific Reports*, *4*, 4134.

Kurenbach, B., Gibson, P. S., Hill, A. M., Bitzer, A. S., Silby, M. W., Godsoe, W., and Heinemann, J. A. (2017). Herbicide ingredients change S*almonella enterica sv. Typhimurium* and *Escherichia coli* antibiotic responses. *Microbiology*, *163*(12), 1791–1801.

Kurenbach, B., Hill, A. M., Godsoe, W., van Hamelsveld, S., and Heinemann, J. A. (2018). Agrichemicals and antibiotics in combination increase antibiotic resistance evolution. *PeerJ*, *6*. https://doi.org/10.7717/peerj.5801

Kurenbach, B., Marjoshi, D., Amábile-Cuevas, C. F., Ferguson, G. C., Godsoe, W., Gibson, P., and Heinemann, J. A. (2015). Sublethal exposure to commercial formulations of the herbicides dicamba, 2, 4-dichlorophenoxyacetic acid, and glyphosate cause changes in antibiotic susceptibility in *Escherichia coli* and *Salmonella enterica serovar Typhimurium*. *MBio*, *6*(2), e00009-15. https://doi.org/10.1128/mBio.00009-15

Kwiatek, M., Parasion, S., Rutyna, P., Mizak, L., Gryko, R., Niemcewicz, M., Olender, A., and Łobocka, M. (2017). Isolation of bacteriophages and their application to control *Pseudomonas aeruginosa* in planktonic and biofilm models. *Research in Microbiology*, *168*(3), 194–207. https://doi.org/10.1016/j.resmic.2016.10.009

Lee, A. L. Z., Ng, V. W. L., Wang, W., Hedrick, J. L., and Yang, Y. Y. (2013). Block copolymer mixtures as antimicrobial hydrogels for biofilm eradication. *Biomaterials*, *34*(38), 10278–10286. https://doi.org/10.1016/j.biomaterials.2013.09.029

Lee, D., Krumdieck, S., and Talwar, S. D. (2013). Scale-up design for industrial development of a PP-MOCVD coating system. *Surface and Coatings Technology*, *230*, 39–45.

Lemire, J. A., Harrison, J. J., and Turner, R. J. (2013). Antimicrobial activity of metals: Mechanisms, molecular targets and applications. *Nature Reviews. Microbiology; London*, *11*(6), 371–384. http://dx.doi.org.ezproxy.canterbury.ac.nz/10.1038/nrmicro3028

Leung, Y. H., Xu, X., Ma, A. P. Y., Liu, F., Ng, A. M. C., Shen, Z., Gethings, L. A., Guo, M. Y., Djurišić, A. B., Lee, P. K. H., Lee, H. K., Chan, W. K., and Leung, F. C. C. (2016). Toxicity of ZnO and TiO_2 to *Escherichia coli* cells. *Scientific Reports*, *6*(1). https://doi.org/10.1038/srep35243

Leveau, J. H. J., and Lindow, S. E. (2002). Bioreporters in microbial ecology. *Current Opinion in Microbiology*, *5*(3), 259–265. https://doi.org/10.1016/s1369-5274 (02)00321-1

Leyland, N. S., Podporska-Carroll, J., Browne, J., Hinder, S. J., Quilty, B., and Pillai, S. C. (2016). Highly Efficient F, Cu doped TiO_2 anti-bacterial visible light active photocatalytic coatings to combat hospital-acquired infections. *Scientific Reports*, *6*(1). https://doi.org/10.1038/srep24770

Li, Y., Leung, P., Yao, L., Song, Q. W., and Newton, E. (2006). Antimicrobial effect of surgical masks coated with nanoparticles. *Journal of Hospital Infection*, *62*(1), 58–63. https://doi.org/10.1016/j.jhin.2005.04.015

Lu, X., Gao, Y., Luo, J., Yan, S., Rengel, Z., and Zhang, Z. (2014). Interaction of veterinary antibiotic tetracyclines and copper on their fates in water and water hyacinth (*Eichhornia*

crassipes). *Journal of Hazardous Materials*, *280*, 389–398. https://doi.org/10.1016/j.jhazmat.2014.08.022

M., S. S., and Natarajan, K. (2015). Antibiofilm activity of epoxy/Ag-TiO_2 polymer nanocomposite coatings against *Staphylococcus aureus* and *Escherichia coli*. *Coatings*, *5*(2), 95–114. https://doi.org/10.3390/coatings5020095

Maness, P.-C., Smolinski, S., Blake, D. M., Huang, Z., Wolfrum, E. J., and Jacoby, W. A. (1999). Bactericidal activity of photocatalytic TiO_2 reaction: Toward an understanding of its killing mechanism. *Applied and Environmental Microbiology*, *65*(9), 4094–4098.

Mangalappalli-Illathu, A. K., and Korber, D. R. (2006). Adaptive resistance and differential protein expression of *Salmonella enterica serovar* Enteritidis biofilms exposed to benzalkonium chloride. *Antimicrobial Agents and Chemotherapy*, *50*(11), 3588–3596.

Mao, K., Zhang, K., Du, W., Ali, W., Feng, X., and Zhang, H. (2020). The potential of wastewater-based epidemiology as surveillance and early warning of infectious disease outbreaks. *Current Opinion in Environmental Science & Health*, *17*, 1–7. https://doi.org/10.1016/j.coesh.2020.04.006

Mehta, A. (2011). Mechanism of action of quinolones and fluoroquinolones. *Retrieved December*, *6*, 2015.

Mehtar, S., Wiid, I., and Todorov, S. D. (2008). The antimicrobial activity of copper and copper alloys against nosocomial pathogens and *Mycobacterium tuberculosis* isolated from healthcare facilities in the Western Cape: An in-vitro study. *Journal of Hospital Infection*, *68*(1), 45–51. https://doi.org/10.1016/j.jhin.2007.10.009

Mendes, G. P., Vieira, P. S., Lanceros-Méndez, S., Kluskens, L. D., and Mota, M. (2015). Transformation of *Escherichia coli* JM109 using pUC19 by the Yoshida effect. *Journal of Microbiological Methods*, *115*, 1–5. https://doi.org/10.1016/j.mimet.2015.05.012

Metcalfe, S., Baker, M. G., Freeman, J., Wilson, N., and Murray, P. (2016). Combating antimicrobial resistance demands nation-wide action and global governance. *The New Zealand Medical Journal (Online); Christchurch*, *129*(1444), 8–14.

Michels, H., Noyce, J., and Keevil, C. (2009). Effects of temperature and humidity on the efficacy of methicillin-resistant *Staphylococcus aureus* challenged antimicrobial materials containing silver and copper. *Letters in Applied Microbiology*, *49*(2), 191–195. https://doi.org/10.1111/j.1472-765X.2009.02637.x

Mills, A. (2012). An overview of the methylene blue ISO test for assessing the activities of photocatalytic films. *Applied Catalysis B: Environmental*, *128*, 144–149.

Mills, A., Hill, C., and Robertson, P. K. (2012). Overview of the current ISO tests for photocatalytic materials. *Journal of Photochemistry and Photobiology A: Chemistry*, *237*, 7–23.

Molina-González, D., Alonso-Calleja, C., Alonso-Hernando, A., and Capita, R. (2014). Effect of sub-lethal concentrations of biocides on the susceptibility to antibiotics of multi-drug resistant *Salmonella enterica* strains. *Food Control*, *40*, 329–334. https://doi.org/10.1016/j.foodcont.2013.11.046

Mun, S.-H., Joung, D.-K., Kim, Y.-S., Kang, O.-H., Kim, S.-B., Seo, Y.-S., Kim, Y.-C., Lee, D.-S., Shin, D.-W., Kweon, K.-T., and Kwon, D.-Y. (2013). Synergistic antibacterial effect of curcumin against methicillin-resistant *Staphylococcus aureus*. *Phytomedicine*, *20*(8), 714–718. https://doi.org/10.1016/j.phymed.2013.02.006

Munson, G. P., Lam, D. L., Outten, F. W., and O'Halloran, T. V. (2000). Identification of a copper-responsive two-component system on the chromosome of *Escherichia coli* K-12. *Journal of Bacteriology*, *182*(20), 5864–5871. https://doi.org/10.1128/jb.182.20.5864-5871.2000

Nadtochenko, V. A., Rincon, A. G., Stanca, S. E., and Kiwi, J. (2005). Dynamics of *E. coli* membrane cell peroxidation during TiO_2 photocatalysis studied by ATR-FTIR spectroscopy and AFM microscopy. *Journal of Photochemistry and Photobiology A: Chemistry*, *169*(2), 131–137.

Naik, K., and Kowshik, M. (2014). Antibiofilm efficacy of low temperature processed AgCl–TiO_2 nanocomposite coating. *Materials Science and Engineering: C*, *34*, 62–68. https://doi.org/10.1016/j.msec.2013.10.008

Nies, D. H. (2003). Efflux-mediated heavy metal resistance in prokaryotes. *FEMS Microbiology Reviews*, *27*(2–3), 313–339. https://doi.org/10.1016/S0168-6445 (03)00048-2

Niño-Martínez, N., Salas Orozco, M. F., Martínez-Castañón, G.-A., Torres Méndez, F., and Ruiz, F. (2019). Molecular mechanisms of bacterial resistance to metal and metal oxide nanoparticles. *International Journal of Molecular Sciences*, *20*(11), 2808. https://doi.org/10.3390/ijms20112808

Nishino, K., Nikaido, E., and Yamaguchi, A. (2007). Regulation of multidrug efflux systems involved in multidrug and metal resistance of *Salmonella enterica Serovar Typhimurium*. *Journal of Bacteriology*, *189*(24), 9066–9075. https://doi.org/10.1128/JB.01045-07

Page, K., Wilson, M., and Parkin, I. P. (2009). Antimicrobial surfaces and their potential in reducing the role of the inanimate environment in the incidence of hospital-acquired infections. *Journal of Materials Chemistry*, *19*(23), 3819. https://doi.org/10.1039/b818698g

Page, M. G. (2012). Beta-lactam antibiotics. In *Antibiotic discovery and development* (pp. 79–117). Springer.

Pantanella, F., Berlutti, F., Passeri, D., Sordi, D., Frioni, A., Natalizi, T., Terranova, M. L., Rossi, M., and Valenti, P. (2011). *Quantitative evaluation of bacteria adherent and in biofilm on single-wall carbon nanotube-coated surfaces* [Research article]. Interdisciplinary Perspectives on Infectious Diseases. https://doi.org/10.1155/2011/291513

Pelaez, M., Nolan, N. T., Pillai, S. C., Seery, M. K., Falaras, P., Kontos, A. G., Dunlop, P. S., Hamilton, J. W., Byrne, J. A., and O'shea, K. (2012). A review on the visible light active titanium dioxide photocatalysts for environmental applications. *Applied Catalysis B: Environmental*, *125*, 331–349.

Peng, J. J.-Y., Botelho, M. G., and Matinlinna, J. P. (2012). Silver compounds used in dentistry for caries management: A review. *Journal of Dentistry*, *40*(7), 531–541. https://doi.org/10.1016/j.jdent.2012.03.009

Percival, S. L., Bowler, P. G., and Russell, D. (2005). Bacterial resistance to silver in wound care. *Journal of Hospital Infection*, *60*(1), 1–7. https://doi.org/10.1016/j.jhin.2004.11.014

Piszczek, P., Muchewicz, ż., Radtke, A., Gryglas, M., Dahm, H., and Różycki, H. (2013). CVD of TiO_2 and TiO_2/Ag antimicrobial layers: Deposition from the hexanuclear μ-oxo Ti (IV) complex as a precursor, and the characterization. *Surface and Coatings Technology*, *222*, 38–43. https://doi.org/10.1016/j.surfcoat.2013.01.057

Prism—Graphpad.com. (n.d.). Retrieved August 31, 2018, from https://www.graphpad.com/scientific-software/prism/

Quick-R: Power Analysis. (n.d.). Retrieved August 31, 2018, from https://www.statmethods.net/stats/power.html

Ramyadevi, J., Jeyasubramanian, K., Marikani, A., Rajakumar, G., and Rahuman, A. A. (2012). Synthesis and antimicrobial activity of copper nanoparticles. *Materials Letters*, *71*, 114–116. https://doi.org/10.1016/j.matlet.2011.12.055

Remus-Emsermann, M. N., and Leveau, J. H. (2010). Linking environmental heterogeneity and reproductive success at single-cell resolution. *The ISME Journal*, *4*(2), 215–222. https://doi.org/10.1038/ismej.2009.110

Remus-Emsermann, M. N. P., Gisler, P., and Drissner, D. (2016). MiniTn *7* -transposon delivery vectors for inducible or constitutive fluorescent protein expression in *Enterobacteriaceae*. *FEMS Microbiology Letters*, *363*(16), fnw178. https://doi.org/10.1093/femsle/fnw178

Remus-Emsermann, M. N. P., and Schlechter, R. O. (2018). Phyllosphere microbiology: At the interface between microbial individuals and the plant host. *New Phytologist*, *218*(4), 1327–1333. https://doi.org/10.1111/nph.15054

Rohde, M. (2019). The Gram-positive bacterial cell wall. *Microbiology Spectrum*, *7*(3). https://doi.org/10.1128/microbiolspec.GPP3-0044-2018

Rosario-Martinez, H. D., Fox, J., and R Core Team. (2015). *phia: Post-Hoc Interaction Analysis* (0.2-1) [Computer software]. https://CRAN.R-project.org/package=phia

Russell A.D. (2002). Introduction of biocides into clinical practice and the impact on antibiotic-resistant bacteria. *Journal of Applied Microbiology*, *92*(s1), 121S-135S. https://doi.org/10.1046/j.1365-2672.92.5s1.12.x

Sader, H. S., Rhomberg, P. R., Fuhrmeister, A. S., Mendes, R. E., Flamm, R. K., and Jones, R. N. (2019). Antimicrobial resistance surveillance and new drug development. *Open Forum Infectious Diseases*, *6*(Supplement_1), S5–S13. https://doi.org/10.1093/ofid/ofy345

Sadowski, R., Strus, M., Buchalska, M., Heczko, P. B., and Macyk, W. (2015). Visible light induced photocatalytic inactivation of bacteria by modified titanium dioxide films on organic polymers. *Photochemical & Photobiological Sciences*, *14*(3), 514–519.

Sandoval-Motta, S., and Aldana, M. (2016). Adaptive resistance to antibiotics in bacteria: A systems biology perspective. *Wiley Interdisciplinary Reviews: Systems Biology and Medicine*, *8*(3), 253–267.

Schindelin, J., Arganda-Carreras, I., Frise, E., Kaynig, V., Longair, M., Pietzsch, T., Preibisch, S., Rueden, C., Saalfeld, S., Schmid, B., Tinevez, J.-Y., White, D. J., Hartenstein, V., Eliceiri, K., Tomancak, P., and Cardona, A. (2012). Fiji: An open-source platform for biological-image analysis. *Nature Methods*, *9*(7), 676–682. https://doi.org/10.1038/nmeth.2019

Schlechter, R. O., Jun, H., Bernach, M., Oso, S., Boyd, E., Muñoz-Lintz, D. A., Dobson, R. C. J., Remus, D. M., and Remus-Emsermann, M. N. P. (2018). Chromatic bacteria – A broad host-range plasmid and chromosomal insertion toolbox for fluorescent protein Eexpression in bacteria. *Frontiers in Microbiology*, *9*. https://doi.org/10.3389/fmicb.2018.03052

Schmidt, M. G., Attaway, H. H., Sharpe, P. A., John, J., Sepkowitz, K. A., Morgan, A., Fairey, S. E., Singh, S., Steed, L. L., Cantey, J. R., Freeman, K. D., Michels, H. T., and Salgado, C. D. (2012). Sustained reduction of microbial burden on common hospital surfaces through introduction of copper. *Journal of Clinical Microbiology*, *50*(7), 2217–2223. https://doi.org/10.1128/JCM.01032-12

Schwarz, S., Kehrenberg, C., Doublet, B., and Cloeckaert, A. (2004). Molecular basis of bacterial resistance to chloramphenicol and florfenicol. *FEMS Microbiology Reviews*, *28*(5), 519–542.

Shankar, S., and Rhim, J.-W. (2014). Effect of copper salts and reducing agents on characteristics and antimicrobial activity of copper nanoparticles. *Materials Letters, 132*, 307–311. https://doi.org/10.1016/j.matlet.2014.06.014

Sikora, R. (2005). Ab initio study of phonons in the rutile structure of TiO_2. *Journal of Physics and Chemistry of Solids*, *66*(6), 1069–1073.

Silver, S., and Phung, L. T. (1996). Bacterial heavy metal resistance: New surprises. *Annual Review of Microbiology, 50*, 753–789. https://doi.org/10.1146/annurev.micro.50.1.753

Silver, Simon, Phung, L. T., and Silver, G. (2006). Silver as biocides in burn and wound dressings and bacterial resistance to silver compounds. *Journal of Industrial Microbiology & Biotechnology*, *33*(7), 627–634. https://doi.org/10.1007/s10295-006-0139-7

Sondi, I., and Salopek-Sondi, B. (2004). Silver nanoparticles as antimicrobial agent: A case study on *E. coli* as a model for Gram-negative bacteria. *Journal of Colloid and Interface Science*, *275*(1), 177–182. https://doi.org/10.1016/j.jcis.2004.02.012

Souli, M., Galani, I., Plachouras, D., Panagea, T., Armaganidis, A., Petrikkos, G., and Giamarellou, H. (2013). Antimicrobial activity of copper surfaces against carbapenemase-producing contemporary Gram-negative clinical isolates. *Journal of Antimicrobial Chemotherapy*, *68*(4), 852–857. https://doi.org/10.1093/jac/dks473

Stoimenov, P. K., Klinger, R. L., Marchin, G. L., and Klabunde, K. J. (2002). Metal oxide nanoparticles as bactericidal agents. *Langmuir*, *18*(17), 6679–6686.

Sunada, K., Watanabe, T., and Hashimoto, K. (2003). Studies on photo killing of bacteria on TiO_2 thin film. *Journal of Photochemistry and Photobiology A: Chemistry*, *156*(1–3), 227–233. https://doi.org/10.1016/S1010-6030 (02)00434-3

Taylor, L., Phillips, P., and Hastings, R. (2009). Reducing bacterial contamination using silver antimicrobial technology. *Nursing Times*, *105*, 24–27.

Tecon, R., and Leveau, J. H. J. (2012). The mechanics of bacterial cluster formation on plant leaf surfaces as revealed by bioreporter technology. *Environmental Microbiology*, *14*(5), 1325–1332. https://doi.org/10.1111/j.1462-2920.2012.02715.x

Tong, F., Zhao, Y., Gu, X., Gu, C., and Lee, C. C. (2015). Joint toxicity of tetracycline with copper (II) and cadmium (II) to *Vibrio fischeri*: Effect of complexation reaction. *Ecotoxicology; New York*, *24*(2), 346–355. http://dx.doi.org/10.1007/s10646-014-1383-7

Tzeng, C.-W. D., Tran Cao, H. S., Lee, J. E., Pisters, P. W. T., Varadhachary, G. R., Wolff, R. A., Abbruzzese, J. L., Crane, C. H., Evans, D. B., Wang, H., Abbott, D. E., Vauthey, J.-N., Aloia, T. A., Fleming, J. B., and Katz, M. H. G. (2014). Treatment sequencing for resectable pancreatic cancer: Influence of early metastases and surgical complications on multimodality therapy completion and survival. *Journal of Gastrointestinal Surgery: Official Journal of the Society for Surgery of the Alimentary Tract*, *18*(1), 16–24; discussion 24-25. https://doi.org/10.1007/s11605-013-2412-1

Van Elsas, J. D., Semenov, A. V., Costa, R., and Trevors, J. T. (2011). Survival of *Escherichia coli* in the environment: Fundamental and public health aspects. *The ISME Journal*, *5*(2), 173–183. https://doi.org/10.1038/ismej.2010.80

Van Hamelsveld, S., Adewale, M. E., Kurenbach, B., Godsoe, W., Harding, J. S., Remus-Emsermann, M. N. P., and Heinemann, J. A. (2019). Prevalence of antibiotic-resistant *Escherichia coli* isolated from urban and agricultural streams in Canterbury, New Zealand. *FEMS Microbiology Letters*, *366*(8). https://doi.org/10.1093/femsle/fnz104

Verdier, T., Coutand, M., Bertron, A., and Roques, C. (2014). Antibacterial activity of TiO_2 photocatalyst alone or in coatings on *E. coli*: The influence of methodological aspects. *Coatings*, *4*(3), 670–686. https://doi.org/10.3390/coatings4030670

Von Nussbaum, F., Brands, M., Hinzen, B., Weigand, S., and Häbich, D. (2006). Antibacterial natural products in medicinal chemistry—Exodus or revival? *Angewandte Chemie International Edition*, *45*(31), 5072–5129.

Wagenvoort, J. H. T., De Brauwer, E. I. G. B., Sijstermans, M. L. H., and Toenbreker, H. M. J. (2005). Risk of re-introduction of methicillin-resistant *Staphylococcus aureus* into the hospital by intrafamilial spread from and to healthcare workers. *Journal of Hospital Infection*, *59*(1), 67–68. https://doi.org/10.1016/j.jhin.2004.07.025

Walker, M. (2003). Scanning electron microscopic examination of bacterial immobilisation in a carboxymethyl cellulose (AQUACEL®) and alginate dressings. *Biomaterials*, *24*(5), 883–890. https://doi.org/10.1016/S0142-9612 (02)00414-3

Walsh, C. (2000). Molecular mechanisms that confer antibacterial drug resistance. *Nature*, *406*(6797), 775.

Wang, J., Li, J., Guo, G., Wang, Q., Tang, J., Zhao, Y., Qin, H., Wahafu, T., Shen, H., Liu, X., and Zhang, X. (2016). Silver-nanoparticles-modified biomaterial surface resistant to staphylococcus: New insight into the antimicrobial action of silver. *Scientific Reports*, *6*(1), 32699. https://doi.org/10.1038/srep32699

Wang, T., El Meouche, I., and Dunlop, M. J. (2017). Bacterial persistence induced by salicylate via reactive oxygen species. *Scientific Reports*, *7*(1), 43839. https://doi.org/10.1038/srep43839

Webber, M. A., and Piddock, L. J. V. (2003). The importance of efflux pumps in bacterial antibiotic resistance. *Journal of Antimicrobial Chemotherapy*, *51*(1), 9–11.

Wei, X., Yang, Z., Tay, S. L., and Gao, W. (2014). Photocatalytic TiO_2 nanoparticles enhanced polymer antimicrobial coating. *Applied Surface Science*, *290*, 274–279. https://doi.org/10.1016/j.apsusc.2013.11.067

Wellington, E. M., Boxall, A. B., Cross, P., Feil, E. J., Gaze, W. H., Hawkey, P. M., Johnson-Rollings, A. S., Jones, D. L., Lee, N. M., Otten, W., Thomas, C. M., and Williams, A. P. (2013). The role of the natural environment in the emergence of antibiotic resistance in Gram-negative bacteria. *The Lancet Infectious Diseases*, *13*(2), 155–165. https://doi.org/10.1016/S1473-3099 (12)70317-1

Weston, N., Sharma, P., Ricci, V., and Piddock, L. J. V. (2018). Regulation of the AcrAB-TolC efflux pump in Enterobacteriaceae. *Research in Microbiology*, *169*(7–8), 425–431. https://doi.org/10.1016/j.resmic.2017.10.005

Wickham, H. (2016). *ggplot2: Elegant Graphics for Data Analysis* (2nd ed.). Springer International Publishing. https://doi.org/10.1007/978-3-319-24277-4

Williamson, D., Baker, M., French, N., and Thomas, M. (2015). Missing in action: An antimicrobial resistance strategy for New Zealand. *The New Zealand Medical Journal (Online); Christchurch*, *128*(1427), 65–67.

Witte, W. (2004). International dissemination of antibiotic resistant strains of bacterial pathogens. *Infection, Genetics and Evolution*, *4*(3), 187–191.

Wright, M. S., Peltier, G. L., Stepanauskas, R., and McArthur, J. V. (2006). Bacterial tolerances to metals and antibiotics in metal-contaminated and reference streams. *FEMS Microbiology Ecology*, *58*(2), 293–302.

Wu, X., Li, J., Wang, L., Huang, D., Zuo, Y., and Li, Y. (2010). The release properties of silver ions from Ag-nHA/TiO_2 /PA66 antimicrobial composite scaffolds. *Biomedical Materials, 5*(4), 044105. https://doi.org/10.1088/1748-6041/5/4/044105

Wu, Y., Vulić, M., Keren, I., and Lewis, K. (2012). Role of oxidative stress in persister tolerance. *Antimicrobial Agents and Chemotherapy*, *56*(9), 4922–4926. https://doi.org/10.1128/AAC.00921-12

Xu, Z., Lai, Y., Wu, D., Huang, W., Huang, S., Zhou, L., and Chen, J. (2015). Antibacterial effects and biocompatibility of titania Nanotubes with Octenidine Dihydrochloride/Poly (lactic-co-glycolic acid). *BioMed Research International*, *2015*. https://doi.org/10.1155/2015/836939

Yang, J.-L., Li, Y.-F., Guo, X.-P., Liang, X., Xu, Y.-F., Ding, D.-W., Bao, W.-Y., and Dobretsov, S. (2016). The effect of carbon nanotubes and titanium dioxide incorporated in PDMS on biofilm community composition and subsequent mussel plantigrade settlement. *Biofouling*, *32*(7), 763–777. https://doi.org/10.1080/08927014.2016.1197210

Yao, Z., Kahne, D., and Kishony, R. (2012). Distinct single-cell morphological dynamics under beta-lactam antibiotics. *Molecular Cell*, *48*(5), 705–712.

Yu, J., Low, J., Xiao, W., Zhou, P., and Jaroniec, M. (2014). Enhanced photocatalytic CO_2-reduction activity of anatase TiO_2 by coexposed ${$001$}$ and ${$101$}$ facets. *Journal of the American Chemical Society*, *136*(25), 8839–8842.

Zaffiri, L., Gardner, J., and Toledo-Pereyra, L. H. (2012). History of antibiotics. From Salvarsan to Cephalosporins. *Journal of Investigative Surgery*, *25*(2), 67–77. https://doi.org/10.3109/08941939.2012.664099

Zhang, H., Li, Y., and Zhu, J.-K. (2018). Developing naturally stress-resistant crops for a sustainable agriculture. *Nature Plants, 4*(12), 989–996. https://doi.org/10.1038/s41477-018-0309-4

Zhang, J., Zhou, P., Liu, J., and Yu, J. (2014). New understanding of the difference of photocatalytic activity among anatase, rutile and brookite TiO_2. *Physical Chemistry Chemical Physics*, *16*(38), 20382–20386.

Zhao, B., Chen, F., Huang, Q., and Zhang, J. (2009). Brookite TiO_2 nanoflowers. *Chemical Communications*, *34*, 5115–5117.

Zhao, Y., Tan, Y., Guo, Y., Gu, X., Wang, X., and Zhang, Y. (2013). Interactions of tetracycline with Cd (II), Cu (II) and Pb (II) and their cosorption behavior in soils. *Environmental Pollution*, *180*, 206–213. https://doi.org/10.1016/j.envpol.2013.05.043

Appendices

Appendix A: Antimicrobial activity experiment

E. coli ATCC 8739 exposed to NsARC and stainless steel for 8 hrs under four different exposure conditions (HI, UV, Dark and Ambient light) using the ISO: 2009 technique.

1. **summary.aov**

	Df	Sum sq	mean Sq.	F value	Pr(>F)	
material	1	28.626	28.626	3562.5	<2.00E-16	***
exposure	3	7.414	2.471	307.5	2.36E-14	***
material:exposure	3	6.915	2.305	286.8	4.08E-14	***
Residuals	16	0.129	0.008			

Signif. Codes: 0 ‘***’ 0.001 ‘**’ 0.01 ‘*’ 0.05 ‘.’ 0.1 ‘ ’ 1

Simultaneous Tests for General Linear Hypotheses

Here is the contrast matrix listing the 6 contrasts of interest:

1)NsARC_al vs steel_al,

2)NsARC_al vs NsARC_dark,

3)NsARC_dark vs steel_dark,

4)NsARC_hi vs steel_hi,

5)NsARC_hi vs NsARC_uv,

6)NsARC_uv vs steel_uv

2. **Bonferroni contrasts**

Linear Hypotheses:

	Estimate	Std. Error	t value	Pr(>|t|)
1 == 0	-2.38055	0.11573	-20.571	<1e-04 ***
2 == 0	-1.47143	0.11573	-12.715	<1e-04 ***
3 == 0	-1.05679	0.07319	-14.439	<1e-04 ***
4 == 0	-3.22481	0.07319	-44.060	<1e-04 ***
5 == 0	0.04969	0.07319	0.679	0.966
6 == 0	-3.28886	0.07319	-44.935	<1e-04 ***

Signif. codes: 0 '***' 0.001 '**' 0.01 '*' 0.05 '.' 0.1 ' ' 1

(Adjusted p values reported -- single-step method.

S. aureus ATCC25923 exposed to NsARC and steel for 8 hrs under four different exposure conditions (HI, UV, Dark and Ambient light) using the ISO:2009 technique.

3. summary.aov

	Df	Sum sq	mean Sq.	F value	Pr(>F)	
material	1	30.411	30.411	864.3	<2.36E-15	***
exposure	3	11.070	3.690	104.84	9.85E-11	***
material:exposure	3	4.757	1.586	45.05	5.01E-08	***
Residuals	16	0.563	0.035			

Signif. Codes: 0 ‘***’ 0.001 ‘**’ 0.01 ‘*’ 0.05 ‘.’ 0.1 ‘ ’ 1

4. Bonferroni contrasts

Linear Hypotheses:

	Estimate	Std. Error	t value	Pr(>|t|)
1 == 0	-4.00675	0.24220	-16.543	<1e-05 ***
2 == 0	-2.99502	0.24220	-12.366	<1e-05 ***
3 == 0	-1.12332	0.15318	-7.333	<1e-05 ***
4 == 0	-3.21455	0.15318	-20.985	<1e-05 ***
5 == 0	0.03219	0.15318	0.210	0.867
6 == 0	-2.99339	0.15318	-19.541	<1e-05 ***

Signif. codes: 0 ‘***’ 0.001 ‘**’ 0.01 ‘*’ 0.05 ‘.’ 0.1 ‘ ’ 1

(Adjusted p values reported -- single-step method.

Pseudomonas aeruginosa ATCC10145 exposed to NsARC and steel for 8 hrs under four different exposure conditions (HI, UV, Dark and Ambient light) using the ISO:2009 technique.

5. summary.aov

	Df	Sum sq	mean Sq.	F value	Pr(>F)	
material	1	22.478	22.478	934.79	<1.27E-15	***
exposure	3	10.966	3.655	152.01	5.73E-12	***
material:exposure	3	4.901	1.634	67.94	2.54E-09	***
Residuals	16	0.385	0.024			

Signif. Codes: 0 '***' 0.001 '**' 0.01 '*' 0.05 '.' 0.1 ' ' 1

6. Bonferroni contrasts

Linear Hypotheses:

	Estimate	Std. Error	t value	Pr(>|t|)
1 == 0	-2.2208	0.2002	-11.093	< 0.001 ***
2 == 0	-1.2904	0.2002	-6.446	< 0.001 ***
3 == 0	-0.9373	0.1266	-7.403	< 0.001 ***
4 == 0	-3.0420	0.1266	-24.026	< 0.001 ***
5 == 0	-0.5367	0.1266	-4.239	0.00334 **
6 == 0	-3.1395	0.1266	-24.796	< 0.001 ***

Signif. codes: 0 '***' 0.001 '**' 0.01 '*' 0.05 '.' 0.1 ' ' 1

(Adjusted p values reported -- single-step method.

S. cerevisiae ATCC10145 exposed to NsARC and stainless steel for 8 hrs under four different exposure conditions (HI, UV, ambient light and Dark) using the ISO:2009 technique.

7. Summary.aov

	Df	Sum sq	mean Sq.	F value	Pr(>F)	
material	1	35.21	35.21	909.61	<1.58E-15	***
exposure	3	4.75	1.58	40.86	9.99E-08	***
material:exposure	3	3.49	1.16	30.07	8.25E-07	***
Residuals	16	0.62	0.04			

Signif. Codes: 0 ‘***’ 0.001 ‘**’ 0.01 ‘*’ 0.05 ‘.’ 0.1 ‘ ’ 1

7. Bonferroni contrasts

Linear Hypotheses:

	Estimate	Std. Error	t value	Pr(>|t|)
1 == 0	-3.8487	0.2540	-15.152	<0.001 ***
2 == 0	-2.3258	0.2540	-9.157	<0.001 ***
3 == 0	-1.5128	0.1606	-9.417	<0.001 ***
4 == 0	-2.8189	0.1606	-17.547	<0.001 ***
5 == 0	0.6293	0.1606	3.917	0.0066 **
6 == 0	-2.8281	0.1606	-17.605	<0.001 ***

Signif. codes: 0 ‘***’ 0.001 ‘**’ 0.01 ‘*’ 0.05 ‘.’ 0.1 ‘ ’ 1

(Adjusted p values reported -- single-step method.

Escherichia coli ATCC8739 survival curve on exposure to NsARC and stainless steel for up to 8 hrs under UV light using the ISO:2009 technique.

8. **summary.aov**

	Df	Sum Sq	Mean Sq	F value	Pr(>F)
material	1	28.043	28.043	1522.1	<2e-16 ***
time	5	18.282	3.656	198.5	<2e-16 ***
material:time	5	18.036	3.607	195.8	<2e-16 ***
Residuals	24	0.442	0.018		

Signif. codes: 0 '***' 0.001 '**' 0.01 '*' 0.05 '.' 0.1 ' ' 1

9. **Bonferroni contrasts**

Linear Hypotheses:

	Estimate	Std. Error	t value	Pr(>|t|)
1 == 0	-0.8852	0.2013	-4.398	0.00112 **
2 == 0	2.2857	0.1273	17.954	< 1e-04 ***
3 == 0	-3.6868	0.1273	-28.960	< 1e-04 ***
4 == 0	-3.8828	0.1273	-30.500	< 1e-04 ***
5 == 0	-1.8120	0.1273	-14.233	< 1e-04 ***
6 == 0	-1.3762	0.1273	-10.810	< 1e-04 ***

Signif. codes: 0 '***' 0.001 '**' 0.01 '*' 0.05 '.' 0.1 ' ' 1

(Adjusted p values reported -- single-step method).

Escherichia coli ATCC8739 survival on steel, Pristine and Annealed NsARC samples for up to 8 hrs under four different exposure conditions (HI, UV, Dark and Ambient light) using the ISO:2009 technique.

10. summary.aov

	Df	Sum Sq	Mean Sq.	F value	Pr(>F)
material	2	53.19	26.594	1093.93	< 2e-16 ***
exposure	3	17.18	5.727	235.59	< 2e-16 ***
material:exposure	6	8.63	1.438	59.15	3.37e-13 ***
Residuals	24	0.58	0.024		

Signif. codes: 0 '***' 0.001 '**' 0.01 '*' 0.05 '.' 0.1 ' ' 1

11. Bonferroni contrasts

Linear Hypotheses:

	Estimate	Std. Error	t value	Pr(>|t|)
1 == 0	-3.25665	0.20129	-16.179	< 0.001 ***
2 == 0	0.14167	0.12731	1.113	0.84987
3 == 0	-0.43954	0.12731	-3.453	0.01474 *
4 == 0	-0.08579	0.12731	-0.674	0.98362
5 == 0	-2.45859	0.20129	-12.214	< 0.001 ***
6 == 0	-0.35852	0.12731	-2.816	0.01269 *
7 == 0	-0.28693	0.12731	-2.254	0.19626
8 == 0	-0.51439	0.12731	-4.041	0.00342 **

Signif. codes: 0 '***' 0.001 '**' 0.01 '*' 0.05 '.' 0.1 ' ' 1

(Adjusted p values reported -- single-step method).

Key:

1="annealed_al" vs "annealed_dark"

2= "annealed_hi" vs "annealed_uv"

3= "pristine_al" vs "pristine_dark"

4= "pristine_hi" vs "pristine_uv"

5=="annealed_al" vs "pristine_al"

6="annealed_dark" vs "pristine_dark"

7="annealed_hi"   vs "pristine_hi"

8="annealed_uv" vs "pristine_uv"

Survival of *E. coli* from the environment on NsARC under high intensity visible light

12. Summary.AOV

	Df	Sum Sq	Mean Sq	F value	Pr(>F)
material	1	0.00	0.00	0.000	0.995
strain	7	94.54	94.54	1163.156	<2e-16 ***
material:strain	7	0.00	0.00	0.036	0.851
Residuals	34	2.60	0.08		

Signif. codes: 0 '***' 0.001 '**' 0.01 '*' 0.05 '.' 0.1 ' ' 1

Key:

Simultaneous Tests for General Linear Hypotheses

Here is the contrast matrix listing the 8 contrasts of interest:

1) NsARC_27 vs steel_27,

2) NsARC_28 vs steel_28,

3) NsARC_42 vs steel_42,

4) NsARC_43 vs steel_43,

5) NsARC_44 vs steel_44,

6) NsARC_45 vs steel_45

7) NsARC_70 vs steel_70

8) NsARC_73 vs steel_73

13. Bonferroni contrasts

Linear Hypotheses:

	Estimate	Std. Error	t value	Pr(>|t|)
1 == 0	-1.04108	0.12618	-13.206	<0.001 ***
2 == 0	-1.25274	0.12618	-15.279	<0.001 ***
3 == 0	-1.44899	0.12618	-11.483	<0.001 ***
4 == 0	-1.43218	0.12618	-11.350	<0.001 ***
5 == 0	-1.22300	0.12618	-11.267	<0.001 ***
6 == 0	-1.74486	0.12618	-13.828	<0.001 ***
7 == 0	-1.4300	0.12618	-11.267	<0.001 ***
8== 0	-1.4086	0.12618	-12.828	<0.001 ***

Survival of *E.coliBWtolC* on NsARC under four different exposure conditions (Hi, UV, Dark and Ambient light)

14. Summary.AOV

	Df	Sum Sq	Mean Sq	F value	Pr(>F)
material	1	34.32	35.21	56.000	0.995
exposure	3	94.54	94.54	163.156	<2e-16 ***
material:exposure	3	0.00	0.00	36.00	0.851
Residuals	16	2.60	0.08		

Signif. codes: 0 '***' 0.001 '**' 0.01 '*' 0.05 '.' 0.1 ' ' 1

15. Bonferroni contrasts

Linear Hypotheses:

	Estimate	Std. Error	t value	Pr(>|t|)
1 == 0	-2.38055	0.11573	-20.571	<1e-04 ***
2 == 0	0.47143	0.11573	0.715	0.67
3 == 0	-1.05679	0.07319	-14.439	<1e-04 ***
4 == 0	-3.22481	0.07319	-44.060	<1e-04 ***
5 == 0	0.04969	0.07319	0.679	0.866
6 == 0	-3.28886	0.07319	-44.935	<1e-04 ***

Signif. codes: 0 '***' 0.001 '**' 0.01 '*' 0.05 '.' 0.1 ' ' 1

Survival of *E. coliBWsoxS* on NsARC under four different exposure conditions (Hi, UV, Dark and Ambient light)

16. Summary.AOV

	Df	Sum Sq	Mean Sq	F value	Pr(>F)
material	1	34.32	35.21	56.000	0.995
exposure	3	94.54	94.54	163.156	<2e-16 ***
material:exposure	3	0.00	0.00	36.00	0.851
Residuals	16	2.60	0.08		

Signif. codes: 0 '***' 0.001 '**' 0.01 '*' 0.05 '.' 0.1 ' ' 1

17. Bonferroni contrasts

Linear Hypotheses:

	Estimate	Std. Error	t value	Pr(>|t|)
1 == 0	-2.38055	0.11573	-20.571	<1e-04 ***
2 == 0	0.47143	0.11573	0.715	0.67
3 == 0	-1.05679	0.07319	-14.439	<1e-04 ***
4 == 0	-3.22481	0.07319	-44.060	<1e-04 ***
5 == 0	0.04969	0.07319	0.679	0.866
6 == 0	-3.28886	0.07319	-44.935	<1e-04 ***

Signif. codes: 0 '***' 0.001 '**' 0.01 '*' 0.05 '.' 0.1 ' ' 1

Key:

Simultaneous Tests for General Linear Hypotheses

Here is the contrast matrix listing the 6 contrasts of interest:

1)NsARC_al vs steel_al,

2)NsARC_al vs NsARC_dark,

3)NsARC_dark vs steel_dark,

4)NsARC_hi vs steel_hi,

5)NsARC_hi vs NsARC_uv,

6)NsARC_uv vs steel_uv

Comparison between BW25113, pFru97, tolC and soxS

18. Summary.AOV

	Df	Sum Sq	Mean Sq	F value	Pr(>F)
material	1	34.32	35.21	156.000	<2e-15 ***
strain	3	94.54	4.54	163.156	<2e-16 ***
material:strain	3	6.40	2.30	36.00	<2e-12 ***
Residuals	16	2.60	0.08		

Signif. codes: 0 '***' 0.001 '**' 0.01 '*' 0.05 '.' 0.1 ' ' 1

Key:

Simultaneous Tests for General Linear Hypotheses

Here is the contrast matrix listing the 4 contrasts of interest:

1)NsARC_BW25113 vs NsARC_BWpFru97,

2) NsARC_BWpFru97 vs NsARC_BWtolC,

3) NsARC_BWpFru97 vs NsARC_BWsoxS,

4) NsARC_BWtolC vs NsARC_BWsoxS,

19. Bonferroni contrasts

Linear Hypotheses:

	Estimate	Std. Error	t value	Pr(>|t|)
1 == 0	0.38055	0.11573	0.571	0.87
2 == 0	-1.47143	0.11573	-30.715	<1e-04 ***
3 == 0	-1.05679	0.07319	-14.439	<1e-04 ***
4 == 0	0.22481	0.07319	0.060	0.77

Signif. codes: 0 '***' 0.001 '**' 0.01 '*' 0.05 '.' 0.1 ' ' 1

Comparison between CMB73, CMB73tolC and CMB73soxS

20. Summary.AOV

	Df	Sum Sq	Mean Sq	F value	Pr(>F)
material	1	24.32	35.21	156.000	<2e-15 ***
strain	2	14.54	4.54	163.156	<2e-16 ***
material:strain	2	6.40	2.30	36.00	<2e-12 ***
Residuals	10	2.60	0.08		

Signif. codes: 0 '***' 0.001 '**' 0.01 '*' 0.05 '.' 0.1 ' ' 1

Key:

Simultaneous Tests for General Linear Hypotheses

Here is the contrast matrix listing the 3 contrasts of interest:

1) NsARC_CMB73tolC vs steel_CMB73,

2) NsARC_CMB73 vs NsARC_CMB73tolC,

3) NsARC_CMB73 vs NsARC_CMB73soxS,

21. Bonferroni contrasts

Linear Hypotheses:

	Estimate	Std. Error	t value	Pr(>|t|)
1 == 0	-4.38055	0.21573	-12.571	<1e-04 ***
2 == 0	-1.47143	0.21573	-25.715	<1e-04 ***
3 == 0	-1.05679	0.27319	-44.439	<1e-04 ***

Signif. codes: 0 '***' 0.001 '**' 0.01 '*' 0.05 '.' 0.1 ' ' 1

Comparison of the Survival of Fluorescent labelled bacteria on NsARC

22. Summary.AOV

	Df	Sum Sq	Mean Sq	F value	Pr(>F)
material	1	24.32	35.21	156.000	<2e-15 ***
strain	4	14.54	4.54	163.156	<2e-16 ***
material:strain	4	6.40	2.30	36.00	<2e-12 ***
Residuals	16	2.60	0.08		

Signif. codes: 0 '***' 0.001 '**' 0.01 '*' 0.05 '.' 0.1 ' ' 1

Key:

Simultaneous Tests for General Linear Hypotheses

Here is the contrast matrix listing the 3 contrasts of interest:

1) NsARC_pMRE132 vs steel_pMRE133,

2) NsARC_pMRE133 vs NsARC_pMRE135,

3) NsARC_pMRE135 vs NsARC_pMRE145,

4) NsARC_pMRE135 vs NsARC_pMRE165

5) NsARC_pMRE145 vs NsARC_pMRE165

23. Bonferroni contrasts

Linear Hypotheses:

	Estimate	Std. Error	t value	Pr(>|t|)
1 == 0	0.038055	0.21573	0.3571	0.844
2 == 0	-1.47143	0.21573	-25.715	<1e-04 ***
3 == 0	-1.05679	0.27319	-44.439	<1e-04 ***
4 == 0	-1.05679	0.27319	-44.439	<1e-04 ***
5 == 0	-1.05679	0.27319	-44.439	<1e-04 ***

Signif. codes: 0 '***' 0.001 '**' 0.01 '*' 0.05 '.' 0.1 ' ' 1

Comparison of the survival between induced and uninduced *E. coli*pUC19 on NsARC under high intensity visible light.

24. Summary.AOV

	Df	Sum Sq	Mean Sq	F value	Pr(>F)
material	1	24.32	35.21	156.000	<2e-15 ***
strain	1	14.54	4.54	163.156	<2e-16 ***
material:strain	1	6.40	2.30	36.00	<2e-12 ***
Residuals	6	2.60	0.08		

Signif. codes: 0 '***' 0.001 '**' 0.01 '*' 0.05 '.' 0.1 ' ' 1

Key:

Simultaneous Tests for General Linear Hypotheses

Here is the contrast matrix listing the 3 contrasts of interest:

1) NsARC_induced vs steel_induced,

2) NsARC_uninduced vs steel_uninduced,

3) NsARC_induced vs NsARC_uninduced,

25. Bonferroni contrasts

Linear Hypotheses:

	Estimate	Std. Error	t value	Pr(>|t|)
1 == 0	-1.5128	0.1606	-9.417	<0.001 ***
2 == 0	-2.8189	0.1606	-17.547	<0.001 ***
3 == 0	-0.08579	0.12731	-0.674	0.98362

Signif. codes: 0 '***' 0.001 '**' 0.01 '*' 0.05 '.' 0.1 ' ' 1

Appendix B: Antibiofilm activity experiment

E. coli ATCC 8739 on NsARC and stainless steel for 12 hrs under four different exposure conditions (HI, UV, Dark and Ambient light) using the ISO:2009 technique.

1. **Summary.AOV**

	Df	Sum Sq	Mean Sq	F value	Pr(>F)
material	1	11.802	11.802	490.937	1.96e-13 ***
exposure	3	4.225	1.408	58.579	7.55e-09 ***
material:exposure	3	0.201	0.067	2.784	0.0745 .
Residuals	16	0.385	0.024		

Signif. codes: 0 '***' 0.001 '**' 0.01 '*' 0.05 '.' 0.1 ' ' 1

Simultaneous Tests for General Linear Hypotheses

Here is the contrast matrix listing the 6 contrasts of interest:

1)NsARC_ambient vs steel_ambient,

2)NsARC_ambient vs NsARC_dark,

3)NsARC_dark vs steel_dark,

4)NsARC_visible vs steel_visible,

5)NsARC_visible vs NsARC_uv,

6)NsARC_uv vs steel_uv

2. **Bonferroni contrasts**

Linear Hypotheses:

	Estimate	Std. Error	t value	Pr(>|t|)
1 == 0	-0.2441	0.2002	-1.219	0.717
2 == 0	1.0699	0.2002	5.345	<0.001 ***
3 == 0	-1.6041	0.1266	-12.671	<0.001 ***
4 == 0	-1.2292	0.1266	-9.710	<0.001 ***
5 == 0	-0.2594	0.1266	-2.049	0.243
6 == 0	-1.4705	0.1266	-11.616	<0.001 ***

Signif. codes: 0 '***' 0.001 '**' 0.01 '*' 0.05 '.' 0.1 ' ' 1

(Adjusted p values reported -- single-step method.

E. coli ATCC 8739 on NsARC and stainless steel for 24 hrs under four different exposure conditions (HI, UV, Dark and Ambient light) using the ISO:2009 technique.

3. **Summary.AOV**

	Df	Sum Sq	Mean Sq	F value	Pr(>F)
material	1	19.673	19.673	1150.347	2.48e-16 ***
exposure	3	7.366	2.455	143.567	8.90e-12 ***
material:exposure	3	0.349	0.116	6.811	0.0036 **
Residuals	16	0.274	0.017		

Signif. codes: 0 '***' 0.001 '**' 0.01 '*' 0.05 '.' 0.1 ' ' 1

4. **Bonferroni contrasts**

Linear Hypotheses:

	Estimate	Std. Error	t value	Pr(>|t|)
1 == 0	-0.3845	0.1688	-2.278	0.16483
2 == 0	0.8448	0.1688	5.004	< 0.001 ***
3 == 0	-1.6871	0.1068	-15.801	< 0.001 ***
4 == 0	-1.8250	0.1068	-17.091	< 0.001 ***
5 == 0	-0.4653	0.1068	-4.358	0.00283 **
6 == 0	-2.0056	0.1068	-18.783	< 0.001 ***

Signif. codes: 0 '***' 0.001 '**' 0.01 '*' 0.05 '.' 0.1 ' ' 1

(Adjusted p values reported -- single-step method).

E. coli ATCC 8739 on NsARC and stainless steel for 48 hrs under four different exposure conditions (HI, UV, Dark and Ambient light) using the ISO:2009 technique.

5. Summary.AOV

	Df	Sum sq	mean Sq.	F value	Pr(>F)	
material	1	19.355	19.355	1146.96	2.54E-16	***
exposure	3	6.139	2.046	121.26	3.25E-11	***
material:exposure	3	0.686	0.229	13.56	0.00017	***
Residuals	16	0.129	0.008			

Signif. Codes: 0 ‘***’ 0.001 ‘**’ 0.01 ‘*’ 0.05 ‘.’ 0.1 ‘ ’ 1

6. Bonferroni contrasts

Linear Hypotheses:

	Estimate	Std. Error	t value	Pr(>|t|)
1 == 0	-0.6426	0.1677	-3.832	0.00754 **
2 == 0	0.6847	0.1677	4.083	0.00472 **
3 == 0	-1.5028	0.1061	-14.169	< 0.001 ***
4 == 0	-1.9427	0.1061	-18.316	< 0.001 ***
5 == 0	-0.6482	0.1061	-6.111	< 0.001 ***
6 == 0	-2.1056	0.1061	-19.852	< 0.001 ***

Signif. codes: 0 ‘***’ 0.001 ‘**’ 0.01 ‘*’ 0.05 ‘.’ 0.1 ‘ ’ 1

(Adjusted p values reported -- single-step method.

S. aureus ATCC25923 on NsARC and steel for 12 hrs under four different exposure conditions (HI, UV, Dark and Ambient light) using the ISO:2009 technique.

7. Summary.AOV

	Df	Sum Sq.	Mean Sq	F value	Pr(>F)
material	1	8.240	8.240	250.751	3.38e-11 ***
exposure	3	3.670	1.223	37.228	1.91e-07 ***
material:exposure	3	0.293	0.098	2.975	0.0629 .
Residuals	16	0.526	0.033		

Signif. codes: 0 '***' 0.001 '**' 0.01 '*' 0.05 '.' 0.1 ' ' 1

8. Bonferroni contrasts

Linear Hypotheses:

	Estimate	Std. Error	t value	Pr(>|t|)
1 == 0	0.2256	0.2340	0.964	0.864
2 == 0	1.6315	0.2340	6.971	<0.001 ***
3 == 0	-1.3735	0.1480	-9.279	<0.001 ***
4 == 0	-0.8022	0.1480	-5.420	<0.001 ***
5 == 0	0.1174	0.1480	0.793	0.934
6 == 0	-1.0935	0.1480	-7.388	<0.001 ***

Signif. codes: 0 '***' 0.001 '**' 0.01 '*' 0.05 '.' 0.1 ' ' 1

(Adjusted p values reported -- single-step method.

S. aureus ATCC25923 on NsARC and steel for 24 hrs under four different exposure conditions (HI, UV, Dark and Ambient light) using the ISO:2009 technique.

9. Summary.AOV

	Df	Sum Sq	Mean Sq	F value	Pr(>F)
material	1	27.723	27.723	1205.86	< 2e-16 ***
exposure	3	2.775	0.925	40.23	1.11e-07 ***
material:exposure	3	0.979	0.326	14.20	8.98e-05 ***
Residuals	16	0.368	0.023		

Signif. codes: 0 '***' 0.001 '**' 0.01 '*' 0.05 '.' 0.1 ' ' 1

10. Bonferroni contrasts

Linear Hypotheses:

	Estimate	Std. Error	t value	Pr(>|t|)
1 == 0	-0.4984	0.1957	-2.546	0.101
2 == 0	1.9074	0.1957	9.744	<0.001 ***
3 == 0	-2.4192	0.1238	-19.541	<0.001 ***
4 == 0	-1.4676	0.1238	-11.855	<0.001 ***
5 == 0	0.7239	0.1238	5.847	<0.001 ***
6 == 0	-1.7544	0.1238	-14.171	<0.001 ***

Signif. codes: 0 '***' 0.001 '**' 0.01 '*' 0.05 '.' 0.1 ' ' 1

(Adjusted p values reported -- single-step method.

S. aureus ATCC25923 on NsARC and steel for 48 hrs under four different exposure conditions (HI, UV, Dark and Ambient light) using the ISO:2009 technique.

11. Summary.AOV

	Df	Sum sq	mean Sq.	F value	Pr(>F)	
material	1	33.68	33.58	1610.845	<2E-16	***
exposure	3	5.36	1.79	85.466	4.61E10	***
material:exposure	3	0.16	0.05	2.598	0.0883	
Residuals	16	0.33	0.02			

Signif. Codes: 0 ‘***’ 0.001 ‘**’ 0.01 ‘*’ 0.05 ‘.’ 0.1 ‘ ’ 1

12. Bonferroni contrasts

Linear Hypotheses:

	Estimate	Std. Error	t value	Pr(>|t|)
1 == 0	-6.934e-01	1.867e-01	-3.715	0.00985 **
2 == 0	1.762e+00	1.867e-01	9.439	< 0.001 ***
3 == 0	-2.581e+00	1.181e-01	-21.863	< 0.001 ***
4 == 0	-2.442e+00	1.181e-01	-20.688	< 0.001 ***
5 == 0	2.220e-16	1.181e-01	0.000	1.00000
6 == 0	-2.133e+00	1.181e-01	-18.064	< 0.001 ***

Signif. codes: 0 ‘***’ 0.001 ‘**’ 0.01 ‘*’ 0.05 ‘.’ 0.1 ‘ ’ 1

(Adjusted p values reported -- single-step method.

Pseudomonas aeruginosa ATCC10145 on NsARC and steel for 12 hrs under four different exposure conditions (HI, UV, Dark and Ambient light) using the ISO:2009 technique.

13. Summary.AOV

	Df	Sum Sq	Mean Sq	F value	Pr(>F)	
material	1	8.208	8.208	309.302	6.88e-12	***
exposure	3	3.497	1.166	43.922	6.00e-08	***
material:exposure	3	0.007	0.002	0.082	0.969	
Residuals	16	0.425	0.027			

Signif. codes: 0 '***' 0.001 '**' 0.01 '*' 0.05 '.' 0.1 ' ' 1

14. Bonferroni contrasts

Linear Hypotheses:

	Estimate	Std. Error	t value	Pr(>|t|)	
1 == 0	0.4475	0.2103	2.128	0.213	
2 == 0	1.6129	0.2103	7.669	<0.001	***
3 == 0	-1.2249	0.1330	-9.209	<0.001	***
4 == 0	-1.1651	0.1330	-8.759	<0.001	***
5 == 0	0.0587	0.1330	0.441	0.996	
6 == 0	-1.0867	0.1330	-8.170	<0.001	***

Signif. codes: 0 '***' 0.001 '**' 0.01 '*' 0.05 '.' 0.1 ' ' 1

(Adjusted p values reported -- single-step method).

Pseudomonas aeruginosa ATCC10145 on NsARC and steel for 24 hrs under four different exposure conditions (HI, UV, Dark and Ambient light) using the ISO:2009 technique.

15. Summary.AOV

	Df	Sum Sq	Mean Sq.	F value	Pr(>F)
material	1	26.172	26.172	509.119	1.48e-13 ***
exposure	3	3.035	1.012	19.677	1.28e-05 ***
material:exposure	3	0.048	0.016	0.309	0.819
Residuals	16	0.822	0.051		

Signif. codes: 0 '***' 0.001 '**' 0.01 '*' 0.05 '.' 0.1 ' ' 1

16. Bonferroni contrasts

Linear Hypotheses:

	Estimate	Std. Error	t value	Pr(>|t|)
1 == 0	-0.2785	0.2927	-0.952	0.869600
2 == 0	1.7215	0.2927	5.881	0.000169 ***
3 == 0	-2.2232	0.1851	-12.010	< 1e-04 ***
4 == 0	-2.1145	0.1851	-11.422	< 1e-04 ***
5 == 0	0.2746	0.1851	1.484	0.545056
6 == 0	-1.7310	0.1851	-9.350	< 1e-04 ***

Signif. codes: 0 '***' 0.001 '**' 0.01 '*' 0.05 '.' 0.1 ' ' 1

(Adjusted p values reported -- single-step method.

Pseudomonas aeruginosa ATCC10145 on NsARC and steel for 48 hrs under four different exposure conditions (HI, UV, Dark and Ambient light) using the ISO:2009 technique.

17. Summary.AOV

	Df	Sum sq	mean Sq.	F value	Pr(>F)	
material	1	29.503	29.503	818.156	3.63E-15	***
exposure	3	5.376	1.792	49.690	2.49E-8	***
material:exposure	3	0.016	0.005	0.151	0.928	
Residuals	16	0.577	0.036			

Signif. Codes: 0 ‘***’ 0.001 ‘**’ 0.01 ‘*’ 0.05 ‘.’ 0.1 ‘ ’ 1

18. Bonferroni contrasts

Linear Hypotheses:

	Estimate	Std. Error	t value	Pr(>|t|)
1 == 0	-0.6758	0.2452	-2.757	0.0677 .
2 == 0	1.4484	0.2452	5.908	<0.001 ***
3 == 0	-2.2030	0.1551	-14.209	<0.001 ***
4 == 0	-2.1613	0.1551	-13.939	<0.001 ***
5 == 0	0.1003	0.1551	0.647	0.9720
6 == 0	-2.1025	0.1551	-13.560	<0.001 ***

Signif. codes: 0 ‘***’ 0.001 ‘**’ 0.01 ‘*’ 0.05 ‘.’ 0.1 ‘ ’ 1

(Adjusted p values reported -- single-step method.

Saccharomyces cerevisiae ATCC10145 on NsARC and steel for 12 hrs under four different exposure conditions (HI, UV, Dark and Ambient light) using the ISO:2009 technique.

19. Summary.AOV

	Df	Sum Sq	Mean Sq	F value	Pr(>F)
material	1	4.662	4.662	368.388	1.8e-12 ***
exposure	3	2.683	0.894	70.679	1.9e-09 ***
material:exposure	3	0.027	0.009	0.721	0.554
Residuals	16	0.202	0.013		

Signif. codes: 0 '***' 0.001 '**' 0.01 '*' 0.05 '.' 0.1 ' ' 1

20. Bonferroni contrasts

Linear Hypotheses:

	Estimate	Std. Error	t value	Pr(>|t|)
1 == 0	0.93523	0.14523	6.439	<0.001 ***
2 == 0	1.84855	0.14523	12.728	<0.001 ***
3 == 0	-0.94429	0.09185	-10.280	<0.001 ***
4 == 0	-0.78234	0.09185	-8.517	<0.001 ***
5 == 0	-0.14587	0.09185	-1.588	0.479
6 == 0	-1.00180	0.09185	-10.907	<0.001 ***

Signif. codes: 0 '***' 0.001 '**' 0.01 '*' 0.05 '.' 0.1 ' ' 1

(Adjusted p values reported -- single-step method.

Saccharomyces cerevisiae ATCC10145 on NsARC and steel for 24 hrs under four different exposure conditions (HI, UV, Dark and Ambient light) using the ISO:2009 technique.

21. Summary.AOV

	Df	Sum Sq	Mean Sq	F value	Pr(>F)
material	1	19.568	19.568	861.08	2.43e-15 ***
exposure	3	4.150	1.383	60.88	5.70e-09 ***
material:exposure	3	0.545	0.182	8.00	0.00176 **
Residuals	16	0.364	0.023		

Signif. codes: 0 '***' 0.001 '**' 0.01 '*' 0.05 '.' 0.1 ' ' 1

22. Bonferroni contrasts

Linear Hypotheses:

	Estimate	Std. Error	t value	Pr(>|t|)
1 == 0	-0.14386	0.19461	-0.739	0.950
2 == 0	1.49909	0.19461	7.703	<1e-04 ***
3 == 0	-1.90542	0.12308	-15.481	<1e-04 ***
4 == 0	-1.50959	0.12308	-12.265	<1e-04 ***
5 == 0	-0.06668	0.12308	-0.542	0.988
6 == 0	-1.61989	0.12308	-13.161	<1e-04 ***

Signif. codes: 0 '***' 0.001 '**' 0.01 '*' 0.05 '.' 0.1 ' ' 1

(Adjusted p values reported -- single-step method.

Saccharomyces cerevisiae ATCC10145 on NsARC and steel for 48 hrs under four different exposure conditions (HI, UV, Dark and Ambient light) using the ISO:2009 technique.

23. Summary.AOV

	Df	Sum sq	mean Sq.	F value	Pr(>F)	
material	1	15.111	15.111	632.709	2.72E-14	***
exposure	3	4.781	1.594	66.733	2.90E-09	***
material:exposure	3	0.263	0.088	3.671	0.0347	*
Residuals	16	0.382	0.024			

Signif. Codes: 0 ‘***’ 0.001 ‘**’ 0.01 ‘*’ 0.05 ‘.’ 0.1 ‘ ’ 1

24. Bonferroni contrasts

Linear Hypotheses:

	Estimate	Std. Error	t value	Pr(>|t|)
1 == 0	0.04108	0.19951	0.206	1.000
2 == 0	1.25274	0.19951	6.279	<0.001 ***
3 == 0	-1.44899	0.12618	-11.483	<0.001 ***
4 == 0	-1.43218	0.12618	-11.350	<0.001 ***
5 == 0	-0.22300	0.12618	-1.767	0.375
6 == 0	-1.74486	0.12618	-13.828	<0.001 ***

Signif. codes: 0 ‘***’ 0.001 ‘**’ 0.01 ‘*’ 0.05 ‘.’ 0.1 ‘ ’ 1

(Adjusted p values reported -- single-step method).

Appendix C: Experiment to determine if exposure of bacteria to NsARC cause the development of resistance to antibiotics

E. coli exposed to NsARC in the dark then plating onto LB and Kanamycin plate

1. **Summary.AOV**

	Df	Sum Sq	Mean Sq	F value	Pr(>F)
material	1	3.61	3.61	2.808	0.104
concentration	1	85.64	85.64	66.572	2.56e-09 ***
material:concentration	1	0.09	0.09	0.069	0.795
Residuals	32	41.17	1.29		

Signif. codes: 0 '***' 0.001 '**' 0.01 '*' 0.05 '.' 0.1 ' ' 1

2. **Bonferroni contrasts**

Linear Hypotheses:

	Estimate	Std. Error	t value	Pr(>|t|)
1(NsARC_0 vs Steel_0) == 0	-0.32304	0.22598	-1.429	0.637
2 (NsARC_4 vs Steel_4)== 0	0.07423	0.14292	0.519	0.995
3 (NsARC_5 vs Steel_5)== 0	-1.36608	0.14292	-9.558	<1e-04 ***
4 (NsARC_6 vs Steel_6)== 0	-1.54810	0.14292	-10.832	<1e-04 ***
5 (NsARC_8 vs Steel_8)== 0	-1.00811	0.14292	-7.053	<1e-04 ***
6 (NsARC_9 vs Steel_9)== 0	0.20834	0.14292	1.458	0.617

Signif. codes: 0 '***' 0.001 '**' 0.01 '*' 0.05 '.' 0.1 ' ' 1

(Adjusted p values reported -- single-step method)

E. coli exposed to NsARC under uv light then plating onto LB and Kanamycin plate

3. **Summary.AOV**

	Df	Sum Sq	Mean Sq	F value	Pr(>F)
material	1	8.86	8.86	8.856	0.00552 **
concentration	1	104.47	104.47	104.474	1.32e-11 ***
material:concentration	1	0.05	0.05	0.052	0.82025
Residuals	32	32.00	1.00		

Signif. codes: 0 ‘***’ 0.001 ‘**’ 0.01 ‘*’ 0.05 ‘.’ 0.1 ‘ ’ 1

4. **Bonferroni contrasts**

Linear Hypotheses:

	Estimate	Std. Error	t value	Pr(>|t|)
1 (NsARC_0 vs Steel_0)== 0	-4.127e-01	1.506e-01	-2.741	0.064 .
2 (NsARC_4 vs Steel_4) == 0	-1.076e+00	9.523e-02	-11.302	<1e-04 ***
3 (NsARC_5 vs Steel_5)== 0	-1.917e+00	9.523e-02	-20.132	<1e-04 ***
4 (NsARC_6 vs Steel_6)== 0	-2.752e+00	9.523e-02	-28.894	<1e-04 ***
5 (NsARC_8 vs Steel_8)== 0	-4.441e-16	9.523e-02	0.000	1.000
6 (NsARC_9 vs Steel_9)== 0	-6.217e-15	9.523e-02	0.000	1.000

Signif. codes: 0 ‘***’ 0.001 ‘**’ 0.01 ‘*’ 0.05 ‘.’ 0.1 ‘ ’ 1

(Adjusted p values reported -- single-step method)

E. coli exposed to NsARC in the dark then plating onto LB and tetracycline plate

5. **Summary.AOV**

	Df	Sum Sq	Mean Sq	F value	Pr(>F)
material	1	0.14	0.14	0.155	0.696
concentration	1	116.90	116.90	129.931	8.39e-13 ***
material:concentration	1	0.01	0.01	0.015	0.903
Residuals	32	28.79	0.90		

Signif. codes: 0 ‘***’ 0.001 ‘**’ 0.01 ‘*’ 0.05 ‘.’ 0.1 ‘ ’ 1

6. **Bonferroni contrasts**

Linear Hypotheses:

		Estimate	Std. Error	t value	Pr(>|t|)
1 (NsARC_0 vs Steel_0)==	0	-2.827e-01	1.602e-01	-1.765	0.412
2 (NsARC_0.5 vs Steel_0.5)==	0	-1.527e-01	1.013e-01	-1.507	0.583
3 (NsARC_0.7 vs Steel_0.7)==	0	-1.013e-01	1.013e-01	-0.999	0.893
4 (NsARC_1 vs Steel_1)==	0	-2.363e-01	1.013e-01	-2.332	0.151
5 (NsARC_1.5 vs Steel_1.5)==	0	-1.159e-01	1.013e-01	-1.144	0.820
6 (NsARC_2 vs Steel_2)==	0	-4.441e-15	1.013e-01	0.000	1.000

(Adjusted p values reported -- single-step method)

E. coli exposed to NsARC under uv light then plating onto LB and tetracycline plate

7. **Summary.AOV**

	Df	Sum Sq	Mean Sq	F value	Pr(>F)
material	1	0.19	0.19	0.199	0.659
concentration	1	107.26	107.26	114.901	4.03e-12 ***
material:concentration	1	0.10	0.10	0.112	0.740
Residuals	32	29.87	0.93		

Signif. codes: 0 '***' 0.001 '**' 0.01 '*' 0.05 '.' 0.1 ' ' 1

8. **Bonferroni contrasts**

Linear Hypotheses:

	Estimate	Std. Error	t value	Pr(>|t|)
1 (NsARC_0 vs Steel_0)== 0	-6.982e-01	1.072e-01	-6.511	< 1e-04 ***
2 (NsARC_0.5 vs Steel_0.5)== 0	-2.404e-01	6.783e-02	-3.544	0.00964 **
3 (NsARC_0.7 vs Steel_0.7)== 0	-1.201e-01	6.783e-02	-1.771	0.40807
4 (NsARC_1 vs Steel_1)== 0	-7.496e-02	6.783e-02	-1.105	0.84167
5 (NsARC_1.5 vs Steel_1.5)== 0	-7.682e-02	6.783e-02	-1.133	0.82685
6 (NsARC_2 vs Steel_2)== 0	-6.217e-15	6.783e-02	0.000	1.00000

Signif. codes: 0 '***' 0.001 '**' 0.01 '*' 0.05 '.' 0.1 ' ' 1

(Adjusted p values reported -- single-step method)

E. coli exposed to NsARC in the dark then plating onto LB and chloramphenicol plate

9. Summary.AOV

	Df	Sum Sq	Mean Sq	F value	Pr(>F)
material	1	1.38	1.38	0.674	0.418
concentration	1	53.05	53.05	25.826	1.57e-05 ***
material:concentration	1	0.01	0.01	0.006	0.939
Residuals	32	65.74	2.05		

Signif. codes: 0 '***' 0.001 '**' 0.01 '*' 0.05 '.' 0.1 ' ' 1

10. Bonferroni contrasts

Linear Hypotheses:

	Estimate	Std. Error	t value	Pr(>|t|)
1 (NsARC_0 vs Steel_0)== 0	-8.731e-01	1.943e-01	-4.494	< 0.001 ***
2 (NsARC_5 vs Steel_5)== 0	-2.664e-01	1.229e-01	-2.169	0.20759
3 (NsARC_6 vs Steel_6)== 0	-3.504e-01	1.229e-01	-2.852	0.04995 *
4 (NsARC_7 vs Steel_7)== 0	-7.518e-01	1.229e-01	-6.118	< 0.001 ***
5 (NsARC_8 vs Steel_8)== 0	-5.478e-01	1.229e-01	-4.459	0.00102 **
6 (NsARC_9 vs Steel_9)== 0	-4.441e-15	1.229e-01	0.000	1.00000

Signif. codes: 0 '***' 0.001 '**' 0.01 '*' 0.05 '.' 0.1 ' ' 1

(Adjusted p values reported -- single-step method)

E. coli exposed to NsARC under uv light then plating onto LB and chloramphenicol plate

11. Summary.AOV

	Df	Sum Sq	Mean Sq	F value	Pr(>F)
material	1	0.07	0.07	0.036	0.851
concentration	1	48.86	48.86	25.381	1.78e-05 ***
material:concentration	1	0.05	0.05	0.024	0.879
Residuals	32	61.60	1.92		

Signif. codes: 0 ‘***’ 0.001 ‘**’ 0.01 ‘*’ 0.05 ‘.’ 0.1 ‘ ’ 1

12. Bonferroni contrasts

Linear Hypotheses:

	Estimate	Std. Error	t value	Pr(>|t|)
1 (NsARC_0 vs Steel_0)== 0	-3.859e-01	2.725e-01	-1.416	0.646
2 (NsARC_5 vs Steel_5)== 0	8.509e-02	1.723e-01	0.494	0.996
3 (NsARC_6 vs Steel_6)== 0	-3.750e-01	1.723e-01	-2.176	0.205
4 (NsARC_7 vs Steel_7)== 0	-3.427e-01	1.723e-01	-1.988	0.287
5 (NsARC_8 vs Steel_8)== 0	3.000e-01	1.723e-01	1.741	0.427
6 (NsARC_9 vs Steel_9)== 0	-4.441e-15	1.723e-01	0.000	1.000

(Adjusted p values reported -- single-step method)

E. coli exposed to NsARC in the dark then plating onto LB and ciprofloxacin plate

13. Summary.AOV

	Df	Sum Sq	Mean Sq	F value	Pr(>F)
material	1	0.01	0.01	0.005	0.942
concentration	1	199.68	199.68	131.559	7.14e-13 ***
material:concentration	1	0.01	0.01	0.006	0.939
Residuals	32	48.57	1.52		

Signif. codes: 0 ‘***’ 0.001 ‘**’ 0.01 ‘*’ 0.05 ‘.’ 0.1 ‘ ’ 1

14. Bonferroni contrasts

Linear Hypotheses:

	Estimate	Std. Error	t value	Pr(>|t|)
1 (NsARC_0 vs Steel_0) == 0	8.606e-02	1.712e-01	0.503	0.996
2 (NsARC_0.1 vs Steel_0.1) == 0	1.491e-01	1.083e-01	1.377	0.673
3 (NsARC_0.2 vs Steel_0.2) == 0	-1.073e-02	1.083e-01	-0.099	1.000
4 (NsARC_0.3 vs Steel_0.3) == 0	-8.882e-16	1.083e-01	0.000	1.000
5 (NsARC_0.4 vs Steel_0.4) == 0	1.776e-15	1.083e-01	0.000	1.000
6 (NsARC_0.5 vs Steel_0.5) == 0	-6.217e-15	1.083e-01	0.000	1.000

(Adjusted p values reported -- single-step method)

E. coli exposed to NsARC under uv light then plating onto LB and ciprofloxacin plate

15. Summary.AOV

	Df	Sum Sq	Mean Sq	F value	Pr(>F)
material	1	0.01	0.01	0.004	0.952
concentration	1	195.18	195.18	131.937	6.88e-13 ***
material:concentration	1	0.02	0.02	0.011	0.916
Residuals	32	47.34	1.48		

Signif. codes: 0 ‘***’ 0.001 ‘**’ 0.01 ‘*’ 0.05 ‘.’ 0.1 ‘ ’ 1

16. Bonferroni contrasts

Linear Hypotheses:

	Estimate	Std. Error	t value	Pr(>|t|)
1 (NsARC_0 vs Steel_0) == 0	-1.923e-01	1.279e-01	-1.504	0.585
2 (NsARC_0.1 vs Steel_0.1)== 0	-1.741e-01	8.087e-02	-2.153	0.214
3 (NsARC_0.2 vs Steel_0.2)== 0	1.241e-01	8.087e-02	1.535	0.564
4 (NsARC_0.3 vs Steel_0.3)== 0	-2.665e-15	8.087e-02	0.000	1.000
5 (NsARC_0.4 vs Steel_0.4)== 0	1.776e-15	8.087e-02	0.000	1.000
6 (NsARC_0.5 vs Steel_0.5)== 0	-7.994e-15	8.087e-02	0.000	1.000

(Adjusted p values reported -- single-step method)

S. aureus exposed to NsARC in the dark then plating onto LB and kanamycin plate

17. Summary.AOV

	Df	Sum Sq	Mean Sq	F value	Pr(>F)
material	1	0.00	0.00	0.001	0.982
concentration	1	178.29	178.29	112.611	5.2e-12 ***
material:concentration	1	0.00	0.00	0.003	0.959
Residuals	32	50.66	1.58		

Signif. codes: 0 ‘***’ 0.001 ‘**’ 0.01 ‘*’ 0.05 ‘.’ 0.1 ‘ ’ 1

18. Bonferroni contrasts

Linear Hypotheses:

	Estimate	Std. Error	t value	Pr(>|t|)
1 (NsARC_0 vs Steel_0)== 0	2.443e-01	1.461e-01	1.672	0.471
2 (NsARC_0.9 vs Steel_0.9)== 0	9.527e-03	9.241e-02	0.103	1.000
3 (NsARC_1 vs Steel_1)== 0	-8.775e-02	9.241e-02	-0.950	0.913
4 (NsARC_2 vs Steel_2)== 0	-1.003e-01	9.241e-02	-1.086	0.852
5 (NsARC_3 vs Steel_3)== 0	1.776e-15	9.241e-02	0.000	1.000
6 (NsARC_4 vs Steel_4)== 0	-7.105e-15	9.241e-02	0.000	1.000

(Adjusted p values reported -- single-step method)

S. aureus exposed to NsARC under uv light then plating onto LB and kanamycin plate

19. Summary.AOV

	Df	Sum Sq	Mean Sq	F value	Pr(>F)
material	1	0.04	0.04	0.025	0.875
concentration	1	166.63	166.63	112.908	5.03e-12 ***
material:concentration	1	0.03	0.03	0.017	0.896
Residuals	32	47.23	1.48		

Signif. codes: 0 ‘***’ 0.001 ‘**’ 0.01 ‘*’ 0.05 ‘.’ 0.1 ‘ ’ 1

20. Bonferroni contrasts

Linear Hypotheses:

	Estimate	Std. Error	t value	Pr(>|t|)
1 (NsARC_0 vs Steel_0)== 0	-2.318e-01	1.193e-01	-1.943	0.3099
2 (NsARC_0.9 vs Steel_0.9)== 0	-3.678e-02	7.545e-02	-0.487	0.9967
3 (NsARC_1 vs Steel_1)== 0	-2.330e-01	7.545e-02	-3.088	0.0289 *
4 (NsARC_2 vs Steel_2)== 0	-2.665e-15	7.545e-02	0.000	1.0000
5 (NsARC_3 vs Steel_3)== 0	0.000e+00	7.545e-02	0.000	1.0000
6 (NsARC_4 vs Steel_4)== 0	-3.553e-15	7.545e-02	0.000	1.0000

Signif. codes: 0 ‘***’ 0.001 ‘**’ 0.01 ‘*’ 0.05 ‘.’ 0.1 ‘ ’ 1

(Adjusted p values reported -- single-step method)

S. aureus exposed to NsARC in the dark then plating onto LB and vancomycin plate

21. Summary.AOV

	Df	Sum Sq	Mean Sq	F value	Pr(>F)
material	1	0.81	0.81	0.693	0.411
concentration	1	152.56	152.56	131.116	7.46e-13 ***
material:concentration	1	0.36	0.36	0.310	0.581
Residuals	32	37.23	1.16		

Signif. codes: 0 '***' 0.001 '**' 0.01 '*' 0.05 '.' 0.1 ' ' 1

22. Bonferroni contrasts

Linear Hypotheses:

	Estimate	Std. Error	t value	Pr(>|t|)
1 (NsARC_0 vs Steel_0)== 0	-9.015e-01	1.230e-01	-7.331	<1e-05 ***
2 (NsARC_0.5 vs Steel_0.5)== 0	-5.101e-01	7.777e-02	-6.560	<1e-05 ***
3 (NsARC_0.8 vs Steel_0.8)== 0	-6.754e-01	7.777e-02	-8.686	<1e-05 ***
4 (NsARC_1 vs Steel_1)== 0	-1.590e-01	7.777e-02	-2.045	0.26
5 (NsARC_1.5 vs Steel_1.5)== 0	8.882e-16	7.777e-02	0.000	1.00
6 (NsARC_2 vs Steel_2)== 0	-4.441e-15	7.777e-02	0.000	1.00

Signif. codes: 0 '***' 0.001 '**' 0.01 '*' 0.05 '.' 0.1 ' ' 1

(Adjusted p values reported -- single-step method)

S. aureus exposed to NsARC under uv light then plating onto LB and vancomycin plate

23. Summary.AOV

	Df	Sum Sq	Mean Sq	F value	Pr(>F)
material	1	0.22	0.22	0.14	0.711
concentration	1	165.42	165.42	104.86	1.26e-11 ***
material:concentration	1	0.00	0.00	0.00	0.995
Residuals	32	50.48	1.58		

Signif. codes: 0 ‘***’ 0.001 ‘**’ 0.01 ‘*’ 0.05 ‘.’ 0.1 ‘ ’ 1

24. Bonferroni contrasts

Linear Hypotheses:

	Estimate	Std. Error	t value	Pr(>|t|)
1 (NsARC_0 vs Steel_0)== 0	-7.521e-03	1.239e-01	-0.061	1.000
2 (NsARC_0.5 vs Steel_0.5)== 0	-3.934e-02	7.835e-02	-0.502	0.996
3 (NsARC_0.8 vs Steel_0.8)== 0	-8.724e-02	7.835e-02	-1.113	0.837
4 (NsARC_1 vs Steel_1)== 0	-8.083e-01	7.835e-02	-10.316	<1e-04 ***
5 (NsARC_1.5 vs Steel_1.5)== 0	8.882e-16	7.835e-02	0.000	1.000
6 (NsARC_2 vs Steel_2)== 0	-4.441e-15	7.835e-02	0.000	1.000

Signif. codes: 0 ‘***’ 0.001 ‘**’ 0.01 ‘*’ 0.05 ‘.’ 0.1 ‘ ’ 1

(Adjusted p values reported -- single-step method)

S. aureus exposed to NsARC in the dark then plating onto LB and erythromycin plate

25. Summary.AOV

	Df	Sum Sq	Mean Sq	F value	Pr(>F)
material	1	0.77	0.77	0.777	0.385
concentration	1	79.96	79.96	81.030	2.78e-10 ***
material:concentration	1	0.04	0.04	0.036	0.851
Residuals	32	31.58	0.99		

Signif. codes: 0 '***' 0.001 '**' 0.01 '*' 0.05 '.' 0.1 ' ' 1

26. Bonferroni contrasts

Linear Hypotheses:

	Estimate	Std. Error	t value	Pr(>|t|)
1 (NsARC_0 vs Steel_0)== 0	-1.230e-01	1.543e-01	-0.797	0.959842
2 (NsARC_1 vs Steel_1)== 0	-6.187e-01	9.759e-02	-6.339	< 1e-04 ***
3 (NsARC_2 vs Steel_2)== 0	-3.597e-01	9.759e-02	-3.686	0.006782 **
4 (NsARC_4 vs Steel_4)== 0	-4.523e-01	9.759e-02	-4.635	0.000603 ***
5 (NsARC_5 vs Steel_5)== 0	-2.587e-01	9.759e-02	-2.651	0.077747 .
6 (NsARC_6 vs Steel_6)== 0	-6.217e-15	9.759e-02	0.000	1.000000

Signif. codes: 0 '***' 0.001 '**' 0.01 '*' 0.05 '.' 0.1 ' ' 1

(Adjusted p values reported -- single-step method)

S. aureus exposed to NsARC under uv light then plating onto LB and erythromycin plate

27. Summary.AOV

	Df	Sum Sq	Mean Sq	F value	Pr(>F)
material	1	0.45	0.45	0.523	0.475
concentration	1	75.13	75.13	87.312	1.16e-10 ***
material:concentration	1	0.06	0.06	0.073	0.789
Residuals	32	27.53	0.86		

Signif. codes: 0 ‘***’ 0.001 ‘**’ 0.01 ‘*’ 0.05 ‘.’ 0.1 ‘ ’ 1

28. Bonferroni contrasts

Linear Hypotheses:

	Estimate	Std. Error	t value	Pr(>|t|)
1 (NsARC_0 vs Steel_0)== 0	-9.706e-03	2.329e-01	-0.042	1.000000
2 (NsARC_1 vs Steel_1)== 0	-7.292e-01	1.473e-01	-4.950	0.000262 ***
3 (NsARC_2 vs Steel_2)== 0	-1.804e-01	1.473e-01	-1.225	0.772686
4 (NsARC_4 vs Steel_4)== 0	-2.817e-01	1.473e-01	-1.912	0.326368
5 (NsARC_5 vs Steel_5)== 0	-1.451e-01	1.473e-01	-0.985	0.898721
6 (NsARC_6 vs Steel_6)== 0	-4.441e-15	1.473e-01	0.000	1.000000

Signif. codes: 0 ‘***’ 0.001 ‘**’ 0.01 ‘*’ 0.05 ‘.’ 0.1 ‘ ’ 1

(Adjusted p values reported -- single-step method)

S. aureus exposed to NsARC in the dark then plating onto LB and oxacillin plate

29. Summary.AOV

	Df	Sum Sq	Mean Sq	F value	Pr(>F)
material	1	0.03	0.03	0.043	0.836
concentration	1	108.58	108.58	163.385	4.08e-14 ***
material:concentration	1	0.00	0.00	0.002	0.961
Residuals	32	21.27	0.66		

Signif. codes: 0 '***' 0.001 '**' 0.01 '*' 0.05 '.' 0.1 ' ' 1

30. Bonferroni contrasts

Linear Hypotheses:

	Estimate	Std. Error	t value	Pr(>|t|)
1 (NsARC_0 vs Steel_0)== 0	-1.232e-01	1.179e-01	-1.045	0.8719
2 (NsARC_0.07 vs Steel_0.07)== 0	-6.151e-02	7.455e-02	-0.825	0.9530
3 (NsARC_0.08 vs Steel_0.08)== 0	-3.923e-03	7.455e-02	-0.053	1.0000
4 (NsARC_0.09 vs Steel_0.09)== 0	-2.027e-08	7.455e-02	0.000	1.0000
5 (NsARC_0.1 vs Steel_0.1)== 0	-2.123e-01	7.455e-02	-2.847	0.0503 .
6 (NsARC_0.2 vs Steel_0.2)== 0	-5.329e-15	7.455e-02	0.000	1.0000

Signif. codes: 0 '***' 0.001 '**' 0.01 '*' 0.05 '.' 0.1 ' ' 1

(Adjusted p values reported -- single-step method)

S. aureus exposed to NsARC under uv light then plating onto LB and oxacillin plate

31. Summary.AOV

	Df	Sum Sq	Mean Sq	F value	Pr(>F)
material	1	0.02	0.02	0.030	0.864
concentration	1	105.08	105.08	168.732	2.64e-14 ***
material:concentration	1	0.00	0.00	0.003	0.960
Residuals	32	19.93	0.62		

Signif. codes: 0 '***' 0.001 '**' 0.01 '*' 0.05 '.' 0.1 ' ' 1

32. Bonferroni contrasts

Linear Hypotheses:

	Estimate	Std. Error	t value	Pr(>|t|)
1 (NsARC_0 vs Steel_0)== 0	-1.679e-02	1.996e-01	-0.084	1.00000
2 (NsARC_0.07 vs Steel_0.07)== 0	1.440e-01	1.263e-01	1.141	0.82225
3 (NsARC_0.08 vs Steel_0.08)== 0	-3.230e-02	1.263e-01	-0.256	0.99992
4 (NsARC_0.09 vs Steel_0.09)== 0	4.601e-01	1.263e-01	3.644	0.00754 **
5 (NsARC_0.1 vs Steel_0.1)== 0	-2.917e-01	1.263e-01	-2.310	0.15808
6 (NsARC_0.2 vs Steel_0.2)== 0	-4.441e-15	1.263e-01	0.000	1.00000

Signif. codes: 0 '***' 0.001 '**' 0.01 '*' 0.05 '.' 0.1 ' ' 1

(Adjusted p values reported -- single-step method)

S. aureus exposed to NsARC in the dark then plating onto LB and tetracycline plate

33. Summary.AOV

	Df	Sum Sq	Mean Sq	F value	Pr(>F)
material	1	0.06	0.06	0.068	0.796
concentration	1	115.66	115.66	122.236	1.84e-12 ***
material:concentration	1	0.00	0.00	0.005	0.944
Residuals	32	30.28	0.95		

Signif. codes: 0 '***' 0.001 '**' 0.01 '*' 0.05 '.' 0.1 ' ' 1

34. Bonferroni contrasts

Linear Hypotheses:

		Estimate	Std. Error	t value	Pr(>|t|)
1 (NsARC_0 vs Steel_0)==	0	-1.036e-03	6.488e-02	-0.016	1.000000
2 (NsARC_0.09 vs Steel_0.09)==	0	2.116e-02	4.103e-02	0.516	0.995550
3 (NsARC_0.1 vs Steel_0.1)==	0	7.682e-02	4.103e-02	1.872	0.348461
4 (NsARC_0.2 vs Steel_0.2)==	0	2.166e-01	4.103e-02	5.280	0.000120 ***
5 (NsARC_0.3 vs Steel_0.3)==	0	1.938e-01	4.103e-02	4.723	0.000515 ***
6 (NsARC_0.4 vs Steel_0.4)==	0	-7.105e-15	4.103e-02	0.000	1.000000

Signif. codes: 0 '***' 0.001 '**' 0.01 '*' 0.05 '.' 0.1 ' ' 1

(Adjusted p values reported -- single-step method)

S. aureus exposed to NsARC under uv light then plating onto LB and tetracycline plate

35. Summary.AOV

	Df	Sum Sq	Mean Sq	F value	Pr(>F)
material	1	0.01	0.01	0.014	0.906
concentration	1	115.23	115.23	118.495	2.73e-12 ***
material:concentration	1	0.00	0.00	0.000	0.993
Residuals	32	31.12	0.97		

Signif. codes: 0 ‘***’ 0.001 ‘**’ 0.01 ‘*’ 0.05 ‘.’ 0.1 ‘ ’ 1

36. Bonferroni contrasts

Linear Hypotheses:

		Estimate	Std. Error	t value	Pr(>|t|)
1 (NsARC_0 vs Steel_0)==	0	-3.760e-03	9.339e-02	-0.040	1.0000
2 (NsARC_0.09 vs Steel_0.09)==	0	-1.757e-02	5.907e-02	-0.297	0.9998
3 (NsARC_0.1 vs Steel_0.1)==	0	6.588e-02	5.907e-02	1.115	0.8362
4 (NsARC_0.2 vs Steel_0.2)==	0	1.624e-01	5.907e-02	2.750	0.0527 *.
5 (NsARC_0.3 vs Steel_0.3)==	0	2.469e-02	5.907e-02	0.418	0.9986
6 (NsARC_0.4 vs Steel_0.4)==	0	-7.105e-15	5.907e-02	0.000	1.0000

Signif. codes: 0 ‘***’ 0.001 ‘**’ 0.01 ‘*’ 0.05 ‘.’ 0.1 ‘ ’ 1

(Adjusted p values reported -- single-step method)

S. aureus exposed to NsARC in the dark then plating onto LB and fusidic acid plate

37. Summary.AOV

	Df	Sum Sq	Mean Sq	F value	Pr(>F)
material	1	0.02	0.02	0.213	0.648
concentration	1	105.37	105.37	1017.558	<2e-16 ***
material:concentration	1	0.00	0.00	0.041	0.842
Residuals	32	3.31	0.10		

Signif. codes: 0 '***' 0.001 '**' 0.01 '*' 0.05 '.' 0.1 ' ' 1

38. Bonferroni contrasts

Linear Hypotheses:

		Estimate	Std. Error	t value	Pr(>|t|)
1 (NsARC_0 vs Steel_0)==	0	-1.361e-01	4.657e-02	-2.922	0.0426 *
2 (NsARC_0.09 vs Steel_0.09)==	0	1.308e-02	2.945e-02	0.444	0.9980
3 (NsARC_0.1 vs Steel_0.1)==	0	3.517e-01	2.945e-02	11.940	<0.001 ***
4 (NsARC_0.2 vs Steel_0.2)==	0	-8.882e-16	2.945e-02	0.000	1.0000
5 (NsARC_0.3 vs Steel_0.3)==	0	0.000e+00	2.945e-02	0.000	1.0000
6 (NsARC_0.4 vs Steel_0.4)==	0	-3.553e-15	2.945e-02	0.000	1.0000

Signif. codes: 0 '***' 0.001 '**' 0.01 '*' 0.05 '.' 0.1 ' ' 1

(Adjusted p values reported -- single-step method)

S. aureus exposed to NsARC under uv light then plating onto LB and fusidic acid plate

39. Summary.AOV

	Df	Sum Sq	Mean Sq	F value	Pr(>F)
material	1	0.00	0.00	0.000	0.995
concentration	1	94.54	94.54	1163.156	<2e-16 ***
material:concentration	1	0.00	0.00	0.036	0.851
Residuals	32	2.60	0.08		

Signif. codes: 0 '***' 0.001 '**' 0.01 '*' 0.05 '.' 0.1 ' ' 1

40. Bonferroni contrasts

Linear Hypotheses:

		Estimate	Std. Error	t value	Pr(>|t|)
1 (NsARC_0 vs Steel_0)==	0	-3.213e-01	1.087e-01	- 2.957	0.0393 *
2 (NsARC_0.09 vs Steel_0.09)==	0	1.089e-01	6.872e-02	1.584	0.5298
3 (NsARC_0.1 vs Steel_0.1)==	0	5.544e-02	6.872e-02	0.807	0.9576
4 (NsARC_0.2 vs Steel_0.2)==	0	-4.441e-16	6.872e-02	0.000	1.0000
5 (NsARC_0.3 vs Steel_0.3)==	0	4.441e-16	6.872e-02	0.000	1.0000
6 (NsARC_0.4 vs Steel_04.)==	0	-5.329e-15	6.872e-02	0.000	1.0000

Signif. codes: 0 '***' 0.001 '**' 0.01 '*' 0.05 '.' 0.1 ' ' 1

(Adjusted p values reported -- single-step method)

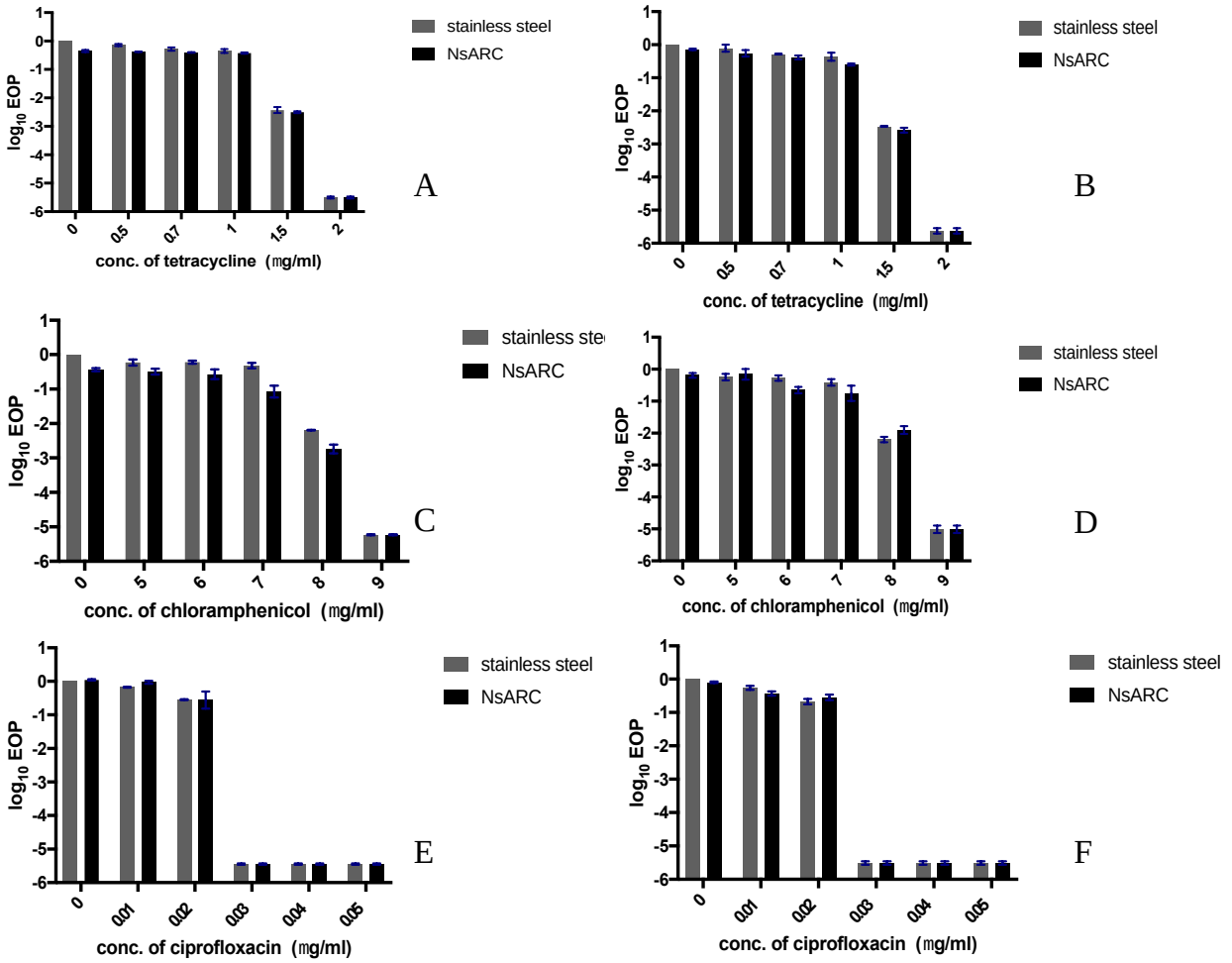

Figure A.1: Response of *E. coli* to (A) Tetracycline after exposure to NsARC in the dark (B) Tetracycline after exposure to NsARC under light (C) Chloramphenicol after exposure to NsARC in the dark (D) Chloramphenicol after exposure to NsARC under light (E) Ciprofloxacin after exposure to NsARC in the dark (F) Ciprofloxacin after exposure to NsARC under light.

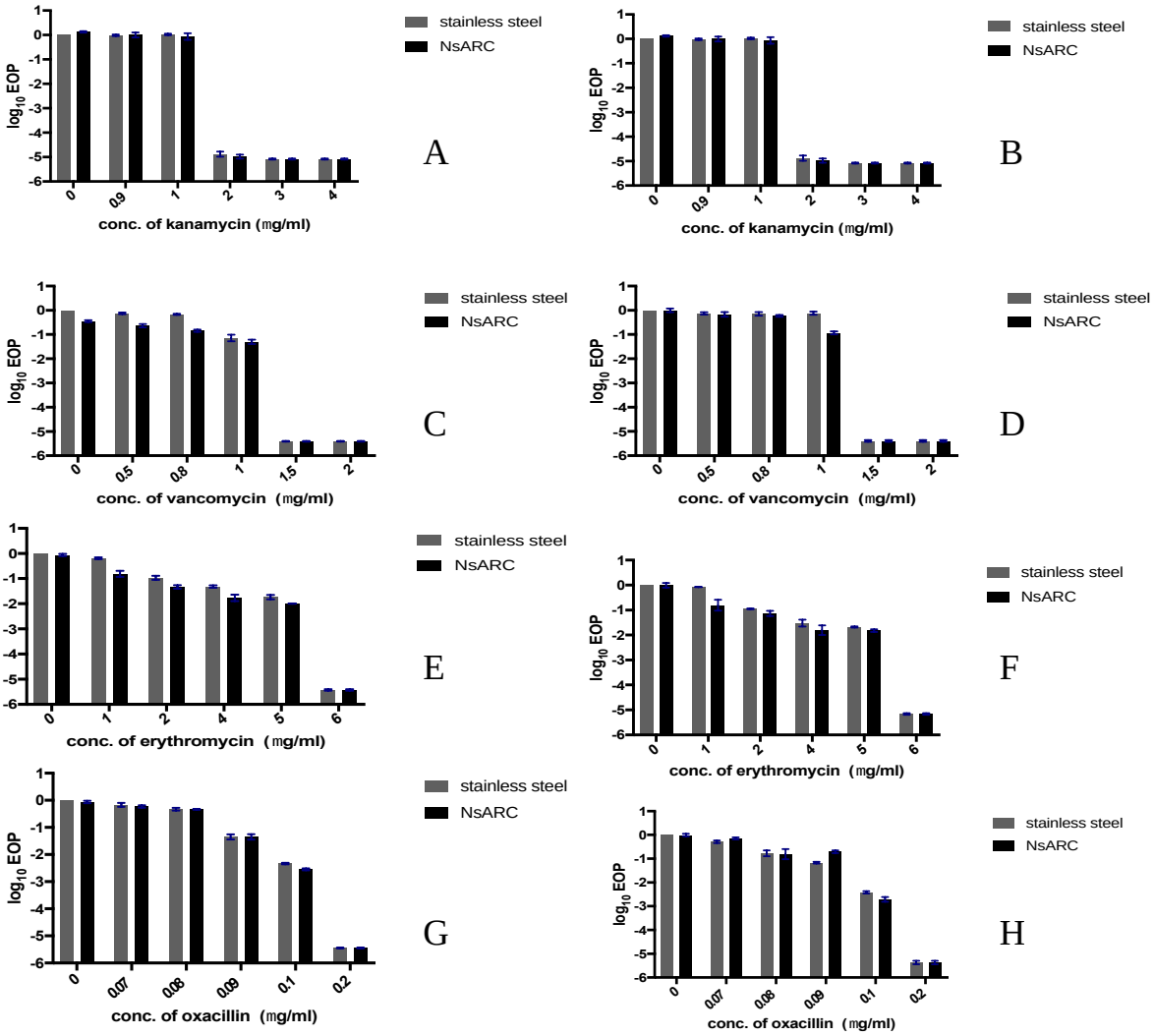
stainless steel
NsARC
log10 EOP
conc. of kanamycin (mg/ml)
A
B
conc. of vancomycin (mg/ml)
C
D
conc. of erythromycin (mg/ml)
E
F
conc. of oxacillin (mg/ml)
G
H

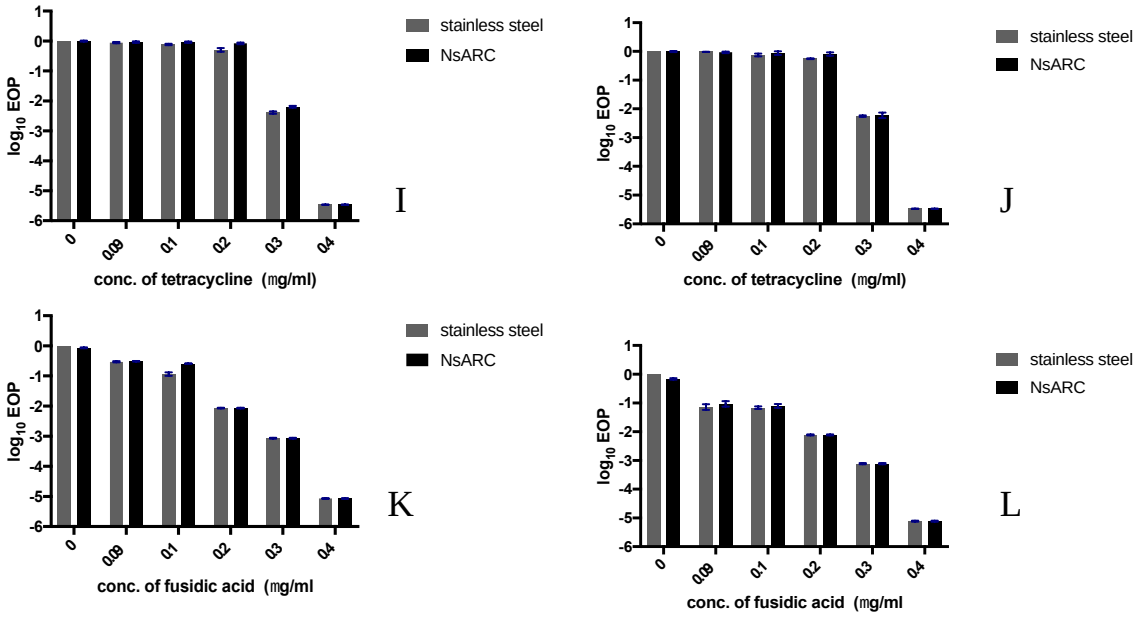

Figure A.2: Response of *S. aureus* to (A) Kanamycin after exposure to NsARC in the dark (B) Kanamycin after exposure to NsARC under light (C) Vancomycin after exposure to NsARC in the dark (D) Vancomycin after exposure to NsARC under light (E) Erythromycin after exposure to NsARC in the dark (F) Erythromycin after exposure to NsARC in the dark (G) Oxacillin after exposure to NsARC in the dark (H) Oxacillin after exposure to NsARC in the dark (I) Tetracycline after exposure to NsARC in the dark (J) Tetracycline after exposure to NsARC in the dark (K) Fusidic acid after exposure to NsARC in the dark (L) Fusidic acid after exposure to NsARC in the dark.

Appendix D: Design and construction of reporter strains

A set of reporter strains that contained plasmids with a fluorescent gene whose expression was controlled by the promoter region of either the *tolC* or *soxS* efflux associated genes was made.

1. Plasmid construction

The design and construction pFru-p*tolC*-mScarlet (Figure A.3) and pFru-p*soxS*-mScarlet (Figure A.4) plasmids were carried out as described by Jun et al. (2019). Primer used are shown in Table A. 1 and A.2. All *E. coli* strains transformed with the plasmids were selected on kanamycin.

Table A. 1: *E. coli* gene promoter regions amplified. Genome regions selected for amplification from *E. coli* BW25113. Regions were upstream of transcription start for each gene.

Gene Name & Sequence location	Sequence
tolC 204bp upstream of transcription start	TGTTAATGTCCTGGCACTAATAGTGAATTAAATGTGAATTTCAGCGACGT TTGACTGCCGTTTGAGCAGTCATGTGTTAAATTGAGGCACATTAACGCCC TATGGCACGTAACGCCAACCTTTTGCGGTAGCGGCTTCTGCTAGAATCCG CAATAATTTTACAGTTTGATCGCGCTAAATACTGCTTCACCACAAGGAAT GCAA
soxS 300bp upstream of	AAATCTGCCTCTTTTCAGTGTTCAGTTCGTTAATTCATCTGTTGGGGAGT ATAATTCCTCAAGTTAACTTGAGGTAAAGCGATTTATGGAAAAGAAATTA CCCCGCATTAAAGCGCTGCTAACCCCCGGCGAAGTGGCGAAACGCAGCGG

transcription start	TGTGGCGGTATCGGCGCTGCATTTCTATGAAAGTAAAGGGTTGATTACCA GTATCCGTAACAGCGGCAATCAGCGGCGATATAAACGTGATGTGTTGCGA TATGTTGCAATTATCAAAATTGCTCAGCGTATTGGCATTCCGCTGGCGAC

Table A. 2: Primers used in this study. Blue regions bonded with vector. Red regions were overlapping primers. Black regions bonded with isolated gene regions on promoter and mScarlet.

Name	Target	Sequence	T_m (C^0)
Gisbon Assembly Primers			
FWD_primer_TolC	*tolC*	5' CAG GAC GCC CGC CAT AAA CTG CCA GGA ATT GGG GAT CGG ATG TTA ATG TCC TGG CAC TAA TAG TGA ATT AAA TGT 3'	87.1
REV_primer_TolC	*tolC*	5' TCG CCC TTG CTC ACC ATG GTT TGC ATT CCT TGT GGT GAA GCA G 3'	81.8
FWD_primer_SoxS	*soxS*	5' CAG GAC GCC CGC CAT AAA CTG CCA GGA ATT GGG GAT CGG AGT CGC CAG CGG AAT GC 3'	89.9

REV_primer_SoxS	*soxS*	5' CCT CGC CCT TGC TCA CCA TGA AAT CTG CCT CTT TTC AGT GTT CAG TT 3'	81.5
TolC_mScarlet_FWD	*tolC* and *mScarlet*	5' CTT CAC CAC AAG GAA TGC AAA CCA TGG TGA GCA AGG GC 3’	78.9
SoxS_mScarlet_FWD	*soxS* and *mScarlet*	5' CAC TGA AAA GAG GCA GAT TTC ATG GTG AGC AAG GGC GAG GC 3’	80.9
mScarlet_REV	*mScarlet*	5' TTA CTG GAT CTA TCA ACA GGA GTC CAA GCT CAG CTA ATT ACT TGT ACA GCT CGT CCA TGC 3'	83.7

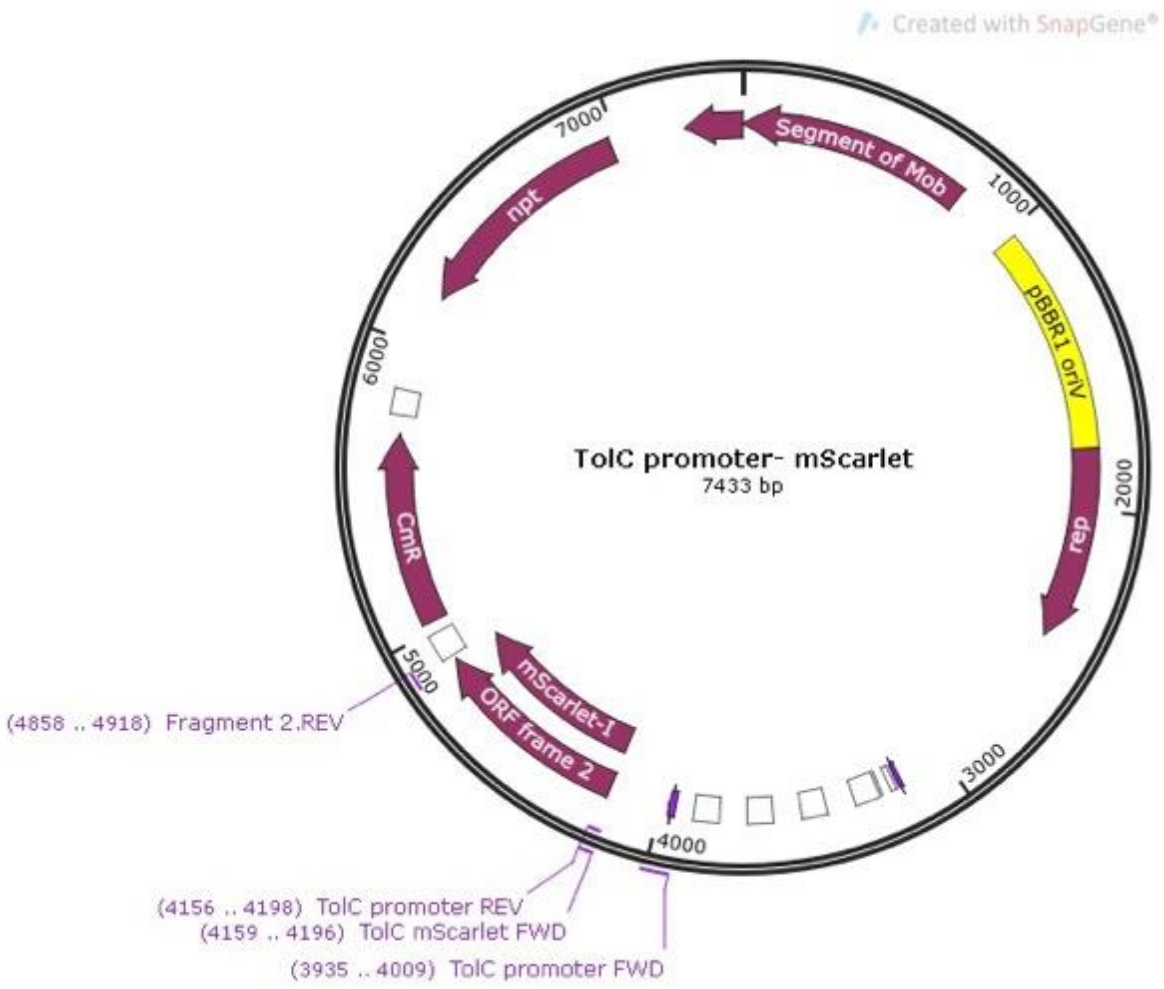

Figure A.3: Plasmid map of pTolC-mScarlet. Relevent genes are marked out. Primer binding regions marked out. Promoter region marked out by between TolC Fwd and TolC Rev

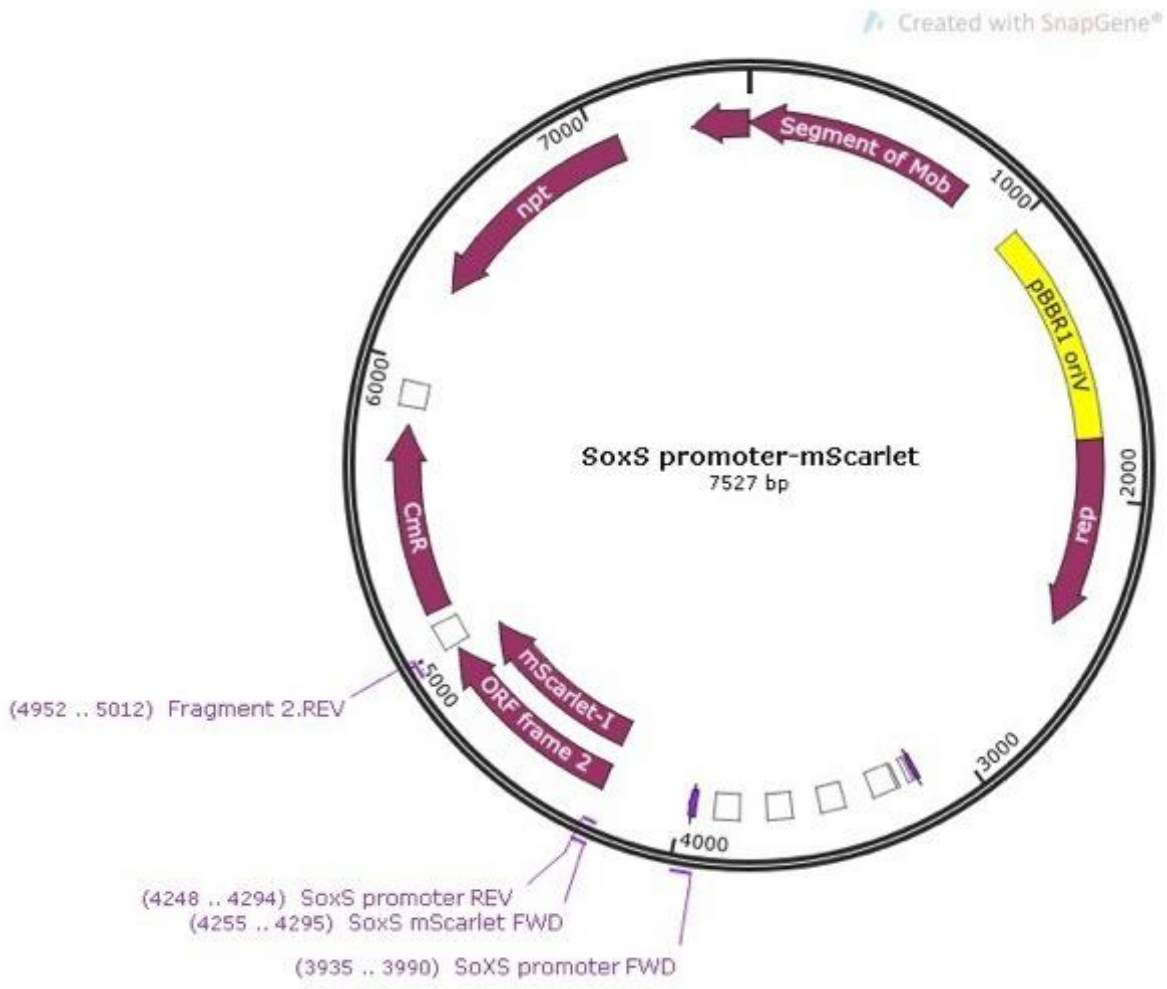

Figure A4: Plasmid map of pSoxS-mScarlet. mScarlet. Relevent genes are marked out. Primer binding regions marked out. Promoter region marked out by between SoxS Fwd and SoxS Rev

2. Extraction of plasmid DNA

The plasmid DNA of choice (pfru97, pUC19, psoxS-mScarlet and ptolC-mScarlet) were extracted from *E. coli* using Zyppy™ Plasmid miniprep kit No: D4036 (Zymo Research Corp). The kit contained suspension buffer, lysis buffer, neutralization buffer, wash buffer and elution buffer. The plasmid DNA extraction was done according to manufacturer's specifications. The plasmid DNA purity and quality was checked using Nanodrop™ 2000 spectrophotometer (ThermoFisher scientific, USA).

3. Making Competent cells

E. coli BW25113 and *E. coli* CMB73 cells were each grown to OD 0.4. The cells were then pelleted by centrifugation and the pellets resuspended in 0.1M $CaCl_2$ and incubated on ice for 4 hours before being spun at 5000rpm for 5 minutes. The pellets are resuspended in 0.1M $CaCl_2$ + 15% glycerol. The cells were then aliquoted in 1.5ml tubes and stored at -80°C.

4. Transformation of *E. coli* BW and CMB73 strain

In ice, 10 ul of the assembled constructs were added to competent *E. coli* Bw25113 and CMB73 cells and incubated for 30 minutes. The assembly is then heat shocked at 42^{o}C for 50 secs and incubated for 2 mins on ice before recovery at 37^{o}C for 1 hours in the incubator and plating on to LB agar plates that contained Kanamycin (4 mg/ml), 100 ul on one plate and 900ul on the other. Colonies were observed for fluorescence daily and colonies showing fluorescence were picked off. Picked off colonies were grown to saturation in LB and kanamycin (40 μg/ml). Saturated cultures were then stored in 15% glycerol at -80^{o}C.

5. Transformation of *E. coli* BW strain with the plasmid backbone (pfru97)

In ice, 10 ul of the pfru97 plasmid was added to competent *E. coli* Bw25113 cells as described in Appendix D4.

6. Transformation of *E. coli* BW strain with pUC19 plasmid

In ice, 10 ul of the pUC19 plasmid was added to competent *E. coli* Bw25113 and incubated for 30 minutes. The assembly is then heat shocked at 42^{o}C for 50 secs and incubated for 2 mins on ice before recovery at 37^{o}C for 1 hours in the incubator and plating on to LB agar plates that contained ampicillin (1 mg/ml), 100 ul on one plate and 900ul on the other.

Colonies were observed for growth daily and colonies were picked off. Picked off colonies were grown to saturation in LB and ampicillin (50 μg/ml). Saturated cultures were then stored in 15% glycerol at -80^{o}C.

Appendix E: Adaptive resistance Experiment

ANOVAs and Tukey's contrasts for experiment comparing the relative fluorescence of *E. coli* BW25113 pHJ01 (pFru - P_{tolC}_mScarlet) that was exposed to copper, NsARC and stainless steel under uv light, High intensity visible light, ambient light and in the dark

Under uv light

1. **ANOVA**

	Df	Sum Sq	Mean Sq	F value	Pr(>F)
material	2	240053	120027	68.52	<2e-16 ***
Residuals	1005	1760453	1752		

Signif. codes: 0 '***' 0.001 '**' 0.01 '*' 0.05 '.' 0.1 ' ' 1

2. **Tukey's contrasts**

Linear Hypotheses:

		Estimate	Std. Error	t value	Pr(>|t|)
NsARC - copper	== 0	-25.839	3.227	-8.007	< 1e-04 ***
steel – copper	== 0	-37.902	3.303	-11.477	< 1e-04 ***
steel - NsARC	== 0	-12.063	3.177	-3.797	0.000458 ***

Signif. codes: 0 '***' 0.001 '**' 0.01 '*' 0.05 '.' 0.1 ' ' 1

(Adjusted p values reported -- single-step method)

Under high intensity visible light

3. **ANOVA**

	Df	Sum Sq	Mean Sq	F value	Pr(>F)	
material	2	393283	196642	183.9	<2e-16	***
Residuals	2730	2918542	1069			

Signif. codes: 0 '***' 0.001 '**' 0.01 '*' 0.05 '.' 0.1 ' ' 1

4. **Tukey's contrasts**

Linear Hypotheses:

	Estimate	Std. Error	t value	Pr(>|t|)	
NsARC - copper == 0	-31.269	2.088	-14.975	< 1e-09	***
steel - copper == 0	-39.597	2.065	-19.175	< 1e-09	***
steel - NsARC == 0	-8.328	1.331	-6.257	1.36e-09	***

Signif. codes: 0 '***' 0.001 '**' 0.01 '*' 0.05 '.' 0.1 ' ' 1

(Adjusted p values reported -- single-step method)

Under Ambient light

5. **ANOVA**

	Df	Sum Sq	Mean Sq	F value	Pr(>F)
material	2	318082	159041	58.22	<2e-16 ***
Residuals	1032	2819314	2732		

Signif. codes: 0 '***' 0.001 '**' 0.01 '*' 0.05 '.' 0.1 ' ' 1

6. **Tukey's contrasts**

Linear Hypotheses:

		Estimate	Std. Error	t value	Pr(>|t|)
NsARC – copper	== 0	-34.162	3.980	-8.584	<1e-04 ***
steel - copper	== 0	-39.613	3.980	-9.954	<1e-04 ***
steel - NsARC	== 0	-5.451	3.980	-1.370	0.357

Signif. codes: 0 '***' 0.001 '**' 0.01 '*' 0.05 '.' 0.1 ' ' 1

(Adjusted p values reported -- single-step method)

In the dark

7. **ANOVA**

	Df	Sum Sq	Mean Sq	F value	Pr(>F)
material	2	188241	94121	44.87	<2e-16 ***
Residuals	1032	2164913	2098		

Signif. codes: 0 '***' 0.001 '**' 0.01 '*' 0.05 '.' 0.1 ' ' 1

8. **Tukey's contrasts**

Linear Hypotheses:

	Estimate	Std. Error	t value	Pr(>|t|)
NsARC - copper == 0	-26.378	3.487	-7.564	<1e-05 ***
steel - copper == 0	-30.411	3.487	-8.721	<1e-05 ***
steel - NsARC == 0	-4.034	3.487	-1.157	0.479

Signif. codes: 0 '***' 0.001 '**' 0.01 '*' 0.05 '.' 0.1 ' ' 1

(Adjusted p values reported -- single-step method)

ANOVAs and Tukey's contrasts for experiment comparing the relative fluorescence of *E. coli* BW25113 pHJ01 (pFru – P_{soxS}_mScarlet) that was exposed to copper, NsARC and stainless steel under uv light, High intensity visible light, ambient light and in the dark.

Under uv light

9. ANOVA

	Df	Sum Sq	Mean Sq	F value	Pr(>F)
material	2	185665	92832	293.2	<2e-16 ***
Residuals	2013	637255	317		

Signif. codes: 0 '***' 0.001 '**' 0.01 '*' 0.05 '.' 0.1 ' ' 1

10. Tukey's contrasts

Linear Hypotheses:

	Estimate	Std. Error	t value	Pr(>|t|)
NsARC - copper == 0	-18.0874	0.9707	-18.634	< 1e-04 ***
steel - copper == 0	-22.0462	0.9707	-22.713	< 1e-04 ***
steel - NsARC == 0	-3.9588	0.9707	-4.078	0.000149 ***

Signif. codes: 0 '***' 0.001 '**' 0.01 '*' 0.05 '.' 0.1 ' ' 1

(Adjusted p values reported -- single-step method)

Under high intensity visible light

11. ANOVA

	Df	Sum Sq	Mean Sq	F value	Pr(>F)
material	2	122804	61402	259	<2e-16 ***
Residuals	1176	278832	237		

Signif. codes: 0 '***' 0.001 '**' 0.01 '*' 0.05 '.' 0.1 ' ' 1

12. Tukey's contrasts

Linear Hypotheses:

	Estimate	Std. Error	t value	Pr(>|t|)
NsARC - copper == 0	-19.617	1.098	-17.859	< 0.001 ***
steel - copper == 0	-23.228	1.098	-21.146	< 0.001 ***
steel - NsARC == 0	-3.611	1.098	-3.288	0.00305 **

Signif. codes: 0 '***' 0.001 '**' 0.01 '*' 0.05 '.' 0.1 ' ' 1

(Adjusted p values reported -- single-step method)

Under Ambient light

13. ANOVA

	Df	Sum Sq	Mean Sq	F value	Pr(>F)
material	2	102237	51118	164.2	<2e-16 ***
Residuals	1230	382986	311		

Signif. codes: 0 '***' 0.001 '**' 0.01 '*' 0.05 '.' 0.1 ' ' 1

14. Tukey's contrasts

Linear Hypotheses:

	Estimate	Std. Error	t value	Pr(>|t|)
NsARC - copper == 0	-17.945	1.231	-14.58	<1e-04 ***
steel - copper == 0	-20.444	1.231	-16.61	<1e-04 ***
steel - NsARC == 0	-2.499	1.231	-2.03	0.105

Signif. codes: 0 '***' 0.001 '**' 0.01 '*' 0.05 '.' 0.1 ' ' 1

(Adjusted p values reported -- single-step method)

In the dark

15. ANOVA

	Df	Sum Sq	Mean Sq	F value	Pr(>F)
material	2	102901	51450	165.8	<2e-16 ***
Residuals	1095	339869	310		

Signif. codes: 0 '***' 0.001 '**' 0.01 '*' 0.05 '.' 0.1 ' ' 1

16. Tukey's contrasts

Linear Hypotheses:

	Estimate	Std. Error	t value	Pr(>|t|)
NsARC - copper == 0	-18.358	1.302	-14.096	< 0.001 ***
steel - copper == 0	-22.178	1.302	-17.029	< 0.001 ***
steel - NsARC == 0	-3.820	1.302	-2.933	0.00957 **

Signif. codes: 0 '***' 0.001 '**' 0.01 '*' 0.05 '.' 0.1 ' ' 1

(Adjusted p values reported -- single-step method)